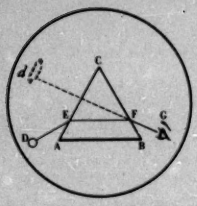

optics and spectroscopy

volume ix
number 6
december 1960

OPTICAL SOCIETY OF AMERICA

USSR ACADEMY OF SCIENCES

RUSSIAN EDITORIAL STAFF FOR
OPTIKA I SPEKTROSKOPIYA sponsored by
USSR ACADEMY OF SCIENCES

Editor: S. E. FRISH

Assistant Editor: P. P. FEOFILOV
Corresponding Secretary: L. S. SAZONOV

Associate Editors:

M. M. GUREVICH M. A. EL'IASHEVICH A. A. LEBEDEV V. P. LINNIK
S. L. MANDEL'SHTAM I. V. OBREIMOV V. K. PROKOF'EV
N. N. SOBOLEV A. N. TERENIN A. I. TUDOROVSKII

Translated from *OPTIKA I SPEKTROSKOPIYA* on the initiative of THE OPTICAL SOCIETY OF AMERICA, INC. with a grant-in-aid from THE NATIONAL SCIENCE FOUNDATION. *Optics and Spectroscopy* is a cover-to-cover translation of *Optika i Spektroskopiya* and no attempt is made to edit the material other than to correct obvious misprints. The views are those of the original authors and do not represent the Optical Society of America.

TRANSLATION EDITORIAL STAFF

Scientific Editors

CYRUS FELDMAN, *Oak Ridge National Laboratory*

CARL W. GARLAND, *Massachusetts Institute of Technology*

MATHEW G. GIBBONS, *Oakland, California*

Administrative Editor: PATRICIA R. WAKELING, *OSA*

Published monthly by the Optical Society of America, Inc. Executive office: 1155 Sixteenth Street, N.W., Washington, D.C. Subscriptions for one year to members of the Society: Associates $13.00; Regular members and Fellows $17.00. Subscriptions for non-members of the Society: One year U. S. and Possessions, $25.00; Foreign $28.00. Back numbers: $3.00 per copy. Subscriptions, changes of address and undeliverable copies should be referred to the Executive offices in Washington, D.C. The office of publication is 2500 South State Street, Ann Arbor, Michigan. Second class postage paid at Ann Arbor, Michigan.

Printed in the U.S.A. by Edwards Brothers, Inc., Ann Arbor, Michigan.

ON QUANTUM TRANSITIONS IN THE SELF-CONSISTENT FIELD APPROXIMATION

I. B. Bersuker

Received 27 January 1960

A different and more exact method of solution of nonstationary problems in the self-consistent field approximation is proposed, in which the probability of quantum transitions is obtained as a solution of a system of nonstationary equations of the self-consistent field, analogous to the equations of Fock for the stationary case. It is shown that the conventional formula for the transition probabilities is an approximation of the zeroth order in the matrix elements of the interaction operator between the electrons. A first approximation correction is obtained for this formula. The specific case of optical dipole transitions in atoms is investigated in more detail and the expression for the correction term is reduced to a form which is convenient for numerical calculations.

1. INTRODUCTION

It is well known that to solve the problem of quantum transitions in a many-electron system in the presence of a perturbation W, one must solve Schrödinger's time-dependent wave equation

$$i\frac{\partial\Psi}{\partial t}=(H+W)\Psi. \qquad (1)$$

The conventional method in solving this equation is based on the assumption that the exact solution of the corresponding stationary equation $H\Psi_k^{(0)}=E_k\Psi_k^{(0)}$ is known. On substituting the expansion $\Psi_k=\sum_n C_{kn}(t)\Psi_n^{(0)}$ into Eq. (1) one obtains the following expressions for the probability of transition of the system from the stationary state k to the stationary state l:

$$|C_{kl}|^2=\left|\int_0^t W_{kl}dt'\right|^2 \qquad (2)$$

To evaluate the matrix elements W_{kl}, it is necessary to use approximate wave functions of the stationary states. These approximate wave functions are obtained by various methods. One of the methods used is the method of the self-consistent field. However, in this case even Eq. (2) is not exact. We propose a different method for solving the problem of quantum transitions, namely, to substitute the approximate wave functions of the system into the exact starting Eq. (1) rather than into the inexact Eq. (2). In the self-consistent field approximation, this means that the wave function Ψ must be represented in Eq. (1) in the form of a determinant built up from one-electron time-dependent wave functions. Equation (1) then transforms into a system of nonstationary equations of the self-consistent field, analogous to the equations of Fock for the stationary case.[1] On solving this system of equations by the method of variation of parameters, one obtains expressions for the transition probabilities which contain Eq. (2) as a zeroth order approximation.

Since the proposed method of solving the problem of quantum transitions in the self-consistent field approximation starts out from the exact Eq. (1) it is in principle more accurate than the conventional method. The improvement obtained in the accuracy of Eq. (2) can be explained by the fact that in the proposed method the transition of every electron is obtained (in the nonstationary case) not only as a function of the external perturbation but also as a function of the character of the time variation of its interaction with the other electrons. It is interesting that an analogous situation exists also in the case of stationary disturbances, where the substitution of the approximate Hartree-Fock wave functions into the starting equations of the perturbation theory leads to more accurate results than the determination of correction terms with the help of these functions.[2]

2. DERIVATION OF THE SELF-CONSISTENT FIELD EQUATIONS FOR THE NONSTATIONARY CASE

For simplicity we will limit ourselves to the case in which the spatial wave function $\Psi(r_1, \ldots, r_N, t)$ of the N-electron system can be represented as a product of two determinants[3] of order p and N−p respectively, built up from one-electron orthonormal functions $\varphi_k(r, t)$, i.e.,

$$\Psi=\left[\sum_P \pm P\prod_{k=1}^{p}\varphi_k(r_k, t)\right]\left[\sum_P \pm P\prod_{k=1}^{N-p}\varphi_k(r_{p+k}, t)\right]. \qquad (3)$$

Here $\pm P$ is a permutation operator of the arguments of the φ-functions, where the minus sign refers to the case of an odd permutation. The representation of the wave function in the form of Eq. (3) assumes that p one-electron states are occupied by electron pairs with compensating spins, and that the remaining (N−2p) spins are not paired, so that the total number of independent one-electron functions is N−p.

The time-dependent equation for each electron can be readily obtained. We recall that Schrödinger's equation for the entire system is equivalent to the variational equation

$$\int\delta\Psi^*\left(H-i\frac{\partial}{\partial t}\right)\Psi d\tau=0. \qquad (4)$$

We now substitute Ψ as given by Eq. (3) into this equation. Independently varying the N−p functions φ_k and also the complex conjugate functions φ_k^*, using the supplementary conditions

$$\int\varphi_k^*\varphi_l d\tau=\delta_{kl} \qquad (5)$$

and equating the coefficients of the independent variations to zero, we obtain

$$i\left\{\frac{\partial\varphi_k(r, t)}{\partial t}+\varphi_k(r, t)\sum_{n=1}^{N-p}\gamma_n\int\varphi_n^*\frac{\partial\varphi_n}{\partial t}d\tau\right.$$

$$\left.-\frac{1}{2}\sum_{n=1}^{N-p}\gamma_n\varphi_n(r, t)\int\varphi_n^*\frac{\partial\varphi_n}{\partial t}d\tau\right\}=\left[H+\sum_{n=1}^{N-p}\gamma_n V_{nn}+W\right]\varphi_k(r, t)$$

$$-\frac{1}{2}\sum_{n=1}^{N-p}(\gamma_n V_{kn}+\varepsilon_{kn})\varphi_n(r, t), \qquad k=1, 2, \ldots, p; \qquad (6)$$

$$i\left\{\frac{\partial\varphi_k(\mathbf{r},t)}{\partial t}+\varphi_k(\mathbf{r},t)\sum_{n=1}^{N-p}\gamma_n\int\varphi_n^*\frac{\partial\varphi_k}{\partial t}\,d\tau-\sum_{n=1}^{N-p}\varphi_n(\mathbf{r},t)\int\varphi_n^*\frac{\partial\varphi_k}{\partial t}\,d\tau\right\}$$

$$=\left[H+\sum_{n=1}^{N-p}\gamma_n V_{nn}+W\right]\varphi_k(\mathbf{r},t)-\sum_{n=1}^{N-p}(V_{kn}+\varepsilon_{kn})\varphi_n(\mathbf{r},t),$$

$$k=p+1,\ p+2,\ \ldots,\ N-p. \tag{7}$$

The following notations are used in the above equations

$$V_{kn}(\mathbf{r},t)=\int\frac{\varphi_n^*(\mathbf{r}',t)\varphi_k(\mathbf{r}',t)}{|r-r'|}\,d\tau', \tag{8}$$

$$\gamma_n=\begin{cases}2, & n\leqslant p,\\ 1, & n>p.\end{cases} \tag{9}$$

H is the Hamiltonian of the electron in the field of the nucleus, the $\varepsilon_{k\alpha}$ are Lagrangrian multipliers (which are generally time-dependent) under supplementary conditions (5), and W(r, t) is the time-dependent potential of the external field.

Equations (6) and (7) represent a system of nonstationary equations of the self-consistent field with exchange for an N-electron system in a variable external field.* It can easily be shown that for the stationary case (W = 0), these equations are reduced to the conventional stationary Fock equations. Indeed, in this case setting $\varphi_k(\mathbf{r},t)=\psi_k(\mathbf{r})\exp(i\beta_k t)$, we find that the functions $\psi_k(\mathbf{r})$ satisfy the conventional Fock equations,* and the constants β_k are related to each other only by the expression $\sum_{k=1}^{N-p}\gamma_k\beta_k=0$, so that they can be all assumed to be zero.

*Similar equations have been obtained first by P. Dirac.[4]

*The factor $\exp(-iEt)$ is not included in the one-electron wave functions ψ and φ and must therefore be added to the wave function ψ of the entire system.

3. TRANSITION PROBABILITY OF THE SYSTEM

Let the unexcited (initial) state of the system be denoted by the index U and the excited (final) state by the index E. The probability of transition between these two stationary states is determined by the square of the amplitude $C_{UE}(t)$ of the stationary state $\Psi_E^{(0)}(\mathbf{r}_1,\ldots,\mathbf{r}_N)$ of the excited configuration in the expansion of the nonstationary state $\Psi_U(\mathbf{r}_1,\ldots,\mathbf{r}_N,t)$ corresponding to the perturbed initial configuration; i.e.,

$$C_{UE}(t)=e^{i(E_E-E_U)t}\times\int\Psi^{(0)*}(\mathbf{r}_1,\ldots,\mathbf{r}_p)\Psi_U(\mathbf{r}_1,\ldots,\mathbf{r}_p,t)\,d\tau_1\ldots d\tau_p. \tag{10}$$

Both the stationary and the nonstationary states of the system are represented as determinants formed from the corresponding one-electron functions, where the nonstationary functions $\varphi(\mathbf{r},t)$ are solutions of systems (6) and (7).

Let us denote by $\psi_{kn}^E(\mathbf{r})$, n = 1, 2, ..., the set of eigenfunctions of the one-electron operator which are obtained when we substitute the wave functions of all other electrons in the excited state of the system under consideration into the Fock equations for the k-th electron. Of the entire ensemble of these functions, only the function which corresponds to the state of the k-th electron in this configuration is self-consistent (the other functions do not represent real self-consistent one-electron states). Expending the nonstationary one-electron functions into such a set of functions, we obtain

$$\varphi_k(\mathbf{r}_j,t)=\psi_{ko}^U(\mathbf{r}_j)+\sum_n a_{kojn}^{no}(t)\,\psi_{jn}^E(\mathbf{r}_j). \tag{11}$$

In writing Eq. (11), the initial condition $\varphi_k(\mathbf{r},t)|_{t=0}=\psi_{ko}^U(\mathbf{r})$ is taken into consideration (so that actually it is the difference $\varphi_k-\psi_{ko}^E$ that is expanded in the orthogonal set ψ_{jn}^E).

Substituting expansion (11) into Eq. (10) and keeping only terms of first power in a, we obtain (with the harmonic factor left out)

$$C_{UE}(t)=\sum_{ko,\,jl}a_{ko,jl}^{UE}D^{UE}(ko\,|\,jl). \tag{12}$$

Where $D^{UE}(ko\,|\,jl)$ is the minor of the element $\beta_{ko,jl}$ of the determinant D^{UE} formed from the overlap integrals of the one-electron wave functions belonging to the different configurations

$$\beta_{ko,jl}=\int\psi_{ko}^U(\mathbf{r})\,\psi_{jl}^{E*}(\mathbf{r})\,d\tau \tag{13}$$

Equation (12) coincides with the expression for the matrix elements of the one-electron operator a obtained in the self-consistent field method.[5] It reduces to the conventional expression for the transition probabilities,[1,6] if we set

$$|a_{ko,jl}^{UE}|^2=|W'_{ko,jl}|^2\,t,$$

where W' is the spatial part of the perturbation. However, it will be shown below that this assumption is only an approximation of the zeroth order to the exact expression for $a_{ko,jl}^{UE}(t)$.

4. CORRECTION OF THE FIRST ORDER APPROXIMATION TO THE CONVENTIONAL FORMULA FOR THE TRANSITION PROBABILITIES

We will limit ourselves to the solution of this problem in the first order of approximation in the matrix elements of the interaction operator V of the electrons.

Substituting expansion (11) into the equation system (6) and (7) and disregarding terms of the order of aV^2 as compared with a and aV, we obtain (the indices "U" and "E" are omitted):

$$i\frac{da_{kokl}}{dt}=-a_{kokl}\omega_{kokl}+W_{kokl}$$

$$+\sum_{n=1}^{N-p}\sum_{n}^{\infty}\gamma_{nk}\left[a_{nonn}(V_{nonn})_{kokl}+a_{nonn}^*(V_{nonn}^*)_{kokl}\right]$$

$$-\sum_{\substack{n=1\\n\neq k}}^{N-p}\sum_{n}^{\infty}\lambda_{nk}\left[a_{nokn}(V_{k,pn})_{kokl}+a_{nokn}^*(V_{knkn}^*)_{nokl}\right]$$

$$-\sum_{\substack{n=1\\n\neq k}}^{N-p}\lambda'_{nk}\left[a_{nokl'kmo}+a_{nokl'kl'o}\right]. \tag{14}$$

where $\omega_{kokl}=\lambda'_k(\varepsilon_{kokn}-\varepsilon_{klkl})$ is the frequency of the electron transition kl → ko, $\gamma_{ok}=\gamma_o-\delta_{ok}$, $\lambda_{ok}=1/2\,\gamma_o$ and $\lambda'_k=1/2$ for $k\leqslant p$ and $\lambda_{ok}=\lambda'_k=1$ for $k>p$, and ε_{kono} are the nondiagonal Lagrange multipliers in the Fock equations.

To establish the order of smallness of the neglected terms in Eqs. (14), a more detailed investigation is required.

Let us assume that the transitions in question occur between two configurations of the system which differ in the quantum numbers of one electron. Let us refer to this electron as the optical electron, and to the remaining

ones as the internal electrons. Furthermore, let H′ be the change in the Hamiltonian of an internal electron caused by the change of state of the optical electron. It can then be readily shown that the change in the Hamiltonian of the optical electron resulting from its change of state and the self-consistency of this change with the states of the internal electrons is determined by the matrix elements of the product H′ · V. The integral $\beta_{k_0 k l}$ will be of the same order of magnitude, where k_0 is the initial and kl the final state of the optical electron. We neglected similar terms in comparison with unity in Eq. (14). Since H′ can be expressed by a difference of the matrix elements of the operator V, it can be assumed that the neglected terms are of the same order of smallness as V^2. All presently known evaluations of integrals of the type $\beta_{k_0 k l}$ justify the validity of these assumptions.[6,7]

An infinite system of linear first order differential equations with constant coefficients (i.e., (14)) is more conveniently written in matrix form, the differential equations being transformed into integral equations of the Volterra type and solved by the method of successive approximations. In the zeroth order approximation, which coincides with the zero order approximation in V, we obtain (a' differs from a only in the unessential harmonic multiplier),

$$a'^{(0)}_{k_0 k l} = -i \int_0^t e^{-i\omega_{k_0 k l} t'} W_{k_0 k l}\, dt'. \tag{15}$$

On substituting this expression into Eq. (12), one obtains the conventional expression for the transition probabilities in the self-consistent field approximation[1,6] which coincides with that obtained on substituting the conventional Hartree-Fock functions into Eq. (2).

In the first order approximation in V we obtain

$$\begin{aligned} a'^{(1)}_{k_0 k l} = -i \int_0^t e^{-i\omega_{k_0 k l} t'} dt' \Bigg\{ & W_{k_0 k l}(t') \\ & + \sum_n^{\infty} \sum_{\alpha=1}^{N-p} \gamma_{nk} \left[(V_{\alpha n n})_{k_0 k l} L_{\alpha n n}(t') + (V^*_{\alpha n n}) L^*_{\alpha n n}(t') \right] \\ & - \sum_n^{\infty} \sum_{\substack{\alpha=1 \\ \alpha \neq k}}^{N-p} \lambda_{nk} \left[(V_{k n n})_{k_0 k l} L_{\alpha k n}(t') + (V^*_{k n k})_{\alpha k l} L_{\alpha k n}(t') \right] \\ & - \sum_{\substack{\alpha=1 \\ \alpha \neq k}}^{N-p} \lambda'_k \left[\varepsilon_{k_0 \alpha} L_{\alpha k l}(t') + \varepsilon_{k l \alpha} L_{\alpha k k_0} \right] \Bigg\}, \end{aligned} \tag{16}$$

where

$$L_{\alpha k n}(t') = -i e^{i\omega_{\alpha k n} t'} \int_n^{t'} e^{-i\omega_{\alpha k n} t''} W_{\alpha k n}\, dt''.$$

The first approximation correction to the conventional formula for the transition probabilities is given by the three sums in the curved brackets in Eq. (16). More detailed calculations show that the main contribution to the first order correction is given by the first sum, which comes from the electrostatic interaction between the electrons. The second sum, which results from the exchange interaction of the electrons, makes a smaller contribution, which for the light atoms is apparently insignificant. The terms in the third sum of the correction, which come from the requirement of mutual orthogonality of the one-electron functions, are different from zero only when these functions are not mutually orthogonal from considerations of symmetry.

Equation (16) was obtained for the general case without specifying the nature of the perturbation W, and can therefore be applied in the self-consistent field approximation to all kinds of transitions in many-electron systems. Corrections involving terms in V higher than the first do not seem to us to be of any real value.

5. OPTICAL DIPOLE TRANSITIONS IN ATOMS (AN EXAMPLE)

We will apply Eq. (16) to the specific case of optical dipole transitions in atoms.

On substituting the expression for the perturbation $W = (\mathbf{E}_0, \mathbf{r}) \sin \omega t$ into the equation, instead of the matrix elements $\mathbf{r}_{k_0 k l}$ which appear in the common formula for the transition probabilities, we obtain matrix elements of the form $\mathbf{r}_{k_0 k l} + (\mathbf{G}(\mathbf{r}))_{k_0 k l}$, where $(\mathbf{G}(\mathbf{r}))_{k_0 k l}$ represents the contribution of the correction terms and is given by

$$\begin{aligned} \mathbf{G}_{k_0 k l} = & \sum_{\alpha=1}^{N-p} \gamma_{nk} \sum_n^{\infty} \left[\frac{(V_{\alpha n n})_{k_0 k l} \cdot \mathbf{r}_{\alpha n n}}{\omega_{\alpha n n} - \omega_{k_0 k l}} (1 - \delta_{nk} \delta_{nl}) \right. \\ & \left. + \frac{(V^*_{\alpha n n})_{k_0 k l} \cdot \mathbf{r}^*_{\alpha n n}}{\omega_{\alpha n n} + \omega_{k_0 k l}} (1 + \delta_{nk} \delta_{nl}) \right] \\ & - \sum_{\substack{\alpha=1 \\ \alpha \neq k}}^{N-p} \lambda_{nk} \sum_n^{\infty} \left[\frac{(V_{k n n})_{k_0 k l} \cdot \mathbf{r}_{\alpha k n}}{\omega_{\alpha k n} - \omega_{k_0 k l}} + \frac{(V^*_{k_0 k})_{\alpha k l} \cdot \mathbf{r}^*_{\alpha k n}}{\omega_{\alpha k n} + \omega_{k_0 k l}} \right] \\ & - \sum_{\substack{\alpha=1 \\ \alpha \neq k}}^{N-p} \lambda'_k \left[\frac{\varepsilon_{k_0 \alpha} \mathbf{r}_{\alpha k l}}{\omega_{\alpha k l} - \omega_{k_0 k l}} + \frac{\varepsilon_{k l \alpha} \mathbf{r}_{\alpha k k_0}}{\omega_{\alpha k k_0} - \omega_{k_0 k l}} \right]. \end{aligned} \tag{17}$$

For the specific case of transitions of the optical electron in a monovalent atom it can be assumed that $\omega^2_{\alpha \alpha n} \gg \omega^2_{k_0 k l}$. If we disregard the exchange terms (the second and third sums), Eq. (17) reduces to the expression for the correction for the influence of the shell on these transitions that was proposed previously by the author,[8] and substantiated in the adiabatic approximation in a paper by Veselov and the author.[9]

In actual calculations on the basis of Eq. (17) most difficulties are presented by the necessity of performing infinite summations. This can be overcome with the help of the following approximation procedure.

We take some average value of $\overline{(1/(\omega_{\alpha \alpha n} \pm \omega_{k_0 k l}))}$ outside of the $\sum_n^{\infty}$ sign. From the relation

$$\begin{aligned} & \overline{(\omega_{\alpha n n} \pm \omega_{k_0 k l})} \sum_n (V_{\alpha n n})_{k_0 k l} \cdot \mathbf{r}_{\alpha n n} \\ & = \sum_n (\omega_{\alpha n n} \pm \omega_{k_0 k l}) (V_{\alpha n n})_{k_0 k l} \cdot \mathbf{r}_{\alpha n n} \end{aligned} \tag{18}$$

we can easily find $\overline{(\omega_{\alpha \alpha n} \pm \omega_{k_0 k l})}$. The sum on the left-hand side of Eq. (18) is found directly as a matrix element of the product. To determine the sum on the right-hand side, one can use the relation $\omega_{\alpha \alpha n} (\alpha_0 | r | \alpha n) = -(\alpha_0 | \nabla | \alpha n)$. The main simplification consists in the assumption that

$$\overline{\left[\frac{1}{(\omega_{\alpha n n} \pm \omega_{k_0 k l})} \right]} \cong \frac{1}{\overline{(\omega_{\alpha n n} \pm \omega_{k_0 k l})}}. \tag{19}$$

This approximation cannot be strictly substantiated. Its justification is based on the consideration that because of the presence of the factors $\mathbf{r}_{\alpha \alpha n}$, only the first few terms with close values of the frequency $\omega_{\alpha \alpha n}$ will have any appreciable contribution to the sums of Eq. (17).

Analogous considerations also apply to the exchange sums in the approximation of first order in V.

For simplicity, we will denote the one-electron states in the atom by a single index. Let the index α apply to the internal electrons, k to the initial state of the optical electron, and l to its final state (it is assumed that the outer shell is not filled). Taking the simplifications discussed above into consideration one obtains

$$G_{kl} = \sum_{\alpha=1}^{N-1} \left\{ \gamma_{\alpha k} \left[\frac{(l \mid (r/r)\, F_{\alpha\alpha}^{(-)} \mid k)}{(l \mid Q_{\alpha\alpha} \mid k)/(l \mid F_{\alpha\alpha}^{(-)} \mid k) - \omega_{kl}} + \frac{(l \mid (r/r)\, F_{\alpha\alpha}^{(+)} \mid k)}{(l \mid Q_{\alpha\alpha} \mid k)/(l \mid F_{\alpha\alpha}^{(+)} \mid k) + \omega_{kl}} \right] \right.$$

$$- \lambda_{\alpha k} (1 - \delta_{\alpha k}) \left[\frac{(\alpha \mid (r/r)\, F_{\alpha l} \mid k)}{(\alpha \mid Q_{\alpha l} \mid k)/(\alpha \mid F_{\alpha l} \mid k) - \omega_{kl}} + \frac{(l \mid (r/r)\, F_{k\alpha} \mid \alpha)}{(l \mid Q_{k\alpha} \mid \alpha)/(l \mid F_{k\alpha} \mid \alpha) + \omega_{kl}} \right] -$$

$$\left. - \lambda'_{k} (1 - \delta_{\alpha k}) \left[\frac{e_k e_\alpha r_{\alpha l}}{\omega_{\alpha l} - \omega_{kl}} + \frac{e_l e_\alpha r_{k\alpha}}{\omega_{k\alpha} - \omega_{kl}} \right] \right\}, \qquad (20)$$

where

$$\left.\begin{aligned} F_{\alpha\alpha}^{(\pm)} &= F_{\alpha\alpha} \pm \Phi_{\alpha l} \lambda_{\alpha k}, \\ (r/r)\, \Phi_{kl}(r) &= (k \mid 1/\mid r - r' \mid \mid l)\, (k \mid r \mid l), \\ (r/r)\, F_{\alpha l}(r) &= (l \mid r'/\mid r - r' \mid \mid \alpha), \\ (r/r)\, Q_{\alpha l}(r) &= (l \mid (1/\mid r - r' \mid)\, \varphi \mid \alpha). \end{aligned}\right\} \qquad (21)$$

If we take the correction term G into consideration, the expression for the oscillator strength in a one-electron transition in atoms can be written in the form:

$$f_{kl} = A_{kl} \omega_{kl} K_{kl}^2 \mid r_{kl} + G_{kl} \mid^2, \qquad (22)$$

where A_k is the ordinary constant for the given transition and K_{kl} is the constant representing the effect of the other electrons on the transition $k \to l$ in the conventional self-consistent field theory.[8] The computation of oscillator strengths from Eq. (22) with the use of Eqs. (20) and (21) for G_{kl} presents no special difficulties.

In conclusion, we would like to express our gratitude to M. G. Veselov and Yu. E. Perlin for their comments during discussions and also to A. V. Ablov for his interest in this work.

Note added in proof: Numerical calculations show that the simplification of Eq. (17) with the help of the relation (19) used in solving the example of optical dipole transitions in atoms is not always justified. Equation (20), which is derived on the basis of this simplification, should therefore be used with caution.

REFERENCES

1. V. A. Fock, Trudy Gosudarst. Opt. Inst. 5, 51 (1931); Z. Physik 61, 126 (1930).
2. A. Dolgarno, Proc. Roy. Soc. A251, 282 (1959).
3. V. A. Fock, Zhur. Eksptl. i Theoret. Fiz. 10, 961 (1940).
4. P. Dirac, "Osnovy Kvantovoi Mekhaniki." Izd. Inostrannoi Lit., Moscow, Leningrad, 1932. "The Principles of Quantum Mechanics," 1st ed., Oxford Univ. Press, London 1930.
5. P. Löwdin, Phys. Rev. 97, 1474 (1955).
6. A. Gold and R. Knox, Phys. Rev. 113, 834 (1959).
7. M. G. Veselov, Zhur. Eksptl. i Theoret. Fiz. 19, 959 (1949).
8. I. B. Bersuker, Kand. diss., Leningrad. Gosudarst. Univ., 1957; Izvest. Akad. Nauk SSSR, Ser. Fiz. 22, 749 (1958).
9. M. G. Veselov and I. B. Bersuker, Izvest. Akad. Nauk SSSR, Ser. Fiz. 22, 662 (1958).

THE ISOTOPE EFFECT IN THE SPECTRUM OF THORIUM

E. A. Vernyi and V. N. Egorov

Received 7 March 1960

The isotope effect was studied in the spectra of Th^{232} and Th^{229}. An isotopic shift of the levels was found, and the even-odd effect was computed. The deformation of the Th^{229} nucleus was evaluated.

INTRODUCTION

The isotope effect in the spectrum of thorium for Th^{232} and Th^{230} has been studied in detail by Stukenbroeker and McNally.[1] The spectrum was excited in an ac arc between copper electrodes. A diffraction grating spectrograph was used. The spectrum was recorded in the first, second, and third orders at linear dispersions of 1.2, 0.6, and 0.4 A/mm respectively. An isotopic shift was detected for 250 lines. In all cases the positive isotopic effect was observed, i.e., the Th^{230} line was shifted to the blue. A calculation of the relative isotopic shifts of levels showed that the isotopic effect in Th II is about 1.5 times greater than in Th I.

A study of the isotopic effect of other isotopes of thorium appears to be of great importance. As it has been previously communicated,[2] we have already investigated the isotope Th^{229}. The results of the investigation of this effect are presented below in detail.

EXPERIMENTAL PART

A 1:1 mixture of Th^{229} and Th^{232} was used for the production of the spectra. The total amount of Th^{229} consumed in the experiments was about 70 μg. The spectra were excited in an ac arc at 4-6 amp. A thorium chloride solution was evaporated on the end of a carbon electrode having a diameter of 4 mm. The material was deposited on the electrode in a thin layer by Zil'bershtein's method.[3] A 30 μg thorium sample produced a well-developed spectrum. Since the Th^{229} isotope shows strong α-activity (half-life 7340 years), the evaporation of the thorium solution and the excitation of the spectrum were carried out in special chambers. In order to suppress the cyanogen bands, the excitation of the spectrum for the exposure in the 2600-4400 A region was performed in a carbon dioxide atmosphere.

The spectrum of the sample was photographed several times at an exposure of 25 sec, until the thorium lines totally disappeared. In this way, it was possible to obtain spectra of various intensities and to measure the isotopic shifts of both weak and strong lines. For recording the spectra, a two-meter spectrograph with a diffraction grating in a Paschen mounting was used. The linear dispersion in the first order was 3.4 A/mm. Individual lines were studied with an autocollimating diffraction spectrograph (DAS) in the 6th and 7th orders. The linear dispersion of this instrument in the 4000-4400 A region was 0.9-0.8 A/mm.

EVALUATION OF RESULTS

a. Isotopic Shifts of Lines

The isotopic shift was determined for 247 thorium lines, of which 178 lines belonged to Th II, 20 to Th I, and 49 were unclassified. Data for the lines of the first and second spectra of thorium are presented in tables 1, 2A, and 2B (the classification of lines is given in refs. 4-8). From the tables, it is seen that on the average, $\Delta\sigma$ of Th II is about 1.2 times greater than $\Delta\sigma$ of Th I. It is surprising to note that none of the thorium lines showed a negative isotopic effect, whereas the spectra of other actinides[9-13] show both positive and negative shifts. This phenomenon can be explained by investigating the types of transition of the observed lines. For example, all Th II lines for which the isotopic effect was observed are produced by the following transitions:[4]

$$6d7s7p \rightarrow 6d7s^2,$$
$$6d^27p \rightarrow 6d^27s,$$
$$5f7s7p \rightarrow 5f7s^2,$$
$$5f6d7p \rightarrow 5f6d7s.$$

It is easy to see that in each case, the lower level belongs to an electron configuration which always has one s-electron more than the configuration of the upper level. Since the s-electrons make the greatest contribution to the isotopic effect, it is obvious that the probability of observing a negative isotopic effect in Th II is very small.

Table 1. Isotopic Shifts of Th I Lines

λ (A)	$\Delta\sigma$ (232–229) (cm^{-1})	λ (A)	$\Delta\sigma$ (232–229) (cm^{-1})
4043.40	0.83	3486.52	0.75
4030.96	0.81	3469.34	0.80
4012.50	0.84	3442.58	1.00
3873.92	0.83	3398.55	0.70
3719.44	0.80	3397.52	0.92
2692.57	0.76	3348.77	0.71
3642.25	0.80	3333.13	0.82
3635.94	0.68	3330.48	0.84
3634.58	0.86	3304.24	0.74
3598.12	0.76	3301.85	0.85

Table 2A. Isotopic Shift of Th II (Group A) Lines

λ (A)	$\Delta\sigma$ (232–229) (cm^{-1})	λ (A)	$\Delta\sigma$ (232–229) (cm^{-1})	λ (A)	$\Delta\sigma$ (232–229) (cm^{-1})	λ (A)	$\Delta\sigma$ (232–229) (cm^{-1})
5989.04	0.97	4034.26	0.91	3499.99	0.79	3119.48	0.84
5707.09	0.96	4019.14	0.64	3469.93	0.72	3097.27	1.05
5639.73	0.85	3937.99	0.51	3463.72	0.86	3078.93	0.97
5247.65	1.11	3929.87	1.13	3450.95	0.87	3068.99	1.01
4850.45	1.10	3904.09	0.88	3435.98	1.13	3019.73	0.94
4832.90	1.09	3823.59	0.74	3389.65	0.93	3002.39	1.04
4752.41	1.08	3754.90	0.88	3351.23	0.71	2972.22	0.92
4281.07	0.45	3741.19	0.76	3337.87	0.68	2971.44	1.21
4277 2	0.88	3632.83	0.79	3334.61	0.84	2965.14	1.09
4179.72	0.99	3625.53	1.03	3324.75	0.84	2965.05	0.97
4123.57	0.78	3615.13	0.79	3220.35	1.23	2879.21	1.02
4094.75	0.84	3610.79	1.20	3174.17	1.17	2870.41	0.97
4086.52	1.14	3609.45	0.74	3169.28	1.06	2747.16	0.97
4036.57	0.88	3539.59	0.76	3154.26	0.91	—	—

These considerations can be used to improve the assignments of the configurations of upper levels when the classification of the lower levels is reliably established. This is clearly demonstrated in the uranium spectrum where both positive and negative shifts are present. Table 3 presents the magnitudes of the mean

Table 2B. Isotopic Shift of Th II (Group B) Lines

λ (A)	Δν (232−229) (cm⁻¹)	λ (A)	Δν (232−229) (cm⁻¹)	λ (A)	Δν (232−229) (cm⁻¹)
4391.11	0.60	3821.43	0.52	3348.56	0.75
4381.86	0.44	3752.57	0.45	3326.47	1.04
4292.04	0.50	3747.55	0.55	3256.27	0.73
4278.81	0.56	3740.85	0.83	3255.51	0.95
4273.36	0.60	3734.60	1.14	3226.12	0.84
4250.34	0.85	3730.75	0.81	3221.29	0.75
4239.46	0.65	3723.29	0.77	3203.28	0.92
4238.89*	0.29	3718.17	0.73	3198.97	1.26
4178.06	0.57	3711.31	0.89	3184.95	1.12
4163.65	0.43	3708.77	0.89	3156.40	0.84
4159.67	0.61	3690.49	0.68	3154.73	0.91
4156.52	0.63	3679.71	0.75	3107.03	0.84
4156.24	0.70	3659.51	0.85	3096.43	0.74
4149.99	0.54	3656.20	0.65	3063.03	0.79
4131.43	0.93	3649.25	0.78	3061.70	1.01
4116.72	0.37	3647.65	0.86	3048.10	1.30
4108.43	0.75	3639.45	0.76	3015.57	0.91
4104.39	0.98	3625.94	0.54	3034.07	1.10
4095.04	0.70	3614.01	0.55	3031.70	1.31
4092.28	0.73	3609.23	0.76	3019.42	1.40
4089.21	0.52	3603.21	0.83	3006.93	0.90
4083.41	0.69	3593.86	0.71	3001.26	1.28
4026.16	0.75	3575.32	0.67	2989.23	1.27
4007.03	0.55	3557.46	0.42	2974.01	1.06
4006.39	0.70	3539.31	0.99	2968.89	1.05
4005.55	0.53	3537.16	0.70	2957.59	1.33
4003.11	0.68	3516.36	1.16	2942.63	1.33
3997.86	0.71	3511.55	1.09	2924.28	1.20
3997.45	0.59	3498.99	0.81	2919.44	1.16
3996.07	0.50	3497.85	0.76	2917.39	1.18
3988.02	0.78	3485.22	1.25	2908.36	1.42
3981.11	0.76	3468.22	0.83	2884.29	1.17
3976.42	0.72	3467.93	0.79	2879.53	1.31
3951.52	0.72	3465.77	0.85	2868.68	1.31
3945.83	0.95	3445.38	0.78	2822.04	1.24
3937.04	0.85	3441.37	0.797	2797.74	1.20
3932.23	0.67	3437.03	1.16	2783.05	1.24
3927.43	0.96	3429.90	1.32	2765.13	1.35
3927.18	0.90	3385.54	1.10	2737.42	1.33
3905.19	0.87	3374.58	0.96		
3884.83	0.49	3367.62	0.86		
3e25.04	0 67	3363.11	1.09		

*In ref. 5 this line is attributed to ThI.

isotopic shifts for permitted types of transitions which occur in the atom of uranium,[9] where the classification of lower levels is reliably known, but that of the upper levels only preliminarily established.[14,15] It is seen from the table that the sign and magnitude of the isotopic shift indicate the most probable type of configuration for the upper level. From the magnitude of the isotopic shift, it is possible to determine with a certain reliability whether the unclassified lines belong to the spectrum of the neutral or the ionized atom, and also to establish the lower electron configurations of the corresponding transitions.

Table 3. Mean Isotopic Shift of Uranium Lines Which Belong to Definite Types of Transitions

State of atom and electron configuration of upper and lower levels	Δν ($U^{238} - U^{235}$) (cm⁻¹)
UI $^*\begin{matrix}5f^36d7s7p\\5f^37s7p\end{matrix}\Big\}\rightarrow 5f^36d7s^2$	+0.40
UI $\rightarrow 5f^36d^27s$	+0.44
UII $^*\begin{matrix}5f^37s7p\\5f^36d7s\end{matrix}\Big\}\rightarrow 5f^37s^2$	+0.84
UII $^*\begin{matrix}5f^37s7p\\5f^36d7p\end{matrix}\Big\}\rightarrow 5f^36d7s$	+0.51
UII $\rightarrow 5f^36d7p$	−0.51
UII $\rightarrow 5f^37p$	+0.76
UII $\rightarrow 5f^37p$	−0.43

The most probable configuration is denoted by an asterisk.

In Table 4, the observed values of maximum and minimum isotopic shifts for various low configurations of Th I and Th II are presented. The most probable partial classification of some thorium lines (Table 5) was based on these data.

b. Isotopic Shifts of Levels

From the theoretical point of view, the isotopic shifts of levels are much more important than the line

Table 4. Isotopic Shifts of Thorium Lines Which Arise from Transitions to Levels of Various Electron Configurations

State of atom and configuration of lower level	Δν ($Th^{232} - Th^{229}$) (cm⁻¹)	
	Maximum	Minimum
ThI $6d^27s^2$	0.92	0.60
ThII $6d^27s^2$	1.23	0.84
ThII $6d^37s$	1.09	0.51
ThII $5f7s^2$	1.42	0.75
ThII $5f6d^27s$	1.01	0.43

Table 5. Isotopic Shifts of Unclassified Lines of Thorium

λ (A)	Possible state of atom and configuration of lower level.	Δν (232−229) (cm⁻¹)	λ (A)	Possible state of atom and configuration of lower level	Δν (232−229) (cm⁻¹)
4270.33	—	0.75	3362.19	—	0.81
4195.83	I or II d^27s or fds	0.73	3360.38	—	0.80
4132.75	I or II d^27s or fds	0.80	3348.96	II	0.83
4122.97	I or II d^27s or fds	0.61	3303.48	—	0.82
4110.87	I or II d^27s or fds	0.67	3295.00	—	0.78
400..07	II fds	0.50	3290.13	I or II d^27s or fds	0.77
3974.23	I or II d^27s or fds	0.80	3273.88	I or II d^27s or fds	0.71
3966.97	—	0.87	3264.13	—	0.83
3963.47	I or II d^27s or fds	0.53	3250.62	I or II d^27s or fds	0.86
3895.43	I or II d^26s or fds	0.56	3248.80	—	0.91
3712.51	I or II d^27s or fds	0.64	3225.62	—	0 90
3688.76	I or II d^27s or fds	0.89	3210.27	—	0.75
3687.86	I or II d^27s or fds	0.69	3198.18	—	0.90
3652.17	—	0.76	3179.05	II	0.96
3648.42	II	1.02	3136.22	II ds^2 or fs^2	1.10
3641.84	I or II d^27s or fds	0.56	3125.46	I или II d^27s или fds	0.89
3641.11	—	0.96	3125.16	II ds^2 or φp^3	1.15
3503.62	I or II d^27s or fds	0.59	3105.05	—	0.92
3501.46	—	0.98	3094.74	II	1.01
3497.26	I or II d^27s or fds	0.74	3069.26	—	0.90
3477.71	—	0.81	3067.73	—	0 86
3434.76	I or II d^27s or fds	0.68	2983.82	—	0.91
3429.00	—	0.91	2921.61	II fs^2	1.36
3427.99	II	0.93	2731.58	II ds^2 or fs^2	1.10
3413.02	II	0.98			

shifts. The absolute values of the shifts of levels can be reliably determined only when the shifts are known for several lines of the same spectral series. By extrapolating these values to the series limit, the values sought can be determined.

The isotopic shifts of levels are frequently measured relative to the levels of configurations with $p_{3/2}$, $d_{3/2}$, $s_{1/2}$, and $f_{7/2}$, $s_{1/2}$ electrons, since the levels of these configurations are usually characterized by insignificant shifts.[16,17] Stukenbroeker and McNally, in determining the isotopic shifts of levels, assigned a value of zero to the shifts for the following levels: 28676 of Th I; 20686, $fd^2\ ^4G^0_{3/2}$, and $fd^2\ ^4G^0_{1/2}$ of Th II (Group A); and 38728 of Th II (Group B).

A comparison of isotope effects for Th^{230} and Th^{229} showed that it seems to be impossible to calculate the isotopic shifts of levels in relation to some chosen level because a large error can be introduced. Even the levels of the fd^2 configuration can have an appreciable isotopic shift. Therefore, we find it more correct to calculate the isotopic shifts of levels (when an isotope effect is observed for a large number of lines) by a successive approximation method. The calculation is carried out as follows: The first approximation to the value of the isotopic shift of each lower level is assumed to be the largest shift displayed by the lines arising from the transition to that level. Then, the mean isotopic shifts of the upper levels are determined. New values of the shifts of lower levels are then calculated on the basis of the mean values of the shifts of the upper levels. This procedure is applied two or three times. At the same time, the degree of reliability of the measurement of the isotopic shifts for each line is considered. It is necessary to note that this method of calculating the isotopic shifts of levels assumes that all levels exhibit a positive isotopic effect; i.e., that the level of a lighter isotope is lower than the level of a heavier isotope. This is reasonable, because

a negative isotopic shift of levels is rarely found[16,17] in the heavy elements.

Individual cases of negative shifts of levels or incorrectly (for unknown reasons) determined isotopic shifts of lines can be easily detected by the above described method from the sharp divergence of the shifts obtained for different lines having a level in common.

The values of the isotopic shifts of the Th II levels are given in Tables 6A and 6B. The error in the determination of the absolute values of level shifts apparently should not exceed 0.1 cm^{-1}. It is necessary to remark that the computation of isotopic shifts of Th II levels (Group B) with respect to the level 38728, as performed in ref. 1, must be considered wrong because it was not confirmed by measurements of the isotopic shifts in the spectrum of Th^{229}. The reversal of positions of levels of Th^{230} and Th^{229} is not probable. No similar cases of inversion have been observed in any spectrum of a heavy element.

The isotopic effect in Th I was detected for a very small number of lines. The isotopic shifts of levels were therefore referred to the level 28676 (Table 7), as in ref. 1. From Tables 6 and 7 it is seen that the isotopic effect in Th II is approximately 1.5 times greater than that in Th I. On the average, the isotopic effect in the thorium spectrum is slightly greater than in the spectra of other heavy elements.[4,9-13,16,18] This qualitatively confirms the presence of a second maximum in the curve showing the isotopic effect as a function of the number of neutrons in the nucleus.[17,19]

Table 6A. Relative Shifts of Th II (Group A) Levels

Electron configuration	Level	Numerical value of level	ΔT_1 (233–229) (cm^{-1})	ΔT_2 (233–230) (cm^{-1})	$\frac{\Delta T_1 - \Delta T_2}{\frac{1}{2}\Delta T_2}$
ds^2	$a^2D_{1/2}$	0.00	1.17	0.71	1.30
	$a^2D_{3/2}$	4113.36	1.23	0.72	1.42
sd^2	$a^4F_{1/2}$	1859.94	1.17	0.70	1.34
	$a^4F_{3/2}$	1521.91	1.07	0.80	1.57
	$a^4F_{5/2}$	4146.57	1.09	0.82	1.52
sd_2	$a^4F_{7/2}$	6213.55	1.08	0.80	1.50
	$a^4P_{1/2}$	8018.19	0.94	—	—
	$a^4P_{3/2}$	9061.08	0.94	0.80	1.13
	$a^2P_{1/2}$	7828.61	0.67	—	—
fd^2	$^4F^*_{1/2}$	18214.47	0.20	—	—
		19050.87	0.06	—	—
fd^2	$^4F^*_{3/2}$	19248.32	0.22	—	—
		20496.23	0.08	—0.05	—
		23372.57	0.29	0.16	—
fd^2	$^4G^*_{5/2}$	23730.81	0.12	—	—
		24414.60	0.33	0.24	—
		24463.86	0.03	0.00	—
fd^2	$^4G^*_{7/2}$	24757.59	0.00	0.00	—
		24873.99	0.53	0.30	—
		25440.26	0.04	0.01	—
$fd^{2?}$	$^4D^*_{1/2}$	26628.45	0.29	0.15	—
$fd^{2?}$	$^4D^*_{3/2}$	27249.56	0.00	0.00	—
		29095.46	0.04	0.00	—
		29720.42	0.25	0.17	—
		30994.30	0.17	—	—
dsp	$^4F^*_{1/2}$	31353.12	0.30	0.12	—
		31800.21	0.03	—	—
		31810.57	0.49	0.28	—
dsp	$^2D^*_{1/2}$	31928.77	0.53	0.31	—
		32933.45	0.10	—	—
		32957.41	0.37	0.28	—
		33215.78	0.20	0.06	—
dsp	$^2F^*_{5/2}$	33355.22	0.00	0.00	—
	$^4F^*_{3/2}$	35156.97	0.00	0.00	—
	$^4F^*_{5/2}$	36193.70	0.24	0.15	—
d^2p	$^4F^*_{1/2}$	36390.49	0.15	0.10	—
		36581.57	0.15	0.09	—
dsp	$^4F^*_{7/2}$	36583.83	0.36	0.28	—
d^2p	$^4G^*_{5/2}$	36687.99	0.22	0.17	—
		37757.29	0.02	—	—
d^2p	$^4G^*_{7/2}$	38764.81	0.26	0.15	—

Table 6B. Relative Shifts of Th II (Group B) Levels

Electron configuration	Level	Numerical value of level	ΔT_1 (233–229) (cm^{-1})	ΔT_2 (233–230) (cm^{-1})	$\frac{\Delta T_1 - \Delta T_2}{\frac{1}{2}\Delta T_2}$
fs^2	$a^2F^*_{5/2}$	4490.29	1.45	0.84	1.45
	$a^2F^*_{7/2}$	8378.85	1.45	0.84	1.45
f	$a^4H^*_{7/2}$	6168.38	0.88	0.50	1.52
	$a^4H^*_{9/2}$	6700.19	0.89	0.49	1.53
	$a^4H^*_{11/2}$	10189.10	0.92	0.51	1.61
	$a^4H^*_{13/2}$	13406.51	0.85	0.50	1.40
	$a^4F^*_{3/2}$	6691.44	0.82	0.45	1.54
	$a^4F^*_{5/2}$	7331.51	0.84	0.48	1.50
	$a^4F^*_{7/2}$	9720.30	0.80	0.45	1.56
	$a^4F^*_{9/2}$	12488.34	0.89	0.53	1.36
	$a^4G^*_{5/2}$	9202.29	0.89	0.50	1.56
	$a^2G^*_{7/2}$	9238.04	0.93	0.51	1.65
fds	$a^4G^*_{5/2}$	9585.41	0.81	0.47	1.45
	$a^4G^*_{7/2}$	11116.61	0.81	0.49	1.31
	$a^4G^*_{9/2}$	13469.00	0.85	0.50	1.40
	$a^4G^*_{11/2}$	15349.93	0.90	0.46	1.91
	$a^2H^*_{9/2}$	10572.09	0.71	0.42	1.39
	$a^2H^*_{11/2}$	14484.37	0.78	0.44	1.55
	$a^2D^*_{3/2}$	11576.43	0.93	0.49	1.80
	$a^2D^*_{5/2}$	12472.18	0.83	—	—
	$b^2F^*_{5/2}$	10673.16	0.78	0.49	1.18
	$b^2F^*_{7/2}$	13818.37	0.67?	0.42	1.18
fsp	$^4G_{5/2}$	27257.19	0.85	0.45	—
fsp?	$^4F_{7/2}$	28011.24	0.80	0.34	—
fsp	$^4F_{3/2}$	28823.68	0.70	0.44	—
		29515.19	0.41	0.17	—
		30452.77	0.51	—	—
		3125o.33	0.30	0.08	—
		31754.25	0.89	—	—
		31773.89	0.85	0.46	—
		32576.77	0.52	—	—
		32736.20	0.46	0.23	—
		33209.43	0.70	0.32	—
		33637.26	0.15	0.08	—
		33730.94	0.37	—	—
		34019.27	0.35	0.19	—
		34174.57	0.59	—	—
		34270.29	0.07	—	—
	$^4F_{5/2}$	34543.63	0.30	—	—
		34661.76	0.24	0.09	—
		34726.60	0.09	0.06	—
		35525.19	0.00	0.00	—
		35545.64	0.04	0.03	—
		35741.36	0.00	0.00	—
fsp	$^2G_{9/2}$	35878.89	0.33	0.13	—
		36065.76	0.20	0.12	—
		36125.43	0.22	0.10	—
		36436.29	0.27	0.11	—
		37063.38	0.20	0.12	—
		37277.39	0.15	0.06	—
		37485.48	0.17	0.05	—
		37787.90	0.15	0.06	—
		37840.91	0.02	0.03	—
		37945.09	0.18	0.14	—
		38105.11	0.37	0.19	—
		38165.40	0.40	0.21	—
		3s291.81	0.12	0.08	—
		38389.43	0.02	0.04	—
		38518.10	0.09	0.00	—
		38724.71	0.29	—0.11	—
		38757.50	0.27	0.12	—
		38s36.24	0.12	0.05	—
fsp	$^4G_{9/2}$	38982.97	0.04	0.06	—
		39867.21	0.00	0.00	—
		39894.75	0.18	0.13	—
		39150.71	0.28	0.16	—
		3.936.90	0.59	—	—
		39458.36	0.03	0.02	—

(continued on next page)

Table 6. (Continued)

Electron configuration	Level	Numerical value of level	ΔT_1 (232—230) (cm^{-1})	ΔT_2 (232—230) (cm^{-1})	$\frac{\Delta T_1 - \Delta T_2}{\frac{1}{2}\Delta T_2}$
fsp	$^2G_{9/2}$	39552.29	0.29	0.11	—
		39893.47	0.03	0.06	—
		39930.14	0.20	0.08	—
		40222.94	0.25	—	—
		40411.52	0.21	0.14	—
		40574.91	0.10	0.08	—
		40644.34	0.10	0.15	—
		40724.89	0.00	0.07	—
		41225.62	0.17	0.15	—
		41326.38	0.35	0.19	—
		41488.20	0.05	0.102	—
		41668.48	0.17	0.03	—
		42146.57	0.09	0.01	—
		42200.27	0.13	0.01	—
		42352.18	0.12	0.04	—
		42518.91	0.25	0.14	—
		43014.187	0.01	—	—
		43096.56	0.14	—	—
		43227.90	0.14	—	—
		43403.94	0.21	0.16	—
		44177.33	0.06	0.00	—
		45126.29	0.10	0.02	—
		45735.11	0.09	0.10	—

c. Even-Odd Effect in the Spectrum of Thorium and the Deformation of the Thorium Nucleus

The even-odd effect permits the evaluation of the ratio of the coefficients of the deformation of the nuclei of the even and odd isotopes of thorium. It is assumed that the even-odd shift is mainly caused by a sudden change in the deformation of the nucleus when a neutron is added to the nucleus.

From Tables 6 and 7 one can see that even-odd effects for Th I and Th II are approximately equal, and that their mean value is 1.49.

The theory of the deformation of the nucleus[17,19] furnishes the following approximate formula for the ratio of the isotopic shift of level caused only by the deformation to the isotopic shift caused by the volume effect.

$$\frac{S_\delta}{S_v} = \frac{3}{10}(2\gamma+3)A\left[\frac{\delta(\alpha^2)}{\delta A}\right]_\beta. \qquad (1)$$

where α is the coefficient of deformation, A is the atomic weight, and $\gamma = (1 - Z^2\alpha^2)^{1/2}$ (in this case $\alpha = e^2/\hbar c$ is the fine structure constant).

Using formula (1), the expression for the total isotopic shift of a level is

$$\Delta T = S_a + S_v - 0.3S_v = S_v\left[0.7 + \frac{3}{10}(2\gamma+3)A\frac{\delta(\alpha^2)}{\delta A}\right], \qquad (2)$$

where 0.3 S_v is the fraction of the isotopic shift caused by all effects except the volume and deformation effects. In the case of an odd-even shift, it is necessary to consider the polarization effect of the nucleus caused by atomic electrons. The direction of the shift of this effect is opposite to the shift due to the volume effect; in magnitude, it does not exceed 20% of the even-odd shift.

Table 7. Relative Shifts of Th I Levels

Electron configuration	Level	Numerical value of level	ΔT_1 (232—230) (cm^{-1})	ΔT_2 (232—230) (cm^{-1})	$\frac{\Delta T_1 - \Delta T_2}{\frac{1}{2}\Delta T_2}$
d^2s^2	$^3F_2$	0.00	0.84	0.48	1.50
	$^3F_3$	2969.26	0.83	0.48	1.46
		26878.16	0.24	0.11	—
		27447.78*	0.04	−0.02	—
		27670.95	0.02	0.09	—
		27784.37	0.04	0.01	—
		29676.29	0.00	0.00	—
		29853.14	0.13	0.00	—
		30017.10	0.00	0.05	—
		30255.45	0.10	0.03	—

The level denoted by an asterisk is taken from ref. 1; the values of the remaining levels are taken from ref. 3.

From formula (2) we obtain

$$\frac{\Delta T\,(229—230)}{\frac{1}{2}\Delta T\,(230—232)} = \frac{0.7 + \frac{3}{10}(2\gamma+3)A\delta_1(\alpha^2)}{0.7 + \frac{3}{10}(2\gamma+3)A\frac{\delta_2(\alpha^2)}{2}}, \qquad (3)$$

where $\delta_1(\alpha^2) = \alpha^2_{230} - \alpha^2_{229}$, $\delta_2(\alpha^2) = \alpha^2_{232} - \alpha^2_{230}$, and $S_v(229 - 230) = 1/2\, S_v(230 - 232)$. According to our data, and considering the correction for the polarization effect, the left-hand side of Eq. (3) is equal to 1.39.

From this we obtain

$$\delta_1(\alpha^2) = 0.8 \cdot 10^{-3} + 0.7 \cdot \delta_2(\alpha^2). \qquad (4)$$

Let us estimate the value of $\delta_2(\alpha^2)$. The theory of the generalized model of the nucleus[21,22] enables us to relate the coefficient of deformation of the nucleus to its permanent quadrupole moment by means of the formula

$$Q_0 = \frac{3}{(5\pi)^{\frac{1}{2}}} ZR_0^2\alpha, \qquad (5)$$

where $R_0 = 1.2 \times 10^{-13}\, A^{1/3}$ cm.

From the lifetime of the first excited state of the Th^{232} nucleus, the quadrupole moment[21,22] determined from the deformation of the nucleus was found to be $Q_0 = 9 \times 10^{-24}$ cm^2. Using formula (5), we obtain $\alpha_{232} = 0.238$.

To evaluate α_{230}, we used the semiempirical formula $\alpha = (1/K)10.4 \times A^{-5/6}\, E_1^{-1/3}$, where E_1 is the energy of the first excited rotational level of the nucleus.[19,21] The coefficient K is found by comparing α_{232} as found by this formula with the value determined from the lifetime of the first excited rotational level of the nucleus. For thorium, K = 2.09. Knowing E_1 for Th^{230}, we find $\alpha_{230} = 0.232$. From this, $\delta_2(\alpha^2) = 2.8 \times 10^{-3}$. Then from formula (4) we obtain

$$\delta_1(\alpha^2) \approx 2.7 \cdot 10^{-3}.$$

It is necessary to emphasize that it is the ratio of $\delta_1(\alpha^2)$ to $\delta_2(\alpha^2)$ which is of interest, rather than the absolute values of the deformation coefficients obtained from the approximate formulas. From formula (4) it is seen that the change of $\delta\alpha(230 - 232)$ $(3 \times 10^{-3} - 3 \times 10^{-2})$ within reasonable limits satisfies the approximate equality $\delta_1(\alpha^2) \approx \delta_2(\alpha^2)$ and from this $\delta_1\alpha \approx \delta_2\alpha$. The last relationship shows that the change in the deformation between the even isotopes Th^{232} and Th^{230} (a difference of two mass units) is approximately the same as that between the isotopes Th^{229} and Th^{230} (a difference of one mass unit).

It is a pleasant duty to express our gratitude to V. K. Markov and M. F. Korinfska for the separation and purification of the Th^{229}, and to Yu. P. Dontsov for valuable advice given in evaluating the results of this work.

REFERENCES

1. G. L. Stukenbroeker and J. R. McNally, J. Opt. Soc. Am. **43**, 36 (1953).
2. E. A. Vernyi and V. N. Egorov, Opt. i Spektr. **6**, 262 (1959), Optics and Spectroscopy **6**, 170 (1959).
3. Kh. I. Zil'bershtein, Zhur. Tekh. Fiz. **25**, 1491 (1955).
4. J. R. McNally, J. Opt. Soc. Am. **35**, 390 (1945).
5. R. Zalubas, J. Research Natl. Bur. Standards **A63**, 275 (1959).
6. W. F. Meggers and R. W. Stanley, J. Research Natl. Bur. Standards **61**, 95 (1958).
7. M. Fred, Astrophys. J. **87**, 176 (1938).
8. J. R. McNally, G. R. Harrison, and H. B. Park, J. Opt. Soc. Am. **32**, 334 (1942).
9. A. R. Striganov and L. A. Korostyleva, Zhur. Eksptl. i Teoret. Fiz. **29**, 393 (1955).

10. D. D. Smith, G. L. Stukenbroeker, and J. R. McNally, Phys. Rev. **84**, 383 (1951).
11. A. R. Striganov, L. A. Korostyleva, and Yu. P. Dontsov, Zhur. Eksptl. i Teoret. Fiz. **28**, 480 (1955).
12. J. G. Conway and M. Fred, J. Opt. Soc. Am. **43**, 216 (1953).
13. M. Fred and F. S. Tomkins, J. Opt. Soc. Am. **47**, 1076 (1957).
14. Van der Bosch, Physica **15**, 503 (1949).
15. M. A. El'yashevich, "Spektry redkikh zemel'" (Spectra of Rare Earths), Moscow, 1953.
16. Landolt-Börnstein Tabellen, Vol. 1, Pt. 5. Berlin, 1952.
17. A. R. Striganov and Yu. P. Dontsov, Uspekhi Fiz. Nauk **55**, 315 (1955).
18. T. E. Manning, C. E. Anderson, and W. W. Watson, Phys. Rev. **78**, 417 (1950).
19. L. Wilets, D. L. Hill, and K. W. Ford, Phys. Rev. **91**, 1488 (1953).
20. L. L. Gol'din, L. K. Peker, and G. I. Novikova, Uspekhi Fiz. Nauk **59**, 459 (1956).
21. K. Alder, A. Bohr, T. Huus, B. Mottelson, and A. Winter, Revs. Modern Phys. **28**, 432 (1956). (See also Symposium: Deformatsiya atomnykh yader (Deformation of Atomic Nuclei), Moscow, 1958.)
22. A. Bohr and B. Mottelson, Kgl. Danske Videnskab. Selskab., Mat.-fys Medd. **27**, 1 (1953). (See also Symposium: Problemy sovremennoi fiziki (Problems of Modern Physics) **9**, 34, 1955.)

f-NUMBER MEASUREMENTS FOR THE SPECTRAL LINES OF BARIUM

Yu. I. Ostrovskii and N. P. Penkin

Received 8 March 1960

The relative oscillator strengths of 65 lines of Ba I between 3889 and 7911 A were measured by the hook method of Rozhdestvenskii. The results of the experiment were compared with theory and with the results of other authors.

Our experimental setup was described in our previous articles.[1,2] The column of barium vapor was formed in a high temperature vacuum furnace, which was placed in the optical path of the interferometer. Barium was introduced into the furnace either as the metal, the nitrate, or the chloride. The exposures were taken at furnace temperatures between 2300 and 3040°K. Under these conditions, it was possible to photograph easily measured hooks for 65 lines of Ba I whose lower energy levels range from 0 to 1.67 ev. Figure 1 shows a sample photograph of the hooks in the 5970-6142 A region. The majority of the lines investigated (36) are not included in the Moore table[3] of multiplets; their assignments were

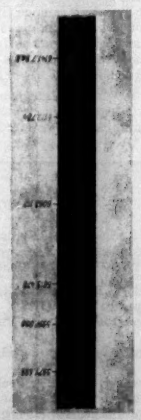

Fig. 1. Spectrogram of hooks in the 5970-6142 A region.

therefore established by using energy level tables.[4] The spectrograms were processed by the procedure usually used for the hook method. In the places where the lines were tightly packed, their mutual influence was calculated by the method suggested by Rozhdestvenskii and Penkin.[5]

The relative population of energy levels of the barium atom was calculated by the Boltzmann formula. At first there seemed to be a deviation from thermal equilibrium in the furnace. Our measured ratios of oscillator strengths of lines corresponding to transitions from normal and excited levels showed a dependence on temperature. In later measurements, it was discovered that this effect was due to distillation of the highly volatile barium from the center of the tube to its cooler ends. As a result, the column of normal atoms appeared to be longer than the column of atoms in the excited states. It appeared that the ratio of these lengths depends on both the temperature of the furnace and the burning time. This effect was carefully studied. To eliminate this effect, it appeared to be sufficient to provide a continuous supply of barium vapor into the graphite tube. This was accomplished by the setup shown in Fig. 2.

Fig. 2. Heating element. 1—Hollow graphite resistance with longitudinal cuts; 2—graphite casing; 3—cement (Al_2O_3); 4—barium.

A graphite casing 2 without electric contacts was fitted onto the tube having longitudinal slits. Barium was placed in the space between the tube and the casing. The junctions between the tube and the casing were sealed with an infusible Al_2O_3-base. When this device was heated, the barium vapor entered into the tube through the longitudinal slits. It is obvious that effects of this nature must be kept in mind when using King's furnace to measure the f-values of highly volatile elements.

The results of our measurements are given in Table 1. The first column gives the multiplet numbers. Arabic numerals are used to indicate these numbers according to the Moore tables,[3] and Roman numerals are used for multiplets which we established from spectral lines of barium using the energy level tables.[4] Subsequent columns give the following: the transitions from which the multiplets arise, the j numbers of the lower and higher levels, the energy of the lower level (in ev), the wavelengths of the lines (in A), and our measurements of f-numbers. We assumed the f-number of the resonance line of Ba I [$\lambda \pm 5535.484$ A ($6\,{}^1S_0$-$6\,{}^1P_1^o$)] to be 1000. According to Wessel's[5] measurements, the absolute value of the f-number for this line is 1.8. The same f-number was also measured by us and Shabanova,[7] and was found to be 1.6.* This allows an easy transition from relative to absolute values of the oscillator strengths of spectral lines contained in Table 1.

*In ref. 7, an arithmetical mistake occurred. Instead of $f_{5536} = 1.7$ it should be $f_{5536} = 1.6$.

Table 1

No. of multiplet	Transition	j – j	$E_{low.}$ (ev)	λ (A)	I	$I_{rad.}$	gf theor.	gf exp.
1	$6^1S - 6^1P^o$	0–1	0.000	7911.38	8.09	—	—	—
2	$6^1S - 6^1P^o$	0–1	0.000	5535.484	1000	—	—	—
I	$6^1S - 6p'^1D^o$	0–1	0.000	4132.43	8.22	—	—	—
II	$6^1S - 6p'^3P^o$	0–1	0.000	3889.32	6.56	—	—	—
5	$5^3D - 5d6p^3F^o$	3–4	1.19	7059.941	420	—	100	108.7
		2–3	1.14	7280.298	370	—	73.5	95.9
		1–2	1.12	7672.092	286	—	55.2	31.0
		3–3	1.19	7488.083	52.8	—	9.9	13.4
		2–2	1.14	7780.479	73.8	—	10.7	13.3
6	$5^3D - 5d6p^3D^o$	3–3	1.19	6498.759	343	—	100	93.2
		2–2	1.14	6527.312	236	—	56.3	45.8
		1–1	1.12	6595.326	295	—	37.3	34.2
		3–2	1.19	6693.842	85.5	—	13.3	23.2
		2–1	1.14	6675.271	88.6	—	12.8	17.2
		2–3	1.14	6341.682	98.5	—	11.9	19.1
		1–2	1.12	6450.854	71.6	—	11.9	8.3
7	$5^3D - 5d6p^3P^o$	3–2	1.19	6110.784	250	240	100	87.8
		2–1	1.14	6063.117	202	211	52.7	50.7
		1–0	1.12	6019.470	165	178	23.1	24.8
		2–2	1.14	5971.699	97.0	—	17.1	24.3
		1–1	1.12	5997.088	157	148	17.2	23.7
		1–2	1.12	5907.65	19.6	—	1.1	3.0
8	$5^3D - 4^3F^o$	3–4	1.19	3993.401	107	143	100	99.5
		2–3	1.14	3935.717	96.2	—	67.1	64.1
		1–2	1.12	3909.910	118	95.4	44.8	47.1
		3–3	1.18	3995.656	13.2	—	8.8	12.3
		2–2	1.14	3937.870	15.8	—	8.6	10.5
III	$5^3D - 6^1D^o$	1–2	1.12	7120.31	168	—	—	—
		3–2	1.19	7417.52	9.32	—	—	—
IV	$5^3D - 6^1F^o$	3–3	1.19	5805.89	12.7	—	—	—
V	$5^3D - 7p^3P^o$	2–2	1.14	4591.83	3.26	—	17.9	23.6
		1–0	1.12	4604.98	5.16	—	23.1	22.4
		2–1	1.14	4628.33	7.25	—	52.6	52.5
		3–2	1.19	4673.62	9.55	—	100	96.7
VI	$5^1D - 6p'^3P^o$	2–2	1.41	6965.71	35.2	—	—	—
VII	$5^1D - 6^1F^o$	2–3	1.41	6452.91	245	—	—	—
VIII	$5^1D - 6^1P^o$	2–1	1.41	5826.30	187	198	—	—
IX	$5^1D - 7^1P^o$	2–1	1.41	4726.45	87.6	94.8	—	—
X	$5^1D - 4^1F^o$	2–3	1.41	4283.11	156	—	—	—
9	$6^3P^o - 6^3D$	2–3	1.87	5777.622	652	556	100	95.7
		2–2	1.87	5800.229	151	—	18.0	22.1
10	$6^3P^o - 7^3S$	2–1	1.87	7905.751	223	—	100	89.6
		1–1	1.56	7392.411	257	—	52.4	61.9
		0–1	1.51	7195.235	354	—	16.6	28.5
XI	$6^3P^o - 8^3S$	0–1	1.51	4619.978	56.4	—	20.7	22.0
		1–1	1.56	4700.44	49.7	—	60	58.0
XII	$6^3P^o - 6^1D$	1–2	1.56	4402.55	214	—	—	—
		2–2	1.87	4579.67	354	—	—	—
XIII	$6^3P^o - 6p^1S$	1–2	1.56	4350.38	179	—	30.8	29.6
		0–1	1.51	4431.90	673	—	25.6	37.2
		1–1	1.56	4505.93	202	—	19.8	33.5
		2–2	1.87	4525.24	185	—	100	51.3
		1–0	1.56	4573.86	192	—	27.3	31.8
		2–1	1.87	4691.62	205	—	35.8	56.8
XIV	$6^3P^o - 6p^1S$	1–0	1.56	4599.75	66.9	—	—	—
XV	$6^3P^o - 6d'^3D$	1–2	1.56	4242.62	16.0	—	51.6	35.9
		2–3	1.87	4325.16	17.4	—	100	65.1
		2–2	1.87	4406.85	15.8	—	18.6	70.4
XVI	$6^3P^o - 7^3D$	2–3	1.87	4488.97	112	—	100	99.4
		2–2	1.87	4493.63	88.3	—	17.9	61.4
		0–1	1.51	4284.39	78.5	—	21.5	13.9
		1–1	1.56	4332.91	27.3	—	16.7	14.5
		1–2	1.56	4323.00	45.0	—	49.7	23.9
XVII	$6^3P^o - 6d^3G$	2–3	1.87	4467.11	17.5	—	—	—
XVIII	$6^3P^o - 9^3S$	2–1	1.87	4239.57	23.9	—	—	—

Our experimental error for lines corresponding to transitions from ground level does not exceed 1-3%. For the lines originating from excited levels, the errors increase to 10-15% because of temperature measurement errors. It should be mentioned that this is true only when the transitions from excited levels are compared with transitions from the ground level. When the ratios between the f-numbers of the lines corresponding to transitions between excited levels are compared, however, the errors vary from 1 to 5% for intense lines ($f > 150$ in our scale), and reach 10% for the remaining faint lines. This decrease of error is due to the fact that the splitting of lower levels of the indicated lines is small and the errors caused by the Boltzman factor are therefore insignificant.

The ratio of oscillator strengths f_{5536}/f_{7911} is 164 ± 5 according to our data (obtained from measurements of 10 exposures). The same ratio measured by Prokof'ev,[8] from two exposures, was found to be $f_{5536}/f_{7911} = 146$. King and Van Vleck[9] calculated this ratio by a quantum mechanical method and found it to be 169.

In the seventh column of Table 1, the relative f-numbers are given for 9 lines of Ba I, which Kruithof[10] measured by the line emission method. Comparison of his data with the results of our measurements shows that they are in satisfactory agreement.

In the last two columns of Table 1, the theoretical[11] and experimental values of gf products for lines of multiplets are given. Attention is called to the fact that the experimental and theoretical values of gf differ considerably for multiplets XV and XVI, and also for a number of lines of other multiplets (6693.8 and 6341.7 A of multiplet No. 6; 5907.6 A of multiplet No. 7; 4431.9 and 4523.2 A of multiplet XIII). This difference is not totally unexpected, because the existence of a large number of intense intercombination lines in the spectrum of barium indicates deviation from LS-coupling.

Adherence to the sum rule by the barium atom is illustrated in Table 2, which gives the sums of f-numbers of spectral lines which end on a given energy level (without intercombination lines). It is seen from this Table that for a majority of levels, Σf is close to 2. The value of Σf for the $5\,{}^1D_2$ and $6\,{}^3P_1$ levels is smaller than for other levels. This is possibly due to the fact that the f-numbers of lines not investigated in the present paper were not taken into account.

Table 2

Level	6^1S_0	5^1D_1	5^1D_2	5^1D_3	6^3P_0	6^3P_1	6^3P_2
Σf	1.77	1.79	2.06	2.06	1.08	1.86	1.55	2.68

REFERENCES

1. N. P. Penkin, Zhur. Eksptl. i Teoret. Fiz. 17, 355, 1114 (1947).
2. Yu. I. Ostrovskii, G. F. Parchevskii, and N. P. Penkin, Opt. i Spektr. 1, 821 (1956).
3. C. E. Moore, Contribs. Princeton Univ. Observ. No. 20 (1945).
4. C. E. Moore, "Atomic Energy Levels," Vol. 3. New York, 1958.
5. D. C. Rozhdestvenskii and N. P. Penkin, J. Phys. USSR 5, 319 (1941).
6. G. Wessel, Z. Physik 26, 440 (1949); 130, 100 (1951).
7. Yu. I. Ostrovskii, N. P. Penkin, and L. N. Shabanova, Doklady Akad. Nauk SSSR 120, 66 (1958).

8. V. K. Prokof'ev, Zhur. Eksptl. i Teoret. Fiz. 1, 111 (1931).
9. G. W. King and J. H. Van-Vleck, Phys. Rev. 56, 464 (1939).
10. A. Kruithof, Physica 10, 493 (1943).
11. E. Condon and G. Shortley, "Teoriya atomnykh spektrov." Izd. Inostrannoi Lit., Moscow, 1949. "Theory of Atomic Spectra." Cambridge Univ. Press, 1935.

THE SCATTERING OF SLOW ELECTRONS BY HELIUM ATOMS, WITH EXCITATION OF THE 2^3S- AND 2^1S-LEVELS*

*A paper presented to the Scientific Committee of the Physics Department of A. A. Zhdanov (Leningrad) University on 25 November 1954.

I. M. Matora

Received 9 March 1960

The method of integral equations[1] was used to calculate the elastic S-scattering of electrons and the excitation functions of the 2^3S- and 2^1S-states of helium by electrons with energies from 0 to 40 ev; results of the calculation are presented. It is shown that the results of the calculation are in quantitative agreement with the experimental data on the extrema of both excitation functions.[2] The calculated excitation function of the 2^1S-level has two maxima. The theoretical curve of the elastic scattering cross section also agrees satisfactorily with experiment;[3] moreover, the calculated limit for the elastic scattering cross section for very slow electrons corresponds more closely to the experimental values given in refs. 4-7 than the results obtained by other authors.[8]

INTRODUCTION

After the publication in 1954 of the results of work by Frish and Zapesochnyi on the excitation of mercury by slow electrons, a great deal of interest was stimulated by the possibility of a more accurate calculation of excitation functions for atoms with two electrons in the outer shell. By this time a new method of calculating electron scattering by atoms (called the method of integral equations) had been developed by Drukarev.[1] The present paper is the first concrete application of this method.

The calculation of electron scattering by helium was carried out over the same energy interval in which the above-mentioned authors[2] found dual maxima in the mercury excitation function. Only the spherically symmetrical part of the scattering was investigated; this part (at least in the neighborhood of the thresholds) apparently yields cross sections closely approximating the total cross section.

1. THE EQUATIONS

When formulated in accordance with Fok's theory,[10] the approximate Schrödinger coordinate wave function of the system "parahelium atom + electron" has the form

$$\psi(r_1 | r_2 r_3) = \sum_{\alpha=0}^{\alpha_{max}} [\chi_\alpha(r_3)\,\psi_\alpha(r_1 | r_2) - \chi_\alpha(r_2)\,\psi_\alpha(r_3 | r_1)] + \sum_{\beta=1}^{\beta_{max}} [\eta_\beta(r_3)\,\psi_\beta(|r_2 r_3) + \eta_\beta(r_2)\,\psi_\beta(|r_3 r_1) + 2\eta_\beta(r_1)\,\psi_\beta(|r_2 r_3)], \quad (1)$$

where χ_0, $\chi_{\alpha>0}$, and η_β describe elastically scattered (along with incident) electrons and electrons exciting singlet and triplet states respectively. They are regular at the origin and behave as follows at infinity:

$$\left.\begin{aligned} \chi_0 &\sim e^{ik_0 r} + a_0(\theta,\varphi)\frac{e^{ik_0 r}}{r}, \\ \chi_\alpha &\sim a_\alpha(\theta,\varphi)\frac{e^{ik_\alpha r}}{r}, \\ \eta_\beta &\sim a_\beta(\theta,\varphi)\frac{e^{ik_\beta r}}{r}. \end{aligned}\right\} \quad (2)$$

ψ_α and ψ_β are the wave functions of the helium atoms.

The problem of describing the S-scattering of electrons with the excitation of 2^3S- and 2^1S-states was reduced to a system of 3 integral equations by using a transformation of the Schrödinger equation:

$$\left.\begin{aligned} x(r) &= b_0 \sin k_0 r - \frac{2a_0}{k_0}\int_0^r \sin k_0 (r-s)\,\text{and}\,(s)\,ds \\ &\quad + \frac{1}{k_0}\int_0^r K_{00}(r,s)\,x(s)\,ds; \\ y(r) &= b_1 \sin k_1 r - \frac{\sqrt{2}\,a_1}{k_1}\int_0^r \sin k_1 (r-s)\,\text{and}\,(s)\,ds \\ &\quad + \frac{1}{k_1}\left\{\int_0^r K_{10}(r,s)\,x(s)\,ds + \int_0^r K_{11}(r,s)\,y(s)\,ds\right\}; \\ z(r) &= b_2 \sin k_2 r - \frac{\sqrt{2}\,a_2}{k_2}\int_0^r \sin k_2 (r-s)\,\text{and}\,(s)\,ds \\ &\quad + \frac{1}{k_2}\left\{\int_0^r K_{20}(r,s)\,x(s)\,ds + \int_0^r K_{22}(r,s)\,z(s)\,ds\right\}. \end{aligned}\right\} \quad (3)$$

x(r)/r, y(r)/r, and z(r)/r are the spherically symmetrical parts of the functions χ_0, χ_1, and η,

$$a_i = \int_0^\infty F_i(r)\,x(r)\,dr \quad (i = 0, 1, 3), \quad (4)$$

where $F_i(r)$ is a known function of discrete wave func-

tions. The complex constants δ_i are determined by giving the solution of the system a proper asymptotic form. The effects which states of the system corresponding to inelastic collisions exercise on elastic scattering are neglected in the derivation of (3). The interaction of the two inelastically scattered waves was also ignored.

Expression (3) was obtained by utilizing the symmetry properties of the atomic wave functions of helium, and by making substitutions which do not change the total function $\psi(r_1 | r_2 r_3)$; i.e., replacing the desired functions x by $x + bu$ and simultaneously substituting $y - 3cv + 3d \cdot w$ and $z + cu + d \cdot w$ for y and z. Here $u(r)/r$, $v(r)/r$, and $w(r)/r$ are the nonnormalized discrete one-electron functions of the helium atom.

The atomic wave functions for the 1^1S, 2^3S, and 2^1S states of helium were formulated from the one-electron analytical functions of Morse et al.[11] The single electron cases are given as

$$\psi_{1s} = \frac{u(r)}{2\sqrt{\pi}r}, \quad u(r) = 2\sqrt{\gamma^3}\, re^{-\gamma r}$$

for the 1^1S-level and

$$\left.\begin{aligned} \psi_{1s} &= \frac{v(r)}{2\sqrt{\pi}r}, \; v(r) = 2\sqrt{\alpha^3}\, re^{-\alpha r}, \\ \psi_{2s} &= \frac{w(r)}{2\sqrt{\pi}r}, \; w(r) = 2\sqrt{\frac{\mu^3}{3N}}\left(re^{-\mu r} - \frac{3A}{\mu}\, re^{-\beta r}\right) \end{aligned}\right| \begin{array}{l} \text{for } 2^3S\text{-} \\ \text{and } 2^1S\text{-levels} \end{array}$$

($\gamma = 1.69$; $\alpha = 2$; $\beta = 1.57$; $A = 0.5966$; $N = 0.8866$). All kernels K_{ik} are degenerate.

The solution of (3) is carried out analytically by iteration to completion in any approximation. The main advantage of the method of integral equations is that it makes it possible to obtain analytical expressions for the desired functions for all r, and not merely their asymptotic forms. This feature apparently can be used to obtain appropriate classes of variation functions associated with the calculation of electron scattering by variational methods.

2. SOLUTION OF THE EQUATIONS

A special feature of system (3) is that on finding the first approximation to the solution of each equation by iteration, we obtain only its formal solution, since the complex constants α_i and δ_i remain unknown. It is possible to obtain two equations for determining α and δ; one of these is formed by inserting the desired solutions into (4). In the solution of (3), it was not the zero approximation which we substituted in (4) (extra-integral terms of the first equation of (3) to the solution of x), but the formal solution $x^{(1)}$ in the first approximation. Thus, noting that the extra-integral terms of the first equation of (3) in a certain sense already have the nature of "distorted" waves, we see that the results of the calculations presented here were obtained by means of a two-stage integration of the "distorted" waves mentioned above.

Initially, the first of equations (3) was solved to a specified approximation at 15 points. Its solution at $k_0 = 0$ was found with the aid of the boundary transition. The cross section obtained for $k_0 = 0$ is in a proper location on the curve plotted against the 15 approximate values.

Graphs of the real and imaginary parts of $\alpha_0 = \alpha_{01} + i\alpha_{02}$ and $\delta_0 = \delta_{01} + i\delta_{02}$ versus energy between 10 and 40 ev are closely approximated by segments of straight lines; α_{01} and α_{02} increase linearly with increasing energy and δ_{01} and δ_{02} are practically constant. In this connection, the solutions of the second and third equations of (3) were found not only for the same electron energy values for which the first equation of (3) was solved directly, but also for several intermediate values for which the quantities α_{01}, α_{02}, δ_{01} and δ_{02} were found by linear interpolation.

3. CROSS SECTION FOR SCATTERING OF ELECTRONS BY HELIUM ATOMS

The differential cross section for electron scattering with excitation of the atom from a p state to a q state, per unit solid angle, in the direction (ϑ, φ) is given by the expression

$$d\sigma_{pq}(\vartheta, \varphi; k_p) = r^2 \frac{J_r(\vartheta, \varphi; k_p)}{J_p}, \tag{5}$$

where $J_p = k_p$ is the current density of incident electrons, and J_r is the radial component of the current density of scattered electrons at a large distance r from the atom. The quantity J has the sense of a quantum-mechanical current density vector in three-dimensional abstract space. Methods for determining this quantity are known for one-electron problems. For multielectron systems, J can be written in the form (using the results of ref. 10; the symbols are those of V. A. Fok)

$$J(r) = \frac{i}{2} \sum_{\sigma_1 \ldots \sigma_N} \nabla_{r'} \left\{ (x \mid r_1 \mid x') - \overline{(x \mid r_1 \mid x')} \right\}_{r'=r}$$

$$= \frac{i}{2} \left\{ m \int d\tau_2 \ldots d\tau_N \nabla_{r'} \left[\psi(r r_2 \ldots r_m \mid r_{m+1} \ldots r_N)\, \bar{\psi}(r' r_2 \ldots r_m \mid r_{m+1} \ldots r_N) \right. \right.$$

$$- \bar{\psi}(r r_2 \ldots r_m \mid r_{m+1} \ldots r_N)\, \psi(r' r_2 \ldots r_m \mid r_{m+1} \ldots r_N) \big]$$

$$+ (N - m) \int d\tau_2 \ldots d\tau_N \nabla_{r'}$$

$$\times \left[\psi(r_2 \ldots r_{m+1} \mid r_{m+2} \ldots r_N r') \bar{\psi}(r_2 \ldots r_{m+1} \mid r_{m+2} \ldots r_N r') \right.$$

$$\left. \left. - \bar{\psi}(r_2 \ldots r_{m+1} \mid r_{m+2} \ldots r_N r') \psi(r_2 \ldots r_{m+1} \mid r_{m+2} \ldots r_N r') \right] \right\}_{r'=r}. \tag{6}$$

When calculating J_r in (5), according to the Schrödinger coordinate wave function (1) one should replace the operator $\nabla_{r'}$ in (6) by $\partial/\partial r'$ and dispose of the asymptotic form χ_0 of the plane wave. Then, making use of the orthonormality of the helium eigenfunctions, we obtain for the system "parahelium atom + electron"

$$d\sigma(\vartheta, \varphi; k_0) = \sum_{\alpha} \frac{k_\alpha}{k_0} |a_\alpha|^2 + 3 \sum_{\beta} \frac{k_\beta}{k_0} |a_\beta|^2. \tag{7}$$

The number of terms in the sums must not violate the conservation of energy law. The effective cross section for elastic scattering for this case is

$$\sigma_0(k_0) = \int_0^{\pi} \int_0^{2\pi} |a_0(\vartheta, \varphi; k_0)|^2 \, d\omega.$$

The effective cross sections for excitation of the para state α and the ortho state β are determined by the expression

$$\sigma_\alpha(k_0) = \frac{k_\alpha}{k_0} \int_0^{\pi} \int_0^{2\pi} |a_\alpha(\vartheta, \varphi; k_0)|^2 \, d\omega; \quad \sigma_\beta(k_0) = \frac{k_\beta}{k_0} \int_0^{\pi} \int_0^{2\pi} |a_\beta(\vartheta, \varphi; k_0)|^2 \, d\omega;$$

In the case of S-scattering,

$$\left.\begin{aligned} \sigma_0(k_0) &= 4\pi |a_0|^2; \\ \sigma_\alpha(k_0) &= 4\pi \frac{k_\alpha}{k_0} |a_\alpha|^2; \\ \sigma_\beta(k_0) &= 12\pi \frac{k_\beta}{k_0} |a_\beta|^2. \end{aligned}\right| \tag{8}$$

4. RESULTS OF THE CALCULATIONS

After analytically solving the system (3) to the approximation described in Section 2, the cross sections for each value of k_0 were determined by simple arithmetic operations. The calculation of one point on the $\sigma_0(k_0)$ curve involves about 250 such operations and a single point for the excitation function—nearly 1000 operations. An automatic electrical computer was used in carrying out the computations. The results of the computations are shown in Figs. 1 and 2.

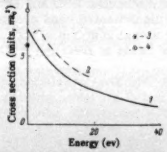

Fig. 1. The cross section for elastic S-scattering of electrons by helium. Curve 1—calculated by the integral equation method; curve 2—experimental, according to the data of ref. 3; curve 3—limit of the cross section, according to the data of ref. 4 (6.1 πa_0^2); curve 4—same as 3, according to the results of calculations in ref. 8 (8.6 πa_0^2).

As is seen from the data presented, both excitation functions exceed the experimental values of Maier-Leibnitz by a factor of 2-4 at the principal maximum (by principal maximum we mean the maximum closest to the excitation threshold). Part of this discrepancy can apparently be attributed to the fact that the electrons used in the experiment were not exactly monoenergetic, which always smooths out such sharp peaks to an appreciable degree. The extrema of both excitation functions show strikingly good agreement with experiment (within an accuracy of 0.2 ev). The calculated excitation function for the 2^1S level has two maxima. The first of these is located 0.2 ev and the second 7 ev from the excitation threshold. We note that the excitation functions for the n^1S levels of mercury that were obtained experimentally by Frish and Zapesochnyi,[9] and also the excitation functions for the n^1S levels of helium determined by Yakhontova[12] have a similar character. Excitation functions with two maxima were also obtained in ref. 12 for the helium triplet level 4^3S.

We point out in closing that the location of the extrema of the optical excitation functions determined by Yakhontova for the 4^1S and 5^1S levels of helium are also

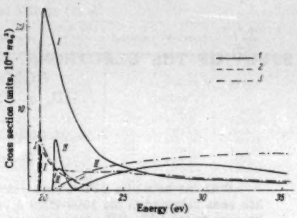

Fig. 2. Excitation functions for helium (I-2^3S-, II-2^1S-levels). Curve 1—calculated by the method of integral equations; curve 2—experimental, according to the data of ref. 2; curve 3—calculated by the method of ref. 13.

in quantitative agreement with the results of the calculation. The excitation functions calculated by Massey and Moiseiwitsch[13] (working simultaneously with us) are shown in Fig. 2 for comparison.

In conclusion I extend my thanks to Academician V. A. Fok; also to G. F. Drukarev and M. G. Veselov for their aid and continued interest in the work.

REFERENCES

1. G. F. Drukarev, Zhur. Eksptl. i Teoret. Fiz. **25**, 139 (1953).
2. H. Maier-Leibnitz, Z. Physik **95**, 499 (1935).
3. C. Ramsauer and R. Kollath, Ann. Phys. **12**, 837 (1932).
4. A. V. Phelps, O. T. Fundingsland, and S. C. Brown, Phys. Rev. **84**, 559 (1951).
5. C. Flinchtbauer, P. Schulz, and A. F. Brandt, Z. Physik **90**, 403 (1934).
6. Tsi-Zé and Shang-Yi, Phys. Rev. **51**, 567 (1937).
7. H. B. Wahlin, Phys. Rev. **37**, 260 (1931).
8. B. L. Moiseiwitsch, Proc. Roy. Soc. **A219**, 102 (1953).
9. S. E. Frish and I. P. Zapesochnyi, Doklady Akad. Nauk SSSR **95**, 971 (1954);
I. P. Zapesochnyi, Vestnik Leningrad. Univ. No. 11, 67 (1954).
10. V. A. Fok, Zhur. Eksptl. i Teoret. Fiz. 10, 961 (1940).
11. P. H. Morse, L. A. Young, and E. S. Gaurwitz, Phys. Rev. **48**, 948 (1935).
12. V. E. Yakhontova, Vestnik Leningrad. Univ. No. 10, 27 (1959).
13. H. S. W. Massey and B. L. Moiseiwitsch, Proc. Roy. Soc. **A227**, 38 (1954).

STUDY OF THE ELECTRONIC SPECTRA AND ISOTOPE EFFECT OF OXYGEN COMPOUNDS OF BORON
III. γ-Bands of the BO Molecule

A. A. Mal'tsev, D. I. Kataev, and V. M. Tatevskii

Received 22 December 1959

With the help of a DFS-5 spectrograph, the γ-band system of the molecules $B^{11}O$ and $B^{10}O$ has been obtained in the 1600-2090 A region. It has been shown that the indicated band system belongs to the $C^3\Pi - X^3\Sigma^+$ transition of the BO molecule, and the vibrational analysis of the spectrum has been refined. From the heads of the R_e branches of the bands of $B^{11}O$ and $B^{10}O$, the corresponding vibrational constants have been determined.

A preliminary rotational analysis of five bands has been carried out. The correlation of the electronic states of the BO molecule with the atomic states of B and O has been considered. In the 1360-2090 A region, the wavelengths of the atomic lines of boron and silicon have been more precisely determined.

INTRODUCTION

In the electronic spectrum of the BO molecule, two band systems are well known and thoroughly investigated: the α-bands (the $A^2\Pi - X^2\Sigma^+$ transition), located in the 3100-8500 A region,[1-4] and the β-bands (the $B^2\Sigma^+ - X^2\Sigma^+$ transition), lying in the 2100-3600 A region.[2,5-9] The combination band system (the $B^2\Sigma^+ - A^2\Pi$ transition), which has been observed only by Mulliken[2] in the 4500-5900 A region, is strongly overlapped by the α-bands and the so-called "fluctuation bands,"[1,10,11] which gives rise to some uncertainty in the existence of the combination band system, regardless of the good agreement of the results of the measurements with the calculated data. As for the fluctuation bands, which are located in the 4800-6200 A region and which Singh[12] assigned to the BO molecule (the $D^2\Sigma^+ - B^2\Sigma^+$ transition), this system belongs not to the BO molecule but to a polyatomic oxygen compound B_xO_y, as has been shown by investigation of the isotopic band shift[13] and also by a number of other factors.[13,14]

Aside from those listed above, there is in the BO spectrum one more band system, discovered by Chretien and Miescher[15,16] and located in the vacuum ultraviolet region (1650-1860 A). The bands of this system, which are shaded toward the long wavelength side, were observed as a contamination—during an investigation of the spectrum of BF in a discharge tube through which a mixture of He with BF_3 vapors was passing. From the most intense heads of 10 bands, the vibrational constants ($\omega_e' = 1300\ cm^{-1}$, $\omega_e'' = 1886\ cm^{-1}$, $\omega_e'x_e' = 15\ cm^{-1}$, $\omega_e''x_e'' \doteq 14\ cm^{-1}$) and the frequency of the electronic transition, $\nu_e = 56{,}670\ cm^{-1}$, were determined. The correspondence of the value $\omega_e'' = 1886\ cm^{-1}$ to the fundamental vibration frequency of the BO molecule ($\omega_e'' = 1885.4\ cm^{-1}$) indicated that this band system might belong to the BO molecule, the β-bands of which were fairly intense under the conditions used in taking the spectra. The rotational band structure was not resolved at a dispersion of 8.3 A/mm; however, the presence of four heads in the bands gave a basis for assigning them to a $^2\Pi - X^2\Sigma^+$ transition. The same bands appeared on introduction of BCl_3 and BBr_3 vapors into the discharge. However, the absence of bands belonging to the isotopic molecule $B^{10}O$ (natural boron contains 82% B^{11} and 18% B^{10}) did not permit Chretien to assign this band system unequivocally to the BO molecule.

Later, Chretien's work was repeated by Zelenskaya and Tunitskii[17] on an instrument of higher dispersion (a DFS-5 spectrograph, dispersion 2.7 A/mm), and the rotational band structure was resolved. Rotational analysis of two bands enabled them to draw the conclusion that Chretien's assignment of the spectrum to the BO molecule was erroneous: the bands cited were assigned to a $^1\Pi - ^1\Pi$ or $^3\Sigma - ^3\Sigma$ transition, while the value $B \approx 8.7\ cm^{-1}$ for the rotational constant indicated that the bands studied had to be assigned to some sort of hydride.

Continuing our investigations of the oxygen compounds of boron,[8,13] we have undertaken an attempt to resolve the contradictions concerning the assignment of the bands lying in the vacuum ultraviolet region; we analyzed the isotopic shifts of the band heads obtained when the boron was enriched in the isotope B^{10}, and we used as a spectral source a discharge tube with a hot hollow cathode in which boric anhydride was placed.

EXPERIMENTAL PART

The spectra were photographed with the aid of a DFS-5 vacuum spectrograph[18] with a concave diffraction grating of 1200 lines/mm and a radius of curvature of 3 meters. The theoretical resolving power of the grating amounts to 120,000, and the dispersion to 2.7 A/mm. To extend the working range of the spectrograph into the region above 2000 A, we increased the inclination of the grating with respect to the incident beam, which enabled us to obtain spectra up to 2090 A.

As in the investigation of the β-bands of BO,[8] we used as a radiation source a discharge tube with a hot hollow cathode, in which boric anhydride was placed. In our work we made use of boric anhydride of the natural isotopic composition (82% B^{11}), and also of material enriched to 92% in the isotope B^{10}, obtained from BF_3 via BCl^3 and H_3BO_3. Helium (7 mm Hg) served to conduct the discharge; it circulated through the discharge tube and was continuously purified in an activated-charcoal trap cooled by liquid nitrogen. We also obtained the spectrum of a discharge[16] in BF_3 in a capillary discharge tube analogous to the one used by Chretien.[16] The bands thus obtained in the 1650-1850 A region coincided completely in position with the spectrum measured when the hollow cathode was used. As photographic material, we used "Schumann" plates of the "Agfa" company, which were developed in fine-grain "Final" developer. The maximum exposure times amounted to 1 hr.

Measurement of the plates was performed on an IZA-2 comparator with a precision of ±0.001 mm, for four portions of the spectrum differing in height. The wavelengths were determined on the basis of the atomic lines of boron, and of silicon and carbon as well. We note

Table 1. Atomic Lines of Boron and Silicon (in A)

Spectrum	Measured	From data of refs. 20-22	Spectrum	Measured	From data of refs. 20-22	Spectrum	Measured	From data of refs. 20-22	Spectrum	Measured	From data of refs. 20-22
				Boron							
BII	1362.47$_0$	1362.46	BI	1600.36$_1$	1600.41	BI	1817.84$_1$	1817.84	BI	2090.28$_1$ **	2090.24
BI	1378.65$_1$	1378.43	BI	1600.44$_1$	1600.83	BI	1818.34$_1$	1818.35		Silicon[20,22]	
BI	1378.85$_1$	1378.89	BI	1600.75$_1$		BI	1825.80$_1$ **	1825.80			
BI	1378.94$_0$		BII	1600.82$_0$	1623.57	BI	1826.39$_1$ **	1826.40	SiII	1526.70$_1$	1526.70
BI	1379.16$_1$	1378.95	BII	1623.56$_0$	1623.78	BII	1824.81$_1$	1824.81	SiII	1533.43$_1$	1533.44
BI	1558.34$_1$	1558.71	BII	1623.78$_0$	1623.99	BIII	2066.45$_2$	2066.443	SiI	1563.16$_0$	1563.1
BI	1559.15$_0$	1559.11	BII	1623.96$_0$	1624.17	BI	2066.94$_1$ *	2066.99	SiI	1565.34$_2$	1565.30
BI	1566.29$_1$	1566.32	BII	1624.16$_0$	1624.35	BI	2067.03$_2$	2067.06	SiI	1583.60$_2$	1583.97
BI	1566.65$_2$	1566.70	BI	1624.36$_1$	1662.62	BI	2067.32$_2$	2067.29	SiI	1616.59$_2$	1616.55
BI	1573.29$_2$	1573.31	BI	1662.65$_0$ *	1663.05	BI	2067.59$_2$	2067.56	SiI	1759.50$_1$	1759.56
BI	1573.67$_1$	1573.67	BI	1663.00$_1$	1666.87	BI	2067.96$_2$	2067.83	SiII	1817.44$_2$	1817.42
			BI	1666.84$_1$	1667.30	BI	2089.58$_1$ **	2089.55	SiI	1847.46$_2$	1847.47
			BI	1667.27$_0$							

*Coincides with a copper line.

**The line is too intense and may be inaccurately measured.

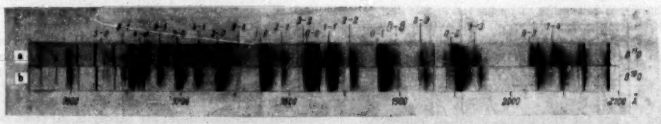

Fig. 1. General view of the bands of the γ-system in the spectrum of the BO molecule.

that the data existing in the literature on the spectra of boron[16,20-22] (and, in part, of silicon) in the vacuum ultraviolet region were obtained on instruments with less resolving power and dispersion than in our case. Therefore, before using these lines as internal standards for measuring the BO spectrum, we obtained a spectrum of boron and copper in the hollow cathode and refined the wavelengths of B and Si on the basis of the most precise literature data on the lines of copper,[23,24] silicon, and carbon.[25] In the refinement of the wavelengths of the atomic lines, and also in the later measurements, a separate dispersion curve was constructed for each plate. The wavelengths obtained by us for the lines of BI, BII, BIII, SiI, and SiII are presented in Table 1. The precision of the comparator measurements and the small scatter of the points on the dispersion curve enable us to estimate the limiting error in the determination of the wavelengths of the atomic lines as being within ±0.01 A. This quantity is confirmed by the determination of the wavelengths of certain copper lines on the basis of others.

EXPERIMENTAL RESULTS

In Fig. 1 are shown the spectra obtained with natural and enriched boric anhydride in the 1500-2090 A region. A well-marked system of bands, shaded toward the long wavelength side, is visible. The bands have 4 heads each (2 of these bands are shown in Fig. 2 under fivefold magnification). In all the bands, the first head from the short wavelength side is of low intensity, and the fourth is covered by the very intense third head. The distance between the second and third heads fluctuates within the limits 25-32 cm^{-1}. The sharp second head is most convenient for measurements. The rotational structure is resolved in all the bands.

The positions of all the bands measured by us are presented in Tables 2 and 3 (the measurements were made at the second head). Of the 22 bands obtained by us with natural boric anhydride, 6 coincide with bands measured at the most intense heads by Chretien.[18] In two cases the heads measured by Chretien coincide not with the second, but with the third heads of our measurements. It should be noted that the bands belonging to the

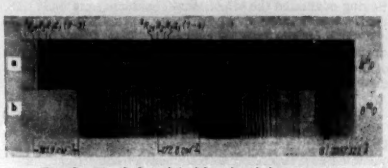

Fig. 2. The 0-3 and 1-4 bands of the γ-system of the BO molecule under fivefold magnification.

isotope B^{10} are almost unnoticeable in the spectrum of the sample with the natural isotopic composition of the boric anhydride (Fig. 1,a). No bands were found in the 1350-1500 A region.

Table 2. Heads of the R_2-Branches of the γ-Bands of the $B^{11}O$ Molecule (in cm^{-1})

v' \ v''	0	1	2	3	4	5
0	55084.2	53222.2	51383.8	49569.0	—	—
1	56376.7	54516.2	—	50863.5	49067.1	—
2	57644.2	55789.8	53947.9	52135.6	—	—
3	58896.1	57035.1	55196.9	—	51560.5	49823.4
4	60124.7	58261.4	—	—	—	—
5	61328.3	59468.5	—	—	—	—
6		60646.3	—	—	—	—

Table 3. Heads of the R_2-Branches of the γ-Bands of the $B^{10}O$ Molecule (in cm^{-1})

v' \ v''	0	1	2	3	4	5
0	55077.4	53162.8	51272.1	49407.1	—	—
1	56408.4	54491.4	—	50735.4	48864.3	—
2	57713.0	55792.5	53908.3	52042.5	—	—
3	58994.8	57079.8	55189.6	—	—	49668.4
4	60255.1	58340.0	—	—	—	—
5	51491.4	59577.7	—	—	—	—
6	—	60789.4	—	—	—	—
7	—	61977.1	—	—	—	—

DISCUSSION OF RESULTS

In the assignment of the bands we started from the fact that, for low values of the vibrational quantum num-

bers, the smallest isotopic shift must be in the 0—0 band. Therefore, the band at 1815.4 A may be taken as the 0—0 band. Furthermore, there are no clearly marked sequences in the spectrum, which permits us to arrange the most intense bands in two progressions on both sides of the 1815.4 A band. These will be the progressions $v' = 0$ (on the side of shorter wavelengths) and $v'' = 0$ (on the side of longer wavelengths). The bands assigned in this way fit well into a Deslandres table for the molecules $B^{11}O$ and $B^{10}O$ (Tables 2 and 3). Our assignment of the bands differs from Chretien's, who took the band at 1773.8 A as the 0—0 band. This error of Chretien's was apparently caused by the fact that, in the spectrum obtained by him, the long wavelength bands were overlapped by the spectrum of the BF molecule, and also by the absence of isotopic bands.

The vibrational constants of the upper and lower electronic states for both isotopic molecules were determined by us from the second heads by the method of least squares from the values

$$\frac{\Delta G\,(v_{m_1}\ v_n)}{(v_m - v_n)} = \omega_e - (v_m + v_n + 1)\,\omega_e x_e,$$

where v_m and v_n are the vibrational quantum numbers of one electronic state while v = const. for the other.[27] Having evaluated the vibrational constants, one can easily determine the value of ν_e from the heads (the constants obtained are presented in Table 4). The discrepancy between the calculated and measured positions of the heads does not fundamentally exceed 1 cm^{-1}. At the same time, the relation

$$\frac{\omega_e^{\delta}}{\omega_e} = \rho = \sqrt{\frac{\mu_{\delta}}{\mu}}, \qquad (1)$$

is well fulfilled, where ω_e and ω_e^{δ} are the vibration frequencies corresponding to the "heavy" and "light" isotopic molecules ($B^{11}O$ and $B^{10}O$), and μ and μ^{δ} are the reduced masses. The reduced masses of $B^{11}O$ and $B^{10}O$ give the value $\rho = 1.0290$, and from the ratio of the vibrational constants of the upper and lower electronic states one obtains respectively $\rho = 1.0285$ and 1.0292. Thus the presence of the isotope effect along with the fulfillment of Eq. (1) confirms the assignment to the BO molecule of the band system here studied.

Table 4. Vibrational Constants and Value of ν_e for the $C^3\Pi$ and $X^2\Sigma^+$ States, Determined from the Heads of the γ-Bands of the Molecules $B^{11}O$ and $B^{10}O$ (in cm^{-1})

Molecule	State	ν_e	T_e	ω_e	$\omega_e x_e$
$B^{11}O$	$A^2\Sigma^+$	0	0	1884.7	11.8
	$C^3\Pi$	55368.5	55346.1	1315.3	11.1
$B^{10}O$	$A^2\Sigma^+$	0	0	1939.7	12.4
	$C^3\Pi$	55370.3	55346.1	1352.7	11.8

The coincidence of the values of the vibrational constants of the lower state of the $B^{10}O$ and $B^{11}O$ molecules with the corresponding values $\omega_e'' = 1940.3$ cm^{-1} and $\omega_e'' = 1885.4$ cm^{-1} obtained from the α-bands[4,9] of BO for the ground state $X^2\Sigma^+$ permits us to consider that the ground state $X^2\Sigma^+$ must be the lower state for the bands studied here. Then, according to the selection rules, the upper state may be either a $^1\Sigma$ or a $^3\Pi$ state. The external appearance of the bands (4 heads in each band) looks very much like bands corresponding to a $^2\Pi - ^2\Sigma$ transition when the spin splitting is not very great. The possibility of a $^2\Sigma - ^2\Sigma$ transition is eliminated, since bands corresponding to this transition have single heads. Therefore the upper state must be a ^{2} state, which is also confirmed by the rotational analysis. Thus each band (Fig. 2) must consist of two subbands corresponding to the transitions $^2\Pi_{1/2} - ^2\Sigma^+$ and $^2\Pi_{3/2} - ^2\Sigma^+$, the first head in the band being the head of the $^5R_{21}$ branch, the second R_2, the third R_1, and the fourth Q_1. By analogy with the α- and β-bands of BO the new band system, corresponding to the transition $C^2\Pi - X^2\Sigma^+$, may be called the γ-system.

The conclusion that the γ-system is to be assigned to the $C^2\Pi - X^2\Sigma^+$ transition of BO is also confirmed by a preliminary rotational analysis which was carried out for the 1—0, 2—0, 0—1, and 0—3 bands of $B^{11}O$ and 2—0 of $B^{10}O$. As a result, the rotational constants $B_v = 1.483$ cm^{-1} and $\alpha_e = 0.018$ cm^{-1} were found for $B^{11}O$, whence, with the help of the isotopic relationships,[27] one obtains $B_e = 1.570$ cm^{-1} and $\alpha_e = 0.020$ cm^{-1} for $B^{10}O$, and it also proves possible to calculate the value $B_2 = 1.520$ cm^{-1}, which agrees well with the experimental result for $B^{10}O$ ($B_2 = 1.521$ cm^{-1}). The spin splitting constant in the case of the nonrotating $C^2\Pi$ state (by analogy with BS)[28] amounts to 46.4 cm^{-1}.

Before we carried out the rotational analysis (after the assignment of the γ-bands to the BO molecule had been established), the previous rotational analysis[17] of two bands of $B^{11}O$ was reexamined by Kuzyakov, Tatevskii, and Tunitskii,[29] the values obtained by them for the rotational constants differing hardly at all from ours. However, in the rotational structure of all the bands we found a series of perturbations. From the values of the rotational constants we also calculated the magnitude of the displacement of the R_2 head relative to the band origin, and determined the magnitude of the electronic excitation to be $T_e = 55346.1$ cm^{-1}. The computed displacement of the R_2 head for $B^{10}O$ proved to be approximately 1.4 cm^{-1} larger than for $B^{11}O$, which explains the experimentally obtained difference of 1.8 cm^{-1} between the ν_e values for the two isotopic molecules. After a final rotational analysis has been carried out, it will be possible to refine the vibrational constants. We note also that one's attention is attracted by the fact of the absence of the 1—2 band for $B^{10}O$ and $B^{11}O$, in the presence of intense 2—2, 1—3, and 2—3 bands. We explain this fact by the low probability of that transition, as also of the 1—2 transition in the case of the β-system of BO.[30]

On the basis of the literature data[4,9] and of the values obtained by us for the vibrational constants of the $C^3\Pi$ state, and using the approximate formula $D_e = \omega_e^2/4\omega_e x_e$, it is possible to estimate the dissociation energies of all the electronic states of the BO molecule. This formula is equivalent, as is well known, to the Birge-Sponer linear extrapolation.[27] It is not yet possible to apply any more precise methods for estimating the dissociation energy for any one of the electronic states of BO, since the higher anharmonicity coefficients $\omega_e y_e$, etc., are unknown. Regardless of the insufficient precision of the estimated values of D_e, consideration of them is important for the reason that it enables us to compare the values of D_e thus obtained and the values of the electronic terms T_e, which have been precisely determined experimentally, with the known energy differences for the state of separate atoms, and to establish, if it is possible, a unique or most probable correlation between the molecular and atomic states. (This in turn enables us to refine the approximate D_e values.) Using the following values (in ev)

$D_e(X^2\Sigma^+) = 9.4$, $D_e(A^2\Pi) = 4.5$, $D_e(B^2\Sigma^+) = 4.8$, $D_e(C^2\Pi) = 4.8$

and

$T_e(X^2\Sigma^+) = 0$, $T_e(A^2\Pi) = 3.0$, $T_e(B^2\Sigma^+) = 5.4$, $T_e(C^2\Pi) = 6.9$

one can set up, on the basis of Morse's formula, an approximate set of potential curves for the BO molecule (the dashed curves in Fig. 3). By considering together the dissociation limits and the various atomic states of oxygen (the first excited state of the boron atom lies

quite high (at 5.0 ev) and may be left out of account), one can see that the energy differences between the dissociation limits are practically equal to the energy differences among the ^3P_g, ^1D_g, and ^1S_g atomic states of oxygen. Such concordance also occurs in the case of the BS molecule.[28] Therefore, it appears at first glance that, on dissociation of a BO molecule, there are formed from its different states a boron and an oxygen atom in those atomic states toward which the dissociation limits obtained by extrapolation converge (Fig. 3). However, in the carrying out of the correlation, the following conditions must be fulfilled: (1) The dissociation limits of the molecular states must converge with the atomic state; and (2) the potential curves for the same kind of state must not intersect. A number of consequences follow from this.

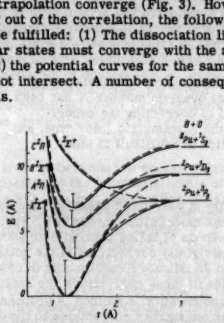

Fig. 3. Potential curves of the BO molecule.

(a) The $X^2\Sigma^+$ state can correlate only with the ground atomic states $B(^2P_u) + O(^3P_g)$, since correlation with higher atomic states would lead to intersection of the potential curves of the $X^2\Sigma^+$ state and the $^2\Sigma^+$ state (the repulsive potential curve in Fig. 3) obtained from $B(^2P_u) + O(^3P_g)$, i.e., to violation of the noncrossing rule.

(b) Under these conditions, the $A^2\Pi$ state can also correlate only with $B(^2P_u) + O(^3P_g)$; otherwise the value of $D_e(A^2\Pi)$ would have to increase by 4 ev (without any basis for it) or else $D_e(X^2\Sigma^+)$ would have to diminish by 1-2 ev and at the same time $D_e(A^2\Pi)$ would have to increase correspondingly by 3-2 ev.

(c) The $B^2\Sigma^+$ state cannot correlate with the atomic states $B(^2P_u) + O(^3P_g)$, since one $^2\Sigma^+$ state already correlates with them (the atomic states $B(^2P_u) + O(^3P_g)$ give the following doublet and quartet molecular states: Σ^+, $\Sigma^-(2)$, and Δ).[27] It is most probable that the $B^2\Sigma^+$ state correlates with the states $B(^2P_u) + O(^1D_g)$, for correlation with $B(^2P_u) + O(^1S_g)$ requires correction of the value of $D_e(B^2\Sigma^+)$ by 1.5 ev.

(d) The $C^2\Pi$ state apparently correlates with $B(^2P_u) + O(^1S_g)$, although it may also correlate with $B(^2P_u) + O(^1D_g)$ if there is a $^2\Pi$ repulsive potential curve for the states $B(^2P_u) + O(^1D_g)$, which must not intersect the $A^2\Pi$ curve (but this would not influence the correlation and D_e of the lower states).

For the proposed correlation, the conditions

$$\left.\begin{aligned} &T_e(A^2\Pi) = D_e(X^2\Sigma^+) - D_e(A^2\Pi);\\ &T_e(B^2\Sigma^+) - \{T[B(^2P_u) + O(^1D_g)] - T[B(^2P_u) + O(^3P_g)]\}\\ &\qquad = D_e(X^2\Sigma^+) - D_e(B^2\Sigma^+);\\ &T_e(C^2\Pi) - \{T[B(^2P_u) + O(^1S_g)] - T[B(^2P_u) + O(^3P_g)]\}\\ &\qquad = D_e(X^2\Sigma^+) - D_e(C^2\Pi). \end{aligned}\right\} \quad (2)$$

must be fulfilled.

The left-hand parts of these equations are known precisely and equal respectively to 3.0, 3.4, and 2.7 ev. Thus the approximate values of D_e presented above must be such as to fulfill Eqs. (2), if the correlation accepted above may be considered correct. In order for Eqs. (2) to be satisfied, it is necessary to correct the D_e values in the following way: either only diminish $D_e(X^2\Sigma^+)$ by ≈2ev, or increase the values of $D_e(A^2\Pi)$, $D_e(B^2\Sigma^+)$, and $D_e(C^2\Pi)$ by ≈2ev, or, finally, diminish $D_e(X^2\Sigma^+)$ by some amount x and increase $D_e(A^2\Pi)$, $D_e(B^2\Sigma^+)$, and $D_e(C^2\Pi)$ by (2 − x). The case in which the linear extrapolation curves of all the electronic states have a positive curvature is not excluded, and then one must diminish $D_e(X^2\Sigma^+)$ by (2 + y) ev and $D_e(A^2\Pi)$, $D_e(B^2\Sigma^+)$, and $D_e(C^2\Pi)$ by y ev.

Thus correction of the D_e values obtained by means of extrapolation is required in any case, the most probable variant being the one which requires correction of only the one value $D_e(X^2\Sigma^+)$ in Eqs. (2) by 2 ev, but not of several D_e's as in the other cases. Hence $D_e(X^2\Sigma^+) \approx 7.5$ ev. The set of potential curves obtained for the BO molecule is shown in Fig. 3 by the solid lines. The value $D_e(X^2\Sigma^+) \approx 7.5$ ev agrees well with the thermochemical data: $D_0 = 7.9$ ev.[31] If we accordingly take $D_e(X^2\Sigma^+) = 8.0$ ev, we obtain the dissociation energies for the remaining states according to Eq. (2): $D_e(A^2\Pi) = 5.0$ ev, $D_e(B^2\Sigma^+) = +4.6$ ev, and $D_e(C^2\Pi) = 5.3$ ev.

REFERENCES

1. W. Jevons, Proc. Roy. Soc. **A91**, 120 (1914).
2. R. S. Mulliken, Phys. Rev. **25**, 259 (1925).
3. W. Scheib, Z. Physik **60**, 74 (1930).
4. F. A. Jenkins and A. McKellar, Phys. Rev. **42**, 464 (1932).
5. A. A. Elliott, Proc. Acad. Sci. Amsterdam **33**, 644 (1930).
6. J. Funke and C. F. E. Simons, Proc. Acad. Sci. Amsterdam **38**, 142 (1935).
7. A. Elliott, Proc. Acad. Sci. Amsterdam **38**, 736 (1935).
8. A. A. Mal'tsev, Yu. Ya. Kuzyakov, and V. M. Tatevskii, Fiz. Sb. L'vovsk. Univ. No. 3(8), 475 (1957).
9. A. Lagerqvist, N. Nilsson and K. Wigartz, Arkiv Fysik **13**, 379 (1958).
10. H. Kayser, "Handbuch der Spectroscopie," Vol. 5. 1910.
11. G. Klihe, Z. wiss. Phot. **4**, 173 (1906).
12. N. L. Singh, Proc. Indian Acad. Sci. **A29**, 424 (1949).
13. A. A. Mal'tsev, V. G. Vinokurov, and V. M. Tatevskii, Fiz. Sb. L'vovsk, Univ. No. 3(8), 480 (1957).
14. J. R. Soulen, P. Sthapitanonda and J. L. Margrave, J. Phys. Chem. **59**, 132 (1955).
15. M. Chretien and E. Miescher, Helv. Phys. Acta **22**, 588 (1949).
16. M. Chretien, Helv. Phys. Acta **23**, 259 (1950).
17. L. G. Zelenskaya and L. N. Tunitskii, Fiz. Sb. L'vovsk. Univ. No. 3(8), 489 (1957).
18. V. K. Prokof'ev, Izvest. Nauk SSSR, Ser. Fiz. **22**, 737 (1958).
19. A. A. Mal'tsev, Opt. i Spektr. **9**, 428 (1960), Optics and Spectroscopy **9**, 225 (1960).
20. B. Edlen, Z. Physik **73**, 476 (1931).
21. H. E. Clearman, J. Opt. Soc. Am. **42**, 373 (1952).
22. E. W. Burke and J. E Mack, J. Opt. Soc. Am. **46**, 100 (1956).
23. A. G. Shenstone, J. Opt. Soc. Am. **45**, 868 (1955).
24. P. G. Wilkinson, J. Opt. Soc. Am. **47**, 182 (1957).
25. P. G. Wilkinson, J. Opt. Soc. Am. **45**, 862 (1955).
26. C. E. Moore, An ultraviolet multiplet table. Washington, 1950.
27. G. Herzberg, "Spektry i stroenie dvukhatomnykh molekul." Izd. Inostrannoi Lit., Moscow, 1949. "Molecular Spectra and Molecular Structure I. Spectra of Diatomic Molecules." Van Nostrand, New York, 1950.
28. P. B. Zeeman, Can. J. Phys. **29**, 336 (1951).

29. Yu. Ya. Kuzyakov, V. M. Tatevskii, and L. N. Tunitskii, Opt. i Spektr. 9, 156 (1960), Optics and Spectroscopy 9, 84 (1960).
30. R. W. Nicholls, P. A. Fraser, and W. R. Jarmain, Combustion and Flame 3, 13 (1959).
31. L. Brewer, Chem. Revs. 52, 1 (1953).

METHOD OF DETERMINING THE NONRIGIDITY CORRECTIONS TO THE HIGHER ROTATIONAL ENERGY LEVELS OF MOLECULES OF THE ASYMMETRIC ROTOR TYPE

G. A. Khachkuruzov

Received 16 March 1960

The character of the regular relationship between the centrifugal displacements of the rotational energy levels of asymmetric rotors and the rotational quantum number J has been established graphically. The possibility has been demonstrated of correcting the experimental values for the rotational energy levels of molecules of the asymmetric rotor type, and of determining the values of higher rotational energy levels which are difficult to study experimentally.

INTRODUCTION

It is known[1] that the rotational energy levels of rigid asymmetric rotors are described by the equation

$$F(J_\tau) = \frac{1}{2}(A+B)J(J+1) + \frac{1}{2}(A-C)\cdot E_{J_\tau}(k), \qquad (1)$$

where A, B, and C are the rotational constants (A ≥ B ≥ C), J is the rotational quantum number, τ is the index by which rotational energy levels having the same J value are labeled, and $E_{J_\tau}(k)$ is a function of J and the asymmetry parameter k. The latter quantity is expressed in the following form in terms of the rotational constants:

$$k = \frac{2B-A-C}{A-C}. \qquad (2)$$

The values of the function $E_{J_\tau}(k)$ are determined by solution of algebraic equations, the degree of which is higher the greater the value of J. The corresponding equations are presented in Herzberg's monograph[1] and in refs. 2-4. The values of the function $E_{J_\tau}(k)$ obtained as a result of numerical solution of such equations have been tabulated by King, Hainer, and Cross[5,6] and by Erlandsson[7] from J = 0 to J = 40.* A procedure has been developed by Baker[8] for computing those rotational energy levels of rigid asymmetric rotors which correspond to large values of J on the basis of the known values for levels with small J. A method has been proposed by Fike[10] for calculating the rotational energy levels for rigid asymmetric rotors with the help of electronic computers.

*In the monograph of Townes and Schawlow,[9] an eight-place table of the function $E_{J_\tau}(k)$ is presented for J = 0-12 and k = 0.00 to 1.00 in steps of 0.01.

Thus the determination, by computational methods, of the rotational energy levels of rigid asymmetric rotors on the basis of the known values of the moments of inertia can be accomplished for any values of J. However, real molecules are not absolutely rigid, in consequence of the finiteness of the forces of intramolecular interaction. Therefore, the rotational energy levels of a real molecule differ from the calculated values of the corresponding levels of its rigid model. In refs. 11-13, some progress has been achieved in working out a theory for the calculation of the centrifugal distortion corrections to the rotational energy levels of asymmetric rotors. However, the equations obtained in these works are applicable only in restricted cases and are associated with a complex calculational procedure. Furthermore, the known methods of taking approximate account of the molecular nonrigidity corrections to the rotational energy levels lead to satisfactory results only in cases where the magnitudes of these corrections are small.

In the present work, a method is proposed for finding the molecular nonrigidity corrections to those rotational energy levels corresponding to large values of J, on the basis of the known experimental values of these corrections for levels corresponding to small J values. The latter can usually be determined with sufficient accuracy from the observed spectra, while the observation of transitions from high rotational energy levels of polyatomic molecules is associated with great experimental difficulties. The present method rests on a new labeling of the rotational energy levels of asymmetric rotors, different from the generally accepted one.

NEW LABELING OF THE ROTATIONAL ENERGY LEVELS OF ASYMMETRIC ROTORS

An asymmetric rotor is converted into a prolate symmetric rotor (A ≠ B = C) when k = −1, and into an oblate symmetric rotor (A = B ≠ C) when k = +1. The rotational energy levels of the latter are determined by the following equations:

(a) for a prolate (rigid) symmetric rotor

$$F(J_\tau) = \frac{1}{2}(A+C)J(J+1) + \frac{1}{2}(A-C)K^2; \qquad (3)$$

(b) for an oblate (rigid) symmetric rotor

$$F(J_\tau) = \frac{1}{2}(A+C)J(J+1) - \frac{1}{2}(B-C)K^2. \qquad (4)$$

In Eqs. (3) and (4), K denotes the quantum number of the projection of the angular momentum vector of the rotor on the symmetry axis; it takes on the values of 0, 1, ..., J for any given J. Thus, in the case of symmetric rotors, the number of levels corresponding to a given value of J equals J + 1. The level corresponding to K = 0 is nondegenerate; the other levels are doubly degenerate. For a given value of the quantum number J, the level with minimum rotational energy in the case of a prolate symmetric rotor corresponds to K = 0, while in the case of an oblate symmetric rotor this level corresponds to K = J. Therefore, during comparison of the rotational energy levels of prolate and oblate symmetric

rotors with each other and with the levels of asymmetric rotors, the quantum number K in the case of a prolate symmetric rotor will be denoted by K_-, and in the case of an oblate symmetric rotor by K_+.

In the case of asymmetric rotors ($|k| < 1$), all the rotational energy levels are nondegenerate. Then the number of levels corresponding to a given value of J equals $2J + 1$. Such levels are labeled by the index $\tau = K_- - K_+$ or by the double index K_-, K_+ in accordance with the correspondence existing between the rotational energy levels of asymmetric and symmetric rotors. To the doubly degenerate rotational energy levels of symmetric rotors, there correspond pairs of very close levels of an asymmetric rotor, which may consequently be called components of doublet levels. Here the lower doublets of an asymmetric rotor, for which $\tau < 0$, correspond to the rotational levels of an oblate symmetric rotor, and the upper doublets of an asymmetric rotor, for which $\tau \geq 0$, correspond to the levels of a prolate symmetric rotor.

The differences between the energy values of the doublet components of the rotational levels of asymmetric rotors are smaller, the smaller the absolute value of the asymmetry parameter k and the larger the value of the rotational quantum number J. It is not difficult to convince oneself of this on the basis of the tables of the function $E_{J_\tau}(k)$,[8-8] and also on the basis of the experimental values for the rotational energy levels of molecules of the asymmetric rotor type. It is important to note that this regularity exists also for the centrifugal distortion corrections to the computed values of the rotational energy levels of rigid asymmetric rotors.

In Table 1 are presented the absolute values of the differences between the experimental values[4,14,15] for the rotational energy levels of the ground vibrational state of the water molecule and the computed values of the corresponding levels calculated according to formula (1).*

*Here the values recommended in ref. 16 were taken for the rotational constants.

Table 1. Experimental Values of the Centrifugal Distortion Corrections to the Rotational Energy Levels of the Ground Vibrational State of the H_2O Molecule (in cm^{-1})

J_τ	n	$\Delta F(J_\tau)$	J_τ	n	$\Delta F(J_\tau)$	J_τ	n	$\Delta F(J_\tau)$	J_τ	n	$\Delta F(J_\tau)$
0_0	0	0	7_0	+6	7.38	10_{10}	+4	88.89	13_{-3}	−4	25.4
			7_{+6}		6.85	10_{+9}		88.89	13_{-2}		24.92
1_{-1}	−0	0.01	7_{+5}	+4	15.13	10_{+7}	+2	138.51	13_{-7}	−6	36.74
1_0	+0	0.03	7_{+3}		15.12	10_{+6}		138.51	13_{-6}		35.7
1_{+1}		0.02	7_{+2}	+2	30.25	10_{+5}	+0	206.96	13_{-5}	−8	50.08
2_{-2}	−0	0.06	7_{+3}	+0	30.25	10_{+10}		206.96	13_{-4}		44.9
2_{-1}		0.05	7_{+6}		56.09				13_{-3}	−10	55.24
2_0	2	0.03	7_{+7}		56.09	11_{-11}	−0	5.75	13_{-2}		54.4
2_{+1}	+0	0.40	8_{-8}	−0	2.07	11_{-10}		5.75	13_{-1}	−12	57.72
2_{+2}		0.42	8_{-7}		2.10	11_{-9}	−2	9.35	13_0	+12	70.42
3_{-3}	−0	0.10	8_{-6}	−2	3.73	11_{-7}	−4	15.93	13_{+1}		70.55
3_{-2}	−2	0.10	8_{-5}		3.52	11_{-6}		15.14	13_{+4}	+10	97.93
3_{-1}	−2	0.15	8_{-4}	−4	6.52	11_{-5}	−6	23.89	13_{+5}		98.01
3_0	+2	0.42	8_{-3}		5.85	11_{-4}		21.11	13_{+4}	+8	140.7
3_{+1}		0.44	8_{-2}	−6	8.51	11_{-3}	−8	28.73	13_{+8}		140.7
3_{+2}	+0	2.06	8_{-1}		9.12	11_{-2}		27.51	13_{+9}	+6	201.1
3_{+3}		2.11	8_0	8	10.03	11_{-1}	−10	30.46	13_{+7}		201.1
4_{-4}	−0	0.28	8_{+1}	+8	16.14	11_0	+10	37.92	13_{+6}	+4	282.5
4_{-3}		0.24	8_{+8}		16.18	11_{+1}		38.29	13_{+10}		282.5
4_{-2}	−2	0.48	8_{+9}	+4	30.33	11_{+3}	+8	57.47	13_{+11}	+2	387.5
4_{-1}	−2	0.50	8_{+4}		30.36	11_{+2}		57.52	13_{+11}	+0	517.3
4_0	4	0.78	8_{+10}	+2	54.67	11_{+5}	+6	89.77	13_{+12}		517.3
4_{+1}	+2	2.05	8_{+8}		54.67	11_{+6}		89.73			
4_{+2}		2.03	8_{+7}	+0	82.13	11_{+8}	+4	137.13	14_{-14}	−0	13.13
4_{+3}	+0	6.48	8_{+6}		82.13	11_{+7}		137.13	14_{-13}		13.13
4_{+4}		6.49	9_{-9}	−0	3.02	11_{+9}	+2	203.04	14_{-12}	−2	19.6
5_{-5}	−0	0.50	9_{-8}		3.09	11_{+10}		203.04	14_{-11}		19.6
5_{-4}		0.51	9_{-7}	−2	5.23	11_{+10}	+0	290.0	14_{-10}	−4	31.3
5_{-3}	−2	0.96	9_{-6}		4.99	11_{+11}		290.0	14_{-9}		31.2
5_{-2}		0.94	9_{-5}	−4	9.26	12_{-12}	−0	7.87	14_{-8}	−6	45.1
5_{-1}	−4	1.40	9_{-4}		8.21	12_{-11}		7.88	14_{-7}		44.8
5_0	+4	2.20	9_{-3}	−6	12.72	12_{-10}	−2	12.24	14_{-6}	−8	60.0
5_{+1}		2.42	9_{-2}		11.92	12_{-9}		12.19	14_{-5}		55.0
5_{+2}	+2	6.30	9_{-1}	−8	14.04	12_{-8}	−4	20.25	14_{-4}	−10	72.1
5_{+3}		6.31	9_0	+8	18.25	12_{-7}		19.74	14_{-3}		66.9
5_{+4}	+0	15.55	9_{+1}		18.80	12_{-6}	−8	29.9	14_{-2}	−12	73.87
5_{+5}		15.56	9_{+6}	+6	31.11	12_{-5}		27.98	14_{-1}		81.94
6_{-6}	−0	0.86	9_{+3}		31.12	12_{-4}	−8	38.72	14_0	14	83.08
6_{-5}		0.85	9_{+4}	+4	54.02	12_{-3}		0.80	14_{+1}	+12	106.79
6_{-4}	−2	1.72	9_{+8}		54.03	12_{-2}	−10	41.23	14_{+7}		106.8
6_{-3}		1.44	9_{+7}	+2	89.86	12_{-1}		44.84	14_{+5}	+10	347.0
6_{-2}	−4	2.72	9_{+8}		89.86	12_0	12	46.06	14_{+6}		347.0
6_{-1}		2.90	9_{+9}	+0	141.70	12_{+1}	+10	63.44	14_{+9}	+8	204.2
6_0	6	3.44			141.70	12_{+5}		62.50	14_{+8}		204.2
6_{+1}	+4	4.48	10_{-10}	−0	4.24	12_{+3}	+8	92.41	14_{+9}	+6	282.5
6_{+2}		6.65	10_{-9}		4.25	12_{+4}		92.43	14_{+8}		282.5
6_{+3}	+2	15.01	10_{-8}	−2	6.99	12_{+6}	+6	137.56	14_{+10}	+4	384
6_{+4}		15.00	10_{-7}		7.47	12_{+6}		137.56	14_{+11}		384
6_{+5}	+0	31.27	10_{-6}	−4	12.28	12_{+7}	+4	200.9	14_{+12}	+2	512
6_{+6}		31.27	10_{-5}		11.40	12_{+8}		200.9	14_{+13}		512
7_{-7}	−0	1.35	10_{-4}	−6	17.97	12_{+9}	+2	285.1	14_{+14}	+0	665
7_{-6}		1.41	10_{-3}		15.93	12_{+10}		285.1			665
7_{-5}	−2	2.83	10_{-2}	−8	20.59	12_{+11}	+0	392.8	15_{-15}	−0	16.81
7_{-4}		2.45	10_{-1}		21.57	12_{+12}		392.8	15_{-14}		16.81
7_{-3}	−4	4.41	10_0	10	23.29	13_{-13}	−0	10.12	15_{-13}	−2	24.4
7_{-2}		4.10	10_{+1}	+8	33.58	13_{-12}		10.12	15_{-12}	−2	24.4
7_{-1}	−6	5.42	10_{+2}		33.67	13_{-11}	−2	15.8	15_{-11}	−4	36.0
7_0			10_{+3}	+8	54.91	13_{-10}		15.8	15_{-10}		37.9
			10_{+4}		54.94						
15_{-0}	−6	54.8	16_{-16}	−6	65.9	17_{-13}	−4	55.1	18_{-2}	−10	129
15_{-4}		53.6	16_{-15}		65.0	17_{-12}		55.1	18_{-1}	−12	155
15_{-7}	−8	58.2	16_{-8}	−8	73.0	17_{-11}	−6	77.8	18_{-0}		157
15_{-6}		62.0	16_{-7}		66.8	17_{-10}		77.2	$18_{-18,19}$	—	—
15_{-5}	−10	87.1	16_{-6}	−10	107	17_{-9}	−8	75.8	19_{-19}	−0	—
15_{-4}		79.5	16_{-5}		93	17_{-8}		71.3	19_{-18}		—
15_{-3}	−12	95.1	16_{-4}	−12	120	17_{-7}	−10	126	19_{-17}	−2	51
15_{-2}		96.7	16_{-3}		111	17_{-6}			19_{-16}		111
15_{-1}	−14	100.0	16_{-2}	−14	121	17_{-5}	−12	143	19_{-15}	−4	81
15_0	+14	119.2	16_{-1}		134	17_{-4}		129	19_{-14}		—
15_{+1}		118.7	16_0	16	132	17_{-3}	−14	142	19_{-13}	−6	107
15_{+2}	+12	156.3	16_{+1}	+14	170	17_{-2}			19_{-12}		—
15_{+3}		156.4	16_{+2}		170	17_{-1}	−16	157	19_{-11}	−8	141
15_{+4}	+10	210	16_{+3}	+12	210	17_0	+16	—	19_{-10}		—
15_{+5}		210	16_{+4}		219	17_{+1}		186	19_{-9}	−10	189
15_{+6}	+8	286	16_{+5}	+10	291	17_{+2}	+14	231	19_{-8}		189
15_{+7}		286	16_{+6}		291	17_{+3}			$19_{-7,-19}$	—	—
15_{+8}	+6	383	16_{+7}	+8	387	17_{+4}	+12	300	20_{-20}	−0	—
15_{+9}		383	16_{+8}		387	$17_{+5,-17}$	—	—	20_{-19}		—
15_{+10}	+4	507	16_{+9}	+6	507				20_{-18}	−2	—
15_{+11}		507	16_{+10}		507	18_{-18}	−0	32.8	20_{-17}		—
15_{+11}	+2	658	16_{+11}	+4	656	18_{-17}		32.8	20_{-16}	−4	—
15_{+12}		658	16_{+12}		656	18_{-16}	−2	44.0	20_{-15}		—
15_{+13}	+0	838	16_{+13}	+2	—	18_{-15}		44.0	20_{-14}	−6	—
15_{+13}		838	16_{+14}		—	18_{-14}	−4	65.6	20_{-13}		123
16_{-16}	−0	21.2	16_{+15}	+0	—	18_{-13}		65.6	20_{-12}	−8	—
16_{-15}		21.2	16_{+16}		—	18_{-12}	−6	91.8	20_{-11}		170
16_{-14}	−2	29.8	17_{-17}	−0	28.5	18_{-11}		92.0	20_{-10}	−10	—
16_{-13}		29.8	17_{-16}		28.5	18_{-10}	−8	118	20_{-9}		185
16_{-12}	−4	45.9	17_{-15}	−2	37.1	18_{-9}		120	$20_{-8,-20}$	—	—
16_{-11}		45.9	17_{-14}		37.1	18_{-8}	−10	148			

It follows from inspection of the data of Table 1 that the centrifugal distortion corrections to the components of the doublet levels differ insignificantly from one another even at small J, and coincide (within the limits of error of the experimental measurements) for $J \geq 10$. In view of this, it appears expedient to introduce, along with the generally accepted labeling for the rotational energy levels of asymmetric rotors by means of the quantum number J and the index τ (or the indices K_-, K_+), a labeling of these levels such that the components of doublet levels should not be labeled differently. For this purpose, we shall label the rotational energy levels of an asymmetric rotor which correspond to a fixed value of the quantum number J by the index n, which takes on the values $\pm 0, \pm 2, \ldots, \pm(J-2), J$, when J is an even number, and the values $\pm 0, \pm 2, \ldots, \pm(J-1)$ when J is an odd number. The correspondence between the values of the indices τ and n in both cases is defined in general form in Table 2 and for specific numerical values of J and τ in Table 1.

CORRESPONDENCE BETWEEN THE VALUES OF THE NONRIGIDITY CORRECTIONS TO THE ROTATIONAL ENERGY LEVELS OF ASYMMETRIC ROTORS AND THE VALUES OF THE QUANTUM NUMBER J

On consideration of the data presented in Table 1, it is evident that there is a regular trend in the changes of the molecular nonrigidity corrections to the values of the rotational energy levels as a function of the changes in the values of the quantum number J and the indices τ or n. In principle, it is not impossible that the character of this regularity may be elucidated by means of mathematical transformations of the corresponding equa-

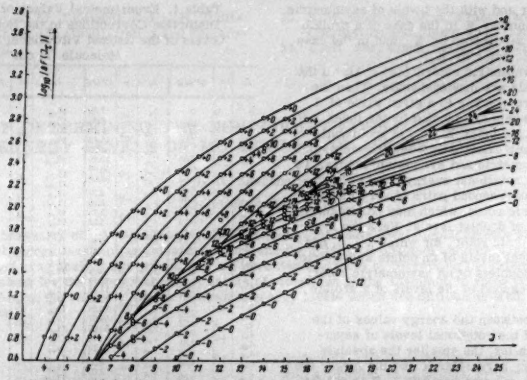

Diagram of the dependence of the logarithm of the centrifugal shift in the rotational energy levels of the ground vibrational state of the H_2O molecule on the quantum number J.

Table 2. Correspondence Between the Values of the Indices τ and n in Cases where the Number J is Even and Odd

Number J is even	τ	$-J$	$-J+1$	$-J+2$	$-J+3$	...	-2	-1	0	$+1$	$+2$	...	$+J-1$	$+J$
	n	-0		-2		...	$-(J-2)$	J	$+(J-2)$		...		$+0$	
Number J is odd	τ	$-J$	$-J+1$	$-J+2$	$-J+3$	...		-1	0	$+1$		...	$+J-1$	$+J$
	n	-0		-2		...	$-(J-1)$	$+(J-1)$			...		$+0$	

tions of the general quantum-mechanical theory of asymmetric rotors. However, the equations of this theory for the higher rotational energy levels are exceedingly complex, in view of which an analysis of the solutions of these equations for the purpose of elucidating their dependence on J and τ could hardly be successfully carried out without previously knowing the approximate character of this dependence, derived on the basis of the existing experimental data. We have succeeded in finding an approximate empirical dependence of this sort for the centrifugal distortion corrections $\Delta F(J_\tau)$ for a typical representative of asymmetric rotors—the water molecule—thanks to the introduction of the index n for labeling the rotational energy levels in place of the index τ previously used.

On the basis of the data presented in Table 1, it is not difficult to construct a diagram (shown in the Figure) of the dependence of $\log \Delta F(J_\tau)$ on the value of the quantum number J (in the Figure, points corresponding to the experimental values presented in Table 1 for the corrections to $\Delta F(J_\tau)$ are indicated by circles). Through those points corresponding to identical values of the index n and to different values of the quantum number J, it has proved possible to pass smooth curves which distinctly group themselves into two families. One family of curves is located in the upper part of the diagram and is formed by lines drawn through points corresponding to positive values of the index n. The second family of curves is located in the lower part of the diagram and is formed by lines passing through points with negative values of the index n. Therefore, for diagrams of the type shown in the Figure, it is appropriate to speak of families of positive and negative lines, i.e., lines corresponding to positive and negative values of the index n. From the Figure it follows that within each family, the lines run roughly parallel to one another, gradually approaching each other as J increases, and almost equidistant. It follows further from the Figure that the families of positive and negative lines intersect (lines with identical absolute values of the index n). The points of intersection of the positive and negative lines also lie on a smooth curve, which is the boundary line between the two families.

The regular placement of the points on the diagram testifies to the presence of a definite dependence of the magnitude of the centrifugal shift in the rotational energy levels of asymmetric rotors on the values of the quantum number J and the index n. The presence of this dependence gives the possibility of correcting the experimental values for the rotational energy levels of asymmetric rotors, and also of determining the magnitude of the centrifugal shift in the higher rotational energy levels, for which the corresponding spectral data are lacking. An example of the use of the diagram for the purposes just stated will be presented in our next communication. Analogous diagrams may also be constructed for other molecules of the asymmetric rotor type, both for the ground vibrational state and for excited states. The dependence found in this work between the centrifugal shifts in the rotational energy levels of asymmetric rotors and the quantum number J may be expressed in analytical form by means of a corresponding use of the method of least squares.

REFERENCES

1. G. Herzberg, "Kolebatel'nye i vrashchatel'nye spektry mnogoatomnykh molekul." Izd. Inostrannoi Lit., Moscow, 1949. "Molecular Spectra and Molecular Structure II. Infrared and Raman Spectra of Polyatomic Molecules." Van Nostrand, New York, 1945.
2. H. H. Nielsen, Phys. Rev. 38, 1432 (1931).
3. H. M. Randall, D. M. Dennison, N. Ginsburg, and L. R. Weber, Phys. Rev. 52, 160 (1937).

4. N. Ginsburg, Phys. Rev. 74, 1052 (1948).
5. G. W. King, R. M. Hainer, and P. C. Cross, J. Chem. Phys. 11, 27 (1943).
6. R. M. Hainer, P. C. Cross, and G. W. King, J. Chem. Phys. 17, 826 (1949).
7. G. Erlandsson, Arkiv Fysik 10, 65 (1955).
8. Ch. Townes and A. Schawlow, "Radiospektroskopiya." Izd. Inostrannoi Lit., Moscow, 1959. "Microwave Spectroscopy." McGraw-Hill, New York, 1955.
9. J. G. Baker, Phys. Rev. 110, 281 (1958).
10. C. T. Fike, J. Chem. Phys. 31, 568 (1959).
11. D. Kivelson and E. B. Wilson, J. Chem. Phys. 20, 1575 (1952).
12. D. Kivelson, J. Chem. Phys. 21, 1229 (1953).
13. E. Gora, J. Mol. Spectrosc. 2, 259 (1958).
14. W. S. Benedict, H. H. Claassen, and J. H. Shaw, J. Res. Natl. Bur. Standards 49, 91 (1952).
15. J. H. Taylor, W. S. Benedict, and J. Strong, J. Chem. Phys. 20, 1884 (1952).
16. W. S. Benedict, N. Gailar, and E. K. Plyler, J. Chem. Phys. 24, 1139 (1956).

VIBRATIONAL SPECTRA AND POTENTIAL ENERGY CONSTANTS OF HELOETHYLENES MONOCHLOROETHYLENE, MONOFLUOROETHYLENE, 1,1-DICHLOROETHYLENE, 1,1-DIBROMOETHYLENE, AND THEIR DEUTERIUM SUBSTITUTION PRODUCTS

L. M. Sverdlov, Yu. V. Klochkovskii, V. S. Kukina, and T. D. Mezhueva

Received 28 March 1960

A calculation of the vibration frequencies and potential energy constants of monochloroethylene, monofluoroethylene, 1,1-dichloroethylene, 1,1-dibromoethylene, and their deuterium substitution products has been carried out according to the method of M. A. El'yashevich and B. I. Stepanov. Good agreement between the calculated and observed frequencies has been obtained. The interpretation now existing in the literature for the vibrational spectra has been confirmed and refined, and the peculiarities of the force field of the molecules listed have been established.

1. We have previously[1] shown that, for the calculation of the vibrational spectra of the haloethylenes (monobromoethylene, cis-trans-dichloroethylene, and 1,1-difluoroethylene being our examples), one may use the force coefficients of ethylene[2] and the halomethanes[3] as a sufficiently good zero-order approximation.

It is of interest to carry out the calculation of the vibrational spectra of other haloethylenes, drawing for this purpose on the force coefficients of ethylene and the halomethanes as well as on the haloethylene force coefficients obtained in the previous calculation. In this work we have carried out the calculation of the normal vibration frequencies and the potential energy constants of monochloroethylene and $CH_2{=}CDCl$, 1,1-dichloroethylene 1,1-dibromoethylene, $CBr_2{=}CHD$, $CBr_2{=}CD_2$, monofluoroethylene, and its 7 deuterium substitution products

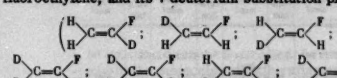

2. The molecules of 1,1-dichloroethylene and 1,1-dibromoethylene belong to the symmetry group C_{2v} and are characterized by vibrations of the following symmetry types:

$$\Gamma = 5A_1 + 4B_1 + A_2 + 2B_2.$$

The molecules of monochloroethylene, monofluoroethylene, and $CBr_2{=}CHD$ belong to the symmetry group C_s. They have 9 symmetric and 3 antisymmetric vibrations.

The Raman spectra of 1,1-dibromoethylene and its deuterium substitution products have been investigated in a work of Hemptinne.[4] The Raman spectra of 1,1-dichloroethylene have been repeatedly studied.[5-8] The most complete data were obtained in the work of Joyner and Glockler,[7] in which are also included the results of polarization measurements. The infrared spectra of 1,1-dichloroethylene have been studied by Thompson and Torkington[9] in the 500-3500 cm^{-1} range and by Evans[8] in the 320-700 cm^{-1} range. The Raman spectra of liquid monochloroethylene have been investigated in refs. 4, 10, and 11, polarization measurements being also carried out in the latter work. The Raman spectrum of gaseous monochloroethylene has been studied in ref. 12. The infrared spectra of gaseous monochloroethylene have been investigated in refs. 9, 12, and 13. The Raman and infrared spectra of the molecule $CH_2{=}CDCl$ have been studied by the authors of ref. 11. The infrared spectra of monofluoroethylene vapors have been investigated in refs. 14 and 15, the spectra of all the deuterium substitution products of monofluoroethylene also being studied in the latter work. An interpretation of the spectra was carried out in all the works cited.

3. The calculation of the frequencies was carried out according to the procedure of El'yashevich and Stepanov.[3] Internal vibrational coordinates were introduced for the calculation.

$1,1\text{-}C_2H_2Cl_2$: q_i, β_i (i = 1-2), Q_a, Q_b, Q_c, α_{12}, γ_{ab}, γ_{ac}, γ_{bc} (Fig. 1), ρ^{CCl_2}, ρ^{CH_2}, $\chi^{CH_2}_{CCl_2}$. Here ρ^{CH_2} and ρ^{CCl_2} are the angles determining the departure of the C=C bond from the plane of the CH_2 and CCl_2 groups respectively; χ is the angle of rotation of the CH_2 and CCl_2 groups relative to each other.

Monochloroethylene: q_i, β_i (i = 1-3), Q_a, Q_b, α_{12}, β_{ba}, γ_{cb} (Fig. 2), ρ^{CH_2}, ρ^{CHCl}, $\chi^{CH_2}_{CHCl}$. There are two additional conditions among the coordinates.

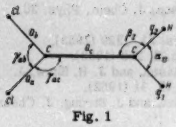

Fig. 1

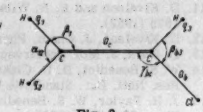

Fig. 2

For the calculation of the kinematic coefficients, the following geometrical parameters were used:

C_2H_3Cl [10, 11]: r (C=C) = 1.33 Å, r (C—Cl) = 1.73 Å, r (C—H) = 1.08 Å, ∠C—C—Cl = 122°, ∠CCH = 120°;

C_2H_3F [12]: r (C=C) = 1.337 Å, r (C—F) = 1.344 Å, r_{CHF} (C—H) = 1.08 Å, r_{CH_2}(C—H) = 1.075 Å, ∠CCF = 121°, ∠CCH = 120°;

1,1-$C_2H_2Cl_2$ [13]: r (C=C) = 1.32 Å, r (C—Cl) = 1.727 Å, r (C—H) = 1.07 Å, ∠CCCl = 123°10′, ∠CCH = 120°;

1,1-$C_2H_2Br_2$: r (C=C) = 1.31 Å, r (C—Br) = 1.9 Å, r (C—H) = 1.07 Å, ∠BrCBr = 114°, ∠HCH = 117°.

To take account of anharmonicity, the "spectroscopic masses" for hydrogen and deuterium were introduced.

In the calculation it was assumed that the force coefficients characterizing the interaction of elements of the molecule distant from one another were equal to zero. The admissibility of such an assumption is confirmed by the results of ref. 1. By the method of variation of constants, the following sets of force coefficients (in units of 10^5 cm^{-2}) were determined.

Monochloroethylene:

K_b (C—H) = 8.63; h_{13} = 0.03; K_b (C—H) = 8.8; K_s (C=C) = 14.2; H_{c_1} = H_{c_2} = 0.1; K_t (C—Cl) = 6; H_{t_1} = 0.28; H_{t_2} = 0.15; k_{23} − l_{23} = 0.77; K_s − $2l_{c_2}$ + l_{22} = 0.5; A_{b_1} − B_s = 0.45; a_3 − b_3 = 0.66; a_s − b_s = 0.43; $A^s_{c_2}$ − $B^s_{c_2}$ = 0.45; $A^s_{t_1}$ − $B^s_{t_1}$ = 0.6; $a^3_{c_2}$ − $b^3_{c_2}$ = 0.6; K_s − $l^{ss}_{c_2}$ − $l^{33}_{c_2}$ + $l^{23}_{c_2}$ = 0.65; K_{b_1} − $l^{ss}_{b_1}$ − $l^{33}_{c_2}$ + $l^{ss}_{c_2}$ = 0.69; K_s − $l^{ss}_{t_1}$ − $l^{33}_{t_1}$ + $l^{23}_{c_2}$ = 1.11; $A^s_{b_1}$ − $B^s_{b_1}$ = 0.8; $a^3_{b_1}$ − $B^3_{b_1}$ = 0.66; $A^s_{t_1}$ − $B^s_{t_1}$ = 0.3; m = 0.095; n = −0.025; K_{HCH_2} = 0.294; K_{HCHCl} = 0.409; $U_{\tau CH_2}$ = 0.053; K_τ = 0.671; $U_{\tau HCCl}$ = −0.05; $U_{\tau CH_2}$ = 0.

1,1-Dichloroethylene:

K_s (C—H) = 8.8; h_{13} = 0.03; K_s (C=C) = 14; K (C—Cl) = 5.78; H_{ab} = 0.67; H_{s_1} = 0.1; H_{as} = 0.28; K_s − l_{23} = 0.77; K_s − $2l_{23}$ + l_{22} = 0.55; a_3 − b_3 = 0.66; a_s − b_s = 0.43; A_s − B_s = 0.45; K_{ss} − l^{ss}_{ss} = 1.1; K_{ab} − $2l^{ab}_{ss}$ + l^{bc}_{ss} = 1.35; A^s_{ss} − B^s_{ss} = 0.5; A^b_{ss} − B^b_{ss} = 0.7; A^a_{ss} − B^a_{ss} = 0.95; n = 0.065; m = 0.005; K_{HCH_2} = 0.27; K_{HCCl_2} = 0.532; $U_{\tau HCl}$ = 0.051; K_τ = 0.672; $U_{\tau H}$ = $U_{\tau Cl}$ = 0.

1,1-Dibromoethylene:

K_s (C—H) = 8.76; h_{13} = 0.03; K_s (C=C) = 14.2; K (C—Br) = 4.91; H_{ab} = 0.5; H_{s_1} = 0.1; H_{as} = 0.1; K_s − l_{23} = 0.74; K_s − $2l_{c_2}$ + l_{22} = 0.52; a_3 − b_3 = 0.66; a_s − b_s = 0.43; A_s − B_s = 0.45; K_{ss} − l^{ss}_{ss} = 0.77; K_{ab} − $2l^{ab}_{ss}$ + l^{bc}_{ss} = 1.32; A^s_{ss} − B^s_{ss} = 0.5; A^b_{ss} − B^b_{ss} = 0.5; A^a_{ss} − B^a_{ss} = 0.8; n = 0.035; m = 0.035; K_{HCH_2} = 0.29; K_{HCBr_2} = 0.371; $U_{\tau HBrCl}$ = 0.049; K_τ = 0.621; $U_{\tau H^{cis}}$ = $U_{\tau Br^{cis}}$ = 0.

Monofluoroethylene:

K_s (C—H) = 8.825; h_{13} = 0.065; K_s (C=C) = 15; H_{c_1} = 0.1; H_{cb} = 0.25; K_b (C—F) = 10.2; H_{bs} = 0.5; H_{sb} = 0.3; K_{23} − l_{23} = = 0.77; K_s − $2l_{23}$ + l_{22} = 0.475; A_{b_1} − B_s = 0.45; a_3 − b_3 = 0.66; a_s − b_s = = 0.43; A^s_{cb} − B^s_{cb} = 0.35; A^b_{cb} − B^b_{cb} = 1.25; a^3_{cb} − b^3_{cb} = 0.9; K_{cb} − l^{bc}_{cb} − − l^{23}_{cb} + l^{bc}_{cb} = 0.77; K_{ab} − l^{ss}_{ab} − l^{23}_{cb} + l^{bc}_{cb} = 0.73; K_s − $l^{ss}_{c_2}$ − $l^{bc}_{c_2}$ + $l^{23}_{c_2}$ = 1.07; $A^b_{c_2}$ − $B^b_{c_2}$ = 1; $a^3_{c_2}$ − $b^3_{c_2}$ = 0.66; $A^s_{c_2}$ − $B^s_{c_2}$ = 1; m^{cb}_{cb} = 0.035; n^{cb}_{cb} = −0.015; $m^{bc}_{c_1}$ = 0.085; n^{cb}_{cb} = 0.035; K_{HCH_2} = 0.268; K_{HCHF} = 0.401; $U_{\tau F_2}$ = 0.05; K_τ = 0.836; $U_{\tau CH_2}$ = −0.01; $U_{\tau CHF}$ = −0.133.

The secular equations were solved by the method of progressive diagonalization. In Tables 1-4 are presented the calculated and observed frequency values, and an interpretation is given for the vibrational spectra of monofluoroethylene and its deuterium substitution products, monochloroethylene and CH_2=CDCl, 1,1-dibromoethylene

Table 2. Calculation and Interpretation of the Vibrational Spectra of Monochloroethylene and CH_2=CDCl (frequencies in cm^{-1})*

Coordinates	Symmetry	CH_2=CHCl					CH_2=CDCl		
		Calculation	Experiment (Ram.)			Exp. (IR)	Exp. (Ram.)		Exp. (IR)
			Liquid		Gas	Gas	Calculation	Liquid	Gas
$\tilde{\nu}_{CH_2}$(C—H)	A'	3104	3112 p		3121 (m)	3120 (s)	3096	3110 p	3111
$\tilde{\nu}_{CH_2}$(C—H)	A'	3012	3027 (w)	p	3027 (s)	3037 (m)	3014	3020 p	3024
$\tilde{\nu}_{CH}$(C—H)	A'	3073	3079 (w)	p	3086 (s)	3086 (s)	2289	2300 p	2308
Q (C=C)	A'	1599	1603 (vs)	p	1607 (vs)	1608 (vs)	1579	1586 p	1593
α (HCH)	A'	1372	1363 (s)	p	1368 (s)	1371 (m)	1348	1349 p	1358
β (CCH)	A'	1041	1028 (m)	p	—	1030 (s)	1134	1100 p	1117
β_{IP} (HCCl)	A'	1258	1274 (m)	p	1279 (s)	1279 (m)	840	861 p	—
Q_8 (C—Cl)	A'	707	706 (m)	p	719 (m)	720 (vs)	705	697 p	714
γ (ClCCl)	A'	403	396 (s)	p	394 (m)	398 (vs)	390	393 p	385
τ_{CH_2}	A''	901	901 (s)	d	—	896 (vs)	901	905 d	900
τ_{CHCl}	A''	612	623 (w)	d	—	620 (vs)	593	590 d	587
$\gamma^{CHCl}_{CH_2}$	A''	949	943		—	941 (vs)	799	803 d	804

*The experimental frequency values are from Raman spectra (Ram.) and infrared absorption spectra (IR). Symbols: p – polarized and d – depolarized lines. For the remaining symbols, see note to Table 1.

Table 1. Calculation and Interpretation of the Vibrational Spectra of Monofluoroethylene and Its Deuterium Substitution Products (frequencies in cm^{-1})*

Coordinates	Symmetry	C_2H_3F		C_2D_3F		CH_2=CFD		CD_2=CFH		t – DHC=CFH		t – HDC=CFD		s – HDC=CFH		s – DHC=CFD	
		Calculation	Experiment	Calculation	Experiment	Calculation	Experiment	Calculation	Experiment	Calculation	Experiment	Calculation	Experiment	Calculation	Experiment	Calculation	Experiment
q_1 (C—H)	A'	3052	—	2243	2240 (w)	3053	—	2257	2265 (w)	2298	2315 (w)	3092	3095 (vw)	3094	3095 (w)	2311	2325 (w)
q_2 (C—H)	A'	3127	3115 (w)	2345	2330 (w)	3126	3120 (vw)	2343	—	3095	3095 (w)	2291	2300 (w)	2296	2315 (w)	3090	3095 (vw)
α (HCH)	A'	1370	1380 (w)	1005	1001 (m)	1369	1368 (w)	973	1005 (w)	1241	1235 (w)	1298	1298 (w)	1310	1318 (w)	1249	1274 (w)
β (CCH)	A'	919	928 (vs)	768	794 (m)	969	985 (w)	816	804 (m)	821	—	934	969 (w)	845	878 (w)	784	798 (w)
Q (C=C)	A'	1640	1654 (vs)	1598	1596 (vs)	1630	1628 (vs)	1603	1620 (s)	1616	1630 (vs)	1616	1615 (vs)	1622	1635 (s)	1612	1603 (vs)
q_3 (C—H)	A'	3074	3080 (w)	2286	2273 (w)	2283	2310 (w)	3076	3085 (w)	3071	3080 (w)	2283	2285 (w)	3074	3080 (w)	2268	2275 (w)
Q (C–F)	A'	1175	1158 (vs)	1145	1142 (s)	1172	1165 (m)	1132	1137 (m)	1136	1137 (s)	1087	1071 (m)	1063	1084 (s)	1129	1145 (m)
β_2 (CCH)	A'	1294	1308 (w)	957	967 (m)	903	902 (w)	1298	1312 (w)	1319	1318 (w)	827	824 (m)	1280	1284 (w)	968	974 (m)
γ (CCF)	A'	473	483 (w)	418	410 (w)	489	477 (w)	421	414 (w)	462	455 (w)	434	428 (w)	456	434 (vw)	441	449 (vw)
ρ_{CH_2}	A''	864	863 (s)	726	728 (w)	865	867 (m)	700	693 (s)	809	815 (m)	846	844 (m)	789	785 (s)	853	868 (m)
ρ_{CHF}	A''	710	711 (w)	570	563(vw)	659	678 (w)	671	688 (m)	589	578 (w)	654	639 (w)	657	642 (w)	722	728 (w)
$\gamma^{CH_2}_{CHF}$	A''	940	940	678	675 (s)	830	—	580	564 (w)	923	928 (s)	678	695 (m)	917	910 (m)	585	575 (w)

*The experimental frequency values are from infrared absorption spectra. Symbols for band intensities (in parentheses): vw – very weak; w – weak; m – medium intensity; s – strong; vs – very strong.

Table 3. Calculation and Interpretation of the Vibrational Spectra of 1,1-Dibromoethylene and Its Deuterium Substitution Products (frequencies in cm^{-1})*

Coordinates	Symmetry	$CBr_2=CH_2$ Calculation	$CBr_2=CH_2$ Experiment	$CBr_2=CD_2$ Calculation	$CBr_2=CD_2$ Experiment	Symmetry	$CBr_2=CHD$ Calculation	$CBr_2=CHD$ Experiment
φ(C—H)	A_1	3042	3023	2254	2230	A'	2286	2282
φ(C—H)	B_1	3113	3108	2328	2339	A'	3079	3061
Q(C=C)	A_1	1617	1593	1564	1536	A'	1596	1563
α(HCH)	A_1	1383	1379	1034	1019	A'	1275	1258
β(CCH)	B_1	1081	1090	956	932	A'	965	949
Q(C—Br)	A_1	442	467	431	453	A'	436	458
Q(C—Br)	B_1	701	696	636	625	A'	647	655
γ(BrCBr)	A_2	189	184	182	183	A''	188	184
γ(CCBr)	B_1	297	322	249	283	A''	292	300
ρ_{CH_2}	B_2	881	886	717	709	A''	828	829
ρ_{CBr_2}	B_2	401	405	383	390	A''	387	391
χ_{CBr_2}	A_2	667	668	479	478	A''	550	545

*The experimental frequency values are from Raman spectra of the liquids.

Table 4. Calculation and Interpretation of the Vibrational Spectra of 1,1-Dichloroethylene (frequency in cm^{-1})*

Coordinates	Symmetry	Calculation	Experiment (Ram.) liquid		Experiment (IR) gas
φ(C—H)	A_1	3041	3035 (vs)	p	3035 (w) (liq.)
φ(C—H)	B_1	3128	3130 (s)	d	3130 (w) (liq.)
Q(C=C)	A_1	1625	1616 (vs)	p	1620 (s)
α(HCH)	A_1	1398	1391 (m)	p	1391 (m)
β(CCH)	B_1	1104	1088 (w)		1094 (s)
Q(C—Cl)	A_1	594	601 (vs)	p	605 (s)
Q(C—Cl)	B_1	792	788 (w)	d	794 (s)
γ(ClCCl)	A_2	308	299 (s)		
γ(CCCl)	B_1	390	375 (s)	d	375 (w)
ρ_{CH_2}	B_2	874	874 (w)	d	872 (s)
ρ_{CCl_2}	B_2	458	458 (w)	d	458 (m)
χ_{CH_2} χ_{CCl_2}	A_2	686	686 (w)	d	—

*For symbols, see notes to Tables 1 and 2

and its deuterium substitution products, and 1,1-dichloroethylene. It is easy to see that there is sufficiently good agreement between the calculated and observed frequencies—the maximum and average errors for the above-listed molecules equal respectively: for the deuteriomonofluoroethylenes, 35 and 10 cm^{-1}; monochloroethylene and CH_2=CDCl, 25 and 11 cm^{-1}; 1,1-dibromoethylene and its deuterium substitution products, 34 and 12 cm^{-1}; 1,1-dichloroethylene, 11 and 5 cm^{-1}.

REFERENCES

1. L. M. Sverdlov, Yu. V. Klochkovskii, and V. S. Kukina, Inzh.-Fiz. Zhur. 1, 43 (1958).
2. L. M. Sverdlov and N. L. Pakhomova, Zhur. Eksptl. i Teoret. Fiz. **26**, 64 (1954).
3. M. V. Vol'kenshtein, M. A. El'yashevich, and B. I. Stepanov, "Kolebaniya molekul" (Molecular Vibrations), Vol. 1. Gosudarst. Izd. Tekh. i Teoret. Lit., Moscow-Leningrad, 1949.
4. M. Hemptinne, Trans. Faraday Soc. **42**, 7 (1946).
5. J. Cabannes, J. chim. phys. **35**, 9 (1938).
6. V. M. Tatevskii and A. V. Frost, Vestnik Moskov. Gosudarst. Univ. No. 3, 65 (1947).
7. P. Joyner and G. Glockler, J. Chem. Phys. **20**, 302 (1952).
8. J. Evans, J. Chem. Phys. **30**, 934 (1959).
9. H. Thompson and P. Torkington, Proc. Roy. Soc. **A184**, 21 (1945).
10. K. Kohlrausch and W. Stockmair, Z. phys. Chem. **B29**, 292 (1935).
11. J. Evans and H. Bernstein, Can. J. Chem. **33**, 1792 (1955).
12. C. Gullikson and J. R. Nielsen, J. Mol. Spectrosc. **1**, 158 (1957).
13. A. Cole and H. Thompson, Proc. Roy. Soc. **A200**, 10 (1949).
14. P. Torkington and H. Thompson, Trans. Faraday Soc **41**, 236 (1945).
15. B. Bak and D. Christensen, Spectrochim, Acta **12**, 355 (1958).
16. J. Goldstein and J. Bragg, Phys. Rev. **75**, 1453 (1949), D. Kivelson and E. Wilson, J. Mol. Spectrosc. **8**, 61 (1959).
17. H. Morgen and J. Goldstein, J. Chem. Phys. **30**, 1025 (1959).
18. S. Sekino and T. Nishikawa, J. Phys. Soc. Japan **12**, 43 (1957).

ON THE INTERPRETATION OF THE VIBRATIONAL SPECTRA OF NAPHTHALENE AND ITS DEUTERIUM ANALOG

N. I. Zhirnov

Received 12 March 1960

On the basis of approximate representations of the character of the force interaction within the molecule, certain refinements in the interpretation of the vibrational spectra of naphthalene and $C_{10}D_8$ are proposed.

INTRODUCTION

Up to the present time, a sufficiently extensive body of experimental data (see refs. 1, 2) on the vibrational spectra of naphthalene and its deuterium substitution products has been collected to enable one to enter upon the calculation of the force constants of the molecule. However, the preliminary study of the experimental material (the choice and assignment of the fundamental frequencies) cannot be considered as complete: up to now the Raman spectra of $C_{10}H_7D$ and $C_{10}H_6D_2$ published in ref. 3 have not been interpreted, and the existing interpretations by Lippincott and O'Reilly[1] and by McClellan and Pimentel[2] for the vibrational spectra of $C_{10}H_8$ and $C_{10}D_8$ cannot be recognized as sufficiently reliable.

The interpretations of refs. 1 and 2 agree only in general outlines, regardless of the fact that the same requirements underlie their construction: the use of spectroscopic data relating to more thoroughly studied aromatic compounds (benzene and the deuteriobenzenes); allowance for the specificity of the vibration frequencies of the separate bonds and atom groups, for the selection rules, and for the Teller-Redlich product rule;[4] the requirement of agreement between the calculated (with the

help of the selected fundamental frequencies) values of the thermodynamic functions of naphthalene at high temperatures and the experimental values. The latter requirement is more strictly fulfilled in ref. 2 and less strictly (but still entirely satisfactorily, in our view) in ref. 1. Therefore, the substantial differences in the interpretation of many frequencies in refs. 1 and 2 are inexplicable. They are evidently to be explained through the incompleteness of the requirements enumerated above, by which the authors of the works cited were guided in their analysis of the spectra. For example, the limited character of the requirement of agreement between the calculated and experimental values of the thermodynamic functions is evident: it is unquestionably useful in the choice of the fundamental frequencies, but at the same time it gives no indications toward the solution of the problem of the assignment of one or another frequency to a particular symmetry type. Furthermore, not one of the requirements formulated above is connected with more or less valid representations of the character of the force field of the molecule.

In analyzing Kovner's works[5,6] on the calculation and interpretation of the vibrational spectra of benzene and its derivatives, we succeeded in formulating one more requirement, which arises from an approximate estimate of the force interaction within the naphthalene molecule. Along with these requirements which were spoken of above, we have set it as the basis for a new, more precise interpretation of the vibrational spectra of naphthalene and octadeuterionaphthalene.

In the present work we have basically employed the experimental values obtained in ref. 1 for the $C_{10}H_8$ and $C_{10}D_8$ frequencies; the values of certain frequencies (3070, 3001, 1576, 1024 cm^{-1} for $C_{10}H_8$ and 1391 cm^{-1} for $C_{10}D_8$) have been taken from ref. 2; the frequency 176 cm^{-1} for the nonplanar B_{1u} vibration of the "butterfly flapping" type has been taken from ref. 7. In this work, approximate values which guarantee that the naphthalene molecule belongs to the symmetry point group D_{2h} and which agree sufficiently well with Robertson's experimental values[8] were used for the interatomic distances and valence angles (see Figure).

DIFFERENCE RULE FOR THE NORMAL VIBRATIONS OF THE NAPHTHALENE AND OCTADEUTERIONAPHTHALENE MOLECULES

Let us consider the secular equation of arbitrary degree n

$$|D - \nu^2 E| = 0; \quad D = A \cdot K, \tag{1}$$

where A and K are the kinematic and dynamic interaction matrices (after introduction of symmetry coordinates and allowance for the additional relationships among them according to the rule set forth in ref. 9, p. 256), E is the unit matrix, and ν^2 is the square of the frequency of a normal vibration of the molecule.

It is well known that the sum of the roots of the secular equation (1) is equal to the sum of the diagonal elements of the matrix D (or its trace), and therefore

$$\mathrm{Sp}\, D_{C_{10}H_8} - \mathrm{Sp}\, D_{C_{10}D_8} = \sum_{i=1}^{n} [\nu_i^2(C_{10}H_8) - \nu_i^2(C_{10}D_8)]. \tag{2}$$

In the general case, the traces of the complete interaction matrices for the $C_{10}H_8$ and $C_{10}D_8$ molecules may be represented in the form

$$\mathrm{Sp}\, D_{C_{10}H_8} = a_{11}K_{11} + a_{12}K_{12} + a_{13}K_{13} + \ldots + a_{1n}K_{1n} + a_{22}K_{22} + \ldots + a_{nn}K_{nn} \tag{3}$$

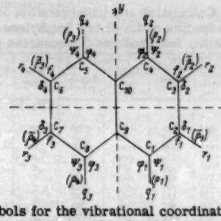

Symbols for the vibrational coordinates of the naphthalene molecule referred to in this work (coordinates of nonplanar vibrations are in parentheses). Symmetry of the molecule is D_{2h} ($\angle C_{10}C_4C_3 = \angle C_{10}C_9C_1 = \angle C_1C_2r_1 = 119°30'$; $\angle C_1C_2C_3 = \angle q_1C_1C_2 = 121°$; $S_{C_1C_9} = 1.42$ A; $S_{C_1C_2} = 1.36$ A, and $S_{C_2C_3} = S_{C_9C_{10}} = 1.395$ A).

and

$$\mathrm{Sp}\, D_{C_{10}D_8} = a'_{11}K_{11} + a'_{12}K_{12} + a'_{13}K_{13} + \ldots + a'_{1n}K_{1n} + a'_{22}K_{22} + \ldots + a'_{nn}K_{nn}, \tag{4}$$

only two (for nonplanar vibrations) or 4 (for planar vibrations) among the coefficients $a'_{11}; a'_{12}; \ldots; a'_{1n}; a'_{22}; \ldots; a'_{nn}$ being different from the corresponding coefficients in (3). This opens the possibility of an approximate estimate of the sum of the differences of the squares of the frequencies in Eq. (2), knowledge of a limited number of force constants of the molecule being sufficient for the indicated purpose.

The difference rule just cited is given below in concrete detail for each type of planar and nonplanar vibration of the $C_{10}H_8$ and $C_{10}D_8$ molecules.

a. PLANAR VIBRATIONS

For the planar vibrations ($9A_{1g} + 8B_{1g} + 8B_{2u} + 8B_{2u}$), in Eqs. (3) and (4), only those coefficients preceding the reduced force constants (q,q), (r,r), $(\varphi,\varphi) + (\psi,\psi) - 2(\varphi,\psi)$, $(\delta,\delta) + (f,f) - 2(\delta,f)$, i.e., A_{qq}, A_{rr}, $A_{\varphi\varphi}$, and $A_{\delta\delta}$, are different, while for all symmetry types

$$A_{qq}(C_{10}H_8) - A_{qq}(C_{10}D_8) = A_{rr}(C_{10}H_8) - A_{rr}(C_{10}D_8) = 0.4882,$$
$$A_{\varphi\varphi}(C_{10}H_8) - A_{\varphi\varphi}(C_{10}D_8) = A_{\delta\delta}(C_{10}H_8) - A_{\delta\delta}(C_{10}D_8) = 0.4964.$$

whence ($\alpha = A_{1g}, B_{1g}, B_{2u}, B_{2u}$):

$$\mathrm{Sp}\, D^{\alpha}_{C_{10}H_8} - \mathrm{Sp}\, D^{\alpha}_{C_{10}D_8} = 0.4882\,[(q,q)^{\alpha} + (r,r)^{\alpha}] + 0.4964\,[(\varphi,\varphi)^{\alpha} + (\psi,\psi)^{\alpha} - 2(\varphi,\psi)^{\alpha} + (\delta,\delta)^{\alpha} + (f,f)^{\alpha} - 2(\delta,f)^{\alpha}], \tag{5}$$

where, for example, for the totally symmetric vibrations

$$(q,q)^{A_{1g}} = K_{q,q_1} + K_{q,q_2} + K_{q,q_3} + K_{q,q_4}; \tag{6}$$

$$(r,r)^{A_{1g}} = K_{r_1r_2} + K_{r_1r_3} + K_{r_1r_4}; \tag{7}$$

$$(\varphi,\varphi)^{A_{1g}} + (\psi,\psi)^{A_{1g}} - 2(\varphi,\psi)^{A_{1g}} = K_{\varphi_1\varphi_2} + K_{\varphi_1\varphi_3} + K_{\varphi_1\varphi_4} + K_{\varphi_2\varphi_3} + K_{\varphi_2\varphi_4} + K_{\varphi_3\varphi_4} - 2(K_{\varphi_1\varphi_2} + K_{\varphi_1\varphi_3} + K_{\varphi_1\varphi_4} + K_{\varphi_2\varphi_3}); \tag{8}$$

$$(\delta,\delta)^{A_{1g}} + (f,f)^{A_{1g}} - 2(\delta,f)^{A_{1g}} = K_{\delta_1\delta_2} + K_{\delta_1\delta_3} + K_{\delta_1\delta_4} + K_{\delta_2\delta_3} + K_{\delta_2\delta_4} + K_{\delta_3\delta_4} + K_{f_1f_2} + K_{f_1f_3} + K_{f_1f_4} + K_{f_2f_3} + K_{f_2f_4} + K_{f_3f_4} - 2(K_{\delta_1f_1} + K_{\delta_1f_2} + K_{\delta_1f_3} + K_{\delta_1f_4}). \tag{9}$$

As was shown in ref. 6, for benzene $K_{q_1q_1} = 8.63$ spectroscopic units and $K_{q_1q_\alpha} = 0$ ($\alpha = 2, \ldots, 6$). There are no serious grounds for considering that the interaction of the C—H bonds in the naphthalene molecule can differ greatly from their interaction in benzene (see also ref. 10, where some additional considerations are presented in favor of this approximation), and therefore we may set

$$(q, q)^{A_{1g}} = (r, r)^{A_{1g}} = 8.63. \quad (10)$$

Furthermore, we may neglect the force interaction of CCH angles which have one atom in common, and the interaction of CCH angles which have no bonds or angles in common, by setting

$$K_{\varphi_1\varphi_2} = K_{\lambda_1 f_1} = 0 \quad (11)$$

and

$$\left.\begin{aligned} K_{\varphi_1\varphi_3} = K_{\varphi_1\varphi_4} = K_{\varphi_1\varphi_5} = K_{\varphi_1\varphi_6} = K_{\lambda_1\lambda_2} = K_{\lambda_1\lambda_3} = K_{f_1f_2} \\ = K_{f_1f_3} = K_{f_1f_4} = K_{\varphi_1\psi_2} = K_{\varphi_1\psi_3} = K_{\varphi_1\psi_4} = K_{\lambda_1 f_2} = K_{\lambda_1 f_3} = 0. \end{aligned}\right\} \quad (12)$$

As for the remaining force constants describing the interaction between CCH angles, they may be considered, as an approximation, to be equal to the corresponding force constants of benzene, i.e.,

$$K_{\varphi_1\psi_1} = K_{\varphi_1\psi_5} = K_{\lambda_1\lambda_5} = K_{f_1f_4} = k_\beta; \quad K_{\varphi_1\psi_1} = K_{\lambda_1 f_4} = l_\beta; \quad K_{\lambda_1\lambda_4} = n_\beta \quad (13)$$

(we employ here the symbols adopted in ref. 6).

Substitution of the force constants from (11)-(13) into (8) and (9) gives

$$\left.\begin{aligned} (\varphi, \varphi)^{A_{1g}} + (\psi, \psi)^{A_{1g}} - 2(\varphi, \psi)^{A_{1g}} = 2(k_\beta - l_\beta) = 1.50, \\ (\lambda, \lambda)^{A_{1g}} + (f, f)^{A_{1g}} - 2(\lambda, f)^{A_{1g}} = 2\left(k_\beta + \frac{1}{2}n_\beta - l_\beta\right) = 1.44, \end{aligned}\right\} \quad (14)$$

where we have used the values

$$k_\beta - l_\beta = 0.75, \quad k_\beta + \frac{1}{2}n_\beta - l_\beta = 0.72 \text{ and } k_\beta - \frac{1}{2}n_\beta - l_\beta = 0.77,$$

which may be obtained from ref. 6 if, in the linear combinations of the benzene force constants there cited, $(\beta_i\beta)^{A_{2g}}$, $(\beta_i\beta)^{B_{2u}}$, $(\beta_{\alpha i}\beta_\alpha)^{E_u}$, and $(\beta_{bi}\beta_b)^{E_g}$, we put $l_{1\beta} = l_{2\beta} = p = p_1 = p_2 = S_\beta = S_{1\beta} = 0$, which is equivalent to the approximations (11) and (12) of the present work. (We note that a certain ambiguity in the definition of n_β is not significant for the approximate estimation of the differences (5).) Substitution (10) and (14) in (5), we find

$$\mathrm{Sp}\, D^{A_{1g}}_{C_{10}H_8} - \mathrm{Sp}\, D^{A_{1g}}_{C_{10}D_8} \simeq 9.886. \quad (15)$$

It may be shown analogously that

$$\mathrm{Sp}\, D^{B_{1g}}_{C_{10}H_8} - \mathrm{Sp}\, D^{B_{1g}}_{C_{10}D_8} - \mathrm{Sp}\, D^{B_{2u}}_{C_{10}H_8} - \mathrm{Sp}\, D^{B_{2u}}_{C_{10}D_8} \simeq 9.935, \quad (16)$$

$$\mathrm{Sp}\, D^{B_{2u}}_{C_{10}H_8} - \mathrm{Sp}\, D^{B_{2u}}_{C_{10}D_8} \simeq 9.886. \quad (17)$$

b. NONPLANAR VIBRATIONS

For the nonplanar vibrations ($4A_{1u} + 4B_{1u} + 3B_{2g} + 4B_{2g}$), only the kinematic coefficients preceding the reduced force constants (ρ,ρ) and ($\bar{\rho},\bar{\rho}$) in Eqs. (3) and (4) are different, while for vibrations of all symmetry types $A_{\rho\rho}(C_{10}H_8) - A_{\bar{\rho}\bar{\rho}}(C_{10}D_8) = A_{\rho\rho}(C_{10}H_8) - A_{\bar{\rho}\bar{\rho}}(C_{10}D_8) = 0.4973$; therefore

$$\mathrm{Sp}\, D^{\alpha}_{C_{10}H_8} - \mathrm{Sp}\, D^{\alpha}_{C_{10}D_8} = 0.4973\,[(\rho, \rho)^\alpha + (\bar{\rho}, \bar{\rho})^\alpha],$$

$$(\alpha = A_{1u};\ B_{1u};\ B_{2g};\ B_{2g}), \quad (18)$$

where, for example, for the vibrations of type B_{1u}

$$(\rho, \rho)^{B_{1u}} + (\bar{\rho}, \bar{\rho})^{B_{1u}} = K_{\rho_1\rho_1} + K_{\rho_1\rho_2} + K_{\rho_1\rho_3} + K_{\rho_1\rho_4} + K_{\bar{\rho}_1\bar{\rho}_1} + K_{\bar{\rho}_1\bar{\rho}_2} + K_{\bar{\rho}_1\bar{\rho}_3} + K_{\bar{\rho}_1\bar{\rho}_4}. \quad (19)$$

In (19), we may neglect the force interaction of $\bar{\rho}_1$ with $\bar{\rho}_3$ and $\bar{\rho}_4$, setting

$$K_{\bar{\rho}_1\bar{\rho}_3} = K_{\bar{\rho}_1\bar{\rho}_4} = 0 \quad (20)$$

(it is unlikely that vibrations of the C_2—H_2 bond could affect the vibrations of the C_8—H_8 and C_7—H_7 bonds to any extent, the latter being located at relatively large distances from it). The same may be asserted (but with a lesser degree of accuracy) with respect to the force interaction of ρ_1 with ρ_3, ρ_3, and ρ_4, reckoning

$$K_{\rho_1\rho_3} = K_{\rho_1\rho_3} = K_{\rho_1\rho_4} = 0. \quad (21)$$

It is also to be expected that the constants $K_{\rho_1\rho_1}$, $K_{\bar{\rho}_1\bar{\rho}_1}$, and $K_{\bar{\rho}_1\bar{\rho}_2}$ differ only insignificantly from the corresponding force constants of benzene evaluated by Kovner,[6] so that as a first approximation we may take

$$K_{\rho_1\rho_2} = K_{\bar{\rho}_1\bar{\rho}_2} = 0.6256 \text{ and } K_{\bar{\rho}_1\bar{\rho}_2} = -0.1006. \quad (22)$$

Substitution of (20)-(22) in (19) and (18) gives

$$\mathrm{Sp}\, D^{B_{1u}}_{C_{10}H_8} - \mathrm{Sp}\, D^{B_{1u}}_{C_{10}D_8} \simeq 0.572. \quad (23)$$

It can be demonstrated analogously that

$$\mathrm{Sp}\, D^{A_{1u}}_{C_{10}H_8} - \mathrm{Sp}\, D^{A_{1u}}_{C_{10}D_8} = \mathrm{Sp}\, D^{B_{2g}}_{C_{10}H_8} - \mathrm{Sp}\, D^{B_{2g}}_{C_{10}D_8} \simeq 0.672 \quad (24)$$

and

$$\mathrm{Sp}\, D^{B_{2g}}_{C_{10}H_8} - \mathrm{Sp}\, D^{B_{2g}}_{C_{10}D_8} \simeq 0.572. \quad (25)$$

The assignment in refs. 1 and 2 of the frequencies 957, 782, 475, and 176 cm^{-1} (naphthalene) and 791, 628, 408, and 160 cm^{-1} ($C_{10}D_8$) to type B_{1u} is not subject to doubt, since it follows directly from the selection rules for intensities. With the help of the frequencies just listed we find

$$\sum_i \left[\nu_i^2(C_{10}H_8) - \nu_i^2(C_{10}D_8)\right] = 0.572.$$

The agreement of this result with (23) confirms the validity of the assumptions which we have made concerning the magnitude of the force constants characterizing the bending of the C—H bonds out of the plane of the molecule.

INTERPRETATION OF THE SPECTRA

In the table are presented the frequencies of the $C_{10}H_8$ and $C_{10}D_8$ molecules which we have assigned as fundamental frequencies. In the same table, the interpretations of refs. 1 and 2 are given for comparison.

As fundamental frequencies of $C_{10}H_8$ we have assigned all the frequencies taken as fundamental in ref. 1, with the exception of 3011, 2947, 1680, 1440 (No. 37), 752, and 585 cm^{-1}, which are to be considered as combinations. In addition, we have taken 3001, 2994, 1716, 1099, 825, and 611 cm^{-1} as fundamental frequencies of naphthalene. Some of these frequencies (3001, 1716, 1099, and 611 cm^{-1}) were taken as fundamental in ref. 2. From the set of fundamental frequencies of the $C_{10}D_8$ molecule listed in ref. 1, we have excluded 1626, 1437, 1120, 929, 831, 777, 756, and 721 cm^{-1}, which may also be considered as combinations. In their place, we have taken 1408, 1391, 1006, 879, 875 (No. 6), 819, 738, and 671 cm^{-1} as fundamental frequencies of the $C_{10}D_8$ molecule.

Fundamental Frequencies of the Naphthalene and $C_{10}D_8$ Molecules

Symmetry type	Frequency No.	Approximate form of the vibration	From the present work		From ref. 1		From ref. 2	
			$C_{10}H_8$	$C_{10}D_8$	$C_{10}H_8$	$C_{10}D_8$	$C_{10}H_8$	$C_{10}D_8$
A_{1g}	1	C–H bond stretching	3063	2288	3063	2268	3058	2268
	2	The same	3028	2257	3028	2257	3001	2257
	3	C–C bond stretching	1578	1548	1578	1548	1576	1548
	4	The same	1380	1380	1393	1380	1379	1379
	5	Planar C–H deformation vibration	1240	1006	1240	929	1240	1006
	6	The same	1144	875	878	752	943	752
	7	Skeletal breathing	1024	962	1025	962	1024	962
	8	Planar skeletal deformation	760	694	760	694	762	694
	9	The same	511	491	511	491	512	491
A_{1u}	10	Nonplanar skeletal deformation	1000	927	700	—	842	—
	11	Out-of-plane C–H bending	875	665	1000	—	1307	—
	12	The same	700	554	875	—	1094	—
	13	Nonplanar skeletal deformation	400	360	400	—	400	—
B_{1g}	14	C–H bond stretching	3051	2302	3051	2302	3025	2302
	15	The same	3001	2260	3015	2260	2960	2257
	16	C–C bond stretching	1628	1573	1628	1573	1625	1573
	17	The same	1586	1408	1586	1437	1586	1437
	18	Planar C–H deformation vibration	1440	1295	1440	1295	1439	1170
	19	Planar skeletal deformation	1337	1219	1337	1219	879	777
	20	Planar C–H deformation vibration	1168	829	1144	829	1145	929
	21	Planar skeletal deformation	611	569	585	541	611	569
B_{1u}	22	Out-of-plane C–H bending	957	791	957	791	956	790
	23	The same	782	628	782	628	780	628
	24	Nonplanar skeletal deformation	475	408	475	408	475	408
	25	"Butterfly flapping"	176	160	176	160	176	160
B_{2g}	26	Out-of-plane C–H bending	941	752	1168	875	1167	875
	27	The same	715	541	941	777	715	541
	28	Nonplanar skeletal deformation	385	339	385	339	191	180
B_{2u}	29	C–H bond stretching	3014	2278	3014	2278	3034	2285
	30	The same	2994	2215	2947	2215	2942	2256
	31	C–C bond stretching	1595	1403	1595	1540	1601	1440
	32	The same	1387	1260	1387	1260	1385	1258
	33	Planar C–H deformation vibration	1268	1039	1268	1039	1268	1050
	34	The same	1139	886	1139	886	1125	885
	35	Planar skeletal formation	825	819	752	721	620	595
	36	The same	361	328	361	328	362	328
B_{3g}	37	Out-of-plane C–H bending	1099	875	1440	1120	1099	829
	38	The same	878	671	715	569	774	671
	39	Nonplanar skeletal deformation	285	270	285	270	588	541
	40	The same	191	180	191	180	285	270
B_{3u}	41	C–H bond stretching	3070	2299	3072	2299	3070	2323
	42	The same	2976	2259	2976	2259	2984	2271
	43	C–C bond stretching	1716	1540	1680	1626	1723	1569
	44	The same	1510	1391	1510	1403	1508	1391
	45	Planar C–H deformation vibration	1211	946	1211	948	1143	905
	46	The same	1012	879	1012	831	1012	830
	47	Skeletal breathing	876	738	876	756	742	680
	48	Planar skeletal deformation	618	593	618	593	581	546

In the table are also indicated the frequencies of the vibrations of type A_{1u} which are inactive in the vibrational spectra of $C_{10}D_8$: 927, 665, 554, and 360 cm^{-1}. Selected by taking account of the product and difference rules, these frequencies in addition combine well with many active fundamental frequencies; this also explains the presence in the infrared spectrum of $C_{10}D_8$ of a large number of combination frequencies and overtones.

The regrouping of the fundamental frequencies with respect to symmetry type which we have carried out agrees excellently with the product rule and the difference rules (15)-(17) and (23)-(25), and the improvement noted in this respect in the values of certain fundamental frequencies of naphthalene guarantees a sufficiently good agreement between the calculated values of the thermodynamic functions of naphthalene and their experimental values.[11] The latter fact confirms the reliability of the set of inactive naphthalene frequencies (1000, 875, 700, and 400 cm^{-1}) listed in ref. 1, while the set of inactive frequencies (1307, 1094, 842, and 400 cm^{-1}) proposed in ref. 2 proves to be precluded by the difference rule (24) and by the product rule. Finally, the question of the assignment of the naphthalene frequencies 941 and 878 cm^{-1}, which has repeatedly aroused disputes, is at last settled by the present work.

ON THE VALUES OF CERTAIN FORCE CONSTANTS OF NAPHTHALENE

With the help of the refined sets of fundamental frequencies of the $C_{10}H_8$ and $C_{10}D_8$ molecules, it is possible to carry out a refinement of the values of these naphthalene force constants about which we previously expressed preliminary considerations.

Considering, as before, that on going from benzene to naphthalene the force constants $K_{q_1q_1}$, $K_{r_1r_1}$, $K_{p_1\bar{p}_1}$, ..., $K_{p_1p_4}$ do not change and remain at $K_{q_1q_1} = K_{r_1r_1} = 8.63$, $K_{\bar{p}_1\bar{p}_1} = 0.6256$, $K_{\bar{p}_1\bar{p}_2} = -0.1006$, and $K_{\bar{p}_1\bar{p}_3} = K_{\bar{p}_1\bar{p}_4} = 0$, then from Eqs. (2), (5), and (18) we find, with the help of the frequencies selected,

$$k_\beta - l_\beta = K_{\varphi_1\varphi_1} - K_{\varphi_1\varphi_2} = K_{\phi_1\phi_1} - K_{\phi_1\phi_2}$$

$$= K_{h_1h_1} - K_{h_1f_1} = K_{f_1f_1} - K_{f_1h_1} = 0.750;$$

$$n_\beta = K_{h_1h_2} = -0.055; \quad K_{p_1p_1} = 0.6294; \quad K_{p_1p_2} = -0.0046;$$

$$K_{p_1p_3} = 0.0012 \text{ and } K_{p_1p_4} = -0.0011.$$

The listed force constants of naphthalene are almost identical with the corresponding force constants of benzene. The constant $K_{p_1p_2}$ undergoes the greatest change in the transition from C_6H_6 to $C_{10}H_8$ (in benzene, it equals −0.0187). The decrease in the constant $K_{p_1p_2}$ is evidently explained by the fact that the benzene rings which are joined in the $C_{10}H_8$ molecule are less mobile and flexible with respect to nonplanar deformations than are free rings. Therefore, the attraction between two opposite C—H bonds in the naphthalene molecule diminishes. The constants $K_{p_1p_3}$ and $K_{p_1p_4}$, which have no analogs among the benzene force constants, prove to be close to zero.

If, in addition, we set $K_{p_1p_3} = 0.6256$ and use the sets of fundamental frequencies proposed in refs. 1 and 2 for naphthalene and octadeuteronaphthalene in calculating the remaining force constants, then we have:

(a) Using the set of frequencies proposed in ref. 1:

$$k_\beta - l_\beta = 0.495, \quad n_\beta = 0.242, \quad K_{p_1p_2} = 0.343,$$

$$K_{p_1p_3} = -0.692 \text{ and } K_{p_1p_4} = 0.348;$$

(b) Using the set of frequencies proposed in ref. 2:

$$k_\beta - l_\beta = 0.558, \quad n_\beta = 0.232, \quad K_{p_1p_2} = 0.259,$$

$$K_{p_1p_3} = -0.322 \text{ and } K_{p_1p_4} = 0.055.$$

Thus the naphthalene force constants calculated with the help of the sets of fundamental frequencies proposed in refs. 1 and 2 have nothing in common with the actual values of the naphthalene force constants. For example, one cannot agree with the values 0.495 and 0.558 for the constant $k_\beta - l_\beta$, since it is well known that $k_\beta - l_\beta$ changes extremely little on going from the simplest hydrocarbons to the most complex aromatic compounds (0.74 in ethane and 0.75 in benzene). It is likewise inadmissible that n_β should be of the same order as $k_\beta - l_\beta$, and that the con-

stants $K_{\rho_1\rho_3}$, $K_{\rho_1\rho_5}$, and $K_{\rho_1\rho_6}$ should agree in order of magnitude with the constant $K_{\rho_1\rho_1}$ which describes the interaction of the coordinate ρ_1 with itself.

The difficulties just mentioned, arising during analysis of the force field of the naphthalene molecule with the help of the interpretations of refs. 1 and 2, also impelled us to reconsideration of these interpretations.

In conclusion, I express my gratitude to E. V. Shpol'skii for his interest in this work.

REFERENCES

1. E. R. Lippincott and E. J. O'Reilly, J. Chem. Phys. 23, 238 (1953).
2. A. L. McClellan and G. C. Pimentel, J. Chem. Phys. 23, 245 (1953).
3. J. Goubeau, H. Luther, K. Feldmann, and G. Braudes, Chem. Ber. 86, 214 (1953).
4. G. Herzberg, "Kolebatel'nye i vrashchatel'nye spektry mnogoatomnykh molekul" (Vibrational and Rotational Spectra of Polyatomic Molecules). Izd. Inostrannoi Lit., Moscow, 1949.
5. M. A. Kovner, Raschet i interpretatsiya kolebatel'nykh spektrov benzola i ego proizvodnykh (Calculation and interpretation of the vibrational spectra of benzene and its derivatives), Dokt. diss. (Doctoral dissertation), Minsk, 1957; Doklady Akad. Nauk SSSR 97, 65 (1954).
6. M. A. Kovner, Zhur. Eksptl. i Teoret. Fiz. 26, 598 (1954).
7. W. B. Person, G. C. Pimentel, and O. Schnepp, J. Chem. Phys. 23, 230 (1953).
8. J. M. Robertson, "Organic Crystals and Molecules." Cornell Univ. Press, Ithaca, N.Y., 1953.
9. M. V. Vol'kenshtein, M. A. El'yashevich, and B. I. Stepanov, "Kolebaniya molekul" (Molecular Vibrations), Vol. 1. Gosudarst. Izd. Tekh. i Teoret. Lit., Moscow, 1949.
10. N. I. Zhirnov, Opt. i Spektr. 6, 162 (1959), Optics and Spectroscopy 6, 105 (1959).
11. G. M. Barrow and A. L. McClellan, J. Am. Chem. Soc. 73, 573 (1951).

INFLUENCE OF TEMPERATURE ON ABSORPTION FOR CERTAIN VIBRATIONAL BANDS OF GASEOUS CHLOROFORM AND BROMOFORM

M. P. Lisitsa and Yu. P. Tsyashchenko

Received 23 March 1960

A quantitative study of the influence of temperature on the intensity of vibrational absorption bands in gases was begun very recently.[1-3] The elucidation of all aspects of this quite complex phenomenon requires the setting up of broad experimental and theoretical investigations.

The temperature dependence of the intensities of the vibrational absorption bands of liquid $CHCl_3$ and $CHBr_3$ has previously been established by the authors.[4,5] In the present communication, we set forth the results of a quantitative study of the same dependence for the bands of the combination frequency $\nu_1 + \nu_4$ of gaseous $CHCl_3$ and $CHBr_3$ and of the fundamental frequency ν_1 of gaseous $CHBr_3$.

Depending on the frequency of the vibration, we used glass and quartz cells with sealed-on windows. The heating of the cells was accomplished with a cylindrical electric furnace, closed at the ends with rock-salt plates. The furnace was surrounded by a water-cooled jacket. The temperature drop between the middle and the ends of the cell did not exceed 10°.

The liquid substance, carefully weighed out in a predetermined amount, was put into the cell in a sealed glass ampoule; the cell was evacuated to a pressure of about 10^{-2} mm Hg and was then detached from the vacuum line. After shaking the cell, the ampoule was broken and the liquid evaporated. The initial temperature of the measurements was determined by that saturated vapor pressure of chloroform or bromoform which was necessary to obtain the optimum optical density when the liquid was completely evaporated. The final temperature was set by the appearance of irreversible processes leading to a diminution of the vapor density of the substance studied. This (as well as the tightness of the cell) could be established by the reproducibility of the absorption band intensities on lowering the temperature to the initial value.

In the calculation of the absorption coefficients, the optical density of the vapor was identified with the optical density of an equivalent layer of liquid;* i.e., a layer possessing the same quantity of absorbing centers in the path of the beam as the vapor did. The values obtained for the integrated absorption coefficients were corrected for the spectral slit width of the apparatus,* calculated with the help of the formula presented in refs. 7 and 8. The correction was introduced on the assumption of a dispersion contour of the bands; however, for the relationships existing between the spectral slit width of the apparatus, the observed halfwidth of the band, and its optical density at the maximum, it differs from the correction introduced on the assumption of a Gaussian contour by only 1-3% in all.[2,5] The correction for the "wings" was not taken into account. No selective emission from the heated vapors was observed. The pronounced (especially at high temperatures) continuous background from the furnace and the cells was allowed for in the measurements. The integrated absorption was determined with an error up to 15% altogether. The relative changes of intensity with temperature are presented with a precision of 5-7%.

*The measurements were performed on an IKS-6 spectrophotometer.

The influence of the liquid-vapor phase transition on the intensity of the three absorption bands studied is illustrated by the data presented in the Table. It is easy to see that in all cases the transition mentioned is accompanied by a significant diminution of the integrated absorption: for the ν_1 vibration of bromoform it diminishes by a factor of 6, and in the two remaining cases by a factor of approximately 3. The differences in the combinations of rotational and vibrational transitions corresponding to the bands under consideration are responsible for the qualitatively opposite change in their halfwidths. While the latter increases approximately twofold

for the band of the fundamental frequency ν_1, it diminishes by a factor of more than 2 for the remaining bands.

Influence of the Liquid-Vapor Phase Transition on the Intensity and Halfwidth of the Absorption Bands of Bromoform and Chloroform

Substance	Vibration	Integrated absorption (cm^{-2})		Halfwidth (cm^{-1})		Temperature (°C)
		Liquid	Vapor	Liquid	Vapor	
$CHBr_3$	ν_1	12000	2000	14	23	150
The same	$\nu_1 + \nu_4$	3300	940	32	12	150
$CHCl_3$	$\nu_1 + \nu_4$	1600	720	25	14	50

The unidentified short wavelength satellite (ν 4248 cm^{-1}) of the band of the $\nu_1 + \nu_4$ combination frequency of $CHCl_3$ is much more distinctly resolved in the gas than in the liquid. As has already been mentioned in ref. 10, its nature is as yet unclarified. However, it may now be noted that the appearance of this satellite is not brought about by resonance interaction of the level $E_{\nu_1 + \nu_4}$ with any higher-order level, since the relative intensity of the band of the combination frequency and of the satellite under consideration remains constant during the liquid-vapor phase transition. In the case of Fermi resonance this cannot happen, as a rule.[6,11]

The results of the temperature measurements are represented in Figs. 1 and 2 in the form of the observed band contours of the $\nu_1 + \nu_4$ combination frequency of chloroform and the ν_1 fundamental vibration of bromoform, and in Fig. 3 in the form of the temperature dependences of the integrated absorption coefficients in the bands of these vibrations and of the $\nu_1 + \nu_4$ bromoform vibration. As follows from Figs. 1 and 2, the halfwidth of the bands of the vibrations $\nu_1 + \nu_4$ of $CHCl_3$ and ν_1 of $CHBr_3$ increases as the temperature rises, from 14 to 25 cm^{-1} in the first case and from 23 to 25.5 cm^{-1}

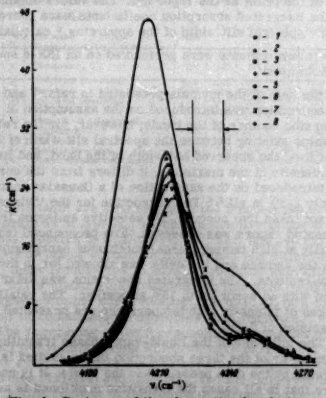

Fig. 1. Contours of the absorption band of the $\nu_1 + \nu_4$ combination frequency of gaseous $CHCl_3$ at various temperatures. Temperature (in °C): 1—50; 2—150; 3—200; 4—250; 5—300; 6—350; 7—400; 8—absorption of an equivalent layer of liquid at a temperature of 50°C.

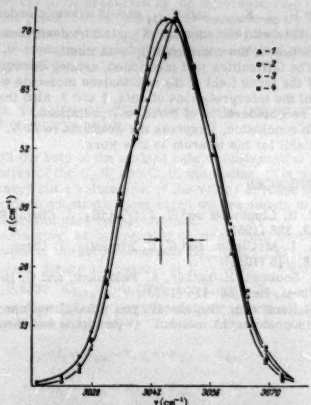

Fig. 2. Contours of the absorption band of the ν_1 fundamental vibration of gaseous $CHBr_3$ at various temperatures. Temperature (in °C): 1—150; 2—200; 3—250; 4—300.

in the second.*

*The values given have been corrected for the magnitude of the spectral slit width.

The integrated absorption in the band of the $\nu_1 + \nu_4$ combination frequency of chloroform was evaluated after separation of the observed doublet into its components. For the lower temperatures, such a separation is easily realizable. In the high temperature case, it may be carried out with a certain error which will be absent only if the change in band contour is symmetrical. If the error referred to actually took place, the temperature-dependence curve being sought would have to run somewhat more steeply than the one presented in Fig. 3.

The experimentally-obtained temperature dependences have been compared with the theoretical ones computed with the help of the well-known formulas of statistical theory.[12] As can be seen from Fig. 3, theory and

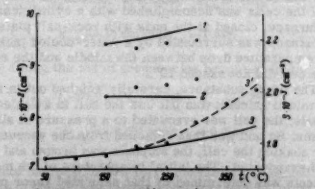

Fig. 3. Experimental (points) and theoretical (solid lines) temperature dependence of the integrated intensity of various bands of gaseous $CHBr_3$ and $CHCl_3$. Curve 1—$\nu_1 + \nu_4$ combination frequency of $CHBr_3$ (left scale); curve 2—ν_1 fundamental frequency of $CHBr_3$ (right scale); curves 3,3'—$\nu_1 + \nu_4$ combination frequency of $CHCl_3$ (left scale).

experiment are in satisfactory agreement within the limits of error for the bands of the ν_1 and $\nu_1 + \nu_4$ bromoform vibrations. An analogous result was previously established during the study of the $\nu_1 + \nu_3$ and $\nu_1 + (\nu_1 + \nu_4)$ resonance doublet of gaseous CCl_4.[3] However, in the case of $CHCl_3$, the temperature increase in the intensity of the band of the $\nu_1 + \nu_4$ vibration somewhat surpasses that predicted by the theory. Similar deviations from theory (sometimes very marked) were also observed in ref. 2. The authors[2] explain them exclusively by intermolecular interactions arising in consequence of molecular collisions. The experiments performed by them to clarify the influence of the isothermal gas pressure* on the band intensity qualitatively confirm such an explanation. However, aside from collisions, it is also necessary to take account of other factors, the influence of which may be substantial in certain cases. Anharmonicity of the vibrations in particular belongs in this group. As was shown in ref. 2, its influence is insignificant for diatomic molecules. Nevertheless, for certain vibrations of polyatomic molecules such a conclusion may prove inadequate.

*The absorption induced by isothermal pressure has been noted in a whole series of cases.[13]

Let us note, finally, that the integrated absorption in the band of the $\nu_1 + \nu_3$ and $\nu_1 + (\nu_1 + \nu_4)$ resonance doublet of gaseous CCl_4, which displays a marked temperature dependence, does not change during an isothermal pressure change within wide limits (by an order of magnitude[14]). Furthermore, the temperature-controlled changes in pressure, which are practically identical in our case, are accompanied by substantially different temperature dependences of the band intensities. For example, during the study of the $\nu_1 + \nu_4$ combination frequency in the temperature interval 150-350°C, the pressure of the $CHCl_3$ and $CHBr_3$ vapors increases from 560 to 760 and from 455 to 620 mm Hg respectively, while the absorption increases by 3 and 11%—in the first case, not exceeding the limits of error of the experiment. These facts apparently indicate that the contribution of intermolecular interaction to the temperature dependence must be determined not only by the number of collisions,[2] but also by their effectiveness,* which depends on the closeness of approach of the colliding molecules. The latter, it is clear, will be different at identical pressures and an identical number of collisions but at different temperatures. Perhaps it is just for this reason that the increase in intensity observed in ref. 2 during an isothermal increase in pressure is markedly less than that brought about by an analogous temperature-controlled pressure change, even when one takes account of the normal distribution of the molecules over the vibrational states.

*At a given temperature, the effectiveness must be determined both by the properties of the molecule itself and by the character of the intramolecular vibration.

REFERENCES

1. M. P. Lisitsa and V. N. Malinko, Ukrain. Fiz. Zhur. 3, 773 (1958); Opt. i Spektr. 6, 694 (1959), Optics and Spectroscopy 6, 450 (1959).
2. P. A. Bazhulin and V. N. Smirnov, Opt. i Spektr. 7, 193 (1959), Optics and Spectroscopy 7, 123 (1959).
3. M. P. Lisitsa and V. L. Strizhevskii, Opt. i Spektr. 7, 478 (1959), Optics and Spectroscopy 7, 305 (1959).
4. M. P. Lisitsa and Yu. P. Tsyashchenko, Opt. i Spektr. 9, 438 (1960), Optics and Spectroscopy 9, 229 (1960).
5. M. P. Lisitsa and Yu. P. Tsyashchenko, Opt. i Spektr. 9, 188 (1960), Optics and Spectroscopy 9, 99 (1960).
6. M. P. Lisitsa and V. N. Malinko, Ukrain. Fiz. Zhur. 3, 482 (1959).
7. A. N. Aleksandrov and V. A. Nikitin, Uspekhi Fiz. Nauk 56, 3 (1955).
8. D. A. Ramsay, J. Am. Chem. Soc. 74, 42 (1952).
9. V. N. Smirnov, Vestnik Moskov. Gosudarst. Univ., Ser. Fiz. 1, 61 (1959).
10. M. P. Lisitsa and Yu. P. Tsyashchenko, Opt. i Spektr. 6, 605 (1959), Optics and Spectroscopy 6, 396 (1959).
11. V. L. Strizhevskii, Opt. i Spektr. 8, 165 (1960), Optics and Spectroscopy 8, 86 (1960).
12. M. V. Vol'kenshtein, M. A. El'yashevich, and B. I. Stepanov, "Kolebaniya molekul" (Molecular Vibrations), Vol. 2. Gosudarst. Izd. Tekh. i Teoret. Lit., Moscow, Leningrad, 1949.
13. V. N. Filimonov, Uspekhi Fiz. Nauk 69, 565 (1959).
14. V. N. Malinko, Kand. diss. (Dissertation), Kiev, 1959.

THE TEMPERATURE DEPENDENCE OF RAMAN BAND INTENSITIES IN CRYSTALLINE AND GLOSSY SOLIDS

I. Experimental Investigation in the Stokes Region of the Spectrum

Ya. S. Bobovich and T. P. Tulub

Received 8 March 1960

The temperature behavior of the Raman band intensities in the Stokes region of the spectra of quartz, Iceland spar, fluorite, corundum, barite, fused quartz, alkaline silica glass, polymethyl methacrylate, and polystyrene has been studied. The results obtained are explained on the basis of proposals concerning the influence of the internal field of the medium (its refractive index and dielectric constant).

I. INTRODUCTION

The influence of temperature on band intensities is one of a number of questions in Raman spectroscopy which have not yet received an adequate theoretical interpretation. In the Stokes region only the temperature behavior of liquids has been studied with sufficient reliability and detail. A fundamental experimental fact established here is a decrease of the integrated band intensity in heated liquids instead of the predicted theoretical increase (a summary of the majority of the investigations of this effect, completed before 1957, is contained in ref. 1). The results of investigations on solids have an indeterminate character (compare refs. 2-4 with refs. 5-7; therefore, it is of considerable importance to begin a systematic investigation of solids, applying new experimental techniques for this purpose.

One possible interpretation of the phenomenon observed in solids is of special interest to us. Earlier, a similarity in the temperature and concentration behavior of band intensities in the spectra of liquids had been established by us[8] and also in a work by one of us and Pivovarov.[9] In the work of Pivovarov[10] concentration anomalies are considered to be a manifestation of the universal influence of the internal field of the medium, given by its refractive index. It is natural to extend this to an interpretation of the temperature phenomena. In solids the refractive index changes only slightly with temperature. Therefore, solids, it would appear, are simpler than liquids as the objects of investigation: at least one source of the anomalies is excluded for them.* It is substantially otherwise. The absence in solids of large temperature changes of the refractive index can, in some cases, permit one to follow the influence of the dielectric constant of the substance (another macroscopic characteristic of the internal field) on the measured quantities. Finally, one should keep in mind that many crystals and glasses can be heated to very high temperatures. This in itself permits the study of new aspects of the phenomena.

*In this sense a comparative investigation of gases and liquids is interesting. However, experiments with gases (but not with solids) by themselves can not be significant in clarifying the role of the internal field in the temperature anomalies of intensities. In gases which are not strongly compressed any intermolecular interactions are practically absent.

2. DESCRIPTION OF THE RESULTS OF THE INVESTIGATION

We measured in the Stokes region the temperature dependence of the majority of Raman bands of crystalline quartz, Iceland spar, fluorite, corundum, barite, fused quartz, alkaline silica glass, polymethyl methacrylate, and polystyrene. The techniques of the experiment, relating to the means of heating the samples and measuring their temperatures, are contained in a preliminary communication.[11] In the following experiments the only additional step taken was to install thermal shields; a glass or quartz tube was placed over the sample with the electric heater. This achieved a more uniform distribution of temperature over the volume of the sample. Application of the heat shield enabled us to improve on the earlier results on fused quartz.

The basic results of the investigation are given in Tables 1 and 2 and are shown graphically in Figs. 1-3. All of the points were obtained by averaging a large number of measurements. We will examine the given data for each of the samples separately.

Crystalline quartz*

*The corresponding graphs are given in a preliminary communication.

Being particularly rich in bands, including bands with low frequencies, the spectrum of this substance is very suitable for study in the sense of interest to us. We succeeded in measuring the temperature dependence of the intensity for practically all of the bands of the sample. No change in intensity of a group of very weak bands lying in the region 800-1230 cm^{-1} was revealed though the sample was heated to approximately 500°K. This agrees well with theoretical predictions since, even for the lowest frequency band of this group, the anticipated temperature effect should be comparable with the experimental error (~9%). The intensity of other bands with the frequencies 460, 200, and 125 cm^{-1} increases with an elevation of the temperature. This change becomes more pronounced as the frequency becomes lower, but the first and second bands change by less than the theoretical amount.

Thus, the spectrum of crystalline quartz behaves with temperature in qualitative agreement with the predictions of theory.

Iceland Spar (Fig. 1)

The spectrum of Iceland spar is not as rich in bands as the spectrum of quartz. The most intense of its bands, which have been studied by a series of other authors, have frequencies of 150, 280, and 1088 cm^{-1}. The first two are assigned to the vibrations of the lattice, the last to the completely symmetrical internal vibration of the CO_3^{--} anion. On a change of the sample temperature from room temperature to 545°K the intensity of the 150 and 280 cm^{-1} bands practically does not change; the intensity of the 1088 cm^{-1} band over the same temperature interval increases by approximately 30%, which significantly ex-

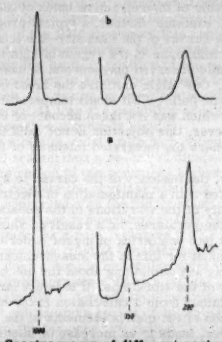

Fig. 1. Spectrograms of different regions of the spectrum of Iceland spar at room temperature (a) and at 540°K (b).

ceeds the mean error of measurement (±5%).

It is possible to assume that our observations are related to the action of a trivial factor—self-absorption of the sample. Indeed, the investigated sample was of a slight brown-yellow color. To verify this, we made measurements of the absorption of the sample on an SF-4 spectrophotometer with special apparatus for three temperature points over a broad spectral interval.* Without citing the results of these measurements we will note only that the correction for self-absorption is of a comparatively very small magnitude. Accordingly, the observed anomalies reflect not an apparatus, but a real physical phenomenon.

*The authors thank V. P. Klochkov for his assistance in making these measurements.

Thus, in the spectrum of Iceland spar in the Stokes region, a temperature anomaly of the intensity, completely analogous to that observed in liquids, is discovered.

Fluorite (Fig. 2)

The single first order band increases in intensity with temperature; however, as also in crystalline quartz, the change is slower than required by theory.

Corundum

Though the crystal absorbs the light considerably, nevertheless the lowest frequency band at 420 cm^{-1} increases in intensity with an increase in temperature. Quantitative evaluation of the growth of the intensity (with consideration of self-absorption) is difficult.

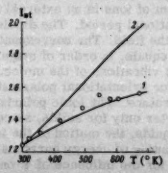

Fig. 2. The temperature dependence of the intensity of the 330 cm^{-1} band in the spectrum of fluorite. Curve 1—experimental; curve 2—theoretical.

Table 1. Intensities of Raman Bands of Barite for Two Temperatures

Frequency (cm^{-1})	Temperature (°K)	$I_{at.} \sim \frac{1}{1-e^{-\frac{h\nu}{kT}}}$ (theor.)	I_{at} (exp.)	$\left(\frac{I_{T_1}}{I_{T_2}}\right)^*_{theor.}$	$\left(\frac{I_{T_1}}{I_{T_2}}\right)^*_{exp.}$
470	300	1.11	437	1.45	1.5
	700	1.61	655		
625	300	1.04	50	1.30	1.4
	700	1.36	70		
965	300	~1.0	240	1.15	1.25
	700	1.15	300		
1140	300	~1.0	~42 **	1.11	~1 **
	700	1.11	~42 **		

*In Tables 1 and 2, T_1 is the room and T_2 the high temperature.

**The measurements are not accurate due to the diffuse nature of the band.

Barite (Table 1)

Since the sample cracked on heating, we are not inclined to assign to the results of the measurements a high quantitative accuracy. However, there is no doubt of the qualitative fulfillment of the theoretical relation.

Fused quartz (Fig. 3)

The sample was investigated over a very broad range of temperatures (up to ~900°K). For the bands at ~800 cm^{-1} the integrated intensity was measured; in two other cases (the 400 and 300 cm^{-1} bands) only the ordinates. The latter is quite correct since the respective bands are particularly wide and broaden little with temperature. All of the measurements (cf. Fig. 3 for the 400 cm^{-1} frequency) showed a growth of intensity with temperature which, as before, was slower than the theoretical.*

*In the results of ref. 11 refinements are introduced.

Silica glass of the composition 12 Na_2O-8 K_2O-80 SiO_2*

*The numbers denote the molecular percents.

The sample was investigated up to ~550°K in the Stokes region of the spectrum (the band at ~500 cm^{-1}). The observed temperature shift of the intensity coincides accurately with the theoretical.

Polymethylmethacrylate (Table 2)

Due to the comparatively low softening temperature of the sample, the heating was limited to temperatures below 390°K. The intensity of all bands decreased with temperature in varying degrees. The least of all susceptible to the heating was the strongly polarized band at 820 cm^{-1}. Thus, the same anomaly is observed in this solid as in liquids.

Polystyrene

For the same reasons the sample could be heated only to 355°K. With this no substantial change of band

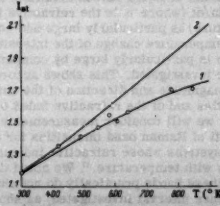

Fig. 3. The temperature dependence of the intensity of the 400 cm^{-1} band in the spectrum of fused quartz. Curve 1—experimental; curve 2—theoretical.

Table 2. The Intensities of Raman Bands of Polymethylmethacrylate for Two Temperatures

Frequency (cm^{-1})	Temperature (°K)	$I_{st} \sim \frac{1}{1-e^{-\frac{h\nu}{kT}}}$ (theor.)	I_{st} (exp.)	$\left(\frac{I_{T_1}}{I_{T_2}}\right)_{theor.}$	$\left(\frac{I_{T_1}}{I_{T_2}}\right)_{exp.}$
380	300	1.22	50	1.10	0.90
	390	1.35	45		
485	300	1.11	45	1.08	0.84
	390	1.20	41		
815	300	1.05	150	1.06	0.84
	390	1.11	127		
820	300	1.02	182	1.03	0.98
	390	1.05	178		
980	300	~1.01	325	1.025	0.89
	390	1.04	290		
1197	300	~1.00	495	1.02	0.90
	390	1.02	446		
1458	300	~1.00	340	~1.00	0.84
	390	~1.00	288		
1720	300	~1.00	80	~1.00	0.87
	390	~1.00	70		

intensities was observed. We note, however, that in liquids over the same temperature interval, anomalies are discovered without trouble.

3. DISCUSSION OF THE RESULTS OF THE MEASUREMENTS

The most substantial fact obtained is that for the majority of the solids the temperature dependence of the intensity of the Stokes bands qualitatively agrees with theory; i.e., the band intensities increase on heating the sample. Such a dependence is truly typical of solids, and deviations from it appear as particular cases. At the same time, in liquids the normal (theoretical) dependence of the same quantities, so far as is known, has not been observed in even one case. Already these facts form definite bases for proposing that the temperature dependence of the intensities of Raman bands is similar to the concentration dependence, being to a certain degree due to the refractive index of the medium.

This picture is confirmed by some other experimental facts, known from the literature. First of all, we note ref. 12, in which it is shown that the temperature shift of Raman band intensities has a different sign for the same substance in the solid and liquid states. Analogous results were obtained in a comparative investigation of liquids and gases by infrared spectroscopy.[13,14] Unfortunately, quantitative measurements of this type for solids are not available. One can, however, propose that in this case no anomalies will be discovered.

Further, according to the data in ref. 15, in the Raman spectrum of liquid carbon disulfide, for which the derivative dn/dt (where n is the refractive index and t the temperature) is particularly large and equals 89×10^{-5},[16] the temperature change of the intensities of the Stokes bands is particularly large by comparison with other liquids investigated. This shows accordingly a parallel in magnitude and direction of the changes of band intensities and of the refractive index of the liquid.

Finally, we will consider measurements of the temperature shift of Raman band intensities for two simple gases, i.e., systems whose refractive indices change very slightly with temperature.[17] We noted that the intensities of these bands practically do not change over the temperature interval investigated, as should be the case from theoretical considerations.

Thus, all of the different investigations show that the temperature anomalies of band intensities in the spectra of liquids can be determined, to a considerable degree, by the behavior of the refractive index of the medium.

We will examine, further, a typical property of the temperature curves of the intensity—the tendency of the curves to a maximum in the region of high temperatures. Evidently, this observed phenomenon is based on a physical reason. One might criticize the fused quartz result because of the definite but small temperature broadening of the band which was not taken account of in the investigation; however, this objection is not valid in the remaining cases where the integrated intensity of the bands was measured.

Earlier, the tendency of the curves to a maximum was connected with a manifestation of electro-optical anharmonicity of the vibrations of the substance, for very large temperatures, as a result of which part of the energy falls into scattering of higher orders.[18] It is difficult to account for this in the measurements. In principle one may say something about the mechanical anharmonicity of the vibrations. If it is not large, then its effect is obtained from a calculation in the anharmonic approximation of the matrix elements of the coordinate. This, however, leads to an increase of intensity in comparison with the harmonic case—an effect opposite to that observed.[1] Therefore, we can reject the influence of mechanical anharmonicity as one of the reasons of the characteristic change of the intensity curves.

We turn now to a possible interpretation of the cases of a weakening of the spectral intensities with temperature.* They are represented by Iceland spar and polymethylmethacrylate. It is more convenient to begin the discussion with the last sample.

*We still are limiting ourselves to a general physical treatment of the phenomenon. The more detailed question will be examined later.

In accordance with the data of a series of references,[19] the refractive index of organic polymers, though subject to a temperature influence to a significantly larger degree than, for example silica glasses and inorganic crystals, still does not change sufficiently to cause the observed changes of the measured band intensities. Therefore, it is not fruitful to attribute the effect in this case to the refractive index.

However, as was noted earlier, a complete account of the total properties of the medium also requires a study of another of its characteristics—the dielectric constant ε. The dielectric constant ε, generally measured at low electrical frequencies, differs from the refractive index n by being related not only with the electronic but also with other forms of the polarization—orientation and ionic. Therefore, it is only for molecules without dipoles and for molecular crystals that the two quantities bear the simple relationship $\varepsilon = n^2$.

Since the vibrational frequencies of the electrons lie in the visible region of the spectrum, they succeed in following the light vector of the incident light. The time for establishment of ions in an external field is of the order of a vibrational period. The dipoles are slowest of all to orient in the field. The corresponding relaxation times for them equals, in order of magnitude, the period of the rotational vibrations of the molecules. Therefore, the value of ε for orientational polarization always depends on temperature. The ionic polarization has a temperature character only for solids, since in solids, in contrast with liquids, the motion of the ions is connected with the surmounting of energy barriers.[20]

To account for the influence of ε on the position and intensity of bands in absorption spectra, and accordingly also on band intensities in Raman spectra, it is necessary to use the value of ε extrapolated to infinitely low field frequencies, i.e., its static value.[21] For each given field

frequency the region of a sharp change of ε with temperature occupies a definite place on the temperature scale. With a decrease of the field frequency this region shifts all the more to low temperatures. In the case of simple molecular liquids the limiting position of the curves $\varepsilon = f(T)$ (the field frequency is zero) corresponds to very low temperatures. Evidently, at these temperatures the dipoles of these solids lose the capability of rotating, i.e., the solid remains absolutely rigid.[22]

A different situation exists with high polymers. For them there is characterized a so-called dipole-elastic jump of ε in the region of temperatures higher than 0°C. The term itself reflects the physical nature of the phenomenon—it is connected with the highly elastic state of a polar polymer at these temperatures. One can say that a high polymer, as a rule, assumes the properties of an absolutely immobile solid at considerably higher temperatures than does a simple molecular solid.[22]

Polymethylmethacrylate acts as a typical polar polymer. Accordingly, its ε depends on temperature, particularly in the temperature region of softening.[23] Corresponding to this, the temperature change of ε, similar to the change of refractive index, should influence the Raman band intensities, which we have indeed observed in our experiments (Table 2). On the other hand, polystyrene is a nonpolar polymer, as a result of which ε for it is constant with temperature.[22] Therefore, within the limits of experimental error the intensity of its Raman bands does not change with temperature.

Special attention is merited by the sign of the anomaly in the case of polymethylmethacrylate—an increase of ε on heating the sample (in contrast to n) corresponds to a decrease of the Raman band intensities. There is nothing surprising in this. In principle it is conceivable that an increase of ε can be accompanied by different changes of the absorption spectra.[21] Such a picture accordingly should also be observed in Raman scattering. Therefore, one can propose that for some solids there exists a "positive" temperature anomaly, i.e., for them the characteristic is a growth of Raman band intensities, depending, despite the theory, not on the magnitude of the vibrational quantum but on the vibrational type and on the chemical nature of the bonds.

The reason for the temperature weakening of the spectrum of Iceland spar is not as clear as in the case of polymethylmethacrylate. If the dielectric constant ε is also responsible for this anomaly, then evidently the role of ionic polarization must be considered. But it is then completely incomprehensible why, in the other typically ionic cases we investigated, the temperature shift of the Stokes bands is normal. A series of authors have established that in a crystal of Iceland spar the selection and polarization rules for spectral bands are not fulfilled.[18] A connection between these anomalies and that observed by us is not excluded.

The authors thank N. G. Bakhshiev for fruitful discussions of the results of this work.

REFERENCES

1. Ya. S. Bobovich and V. M. Pivovarov, Opt. i Spektr. 3, 227 (1957).
2. F. G. Brickwede and M. F. Peters, Phys. Rev. 33, 116 (1929).
3. L. S. Ornstein and I. I. Went, Physica 2, 503 (1935).
4. S. Venkateswarlu, Proc. Indian Acad. Sci A14, 529 (1941).
5. G. S. Landsberg and L. I. Mandel'shtam, Z. Physik 60, 354 (1930).
6. M. Harraud, Ann. Phys. 2, 309 (1957).
7. A. I. Stekhanov and E. V. Chisler, Vestnik Leningrad. Gosudarst. Univ. Ser. Fiz. i Khim No. 4, Pt. 1, 159 (1959).
8. Ya. S. Bobovich and T. P. Tulub, Zhur. Eksptl. Teoret. Fiz. 30, 189 (1956).
9. V. M. Pivovarov and Ya. S. Bobovich, Opt. i Spektr. 3, 134 (1957).
10. V. M. Pivovarov, Opt. i Spektr. 6, 101 (1959), Optics and Spectroscopy 6, 60 (1959).
11. Ya. S. Bobovich and T. P. Tulub, Opt. i Spektr. 6, 566 (1959), Optics and Spectroscopy 6, 362 (1959).
12. T. P. Tulub and Ya. S. Bobovich, Opt. i Spektr. 9, 669 (1960), Optics and Spectroscopy 9, 352 (1960).
13. P. A. Bazhulin and V. N. Smirnov, Opt. i Spektr. 6, 745 (1959), Optics and Spectroscopy 6, 485 (1959).
14. V. N. Smirnov and P. A. Bazhulin, Opt. i Spektr. 7, 193 (1959), Optics and Spectroscopy 7, 123 (1959).
15. A. I. Sokolovskaya and P. A. Bazhulin, Izvest. Akad. Nauk SSSR. Ser. Fiz. 25. 1068 (1958).
16. Landolt-Börnstein, Phys. Chem. Tabellen 2, 958 (1923).
17. V. M. Pivovarov and Ya. S. Bobovich, Opt. i Spektr. 6, 249 (1959), Optics and Spectroscopy 6, 160 (1959).
18. O. T. Theimer, Can. J. Phys. 34, 312 (1956).
19. B. N. Putovskii and N. Ya. Parlashkevich, "Akrilovye smoly" (Acrylic Resins). GUUZ NKKhP, 1940.
20. G. I. Skanavi, "Fizika Dielektrikov" (The Physics of Dielectrics). Gosudarst. Izd. Tekh. i Teoret. Lit., Moscow, Leningrad, 1949.
21. B. S. Neporent and N. G. Bakhshiev, Opt. i Spektr. 5, 643 (1958);
N. G. Bakhshiev, Opt. i Spektr. 5, 646 (1958); Ibid. 7, 52 (1959), Optics and Spectroscopy 7, 29 (1959).
22. P. P. Kobeko, "Amorfnye Veshchestva" (Amorphous Materials). Izd. Akad. Nauk SSSR, Moscow, Leningrad, 1952.

ON THE ANTISTOKES PHOSPHORESCENCE OF ORGANOPHOSPHORS

V. A. Pilipovich

Received 21 March 1960

We investigated the quenching and degree of polarization of the afterglow of a number of organophosphors excited by radiation of different wavelengths, including the antistokes region. It is shown that in the case of both α- and β-phosphorescence the rate of quenching of the glow at room temperature increases considerably when excitation occurs in the antistokes region, while the degree of polarization remains constant.

According to literature data, the lifetime of the excited fluorescence state remains constant when the wavelength of the exciting radiation moves from the stokes to the antistokes region. Investigations of solutions[1,2] and of vapors[3] provided the evidence for the above generalization. At the same time, when the exciting radiation reaches the antistokes region, the fluorescence yield decreases sharply and the luminescence spectra, in many cases, shift to longer wavelengths. According to several authors[4-6] the difference in behavior between the variation in the quantum yield and the average lifetime of the excited state in antistokes excitation is due to the presence of inactive absorption. According to Stepanov,[6] the shift of the luminescence spectra can also be explained if it is assumed that in antistokes excitation thermal equilibrium between the medium and the excited molecule is not reached, as a result of which, the distribution function is not given any more by the Gibbs formula. At the same time, it is assumed that complete equilibrium could be reached in a time exceeding the lifetime of the excited state. Levshin[5] has proposed another explanation for the stokes cutoff. Pointing out that the Stokes rule is fulfilled for substances possessing very wide emission spectra, Levshin considers that emission spectra in this case can be complex, i.e., can be the result of radiation due to two different electronic transitions. However, this viewpoint is not in agreement with the polarization measurements of Feofilov,[7] who showed that the limiting polarization of rhodamine B extra and fluoroscein remains constant irrespective of whether excitation occurs in the 500-630 mμ or 450-550 mμ regions.

The investigation of the phosphorescence spectra of organophosphors with antistokes excitation, by Kudryashov and Sveshnikov,[8] showed that in the case of fluorescence as well as in α- and β-phosphorescence, there occurs a weakening in the short wavelength region of the afterglow spectrum, while the quenching constant remains constant within experimental error whether excitation is achieved by 436 mμ or 578 mμ radiation. On the basis of these results the authors consider that in the case of antistokes excitation, the fluorescing and phosphorescing states behave according to a general mechanism.

In earlier works[8,9] the quenching rate and the degree of polarization of the phosphorescence in various regions of the emission spectrum was investigated. It was shown that the quenching rate and polarization of phosphorescence, unlike those of fluorescence, do not remain constant throughout the emission spectrum. In order to explain the experimental facts, it was supposed that the metastable level was not simple. Such a hypothesis, as noted in an earlier paper by the author and Sveshnikov,[9] agrees well with the result obtained by Kudryashev and Sveshnikov[8] mentioned above. However, because of the absence of reliable data on the quenching rate of phosphorescence as a function of the wavelength of the exciting radiation, the agreement was not considered to be conclusive.

In the present work we investigated the mechanism of quenching of the afterglow of some organophosphors excited by radiation of different wavelengths, including the antistokes region.

The experimental setup has been described earlier.[10-11] Measurements were performed at room temperature and at liquid air temperature. A mercury lamp was used to provide the exciting radiation. The mercury lines were resolved by means of a filter and a concave diffraction grating. We also investigated the polarization of the phosphorescence as a function of the wavelength of the exciting radiation. An SF-4 monochromator was used as the source of excitation. The polarization of the phosphorescence was measured by a photoelectric method. Filters were used besides the monochromator to reduce the effect of scattered radiation.

Figure 1 shows the quenching of the phosphorescence of trypaflavin in gelatin as a function of wavelength of the exciting radiation. Comparison of curves 3 and 4 shows that quenching of the afterglow is not affected by the change in the wavelength of the exciting radiation from 404 mμ (curve 4) to 436 mμ (curve 3). Curve 2, corresponding to the exciting radiation of 492 mμ, has a slope that differs very little from that of curves 3 and 4 (the wavelengths of these exciting radiations fall within the stokes region). The quenching constant calculated in the 0-1 sec region is the same for all three cases ($\tau = 0.415$ sec). A completely different result is obtained in the antistokes region of excitation ($\lambda_{exc.} = 510$ mμ). The quenching constant calculated from the slope of the curve in the same region is 0.214 sec.*

*Kislyak[12,13] obtained a similar dependence of τ on $\lambda_{exc.}$ for trypaflavin in acetic acid.

An analogous behavior of the rate of quenching of the phosphorescence as a function of the wavelength of the

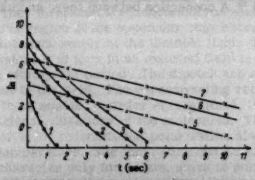

Fig. 1. Quenching of the phosphorescence of trypaflavin in gelatin as a function of the wavelength of the exciting radiation; at room temperature (curves 1-4) and liquid air temperature (curves 5-7). $\lambda_{exc.}$ (in mμ): curve 1—510; curves 2,5—492; curves 3,6—436; curves 4,7—404.

exciting radiation is observed in the case of acridine orange in sugar glass (Fig. 2, curves 1-5). Curves 2-5 correspond to the quenching of phosphorescence excited in the stokes region, while curve 1 corresponds to the one in the antistokes region. Kudryashev and Sveshnikov[8] have shown that only a slight change occurs in the phosphorescence spectra of acridine orange excited in the stokes region ($\lambda_{exc.}$ = 436 and 546 mμ). In our experiments, this corresponds to the observed constancy of the quenching constant. When the exciting radiation is 578 mμ there occurs a substantial change in the phosphorescence spectrum. According to our experiments, in this case, the phosphorescence is quenched much more rapidly.

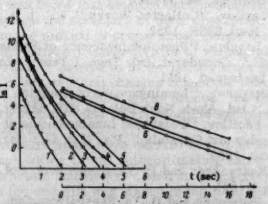

Fig. 2. Quenching of a phosphorescence of acridine orange in sugar glass as a function of the wavelength of the exciting radiation; at room temperature (curves 1-5) and liquid air temperature (curves 6-8). $\lambda_{exc.}$ (in mμ): curve 1—578; curve 2—546; curves 3,6—492; curves 4,7—404; curves 5,8—436.

It is known that in antistokes excitation the absorption of a quantum of light and its subsequent emission is related to the transformation of thermal energy into radiation energy. This makes the antistokes luminescence strongly temperature dependent; thus it can be eliminated at low enough temperatures. The curves 5-7 in Fig. 1 and the curves 6-8 in Fig. 2 describe the quenching of the afterglow of trypoflavin and acridine at liquid air temperature. At this temperature the absorption of the two compounds in the region of 510 mμ is almost absent, while at room temperature it was always possible to excite a phosphorescence in this region. As can be seen from the figures, the character of the quenching of the afterglow of both compounds is not affected by the wavelength of exciting radiation occurring in the stokes region.

Our results and those of Kudryashov and Sveshnikov can not be explained by the influence of luminescing impurities in the compound under investigation, since it is hard to assume that decrease in temperature narrows or shifts the absorption spectrum of the impurities more than that of the compound. It is likewise hard to assume that the various aggregations of the activator molecules could influence the phosphorescence excited in the antistokes region, since the concentrations did not exceed 5×10^{-8} gm/gm.

The phosphorescence at room temperature of the dyes so far examined belongs to α-phosphorescence. However, the fact that at low temperatures we did not observe a variation in the rate of quenching as the wavelength of the exciting radiation was changed, does not indicate that the decrease in duration in antistokes excitation is characteristic only of α-phosphorescence. Investigation of the mechanism of quenching of the phosphorescence of esculin in sugar glass (where only the β-process is operative at all temperatures) as a function of the wavelength of the exciting radiation, shows (Fig. 3) that in this case also there exists a relation between the rate of quenching and the wavelength of the exciting radiation. Curves 1 and 2 correspond to excitation in the antistokes region while curves 3 and 4 correspond to excitation in the stokes region. It can be seen from comparison of the curves, that the rate of quenching of the afterglow increases as the wavelength of the exciting radiation is increased. It must be noted that there does not exist a sharp change in the rate of quenching on transition to excitation at longer wavelengths. Curves 5 and 6 illustrate the quenching of the afterglow at low temperatures for different wavelengths of the exciting radiation. We were not able to observe the antistokes phosphorescence of trypoflavin, acridine, or esculin at liquid air temperature.

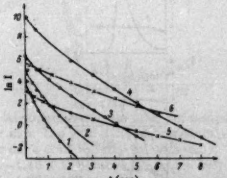

Fig. 3. The quenching of the phosphorescence of esculin in sugar glass as a function of the wavelength of exciting radiation; at room temperature (curves 1-4) and liquid air temperature (curves 5 and 6). $\lambda_{exc.}$ (in mμ): curve 1—436; curve 2—404; curves 3,5—313; curves 4,6—365.

Thus, in contrast to antistokes fluorescence where the stokes cutoff is not accompanied by a change in the average lifetime of the fluorescence, in the case of antistokes phosphorescence the shift of the emission spectra to longer wavelengths causes a noticeable decrease in the average lifetime of the metastable state. If we add to this the fact that in the case of phosphorescence the rate of quenching and the degree of polarization do not remain constant throughout the emission spectrum in contrast to fluorescence, then it becomes natural to suppose that there exists a difference between the sources of antistokes fluorescence and antistokes phosphorescence. In particular, it can be assumed that the shift in the phosphorescence spectrum in antistokes excitation is caused by a decrease in the probability of transition from the metastable state to the labile state. This would have indicated that the afterglow observed in antistokes excitation consists mainly of the β-process. Such an assumption seems justified since together with a decrease in the lifetime of the excited state in antistokes excitation the relative quantum yield of phosphorescence is also strongly decreased.[14] The latter circumstance can lead to the observed change in the spectrum and average lifetime of phosphorescence subject to the condition that the probability of the return of a metastable molecule to the labile state changes with change in the wavelength of the exciting radiation less than the probability of quenching in the metastable state.

In order to verify the supposition made above, it is necessary to determine which of the processes (α- or β-) determines the afterglow in antistokes excitation. With this purpose in mind, it was natural to investigate the polarization of phosphorescence as a function of the wave-

length of the exciting radiation, since it is known that the long wavelength phosphorescence (β-phosphorescence) has a negative value of polarization in contrast to the short wavelength phosphorescence.[10]

Figure 4 shows the absorption spectra (first band) and degree of polarization of the phosphorescence as a function of the wavelength of exciting radiation for acridine orange (I), trypaflavin (II), and auramine (III) in sugar glasses. It can be seen from the figure that in the case of all the compounds investigated, the anisotropy of the lengthy afterglow does not change with transition from the stokes region of excitation to the antistokes region. This result indicates that the phosphorescence of organophosphors at room temperature is determined by the α-process, irrespective of the conditions of excitation, and hence that the shift in the emission spectrum in antistokes excitation toward lower frequencies is not related to the presence of the β-process in the afterglow.

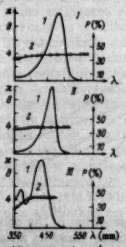

Fig. 4. Absorption spectra (curve 1) and degree of polarization of the phosphorescence as function of the wavelength of the exciting radiation (curve 2) for acridine orange (I), trypaflavin (II), and auramine (III) in sugar glasses.

The author would like to thank B. Ya. Sveshnikov for his interest in the present investigation and B. I. Stepanov for valuable advice.

REFERENCES

1. B. Ya. Sveshnikov, Trudy Gosudarst. Opt. Inst. 108, 1 (1938).
2. L. A. Tumerman, Trudy Fiz. Inst., Akad. Nauk SSSR 1, 77 (1938).
3. B. S. Neporent and N. A. Borisevich, Doklady Akad. Nauk SSSR 94, 447 (1954).
4. S. I. Vavilov, "Collected Works," Vol. 1, p. 424, Izd. Akad. Nauk SSSR, 1952.
5. V. L. Levshin, "Photoluminescence of Solids and Liquids." Gosudarst. Izd. Tekh. i Teoret. Lit., Moscow, Leningrad, 1951.
6. B. I. Stepanov, "Luminescence of Complex Molecules." Izd. Akad. Nauk Belorus.SSR, Minsk, 1955.
7. P. P. Feofilov, "Polarized Luminescence of Atoms Molecules and Crystals." Fiz. Mat. Gosudarst. Izd., Moscow, 1959.
8. P. I. Kudryashov and B. Ya. Sveshnikov, Opt. i Spektr. 1, 554 (1956).
9. V. A. Pilipovich and B. Ya. Sveshnikov, Opt. i Spektr. 5, 290 (1958).
10. V. A. Pilipovich and B. Ya. Sveshnikov, Doklady Akad. Nauk SSSR 119, 59 (1958).
11. V. A. Pilipovich and B. Ya. Sveshnikov, Opt. i Spektr. 4, 116 (1958).
12. G. M. Kislyak, Opt. i Spektr. 5, 297 (1958).
13. G. M. Kislyak, Opt. i Spektr. 6, 226 (1959), Optics and Spectroscopy 6, 144 (1959).
14. R. Bauer and A. Baczynski, Bull. acad. polon. sci. 6, 113 (1958).

QUANTITATIVE STUDIES OF THE ABSORPTION SPECTRUM OF CUPROUS OXIDE*

*The results of this work were presented at an Extraordinary Session of the Commission for Semiconductors of the Academy of Sciences of the Ukrainian S.S.R. at Odessa in 1959.

I. S. Gorban'

Received 26 November 1959

A quantitative study of the absorption spectra of Cu_2O crystals was carried out in the visible part of the spectrum. The assumption that the hydrogenlike series of bands at the edge of the main band represents the fundamental absorption of the crystal was confirmed. The features of the structure of the edge—the fundamental absorption bands of the Cu_2O spectrum—can be explained theoretically if one assumes that this absorption band is due to transitions between states of equal parity.

FORMULATION OF THE PROBLEM

In spite of the large number of investigations devoted to the study of the absorption spectrum of cuprous oxide, there are still insufficient detailed numerical data to permit forming a picture of the absolute values of the absorption coefficient and its dependence on wavelength. The aim of the early investigations[1] was to determine the general outlines of the spectrum; as a result of this, some very essential details were overlooked. In later investigations,[2] special attention was given to the hydrogenlike series observed in the spectra of Cu_2O at low temperatures. The data in refs. 3 and 4 referred to special cases and agreed with one another only qualitatively.

It is well known that the investigation of the absorption band series at the edge of the fundamental band, by E. F. Gross and his co-workers, involved the excitation of the exciton state of the crystal. The basis for this assumption is the location of the absorption bands in the spectrum, and also their magneto-optic properties.[5] However, these facts should not be regarded as sufficient proof of the exciton origin of the series because the spectra of some of the impurities in the crystals may be hydrogenlike and may have "crystal-like" magneto optic properties.[6]

For a final solution of the problem of the nature of the hydrogenlike series in the Cu_2O spectrum, it is necessary to make quantitative measurements of the intensity of absorption lines as a function of the concentration of impurities. In addition to this, it is interesting to investigate the rules governing the distribution of the intensity among the absorption bands in a given series and also between different series.

EXPERIMENTAL PROCEDURE

About thirty mono- and polycrystalline samples of cuprous oxide with different dark conductivities were examined. It was found that both the dark conductivity of the samples and the structure of their absorption bands depended on the method of preparation. Hence the main cause for the different conductivities of the samples in these experiments proved to be deviations from stoichiometry or other structual changes connected with the oxygen or copper. The differences between the absorption spectra of mono- and polycrystalline samples proved to be immaterial.

The measurements were carried out on an ISP-51 spectrograph with a UF-85 autocollimating camera. A photoelectric attachment was constructed for recording intensities (an exit slit was placed in the focal plane of the spectrograph with a photomultiplier located immediately behind it). The signal from the photomultiplier was amplified and recorded on an electronic potentiometer. The scanning was accomplished with the rotating mechanism of the prism table; this motion was synchronized with the chart-paper-feeding mechanism of the recorder. The spectrum was recorded in sections, for each of which the camera was focused. An example of a trace is shown in Fig. 1. This figure clearly shows the four absorption bands of the yellow series in the spectrum of a 15μ thick Cu_2O platelet which was cooled to −180°C in a special cryostat.

Fig. 1. Example of a spectrogram of a Cu_2O absorption band series.

With the aid of the spectrograph we succeeded in recording the distribution of the absorption coefficients in those bands of the series which, according to ref. 2, correspond to transitions to levels with quantum numbers $n \geq 2$. It is well known that the line corresponding to $n = 1$ is very narrow and has a very weak absorption; hence it cannot be recorded with the above spectrometer in such thin specimens. Measurements of the absorption coefficient of this line were performed on thick specimens (0.7 mm) with a Fabry-Perot interferometer used in conjunction with a spectrograph. A detailed description of the procedure used for these measurements will be the subject of a separate article.

RESULTS OF THE MEASUREMENTS

Figure 2 represents three absorption curves in the region of the long wavelength edge of the fundamental Cu_2O band at room temperature. The absorption coefficient is expressed in cm^{-1}. It can readily be seen that the absorption on the long wavelength side of 6750 A does not display a direct relationship to the dark conductivity of the specimen, but depends on its thermal history, and according to ref. 6 is due to impurities.

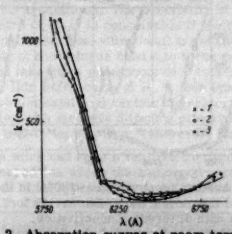

Fig. 2. Absorption curves at room temperature for samples with different conductivities. Specific dark conductivity (in ohm-cm): curve 1—1.26×10^3; curve 2—1.11×10^4; curve 3—1.02×10^6.

Between 6730 and 6100 A, a strong dependence of the absorption on the dark conductivity was observed; in the range of conductivities examined, high specific resistance always corresponded to low absorptivity. It is known from ref. 2 that in the wavelength interval under consideration there are two absorption steps which are slightly displaced along the wavelength scale between one sample and another; their edges are usually between 6371 and 6284 A. Special measurements have shown that the absolute values of the absorption coefficient in the region of these steps is different for different samples and varies with the absorptivity over the whole 6730-6100 A range. However, the relative distribution of the absorption in these steps varies a little, and according to a different rule. According to ref. 7, the absorption of light in Cu_2O between 6730 and 6100 A depends for the most part on impurity centers of the acceptor type, whose concentration over the conductivity range studied is determined by the nonstoichiometric content of oxygen.[6,7] The absorption in the region of the steps is apparently of a different nature.

The absorption curves rise steeply on the short wavelength side of 6100 A; the higher the dark conductivity of the sample, the further the foot of the steep edge is shifted towards the short wavelength side. In the vicinity of 6000 A, the absorption curve for samples with high conductivities has a small kink which apparently depends on the yellow hydrogenlike series. In samples of even higher resistance, this kink is partly smoothed out and partly passes into the region of very high optical density. For specimens of this thickness measurements become impossible in this region because of the strong absorption.

Thus an increase in the concentration of impurity centers of the acceptor type in Cu_2O at room temperature is accompanied by an increase in the absorption in the 6300-6100 A region, and a simultaneous decrease at shorter wavelengths.

The results of measurements at −180°C are shown in Fig. 3. The curves A illustrate the over-all appearance of the edge of the absorption spectra of the two samples which have the extreme conductivity values. Series

length of the exciting radiation, since it is known that the long wavelength phosphorescence (β-phosphorescence) has a negative value of polarization in contrast to the short wavelength phosphorescence.[10]

Figure 4 shows the absorption spectra (first band) and degree of polarization of the phosphorescence as a function of the wavelength of exciting radiation for acridine orange (I), trypaflavin (II), and auramine (III) in sugar glasses. It can be seen from the figure that in the case of all the compounds investigated, the anisotropy of the lengthy afterglow does not change with transition from the stokes region of excitation to the antistokes region. This result indicates that the phosphorescence of organophosphors at room temperature is determined by the α-process, irrespective of the conditions of excitation, and hence that the shift in the emission spectrum in antistokes excitation toward lower frequencies is not related to the presence of the β-process in the afterglow.

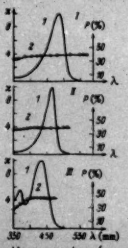

Fig. 4. Absorption spectra (curve 1) and degree of polarization of the phosphorescence as function of the wavelength of the exciting radiation (curve 2) for acridine orange (I), trypaflavin (II), and auramine (III) in sugar glasses.

The author would like to thank B. Ya. Sveshnikov for his interest in the present investigation and B. I. Stepanov for valuable advice.

REFERENCES

1. B. Ya. Sveshnikov, Trudy Gosudarst. Opt. Inst. 108, 1 (1938).
2. L. A. Tumerman, Trudy Fiz. Inst., Akad. Nauk SSSR 1, 77 (1938).
3. B. S. Neporent and N. A. Borisevich, Doklady Akad. Nauk SSSR 94, 447 (1954).
4. S. I. Vavilov, "Collected Works," Vol. 1, p. 424, Izd. Akad. Nauk SSSR, 1952.
5. V. L. Levshin, "Photoluminescence of Solids and Liquids." Gosudarst. Izd. Tekh. i Teoret. Lit., Moscow, Leningrad, 1951.
6. B. I. Stepanov, "Luminescence of Complex Molecules." Izd. Akad. Nauk Belorus.SSR, Minsk, 1955.
7. P. P. Feofilov, "Polarized Luminescence of Atoms Molecules and Crystals." Fiz. Mat. Gosudarst. Izd., Moscow, 1959.
8. P. I. Kudryashov and B. Ya. Sveshnikov, Opt. i Spektr. 1, 554 (1956).
9. V. A. Pilipovich and B. Ya. Sveshnikov, Opt. i Spektr. 5, 290 (1958).
10. V. A. Pilipovich and B. Ya. Sveshnikov, Doklady Akad. Nauk SSSR 119, 59 (1958).
11. V. A. Pilipovich and B. Ya. Sveshnikov, Opt. i Spektr. 4, 116 (1958).
12. G. M. Kislyak, Opt. i Spektr. 5, 297 (1958).
13. G. M. Kislyak, Opt. i Spektr. 6, 226 (1959), Optics and Spectroscopy 6, 144 (1959).
14. R. Bauer and A. Baczynski, Bull. acad. polon. sci. 6, 113 (1958).

QUANTITATIVE STUDIES OF THE ABSORPTION SPECTRUM OF CUPROUS OXIDE*

*The results of this work were presented at an Extraordinary Session of the Commission for Semiconductors of the Academy of Sciences of the Ukrainian S.S.R. at Odessa in 1959.

I. S. Gorban'

Received 26 November 1959

A quantitative study of the absorption spectra of Cu_2O crystals was carried out in the visible part of the spectrum. The assumption that the hydrogenlike series of bands at the edge of the main band represents the fundamental absorption of the crystal was confirmed. The features of the structure of the edge—the fundamental absorption bands of the Cu_2O spectrum—can be explained theoretically if one assumes that this absorption band is due to transitions between states of equal parity.

FORMULATION OF THE PROBLEM

In spite of the large number of investigations devoted to the study of the absorption spectrum of cuprous oxide, there are still insufficient detailed numerical data to permit forming a picture of the absolute values of the absorption coefficient and its dependence on wavelength. The aim of the early investigations[1] was to determine the general outlines of the spectrum; as a result of this, some very essential details were overlooked. In later investigations,[2] special attention was given to the hydrogenlike series observed in the spectra of Cu_2O at low temperatures. The data in refs. 3 and 4 referred to special cases and agreed with one another only qualitatively.

It is well known that the investigation of the absorption band series at the edge of the fundamental band, by E. F. Gross and his co-workers, involved the excitation of the exciton state of the crystal. The basis for this assumption is the location of the absorption bands in the spectrum, and also their magneto-optic properties.[3] However, these facts should not be regarded as sufficient proof of the exciton origin of the series because the spectra of some of the impurities in the crystals may be hydrogenlike and may have "crystal-like" magneto optic properties.[5]

For a final solution of the problem of the nature of the hydrogenlike series in the Cu_2O spectrum, it is necessary to make quantitative measurements of the intensity of absorption lines as a function of the concentration of impurities. In addition to this, it is interesting to investigate the rules governing the distribution of the intensity among the absorption bands in a given series and also between different series.

EXPERIMENTAL PROCEDURE

About thirty mono- and polycrystalline samples of cuprous oxide with different dark conductivities were examined. It was found that both the dark conductivity of the samples and the structure of their absorption bands depended on the method of preparation. Hence the main cause for the different conductivities of the samples in these experiments proved to be deviations from stoichiometry or other structual changes connected with the oxygen or copper. The differences between the absorption spectra of mono- and polycrystalline samples proved to be immaterial.

The measurements were carried out on an ISP-51 spectrograph with a UF-85 autocollimating camera. A photoelectric attachment was constructed for recording intensities (an exit slit was placed in the focal plane of the spectrograph with a photomultiplier located immediately behind it). The signal from the photomultiplier was amplified and recorded on an electronic potentiometer. The scanning was accomplished with the rotating mechanism of the prism table; this motion was synchronized with the chart-paper-feeding mechanism of the recorder. The spectrum was recorded in sections, for each of which the camera was focused. An example of a trace is shown in Fig. 1. This figure clearly shows the four absorption bands of the yellow series in the spectrum of a 15μ thick Cu_2O platelet which was cooled to $-180°C$ in a special cryostat.

Fig. 1. Example of a spectrogram of a Cu_2O absorption band series.

With the aid of the spectrograph we succeeded in recording the distribution of the absorption coefficients in those bands of the series which, according to ref. 2, correspond to transitions to levels with quantum numbers $n \geq 2$. It is well known that the line corresponding to $n = 1$ is very narrow and has a very weak absorption; hence it cannot be recorded with the above spectrometer in such thin specimens. Measurements of the absorption coefficient of this line were performed on thick specimens (0.7 mm) with a Fabry-Perot interferometer used in conjunction with a spectrograph. A detailed description of the procedure used for these measurements will be the subject of a separate article.

RESULTS OF THE MEASUREMENTS

Figure 2 represents three absorption curves in the region of the long wavelength edge of the fundamental Cu_2O band at room temperature. The absorption coefficient is expressed in cm^{-1}. It can readily be seen that the absorption on the long wavelength side of 6750 A does not display a direct relationship to the dark conductivity of the specimen, but depends on its thermal history, and according to ref. 6 is due to impurities.

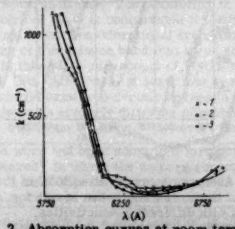

Fig. 2. Absorption curves at room temperature for samples with different conductivities. Specific dark conductivity (in ohm-cm): curve 1—1.26×10^3; curve 2—1.11×10^4; curve 3—1.02×10^6.

Between 6730 and 6100 A, a strong dependence of the absorption on the dark conductivity was observed; in the range of conductivities examined, high specific resistance always corresponded to low absorptivity. It is known from ref. 2 that in the wavelength interval under consideration there are two absorption steps which are slightly displaced along the wavelength scale between one sample and another; their edges are usually between 6371 and 6284 A. Special measurements have shown that the absolute values of the absorption coefficient in the region of these steps is different for different samples and varies with the absorptivity over the whole 6730-6100 A range. However, the relative distribution of the absorption in these steps varies a little, and according to a different rule. According to ref. 7, the absorption of light in Cu_2O between 6730 and 6100 A depends for the most part on impurity centers of the acceptor type, whose concentration over the conductivity range studied is determined by the nonstoichiometric content of oxygen.[4,7] The absorption in the region of the steps is apparently of a different nature.

The absorption curves rise steeply on the short wavelength side of 6100 A; the higher the dark conductivity of the sample, the further the foot of the steep edge is shifted towards the short wavelength side. In the vicinity of 6000 A, the absorption curve for samples with high conductivities has a small kink which apparently depends on the yellow hydrogenlike series. In samples of even higher resistance, this kink is partly smoothed out and partly passes into the region of very high optical density. For specimens of this thickness measurements become impossible in this region because of the strong absorption.

Thus an increase in the concentration of impurity centers of the acceptor type in Cu_2O at room temperature is accompanied by an increase in the absorption in the 6300-6100 A region, and a simultaneous decrease at shorter wavelengths.

The results of measurements at $-180°C$ are shown in Fig. 3. The curves A illustrate the over-all appearance of the edge of the absorption spectra of the two samples which have the extreme conductivity values. Series

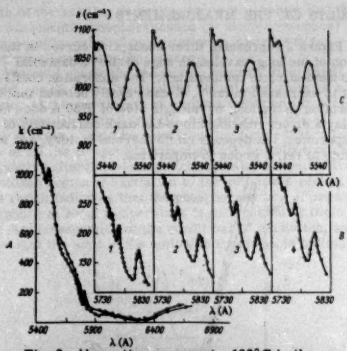

Fig. 3. Absorption curves at −180°C in the region of the yellow and green series for samples with different conductivities. Specific dark conductivities (in ohm-cm) at room temperature: curve 1—1.26×10^3; curve 2—1.11×10^4; curve 3—1.03×10^5; curve 4—1.02×10^6.

B and C are enlarged views of the absorption curves in the regions of the yellow and green hydrogenlike series respectively.

A comparison of curves A with the corresponding curves in Fig. 2 reveals that the transparency of the samples increases significantly at low temperatures, and that the whole spectrum is moved towards the blue. At the same time, the absorption associated with impurity centers weakens. The absorption in the 6100-5700 A region, and also in the corresponding region at room temperature, is weaker in low-resistance samples which have a high concentration of nonstoichiometric oxygen (acceptors)[6,7] than in the case of high-resistance samples. This difference, however, is small. No noticeable difference in the absorption of samples of different conductivities is observed on the blue side of 5700 A.

The yellow hydrogenlike series falls in that part of the spectrum in which the total absorption decreases with increasing concentration of impurities. These bands rise above the continuous background, which rises sharply towards the blue. The most intense band corresponds to n = 2; beyond it, on the short wavelength side, the other members of the series appear one by one. The integrated absorption in the peaks appearing above the background does not depend on the concentration of the excess oxygen. One can satisfy oneself of this by measuring the areas of the appropriate peaks in the spectra which are represented in a magnified form by Series B in Fig. 3. In addition to this, the values of the absorption coefficients at the maxima of these peaks are also independent of the impurity content. A barely noticeable exception is the absorption spectrum of samples 2 in which the peaks are lower and have a greater halfwidth. This departure can be explained by the fact that samples 2 were not annealed after preparation, so that a slight amount of disorder existed in the crystalline structure.

In the region of the green series the effect of a change in the concentration of the impurities on the absorption is very small.

Figure 4 shows the absorption curve which, according to ref. 2, corresponds to the first component of the yellow series (n = 1). The shape of this line was measured for a specimen for which $\rho = 1.93 \times 10^3$ ohm-cm, using a Fabry-Perot interferometer.

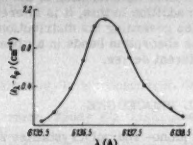

Fig. 4. The contour of the narrow absorption line at λ = 6137 A.

The more important properties of the yellow hydrogenlike series at −180°C are shown in the Table.

n	1	2	3	4	5
λ_{max} (A)	6137	5803	5770	5758	5752
k_{max} (cm⁻¹)	1.1	48	23	~7.5	4
Δ (A)	1.1	10	5	2.5	~1.4
$\frac{S_n}{S_1}$	$2 \cdot 10^{-3}$	1	0.194	0.041	0.025
$\frac{k_n}{k_1}$	$2.3 \cdot 10^{-3}$	1	0.48	0.156	0.086
$\frac{n_1^2}{n_n^2}$	8	1	0.296	0.125	0.064
$\frac{n_n^2-1}{n_n^2} : \frac{n_1^2-1}{n_1^2}$	0	1	0.351	0.145	0.089

Here n is the number of the band or the principal quantum number; λ_{max} is the location of the maxima on the wavelength scale; k_{max} is the absorption coefficient at the maximum which describes the height of the band above background; Δ is the halfwidth of the band; S_n/S_1 is the ratio of the area of the n-th band to the area of the band for which n = 2; k_n/k_1 is the same ratio for the absorption coefficients at the maxima; the two lowest lines list the values of functions of the quantum numbers (see also ref. 10). The intensity of the bands of the green series is higher than that of the yellow series. Thus, for bands for which n = 2 the ratio of the areas is $S_{green}/S_{yellow} = 4.79$ and the ratio of the absorption coefficients at the maxima is $k_{green}/k_{yellow} = 1.7$. Since the absorption was measured for only two members of the green series, there was no point in compiling a detailed table. We shall only note that $k_{max} = 7.7$ cm⁻¹ and Δ = 25 A for n = 2.

DISCUSSION OF RESULTS

The intensities of the bands which rise above the continuous background and form the yellow and green hydrogenlike series in the spectra of Cu_2O do not depend on the impurity content of the samples. This strongly indicates that the hydrogenlike series of Cu_2O is due to the fundamental absorption of the crystal.

The intensity of the continuous background which underlies the yellow series is slightly dependent on the dark conductivity of the specimens. The absorption increases with an increase in the specific resistance; it varies rapidly for low-resistance samples and tends toward a saturation value for high-resistance samples (Fig. 3). Since the variation in the intensity of the background is not accompanied by simultaneous changes in the intensity of the peaks of the yellow series, one cannot (at least, fully) ascribe the origin of the continuous background underlying the yellow series to the nature of

that series, by considering, for example, that it represents a mutual overlapping of neighboring bands. On the other hand, one cannot explain the origin of the background by transitions from the acceptor levels into the conduction band (photoionization of the acceptors) because the intensity of the background decreases with an increase in the concentration of the excess oxygen.

The assumption that the observed continuous absorption underlying the yellow series arises as a result of the excitation of the crystal into impurity states formed by excess Cu^+ ions also does not agree with the experiments in a number of points. The existence of excess Cu^+ ions in the crystal can no doubt be considered if one assumes that their presence is accompanied by a simultaneous presence of excess oxygen. The concentration of the excess oxygen must be larger than the concentration of the copper, because cuprous oxide has p-type conductivity. Consequently, the absorption which depends on the excess oxygen should be more intense. But experiments have shown that the absorption due to oxygen is much smaller than the background underlying the yellow series.

The intensity of an impurity absorption should be strongly dependent on the frequency; as a rule, the bands have a shape such that the absorption coefficient decreases from the peak toward the blue[8] as $1/\nu^{2\cdot5}$. Experiment shows that as the frequency increases, the intensity of the background rises continuously.

Thus, on the basis of the above qualitative considerations, one can conclude that the continuous absorption underlying the yellow series is not due to impurities.

Nikitine and his co-workers have discussed the origin of some of the absorption series in the Cu_2O spectra. They assumed that the yellow series is the fundamental series, that it arises from direct transitions, and that the green and the longest wavelength series (the so-called "red series" which also has a narrow line to which the number $n = 2$ is ascribed) are formed as a result of diagonal transitions and are accompanied by the absorption or emission of a phonon with an energy of 0.133 ev. The experimental data now available cannot be reconciled with this point of view. First of all, neither we nor other authors[4] were able to observe members of the red series for which n was higher than 2. If the green and the red series are satellites, their intensity in the Cu_2O spectrum should be lower than the intensity of the yellow series. Apart from this, they should be strongly dependent on temperature, following a law which is substantially different from that of the yellow series. Beyond the limit of convergence of the satellite series, the continuous background should increase with increasing frequency[10] as $(\Delta\nu)^2$ and the convergence constant R' should be approximately equal for all three series. However, none of these conclusions, which result from the assumption of a vibrational origin for some of the series, agree with the experimental data.

The author of this communication made an attempt to analyze the structure of the long wavelength edge of the fundamental absorption of Cu_2O from the point of view of the theory given in ref. 10. On making certain assumptions, the ratio of the intensities of different members of the series and the properties of the continuous background beyond the boundaries of their convergence can be explained from the point of view of the theory of forbidden direct transitions. The possibility of three series in the spectra of Cu_2O is conceivable if their origin is ascribed, not to exciton-vibrational transitions, but to the splitting of the valence band into three components, which could take place on account of a spin-orbit interaction.[12] If this is the case, at least four types of current carriers should exist to a certain degree in Cu_2O. Three will be holes with strongly differing effective masses and the fourth will be an electron.* However, further research is necessary for a final solution of this problem.

*After this work had been submitted for publication, a paper appeared[13] in which the authors reported the observation of three types of current carriers in Cu_2O with substantially different effective masses.

The author is grateful to A. A. Shishlovski, K. B. Tolpyg, and S. A. Moskalenko for valuable discussions.

REFERENCES

1. A. V. Ioffe and A. F. Ioffe, Zhur. Eksptl. i Teoret. Fiz. **6**, 737 (1936).
2. E. F. Gross, Uspekhi Fiz. Nauk, **63**, 575 (1957).
3. I. S. Gorban', Visnik K.D.U. 1 (Fizika, Khimiya), 48 (1959).
4. I. Pastrnyak, Fiz. Tverd. Tel. **1**, 973 (1959).
5. Trudy Kievsk. soveshch. po optich. i fotoelektrich. svoistvam poluprovodnikov (Transactions of the Kiev Conference on the Optical and Photoelectric Properties of Semiconductors). Izd. Akad. Nauk USSR, Kiev, 1959.
6. O. Schönwald, Ann. Phys. **15**, 395 (1932).
7. J. Bloem, Philips Res. Repts. **13**, 167 (1958).
8. N. I. Fan', Uspekhi Fiz. Nauk, **64**, 315 (1958).
9. S. Nikitine, Helv. Phys. Acta. **28**, 247 (1954); S. Nikitine, G. Perny, and M. Sieskind, Compt. rend. acad. sci. **239**, 247 (1954).
10. R. J. Elliott, Phys. Rev. **108**, 1384 (1957).
11. I. S. Gorban', Ukrain. Fiz. Zhur. **5**, No. 2 (1960).
12. S. A. Moskalenko, Fiz. Tverd. Tel. **2**, 1755 (1960).
13. A. I. Gubanov, N. I. Krivko, and N. M. Reinov, Zhur. Eksptl. i Teoret. Fiz. **38**, No. 2 (1960).

OPTICAL TRANSITIONS IN U-CENTERS IN NaCl CRYSTALS

A. A. Kiselev and I. V. Abarenkov

Received 9 March 1960

U-center in NaCl crystals are considered. Using the polarized point lattice approximation, the energies of the transitions corresponding to the absorption and emission maxima of the U-bands are calculated along with the halfwidth of the U-band. It is shown that the results obtained agree satisfactorily with the experimental data.

When coloring alkali halide crystals, another series of absorption bands, in addition to the F-bands, is often produced in the ultraviolet. One such band (λ_{max} = 192 mμ in the NaCl spectrum) and the center producing it are called the U-band and U-center, respectively. One can explain all the properties of a crystal having a U-band if one supposes that the U-center is a negative hydrogen ion localized at an anion vacancy.[1] For example, the widely known weakening of the F-band and proportional intensification of the U-band upon heating a crystal with F-centers in an atmosphere of hydrogen is explained by the fact that the hydrogen atoms permeate the crystal and combine with F-centers to produce U-centers. The assumed model of the U-center permits one to explain more complicated processes (for example, processes which occur upon irradiation of a crystal having U-centers with light in the U-band). During such irradiation, the U-band is weakened and simultaneously certain other bands are produced: at temperatures lower than about 90° K, an α-band and a U_1-band are produced,[1] but at temperatures greater than 90° K, an F-band and a U_2-band are produced.*[2] The appearance of new bands and, consequently, new color centers is of course connected with the decay of the excited state of the U-center. Let us consider the possible decay paths.

*At the present time it is assumed that the α-band is caused by an anion vacancy, and U_2- and U_1-bands are caused by an interstitial atom and negative hydrogen ion, respectively.[1,2]

The excited U-center might decay to the ground state with the emission of light. In this case other centers do not appear. The excited U-center might also decay to the ground state without light emission. The radiationless transition either does not produce other centers or leads to the ejection of a negative hydrogen ion into an interstitial position at the expense of the energy released during the transition, i.e., α-centers and U_1-centers appear. The third possibility is that before the excited electron of the U-center falls to the ground state, a thermal fluctuation might arise which is able to eject a hydrogen atom into an interstitial position and leave an excited electron in the vacancy; this leads to the formation of an F-center or U_2-center. Qualitative considerations indicate that the remaining possible means of decay, for example, the ejection of a hydrogen atom into an interstitial position as the result of a nonradiative transition of the U-center to the ground state are unlikely.

At low temperatures, the probability of a sufficiently large thermal fluctuation is small, and the formation of other color centers takes place mainly by nonradiative transitions of U-centers to the ground state. Since the diffusion rate of the ions is also small, recombination processes are practically negligible. Consequently, α-centers and U_1-centers must be the products of the decay; this is confirmed by experiment. At sufficiently high temperatures, the formation of color centers also begins to take place by the effect of thermal fluctuations on the excited U-centers; therefore, during the decay of U-centers, F- and U_2-centers appear, as well as α- and U_1-centers. However, since the diffusion rate of the ions increases with temperature, recombination begins to be appreciable. Thus the oppositely charged α- and U_1-centers recombine practically completely, which leads to the disappearance of the α- and U_1-bands. The recombination rate of F- and U_2-centers is significantly smaller. In this case, therefore, F- and U_2-centers must be the products of the decay, which also agrees with experiment.

The model of the U-center as a negative hydrogen ion in an anion vacancy agrees qualitatively with the experimental data. It is of interest to calculate this model quantitatively in order to confirm it once again, and also to obtain characteristics of the U-center which have not been or cannot be measured experimentally (for example, the energy of a radiative transition and adiabatic potentials). In the present paper, the calculation of the U-center is carried out using the approximation of a polarized point lattice. One can find a detailed description and some justification for this approximation in a paper by one of the authors[3] which used the approximation of a polarized point lattice for the calculation of F-centers. Here we present only the necessary details.

1. In the approximation of a polarized point lattice, the structure of the ions of the crystal is considered by introducing repulsive forces between the point ions, and by assuming that dipole moments can be induced in the point ions under the influence of an electric field. Thus our problem reduces to the consideration of a system consisting of two electrons, a proton, and N point ions. The Hamiltonian of such a system can be written as a sum (in atomic units, a.u.):

$$H = H_1 + H_2 + H_3 + H_4, \tag{1}$$

where

$$H_1 = -\frac{1}{2}\Delta_1 - \frac{1}{2}\Delta_2 + \frac{1}{|r_1 - r_2|} - \sum_{i=1}^{2}\sum_{j=1}^{N+1}\frac{Z_j}{|r_i - R_j|} \tag{2}$$

is the operator for the kinetic energy of the electrons, the interaction energy of the electrons with each other, and the interaction energy of the electrons with the point ions and the proton;

$$H_2 = -\sum_{i=1}^{N+1}\frac{1}{2M_i}\Delta_i \tag{3}$$

is the kinetic energy operator of the point ions and the proton, and

$$H_3 = \frac{1}{2}\sum_{i,j=1}^{N+1}\frac{Z_i Z_j}{|R_i - R_j|} + \frac{1}{2}\sum_{i,j=1}^{N}W_{rep}(R_i, R_j) \tag{4}$$

is the operator for Coulomb interaction between the point

ions themselves, between point ions and the proton, and for the repulsive energy between the point ions. The last term H_4 is the interaction energy of the electrons, point ions, and the proton with the dipole moments. One can find the explicit form of this nonlinear operator in ref. 3. The polarization values of the point ions appearing in H_4 were taken from ref. 4.

We shall solve this problem in the adiabatic approximation; i.e., we approximate the wave function of the system by*

*r and R, without indices, denote collectively all the electronic and ionic coordinates, respectively.

$$\Psi_{\alpha n}(r, R) = \psi_\alpha(r \mid R)\,\varphi_{\alpha n}(R), \quad (5)$$

where the functions $\psi_\alpha(r \mid R)$ and $\varphi_{\alpha n}(R)$ satisfy the equations

$$H_1\psi_\alpha(r \mid R) = W_\alpha(R)\,\psi_\alpha(r \mid R) \quad (6)$$

and

$$[H_2 + E_\alpha(R)]\,\varphi_{\alpha n}(R) = E_{\alpha n}\varphi_{\alpha n}(R), \quad (7)$$

where

$$E_\alpha(R) = W_\alpha(R) + H_3 + \int \psi_\alpha^*(r' \mid R)\,H_4\psi_\alpha(r' \mid R)\,dr'. \quad (8)$$

The quantity $E_\alpha(R)$ which plays the role of the potential energy in Eq. (8) is designated as the adiabatic potential.

2. Thus the problem reduces to the solution of Eqs. (6) and (7), the first of which describes the motion of the electrons, and the second which describes the motion of the point ions and the proton. Since it is the optical properties of the U-center which interest us, we consider only small oscillations of the point ions (and proton); i.e., it is necessary for us to know the values of the adiabatic potential only close to their equilibrium positions. Starting from this, one can look for the eigenfunctions and eigenvalues of Eq. (6) which depend on the coordinate R (and on the parameters) of the point ions—not for the entire range of R, but only near the equilibrium positions of the ions. As a consequence of the small range of variation of R, it is expedient to solve this problem by the following method: find the eigenfunctions and eigenvalues of Eq. (6) corresponding to a certain configuration of the point ions close to equilibrium, and determine the quantity $W_\alpha(R)$ as a function of R for the region of interest by first approximation perturbation theory. In this case, one can use the results of Gourary,[5] who solved Eq. (6) approximately for a configuration of ions which corresponds to an ideal point lattice of the NaCl type with the parameter $a_0' = 5.31$ a.u. (experimental value at room temperature). Solving the variational problem equivalent to Eq. (6) and using the function

$$\psi_1(r_1, r_2) = \frac{L}{4\pi}\left(e^{-\mu r_1}e^{-\nu r_2} + e^{-\mu r_2}e^{-\nu r_1}\right), \quad (9)$$

as a comparison function for the ground state, where L is a normalization constant, and for the excited state the function

$$\psi_2(r_1, r_2) = \frac{1}{\sqrt{2}}\left[\psi_1(r_1)\,\psi_2(r_2) + \psi_1(r_2)\,\psi_2(r_1)\right], \quad (10)$$

where

$$\psi_1(r) = \pi^{-\frac{1}{2}}\gamma^{\frac{3}{2}}e^{-\gamma r},$$

$$\psi_2(r) = \pi^{-\frac{1}{2}}\lambda^{\frac{5}{2}}re^{-\lambda r}\cos\theta.$$

Gourary found: $\mu = 0.998$; $\nu = 0.471$; $\gamma = 1$; $\lambda = 0.452$; $W_1(R_0') = -1.142$ a.u.; $W_2(R_0') = -0.954$ a.u. The transition energy ΔE was found to be 0.188 a.u. The experimental value of ΔE at room temperature is 0.238 a.u.

3. From first order perturbation theory we obtain the formula for the function $W_\alpha(R)$

$$W_\alpha(R) = \int \psi_\alpha^*(r \mid R_0')\,H_1(r, R)\,\psi_\alpha(r \mid R_0')\,dr, \quad (11)$$

where $\alpha = 1,2$ (we denote function (9) by $\psi_1(r \mid R_0')$ and function (10) by $\psi_2(r \mid R_0')$). We use these same functions for calculation of the third term in formula (8). The second term in formula (8) is calculated directly.

As was indicated, it is necessary to know the values of the adiabatic potentials only near the equilibrium positions of the point ions. The equilibrium positions of ions in a crystal with U-centers are easily determined if one starts from the equilibrium positions of ions in an ideal crystal. The latter were obtained theoretically by Löwdin from the condition for a minimum of the expression

$$\frac{1}{2}\sum_{i,j=0}^{N}\left[\frac{Z_iZ_j}{|R_i - R_j|} + W_{\text{rep}}(R_i, R_j)\right], \quad (12)$$

the lattice parameter a_0 for a NaCl crystal was found equal to 5.19 a.u. (this value corresponds to 0° K). When a single anion is replaced by a negative hydrogen ion, only the cations nearest the hydrogen ion are displaced appreciably, since the charges of the anion and negative hydrogen ion are equal. In computing the adiabatic potentials we therefore consider only the displacements of the equilibrium positions of the cations nearest the hydrogen ion.

In the ground state ($\alpha = 1$) the electron cloud of the U-center is spherically symmetrical; consequently, the displacement of the equilibrium positions of the cations takes place in such a way that the point symmetry of the lattice is preserved (see Fig. 1); i.e., $R_1 = R_2 = \cdots = R_6 \equiv R$. In order to find the value of $R_{\min}$ corresponding to the equilibrium configuration of the cations, it is sufficient to plot the curve $E_1(R, \cdots R, R_7^0, \cdots R_{N+1}^0) \equiv E_1(R)$ as a function of R and find its minimum. In the first excited state ($\alpha = 2$), the electron cloud of the U-center possesses a lower symmetry, and the equilibrium positions of the cations will be shifted as indicated in Fig. 2, i.e., $R_1 = R_2 \equiv R_I$, $R_3 = \cdots = R_6 = R_{II}$. To determine the values of $R_{I\min}$ and $R_{II\min}$ corresponding to the equilibrium positions of the cations, it is sufficient to plot the surface $E_2(R_I, R_I, R_{II}, \cdots R_{II}, R_7^0, \cdots R_{N+1}^0) \equiv E_2(R_I, R_{II})$ as a function of R_I and R_{II} and find its minimum.

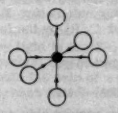

Fig. 1

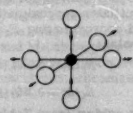

Fig. 2

Fig. 1. Displacement of the equilibrium positions of the cations (U-center is in the ground state). The origin is at the point of the ideal lattice corresponding to the anion which has been replaced by H^-.
Fig. 2. Displacement of the equilibrium positions of the cations (U-center is in an excited state).

The calculated values of $E_1(R)$ and $E_2(R_I, R_{II})$ are given in Tables 1 and 2, respectively. Detailed formulas for the calculations are given in the Appendix. It is shown that the minimum of the curve $E_1(R)$ lies at $R_{\min} =$

4.64 a.u., and the minimum of the surface $E_2(R_I, R_{II})$ lies at the point with coordinates $R_{I\,min} = 4.91$ a.u. and $R_{II\,min} = 5.49$ a.u. To find the transition energies, the following values of the adiabatic potentials were calculated at the minimum points corresponding to the ground and excited states:

$E_1(R_{min}) = -0.835$ a.u.; $E_1(R_{I\,min}, R_{II\,min}) = -0.787$ a.u.

$E_2(R_{min}, R_{min}) = -0.579$ a.u.; $E_2(R_{I\,min}, R_{II\,min}) = -0.623$ a.u.

Table 1. Adiabatic Potentials $E_1(R)$ and $E_2(R)$

R (a. u.)	$E_1(R)$ (a. u.)	$E_2(R)$ (a. u.)
4.4	−0.8320	−0.5381
4.5	−0.8341	−0.5556
4.6	−0.8354	−0.5705
4.7	−0.8352	−0.5824
4.8	−0.8337	−0.5925
4.9	−0.8315	−0.6005

Table 2. Adiabatic Potential $E_2(R_I, R_{II})$(in a.u.)

R_{II} (a. u.)	R_I (a. u.)			
	4.8	4.9	5.0	5.1
5.4	−0.6223	−0.6228	−0.6227	−0.6223
5.5	−0.6230	−0.6234	−0.6233	−0.6226
5.6	−0.6222	−0.6225	−0.6220	−0.6213
5.7	−0.6194	−0.6196	−0.6190	−0.6180

The energies for transition with the absorption (ΔE_{abs}) and emission (ΔE_{em}) of light which follow from this are given in Table 3.

Table 3. Comparison of Calculated Quantities with Experimental Data

Quantity	Theoretical value (a. u.)	Experimental value (a. u.)
ΔE_{abs} (0)	0.257	0.245 [7]
ΔE_{abs} (77)	—	0.242 [8]
ΔE_{em} (0)	0.164	
$\mathcal{H}$ (77)	0.018	0.019 [8]
$\mathcal{H}$ (293)	0.030	0.028 [8]

(Numbers in parentheses are temperatures in °K.)

Besides the transition energies, it was possible on the basis of the calculations to estimate the halfwidth of the U-band, if one assumes that the symmetrical oscillations of the six cations nearest the hydrogen ion provide the main contribution to this halfwidth. One can find values of the halfwidth $\mathcal{H}$ for different temperatures in the single oscillator approximation after calculating $E_2(R, R) \equiv E_2(R)$ and approximating $E_1(R)$ and $E_2(R)$ by the following parabolas:

$$E_1(R) = 0.0484\,(R - 4.62)^2 - 0.835;$$

$$E_2(R) = 0.0954\,(R - 5.29)^2 - 0.619.$$

As is evident from Table 3, the results obtained on the basis of a polarized point lattice agree well with experiment.

In conclusion, we express our gratitude to M. I. Petrashen' for suggesting this investigation and for his constant interest, and also to M. G. Veselov and N. N. Kristofel for valuable discussions.

APPENDIX

Let us consider in order the terms which enter in formula (8) for the adiabatic potentials $E_n(R)$.

Calculating $W_n(R)$, we find that starting from values of the functions $W_n(R_0')$ which correspond to an ideal lattice with the parameter $a_0' = 5.31$ a.u., we must first determine values of the functions $W_n(R_0)$ which correspond to an ideal lattice with the parameter $a_0 = 5.19$ a.u. Secondly, we must find the expressions $W_n(R)$ as functions of the coordinates of the cations nearest the hydrogen ion for values of R close to a_0. From formula (11), using (9) and (10), we obtain for $W_1(R_0)$ and $W_2(R_0)$

$$W_1(R_0) = W_1(R_0') + \beta \int \psi_1^*(r \mid R_0')\, V(r, R_0')\, \psi_1(r \mid R_0')\, d\tau \qquad (I)$$

$$+ 2 \sum_m n_m \frac{L^3}{8\pi^3 s^3} \left\{ \frac{1+\beta}{R_m'} \int_0^{R_m'} K(r)\, r^2 dr + \beta \int_{R_m'}^{\infty} K(r)\, r dr - \int_0^{R_m'} K(r)\, r dr \right\},$$

where

$$K(r) = \frac{\varkappa^3}{2} e^{-\varkappa r} + \frac{\mu^3}{2} e^{-\mu r} + 4 \left(\frac{2\mu\nu}{\mu+\nu} \right)^3 e^{-(\mu+\nu)r},$$

$$V(r, R_0') = \sum_{i=1}^{s} \sum_m \frac{n_m Z_m}{|r_i - R_m'|}.$$

n_m is the number of point ions in the m-th layer,* z_m is the charge of an ion belonging to the m-th layer, $R_m' = a_0\sqrt{m}$, $R_m' = a_0'\sqrt{m}$, $\beta = (a_0' - a_0)/a_0'$ (summation is over all positive integers);

*Ions with the same value of R_m form the m-th layer. Ions belonging to one and the same layer have the same charge.

$$W_2(R_0) = W_2(R_0') + \beta \int \psi_2^*(r \mid R_0')\, V(r, R_0')\, \psi_2(r \mid R_0')\, d\tau \qquad (II)$$

$$+ 4\gamma^3 \sum_m n_m \left[\frac{1+\beta}{R_m'} \int_0^{R_m'} e^{-2\gamma r} r^2 dr + \beta \int_{R_m'}^{\infty} e^{-2\gamma r} r dr - \int_0^{R_m'} e^{-2\gamma r} r dr \right]$$

$$+ \frac{4\gamma^5}{3} \sum_m n_m \left[\frac{1+\beta}{R_m'} \int_0^{R_m'} e^{-2\gamma r} r^4 dr + \beta \int_{R_m'}^{\infty} e^{-2\gamma r} r^2 dr - \int_0^{R_m'} e^{-2\gamma r} r^2 dr \right],$$

where the notation is the same as in (I).

It was found from formulas (I) and (II) that $W_1(R_0) = -1.148$ a.u. and $W_2(R_0) = -0.940$ a.u.

In exactly the same way one can obtain the following expressions for the functions $W_n(R)$ intended for calculation of the transition energies with emission of light:

$$W_1(R) = W_1(R_0) - 2 \sum_{i=1}^{II} n_i \left\{ \left(\frac{1}{R_i} - \frac{1}{a_0} \right) + \frac{L^3}{8\pi^3 s^3} \left[\frac{1}{R_i} \int_0^{R_i} K(r)\, r^2 dr \right. \right.$$

$$\left. \left. - \int_{R_i}^{\infty} K(r)\, r dr + \int_{a_0}^{\infty} K(r)\, r dr - \frac{1}{a_0} \int_{a_0}^{\infty} K(r)\, r^2 dr \right] \right\}, \qquad (III)$$

where $n_1 = 2$, $n_{11} = 4$, and the remaining notation is the same as in (I);

$$W_2(R) = W_2(R_0) - \sum_{i=1}^{II} n_i \left\{ 2 \left(\frac{1}{R_i} - \frac{1}{a_0} \right) \right.$$

$$\left. - G(R_i) + F(R_i)\, P_2(\cos \vartheta_i) \right\}. \qquad (IV)$$

Here

$$G(R_i) = 4\gamma^3 \left[\frac{1}{R_i} \Gamma_2(R_i) - \Gamma_1(R_i) - \frac{1}{a_0} \Gamma_2(a_0) + \Gamma_1(a_0) \right]$$

$$+ \frac{4\gamma^5}{3} \left[A_2(R_i) - \frac{1}{R_i} A_1(R_i) - A_2(a_0) + \frac{1}{a_0} A_1(a_0) \right],$$

$$F(R_i)=\frac{8\lambda^5}{15}\left\{\frac{1}{R_i}[\Lambda-\Lambda_0(R_i)]+R_i^2\Lambda_1(R_i)\right.$$

$$\left.-\frac{1}{a_0^5}[\Lambda-\Lambda_0(a_0)]-a_0^2\Lambda_1(a_0)\right\};$$

$$\Gamma_n(R)=\int_R^\infty e^{-2\gamma r}r^n dr;\qquad \Lambda_n(R)=\int_R^\infty e^{-2\lambda r}r^n dr;\qquad \Lambda=\int_0^\infty e^{-2\lambda r}r^2 dr,$$

$P_2(\cos\theta)$ is the Legendre polynomial of order two.

For calculation of the characteristics of the absorption it is necessary to set $R_I = R_{II}$ in formulas (III) and (IV).

One can find the detailed expression for the function H_3 in ref. 3. The expression for the function $H_4(R)$ differs from the analagous expression given in ref. 3 only by terms containing the intensity $\mathcal{E}_0(R)$ of the electric field of the negative hydrogen ion. The latter are written in the following manner:

$$\mathcal{E}_{1R}(R)=-\frac{1}{R^2}+\frac{32\pi^2L^2}{R^2}\int_R^\infty K(r)\,r^2dr,$$

$$\mathcal{E}_{2R}(R,\theta)=-\frac{1}{R^3}+\frac{4\gamma^3}{R^3}\Gamma_3(R)+\frac{4\lambda^5}{3R^3}\Lambda_4(R)$$

$$+\frac{8\lambda^5}{15}P_2(\cos\theta)\left\{2R\Lambda_1(R)-\frac{3}{R^3}[\Lambda-\Lambda_4(R)]\right\}, \qquad (V)$$

$$\mathcal{E}_{2\theta}(R,\theta)=-\frac{4\lambda^5}{5}\sin 2\theta\left\{\frac{1}{R^3}[\Lambda-\Lambda_4(R)]+R\Lambda_1(R)\right\},$$

where $\mathcal{E}_{nR}(R,\theta)$ is the radial and $\mathcal{E}_{n\theta}(R,\theta)$ the angular components of the electric intensity of the hydrogen ion field. It is obvious that $\mathcal{E}_{1\theta}(R,\theta)=0$.

REFERENCES

1. F. Seitz, Revs. Modern Phys. **26**, 7 (1954).
2. C. Delbecq, B. Smaller, and P. Yuster, Phys. Rev. **104**, 599 (1956).
3. I. V. Abarenkov, Vestnik Leningrad. Gosudarst. Univ., in press.
4. W. Shockley, Phys. Rev. **70**, 105 (A) (1946).
5. B. Gourary, Phys. Rev. **112**, 337 (1958).
6. P-O. Löwdin, A Theoretical Investigation into Some Properties of Solids, Uppsala, 1948.
7. H. Ivey, Phys. Rev. **72**, 341 (1947).
8. H. Etzel and D. Patterson, Phys. Rev. **112**, 1112 (1958).

THE ROLE OF M-, R-, AND F′- COLOR CENTERS IN THE INFRARED FLUORESCENCE OF F-CENTERS IN ALKALI HALIDE CRYSTALS

I. I. Ezhik and S. T. Shovlo

Received 28 October 1959

Infrared fluorescence of F-centers is observed between 1 and 1.5 μ in both additively colored[1] and x-rayed[2,3] alkali halide crystals. In both cases it originates during irradiation of the colored crystals with light in the F-center absorption band. In additively colored crystals the infrared luminescence is observed only at low temperatures, and practically disappears at 100-150°K.[1]

In x-rayed crystals the infrared fluorescence of F-centers is observed at both high and low temperatures.[2,3] On the infrared F-center fluorescence vs. temperature curves in the 77-400°K range, peaks are observed at 218°K in NaCl, at 140, 224, 270, and 312°K in KCl, and at 162 and 254°K in KBr crystals.[2,3] No such infrared luminescence peaks were observed in additively colored crystals.[1]

No explanation has yet been found[1] for the absence of infrared fluorescence peaks in the temperature dependence curves additively colored crystals, for the sharp drop in the intensity of infrared fluorescence in the 100-150°K range, or for the disappearance of fluorescence at certain temperatures. The role of color centers (M-, R-, and F′- centers) in the infrared fluorescence of F- centers is also of great theoretical and practical interest. The present paper is devoted to these questions.

The investigation was performed on crystals additively colored by the method of Artsybyshev.[4] After additive coloring the crystals were cooled in the dark to liquid nitrogen temperature, and thus contained only F-centers. An FS-A1 photoresistor was used as the infrared fluorescence indicator. Weak currents were amplified with an ac resonance amplifier.[2] The crystals were uniformly heated at a rate of 5-6 deg/min by means of a heating element which permitted the temperature to change from 77 to 600°K. The intensity of the infrared F-center fluorescence was measured over this temperature range.

We performed the following experiments with additively colored crystals in order to determine the role of F′-, M-, and R- centers in the infrared fluorescence of F-centers: (1) The crystal was simultaneously excited by light in the F- and M-absorption bands. (2) The crystal was simultaneously excited by light in the F- and F′- absorption bands. (3) The crystal was simultaneously excited by light in the F-, F′-, and M- absorption bands. The spectral regions necessary for excitation were isolated with the help of a fast quartz monochromator and interference filters (see Table).

Type of crystal	F-band $\lambda_{max.}$ (A)	M-band $\lambda_{max.}$ (A)	F′-band $\lambda_{max.}$ (A)
NaCl . . .	4700	7100	5200
KCl . . .	5600	7900	7400
KBr . . .	6300	8000	7800

The experimental results are shown in Figs. 1 and 2.

Upon simultaneous excitation of additively colored KCl crystals in the F′ and M-bands, a large drop is observed in the intensity of infrared fluorescence at approximately 220°K (curve 2, Fig. 1). Completely unexpected results were obtained upon simultaneous excitation of crystals in the F- and F′- absorption bands. In this case, a sharp peak is observed at 325°K in the infra-

Fig. 1. Infrared fluorescence of F-centers in additively colored KCl crystals. Curve 1—Upon simultaneous excitation in F- and F′- absorption bands; curve 2—same in F-, F′-, and M- absorption bands; curve 3—same in F′- and M- absorption bands.

red fluorescence intensity vs. temperature curve (curve 1). The intensity of luminescence does not change between 77 and 220°K. A drop in the intensity of infrared fluorescence is observed above 220°K; as will be shown later, this is the temperature of thermal decomposition of F′- centers. An infrared fluorescence peak can also be observed at 210°K upon simultaneous excitation of KCl crystals in the F- and M- absorption bands (curve 3). Qualitatively similar results were obtained with KBr crystals (Fig. 2). A peak is observed at 240°K on the intensity of infrared fluorescence vs. temperature curve when additively colored KBr crystals are simultaneously excited in the F- and F′- absorption bands. Upon simultaneous excitation of KBr crystals in the F- and M- absorption bands, a peak is observed at 150°K (curve 3). Finally, a most intense infrared fluorescence of F-centers is observed when the crystals are excited in the F′- and M- absorption bands (the drop in luminescence intensity begins at about 150°K.)

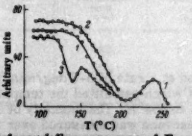

Fig. 2. Infrared fluorescence of F-centers in additively colored KBr crystals. Curve 1—Upon simultaneous excitation in F- and in F′- absorption bands; curve 2—same in F-, F′- and M- absorption bands; curve 3—same in F- and M- absorption bands.

If the location of the peaks of the infrared F- center fluorescence on the curves of Figs. 1 and 2 is compared to corresponding data for the visible and ultraviolet luminescence of the same crystals, it turns out that the temperatures at which the peaks of infrared fluorescence are located coincide with the corresponding peaks on thermal de-excitation curves. The infrared fluorescence peak at 325°K in KCl crystals coincides with a peak corresponding to the thermal decomposition of M-centers;[3] the infrared fluorescence peak at 220°K corresponds to the thermal decomposition of F′-centers.[3,4] In KBr crystals the infrared fluorescence peak at 240°K corresponds to the thermal decomposition of M-centers, and the peak at 150°K corresponds to the thermal decomposition of F′- centers.[4]

Thus a direct connection has been established in the present paper between the infrared luminescence of F-centers and M- and F′- centers. It also follows from our experiments that the yield of infrared fluorescence is considerably increased by an additional excitation of crystals in the F′- and M- absorption bands or by a simultaneous excitation in the F′- and M- absorption bands. This increase in yield obviously comes from newly formed F-centers. The electrons used in the formation of new F-centers are those resulting from the destruction of F′- and M- centers by the exciting light. Not all of the electrons form F-centers; some participate in transitions involving the emission of visible or ultraviolet light (also nonradiative transitions).

The formation of infrared fluorescence peaks (which are observed on the curves in Figs. 1 and 2) can be explained on the basis of a kinetic scheme in which the F-center is represented by two levels—a ground level k and an excited level i. Local F′-, M-, and R- levels are considered to be electron acceptor levels (Fig. 3). Electrons will be captured at these levels if there is no excitation by light in the F′-, M-, and R- bands. It was previously shown[2] that infrared fluorescence arises as a result of a transition of an excited F-center from the 2p state to the ground state 1s (transition n_1, Fig. 3). In this case, the excitation is accomplished by light in the F-center absorption band. If an additively colored crystal is illuminated only in the F-absorption band, the intensity of infrared emission suffers a characteristic loss with increasing temperature in the 100-150°K range.[1] This can be explained by assuming that at 100°K and above, a transition of F-center electrons through the conduction band takes place, accompanied by the formation of F′-, M-, R-, and other color centers (transitions 2, 3, and 4); some of these electrons are also spent on transitions 5-8. The destruction of F-centers (transitions L_i) predominates over the formation of new F-centers (transition 1) and, consequently, the intensity of the infrared fluorescence of F-centers rapidly decreases.

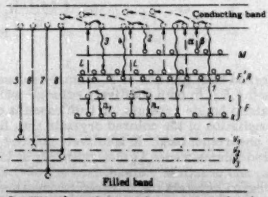

Fig. 3. Kinetic scheme of processes leading to the formation of the infrared luminescence of additively colored crystals.

It is known that F′- centers are formed as a result of F-center destruction, and that two F- centers are formed when one F′- center is destroyed. Therefore a considerable restoration of destroyed F-centers takes place upon excitation of additively colored crystals in the F′- band at certain temperatures; as a result of this restoration the intensity of infrared emission is in this case considerably increased (transitions α, 1). A similar restoration of F- centers and, consequently, an increase in the intensity of the infrared fluorescence of F-centers is also observed in the case of an additional excitation in the M- absorption band (transitions β, 1).

A formation of M- centers takes place during the excitation of additively colored crystals with light in the F- and F′- center absorption bands at 77°K; these M- centers are destroyed upon further heating. The thermal destruction of M- centers occurs at a definite temperature. The formation of new F- centers (transitions β, 1) takes place

at the same temperature, and they account for the infrared fluorescence peaks shown in Figs. 1 and 2. A similar mechanism for the formation of infrared fluorescence peaks also operates during the excitation of the crystals in the absorption band of F- and M- centers. In this case F'- centers are formed at 77°K, which produce new F-centers upon thermal destruction, which in turn account for the infrared fluorescence peaks.

REFERENCES

1. P. J. Botden, C. Z. Doorn, and Y. Haven, Philips Res. Repts. 9, 469 (1954).
2. I. I. Ezhik, Ukrain. Fiz. Zhur. 3, 56 (1958).
3. I. I. Ezhik and S. T. Shovlo, Izvest. Ministerstva Vysshego Obrazovaniya SSSR, Fiz. No. 3, 62 (1959).
4. S. A. Artsybyshev, Trudy Fiz. Inst., Akad. Nauk SSSR 1, 5 (1938).
5. Ch. B. Lushchik, Trudy Inst. Fiz. i Astron., Akad. Nauk Eston.SSR No. 3, 3 (1955).
6. D. D. Dutton and R. Maurer, Phys. Rev. 90, 126 (1953).

MAIN PEAKS IN THE LIGHT PULSES OF ELECTROLUMINESCENCE

A. N. Georgobiani and M. N. Fok

Received 26 May 1960

By investigating the shape of the light pulse, it is shown that at high voltages the process of electron release is regulated basically by the field. Electron liberation takes place at low temperatures by collision ionization and at high temperatures by tunneling through a potential barrier (Zener effect). A comparison of experimental and theoretical temperature dependence curves of the fields at which a total release of electrons is obtained has made it possible to calculate the value of optical phonons in ZnS and the energy depth of localized levels. These values are in good agreement with the value of the optical phonon obtained from the vibrational structure of the edge emission spectrum, and with the energy depth of levels calculated from the equilibrium concentration of donor free electrons in an electroluminescent ZnS-Cu crystal.

INTRODUCTION

The present investigation was performed with ZnS-Cu electroluminors (Cu ~ 10^{-3}, Al ~ 10^{-4} gm atom/gm mol). A polymerized mixture of melamine formaldehyde and aldehyde-resyl resins was used as a dielectric. The electroluminor was insulated from the electrodes. This was indicated by the following facts: First, the current passing through the electroluminescent cell was capacitative in nature; secondly, a mica strip placed between the electrode and the electroluminescent layer produced changes which could be compensated by a simple increase in voltage.

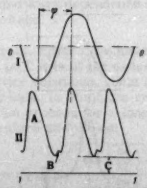

Fig. 1. Oscillograms of the brightness of electroluminescence (curve II) and of the exciting voltage (curve I). 0,0—Zero voltage line; 1,1—zero brightness line. A—main peak of brightness wave; B—additional peak of brightness wave; C—real component of electroluminescent brightness. φ—phase shift between the start of voltage switching and the maximum of the main peak of the brightness wave.

An oscillogram of the electroluminescence intensity is shown in Fig. 1 (curve II). together with an oscillogram of the sinusoidal exciting voltage (curve I). It is easy to see that the intensity oscillogram consists of an alternating component (usually called the light pulse) and a constant (dc) component, designated on the drawing by the letter C. The nature of the dc component was investigated in ref. 1. In each half-cycle of the exciting voltage the light pulse has a main peak, denoted by the letter A. Additional peaks B appear in certain phosphors under some specific conditions, these peaks being usually smaller than the main peaks. The components of the light pulse are better resolved if the exciting voltage has a trapezoidal shape (Fig. 2).

The formation of a light pulse is evidently connected with electron displacement within the crystal, which is to some degree regulated by the electrical field. We assume, in accordance with a widespread point of view, that an ionization of luminescence centers takes place at one end of the crystal in each half-cycle of the exciting voltage, and that electrons are transferred to the other end. In the next half-cycle electrons return to the ionized centers and recombine with them, emitting radiation. This two-stage model of the electroluminescent cycle is corroborated by the following facts: First, the probability of recombination is very small in the region of high field strength (where the ionization of luminescence centers takes place), because the electrons leave the excitation region very rapidly, the electron mobility in ZnS being 120 cm^2/volt-sec^2 and the crystal dimensions being of the order of 10^{-3} cm. Secondly, when the voltage pulse

Fig. 2. Oscillogram of electroluminescence brightness in the case of trapezoidal exciting voltage.

is applied to an electroluminescent cell with a well de-excited phosphor, a noticeable emission is observed only on the removal (or change of polarity) of the voltage applied to the cell;[1] i.e., apparently at the time when electrons may possibly return to the region of excitation. Thirdly, the insertion of a single weak pulse into the sinusoidal exciting voltage does not act on the light pulse then in progress, but on the next one.[3] This can be explained by assuming that electrons can return to luminescence centers which were ionized in a given half-cycle of the exciting voltage only after a change in the polarity of the field, that is, in the next half-cycle.

In our opinion, it was convincingly demonstrated in ref. 4 that additional light pulses are associated with a return to the excitation region of electrons liberated by thermal ionization of trapping centers at a depth smaller than 0.4 ev.

The mechanism of formation of the main peaks of light pulses has not yet been explained. Many authors, including Zalm[3] and Haake,[4] believe that the main peak is caused by the return of free electrons to the excitation region. The additional peak, however, follows the main peak after some delay, as it is formed as a result of the return of trapped electrons to the excitation region. However, since the mobility of an electron in ZnS is about 120 cm^2/volt-sec,[5] the return of electrons should occur without inertia for an exciting voltage whose half-cycle lasts approximately 10^{-3} sec. It should therefore be expected that the main peak be near the maximum and not near the zero point of the derivative of the field as is observed experimentally.

The present work is devoted to an experimental clarification of the formation mechanism of the main peaks of light pulses.

THE MAXIMUM OF THE MAIN PEAK OF THE LIGHT PULSE

According to our observations, the phase φ of the maximum of the main peak of the light pulse (see Fig. 1) remained practically constant when the temperature T was varied from 77°K to 373°K and the frequency f of the exciting sinusoidal voltage was varied from 200 to 5500 cycles. The value of the phase φ is counted from the moment when the external voltage reverses polarity; that is, from the moment when it becomes possible for the electrons to return to the region of excitation (see Fig. 2). The data are shown in Table 1.

Table 1

f = 200 cycles		f = 5500 cycles	
T (°K)	$\frac{\varphi}{\pi}$	T (°K)	$\frac{\varphi}{\pi}$
77	0.74	77	0.79
293	0.79	293	0.86
373	0.81	373	0.89

The appearance of the main peak of the light pulse cannot consequently be explained by a return of electrons liberated by thermal ionization from shallow local levels, as is probably the case for the formation of the additional peak. As it was shown above, it is likewise necessary to reject the hypothesis that the main peaks of the light pulse are caused by the return of free electrons to the region of excitation. These facts indicate that the shape of the main peak of the light pulse is basically determined by the electric field.

We assume that the main peak of the light pulse is basically related to the return to the excited region of electrons released from local levels either by collision ionization or by field ionization (Zener effect). It follows from this hypothesis that with an increase of the electrical field strength, the shallow trapping levels will be the first to be emptied, followed by the deeper trapping levels; when a certain "critical" value of the electrical field is finally reached, a practically total release of electrons must take place even from the deepest trapping levels. As a result, any further increase in the electric field must be accompanied by a decrease in brightness because of the emptying of the traps, which are the source of the electrons. This effect was actually observed by us at field strengths across the electroluminescent capacitor in excess of 10^5 volts/cm (Fig. 3).

Fig. 3. Oscillogram of intensity of electroluminescence with a trapezoidal exciting voltage corresponding to an average field greater than 10^5 volts/cm.

In oscillogram a (Fig. 4) the pulse amplitude of the

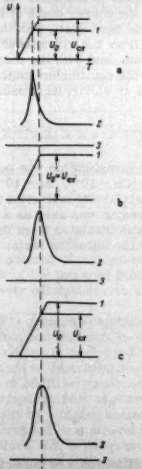

Fig. 4. Dependence of the location of the maximum of the main peak of the light pulse on the voltage pulse amplitude. 1—Oscillogram of the exciting voltage; 2—oscillogram of the intensity of electroluminescence; 3—zero intensity line of electroluminescence. U_0—amplitude of the exciting voltage; U_{cr}.—critical voltage. a—pulse amplitude smaller, b—equal, c—greater than the critical voltage.

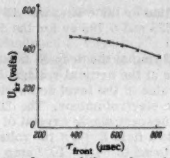

Fig. 5. Dependence of the value of critical voltage on the steepness of the pulse front of the exciting voltage.

exciting voltage U_0 is smaller than the critical voltage $U_{cr.}$. The light pulse in this case reaches a maximum at the end of the front of the voltage pulse. In oscillogram b, the voltage pulse amplitude equals the critical voltage, and in oscillogram c exceeds it. In this case, the light pulse reaches a maximum at the moment when the exciting voltage pulse reaches the critical value. Let us also note that the value of the critical voltage is only slightly dependent on the steepness of the pulse front (Fig. 5).

TEMPERATURE DEPENDENCE OF THE CRITICAL VOLTAGE VALUE

The temperature dependence of the critical voltage value is shown in Fig. 6. Let us compare our curve with the temperature dependence of critical fields in collision ionization processes and in tunneling electron release processes. (The mechanism of collision ionization was theoretically investigated by Chuenkov[8] and by Keldysh.)[9]

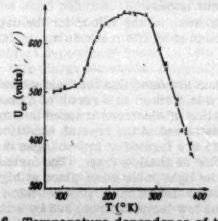

Fig. 6. Temperature dependence of the value of critical voltage.

According to refs. 2 and 3 the mean free path for thermal electrons in ZnS is of the order of 10^{-5} cm, i.e., several tens of lattice constants. This is a very large value for ionic crystals, in which the critical field for a collision ionization process for a long mean free path depends on temperature as follows:

$$E_{cr.} = A \cdot \sqrt{\frac{\exp\left(\frac{\hbar\omega}{kT}\right)+1}{\exp\left(\frac{\hbar\omega}{kT}\right)-1}}, \qquad (1)$$

where $\hbar\omega$ is the value of the optical phonon and A—which is independent of temperature—is equal to the critical field at 0°K. According to this formula, the magnitude of the critical field drops with decreasing temperature until kT becomes much smaller than $\hbar\omega$, whereupon $E_{cr.} \approx A$, that is, $E_{cr.}$ becomes independent of temperature. This is exactly the shape of the low temperature side of the curve in Fig. 6.

Equation (1) can be reduced to a form which is convenient for the calculation of the value of the optical phonon

$$\hbar\omega = kT \ln \frac{E^2_{cr.}(T) + A^2}{E^2_{cr.}(T) - A^2} \qquad (2)$$

Since the probabilities of collision ionization and tunneling release of electrons increase greatly with increasing electrical field, it is obvious that the processes which release electrons from traps are most effective in the region of a concentrated field, that is, at the edge of the crystal. According to the Schottky model, the field at the crystal edge is proportional to the square root of the applied voltage. (The ordinates in Fig. 6 are therefore proportional to the square of the critical field, that is, $U_{cr.} \sim E^2_{cr.}$.) As seen in Fig. 6, the critical voltage is already practically independent of temperature at 80°K, and we therefore assume that $E_{cr.}(80°K) \approx A$. A comparison is made in Table 2 between the values of optical phonons calculated from Eq. (2) and the values of the longitudinal ($\hbar\omega_{long.}$) and transversal ($\hbar\omega_{tr.}$) optical phonons obtained in refs. 7 and 8 from the vibrational structure of the edge emission spectrum.

Table 2

$\hbar\omega$ (from electroluminescence)	$3.8 \cdot 10^{-2}$ ev
$\hbar\omega_{long.}$ (from the fluorescence spectrum)	$4.3 \cdot 10^{-2}$ ev
$\hbar\omega_{tr.}$ (from the fluorescence spectrum)	$3.4 \cdot 10^{-2}$ ev

Inasmuch as both longitudinal and transversal optical phonons participate in electron scattering, our calculated effective value must lie between the two indicated values, which is experimentally the case. If it were assumed, however, that there is no concentration of the field, the value obtained for the phonons would be 2.55×10^{-2} ev, which is not in agreement with phonon values obtained from the fluorescence spectrum. This can serve as additional proof of the occurrence of field concentration in electroluminescence.

The temperature dependence of the tunneling release of electrons has been theoretically investigated by Keldysh.[9] The critical field for this mechanism decreases slightly with increasing temperature, because of the change in lattice parameters and the increase in the number of phonons. The presence of phonons is necessary to fulfill the law of the conservation of momentum in a tunneling transition. In the region of high temperatures, in which the condition

$$T > \frac{eEd}{k}, \qquad (3)$$

is fulfilled (where e is the electron charge, d the lattice constant, and k the Boltzmann constant), the critical field begins to decrease rapidly with increasing temperature, due to the energy contribution of phonons to the electron release process. Let us attempt to compare this effect with the drop of critical voltage on the high temperature side of curve Fig. 6. In this temperature range, the probability of tunneling release of electrons has the following form, according to Keldysh:[9]

$$W_t = b \cdot \exp\left\{-\frac{\Delta}{kT} + \frac{1}{24m}\frac{(eaE)^2}{(kT)^3}\right\}, \qquad (4)$$

where Δ is the depth of the level from which the release is taking place, m is the electron mass, and b is weakly dependent on the field and temperature. The "critical" field is the field at which probability of release during the time of observation is of the order of unity. If the exponent in Eq. (4) is designated by $-a$ at the critical value of the electrical field, then

$$e \cdot E_{cr.} = \frac{\sqrt{2\Delta}\, mkT\sqrt{\Delta}}{\hbar} \sqrt{1 - \frac{akT}{\Delta}}$$

This expression can be rewritten as follows:

$$\frac{E_{cr.}(T)}{E_0} = \frac{T}{T_0}\sqrt{1 - \frac{T}{T_0}}, \qquad (5)$$

introducing the designations

$$T_0 = \frac{\Delta}{ak}, \quad E_0 = \frac{\sqrt{2}(m\Delta)^{\frac{3}{2}}}{a\hbar e}. \qquad (6)$$

Figure 7 compares the experimental temperature dependence of the critical field with the theoretical dependence computed from Eq. (5), under the assumption that electron release is most effective in the region of field concentration, where $E^2 \sim U$. The graph is plotted in log-log coordinates in order to eliminate the influence of scale factors on the shape of the curves.

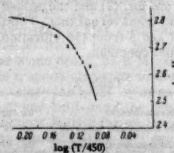

Fig. 7. Temperature dependence of the value of the critical field in the region of high temperature drop, plotted in log-log coordinates. Points—experimental; solid line—theory.

By superposing theoretical and experimental curves in Fig. 7, a value was obtained for T_0, namely, 398-403° K. The depth of the level can be obtained according to definition (6) from the equation

$$\Delta = akT_0. \qquad (7)$$

For this purpose it is necessary to calculate a in advance.

We used pulses with a rise time of $\tau_{fr.} = 10^{-3}$ sec to measure the value of critical voltage. When the critical value of the field is reached, the electron must be released during the time of observation $\tau_{obs.} = \tau_{fr.}$. In other words, when $E = E_{cr.}$

$$W_i \cdot \tau_{obs.} \approx 1. \qquad (8)$$

At a critical value of the electric field, Eq. (4) can be converted to the form

$$\frac{1}{\tau_{obs.}} \approx b \cdot e^{-a}$$

or, after changing to logarithms,

$$a \approx \ln b + \ln \tau_{obs.} \qquad (9)$$

The factor b in front of the exponential is not calculated for the temperature range (3), but, inasmuch as it varies slightly with temperature and appears as a logarithm when substituted in Eq. (9), we obtained its value from the equation for the tunneling release of electrons at low temperatures ($T \ll eEd/k$) which in this temperature range, according to ref. 10, takes the form

$$b = 1.48 \cdot 10^7 \frac{E}{\sqrt{\Delta}}. \qquad (10)$$

In our case, $E \sim 10^5$ volts/cm and $\Delta \sim 1$ ev, hence $b = 10^{12}$. The value of a then becomes 21 and the depth of the level calculated from (7) $\Delta = 0.710 + 0.005$. If b differs from the indicated value by one order of magnitude in one direction or the other, we will obtain a value between 0.635 and 0.795 ev for the depth of the level Δ.

Since an emptying of the deepest traps or donor levels takes place at the critical voltage, it is interesting to compare our value of the level depth with the value of donor levels in an electroluminor. The dark conductivity of an electroluminescent single crystal of ZnS was measured in ref. 11. In a field $E = 2 \times 10^3$ volts/cm, the current density was found to be $j = 10^{-4}$ amp/cm^2.

As is well known, the equilibrium electron concentration in the conduction band is

$$n_0 = \frac{j}{\mu e E}, \qquad (11)$$

where μ is the electron mobility. According to Kröger's data[2] $\mu = 120$ cm^2/volt-sec for ZnS and therefore $n_0 = 10^{12}$ cm^{-3}. If the width of the forbidden band is ~3.7 ev, such a value of the equilibrium concentration of electrons in the conduction band can only be caused by donors. When a negligible fraction of the donors is ionized, the relation between the equilibrium concentration of electrons and the depth of donor levels has the following form:[12,13]

$$n_0 = \sqrt{N_d \cdot N_{eff.}} \cdot e^{-\frac{\Delta_d}{2kT}}, \qquad (12)$$

where N_d is the donor concentration, Δ_d is the depth of donor levels, and $N_{eff.} = 2.5 \times 10^{19}$ cm^{-3}. In electroluminescent single crystals of ZnS, the concentration of the activator Cu ~ 10^{-3} gm atom/gm mole; that is, $N_d \sim 10^{17}$ cm^{-3}. In this case the depth of donor levels determined from Eq. (12) is 0.725 ev. If the donor concentration deviates from the indicated value by one order of magnitude in either direction, we obtain $\Delta_d = 0.685$-0.810 ev for the depth of the donor levels.

It is easy to see that the values for the depth of donor levels obtained by two methods are in fairly good agreement.

It can be thus assumed that the light pulse of electroluminescence is formed as a result of a return to the region of excitation of electrons trapped in trapping centers at the opposite end of the crystal. Additional peaks in the light pulse are formed at low voltages due to the thermal ionization of shallow traps. The formation of the main peaks of the light pulse takes place at high voltages due to an electron release, mainly by collision ionization of local levels at low temperatures, and by a tunneling release of electrons at high temperatures. At field strengths of the order of 10^5 volts/cm across the capacitor, an effective emptying of the deepest levels of the ZnS-Cu crystal takes place, these levels participating in the electroluminescence as a source of electrons.

REFERENCES

1. A. N. Georgobiani and M. V. Fok, Opt. i Spektr. 5, 167 (1958).
2. F. A. Kröger, Physica, 22, 637 (1958).
3. P. Zalm, Philips Res. Repts. 11, 353 (1956).
4. C. H. Haake, J. Appl. Phys. 28, 117 (1957).
5. V. A. Chuenkov, Izvest. Akad. Nauk SSSR, Ser. Fiz. 22, 369 (1958).
6. L. V. Keldysh, Zhur. Eksptl. i Teoret. Fiz. 37, 713 (1959).
7. F. A. Kröger and H. I. G. Mayer, Physica 20, 1149 (1954).
8. L. I. Lambe, C. C. Klick, and D. L. Dexter, Phys. Rev. 103, 1715 (1956).

9. L. V. Keldysh, Zhur. Eksptl. i Teoret. Fiz. 34, 962 (1958).
10. W. Franz, Handbuch d. Physik. 17, 155 (1956).
11. A. Lempicki, D. R. Frankl, and V. A. Brophy, Phys. Rev. 107, 1238 (1957).
12. E. I. Adirovich, G. M. Guro, V. F. Kuleshov, and V. A. Chuenkov, Trudy Fiz. Inst. Akad. Nauk SSSR 8, 127 (1960).
13. Yu. M. Popov, Opt. i Spektr. 6, 764 (1959), Optics and Spectroscopy 6, 497 (1959).

SHORT COMMUNICATIONS

HALF-WIDTH OF THE F-BAND AND DENSITY OF F-CENTERS IN SOLID SOLUTIONS OF KCl-KBr SINGLE CRYSTALS

I. Ya. Melik-Gaikazyan, M. N. Treskina, and E. K. Zavadovskaya

Received 3 May 1960

The dependence of the halfwidth of the F-band on the composition of mixed crystals of alkali halides was studied experimentally in 1953 by Gnaedinger[1] and Miessner.[2] KCl-RbCl crystals were investigated in ref. 1 (the crystal KCl-KBr was studied only for nearly equimolar compositions). In ref. 2, KCl-KBr crystals were studied, as well as KCl-RbCl crystals; however, their compositions were assumed to be the same as those of the mixtures from which the crystals were grown. A subsequent chemical analysis was not performed; this could not help but lead to errors. The experimental deviation of the values of the halfwidth of the F-bands in the solid solutions from the additive values was explained by Gnaedinger by the complexity of the F-bands, which in this case consisted of seven components, in agreement with the proposed model of the solid solution. However, the experimental dependence of the halfwidth γ on the composition of the crystal found in ref. 1 does not agree with the theoretically calculated dependence based on this model. The reason for this disagreement is, evidently, that the proposed model does not take account of the significant number of Schottky defects which is different for solid solution crystals of different compositions.

Imperfections in solid solutions of alkali halides have been investigated previously.[3-5] In these investigations the difference between the x-ray and experimental densities of the crystals was taken as the measure of the degree of imperfection. If the presence of Schottky defects determines the over-all imperfection, then the maximum number of defects must occur at the composition for which the halfwidth of the F-band is the greatest. This supposition was confirmed for crystals of KCl-RbCl, whose defects were investigated by Makarov and collaborators:[5] the maximum halfwidth of the F-band (according to Gnaedinger's data) and the maximum number of Schottky defects occur at a composition of 60 mole % RbCl in KCl.

In the crystals of KCl-KBr investigated by us, grown both from the melt and water solution, the Schottky defect maximum χ_v is shifted in the direction of the composition in which the component with the smaller lattice energy predominates (see Fig. 1).

The halfwidth of the F-band and the concentration of F-centers in single crystals of KCl-KBr obtained from the melt by the Kyropulos method were determined as follows: Plates with a thickness of 0.3-0.5 mm were chosen from among the crystals and polished with a suspension of Al_2O_3 in absolute ethyl alcohol. The polished samples were irradiated for 4 hr by x-rays with a URS-70, using a tube with a tungsten target and a zirconium filter (50 kv and 14 ma). The sample, shielded from visible light, was placed at a distance of 3 cm from the

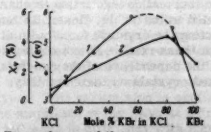

Fig. 1. Dependence of the vacancy concentration χ_v (curve 1) and the halfwidth of the F-band γ (curve 2) on composition of the system KCl-KBr.

window of the tube. To secure homogeneous coloring, the sample was rotated by 180° after the first 2 hr of exposure. The absorption spectrum of the colored crystal was investigated by means of an SF-4 quartz spectrophotometer. The composition of the crystals was determined by potentiometric titration for the percentage of the halide. We obtained reliable evidence that this composition differed significantly from the composition of the complexes in the starting mixture.

The concentration of F-centers was calculated by Smakula's formula[6]

$$n_0 f = 1.31 \cdot 10^{17} \frac{n}{(n^2+2)^2} \alpha_{max} \gamma,$$

where n_0 is the number of F-centers per cm³, f is the oscillator strength (assumed by us to be unity in all cases), n is the index of refraction of the crystal, γ is the halfwidth of the F-bands in ev, and α_{max} is the absorption coefficient at the band maximum.

The dependence of the halfwidth of the F-band on the composition of the solid solutions of KCl-KBr is given in Fig. 1. The maximum deviation of the halfwidth from the additive value occurs at a composition of 80 mole % KBr and 20 mole % KCl, which corresponds to the greatest concentration of Schottky defects. The maximum value of the ionic conductivity of the crystals also occurs at a composition close to this.

The dependence of the F-center concentration on the composition of the solid solutions is indicated in Fig. 2.

Solid solutions of KCl-KBr show a smaller tendency toward coloration than do pure crystals of KCl and KBr. It is easy to see that the dependence of n_0 is symmetric with respect to the percentage composition of KBr in KCl. According to V. V. Boldyrev, the reduced concentration of F-centers in crystals of KCl-KBr is a consequence of the instability of F-centers in solid solutions caused by the asymmetry of the surroundings of the color center in a mixed crystal.

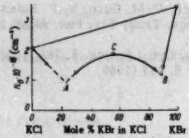

Fig. 2. F-center density, n_0, dependence on the composition of the system KCl-KBr for identical x-ray irradiation of the crystals.

The curve for the dependence of the degree of asymmetry on the composition of crystals of KCl-KBr possesses two maxima (points A and B in Fig. 2) and must have a relative maximum for solid solutions of equimolar composition (point C).

The stability of F-centers of certain solid solutions with respect to thermal de-excitation is characterized by data presented in the Table. De-excitation was carried out by heating the crystals for 30 min at 70°C. It is easy to see that these results do not contradict the hypothesis about the dependence of the concentration of F-centers in mixed crystals on their stability.

Composition of the crystal	KCl	KCl-KBr (90–10) mole %	KCl-KBr (44–56) mole %	KCl-KBr (10–90) mole %	KBr
Relative number of F-centers destroyed $\frac{\Delta n}{n}$ (%)	18	19	25	60	15

The authors thank V. V. Boldyrev and A. D. Shchelokov for discussion of the results of this investigation.

REFERENCES

1. R. Gnaedinger, J. Chem. Phys. 21, 323 (1953).
2. G. Miessner, Z. Physik 134, 576 (1953).
3. N. Wallace and R. Flin, Nature 172, 681 (1953).
4. M. S. Ivankina, Kand. Diss., Tomsk, 1960.
5. L. L. Makarov, B. G. Lur'e, and V. N. Malyshev, Fiz. Tver. Tel. 11, 1 (1960).
6. F. Seitz, "Sovremennaya Teoriya Tverdogo Tela." Izd. Inostrannoi Lit., Moscow, Leningrad, 1949. Translation of "The Modern Theory of Solids." McGraw-Hill, New York, 1940.

SOME RESULTS OF A SPECTRAL INVESTIGATION OF AN ULTRAHIGH FREQUENCY IMPULSE DISCHARGE IN A RESTRICTED DISCHARGE GAP

V. V. Bakakina

Received 1 July 1960

Observations were made of the radiation emitted by discharges in helium and neon excited by a powerful ultrahigh frequency (uhf) impulse in a narrow gap placed across a coaxial line (Fig. 1). The change in the intensity of individual lines with time was investigated for 2-12 μsec pulses at 1-100 mm Hg in the decimeter wavelength range. The experimental models consisted of sections of uniform coaxial lines; the center and outer electrodes did not differ essentially in their dimensions from the center and outer conductors of the coaxial line to which the models were connected.

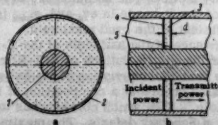

Fig. 1. Schematic view of a confined discharge gap in a coaxial line. a—Front view: 1—center electrode, 2—outer electrode; b—side view: 3—discharge gap, 4—entrance window, 5—exit window.

The gas reservoir was a toroidal shell with a small discharge gap volume. The width of the gap (for various models) was 0.2-1 mm. Windows made of ZS-5 glass permitted observation along the axis of the models from the power input and output ends. Evacuation was carried out under continuous heating, making use of liquid air. Spectrally pure gases were used for filling.

The change in intensity of an individual line with time was observed with the help of a UM-2 monochromator having a photoelectric attachment. The measuring setup contained elements necessary to obtain on the oscillograph the envelope of the uhf impulse which excited the discharge and provision for controlling the duration and shape of this impulse. It was also possible to record the envelope of the uhf power impulse leaking through the plasma, the form of this pulse being conditioned by the characteristics of the various phases of the uhf-impulse gas discharge.

The uhf power in the impulse channel was determined on the basis of average power measurements made by the calorimetric method usually used in uhf technique, and amounted to several hundred kilowatts. The channel passband of the oscillograph amplifier was at least 1 Mc wide, which assured the absence of distortion in observing impulses lasting longer than 2 μsec. Particular attention was paid to assuring accurate synchronization of the photomultiplier output with the input into the oscillograph. A cathode follower was used; the wave impedance of the cable was also taken into account.

The radiation was fed to the monochromator without intermediate lenses. The slit width of the monochromator was not more than 0.1 mm at the entrance and not more than 0.2 mm at the exit when the helium line was observed. For the observations of the neon line, the slit width did not exceed 0.05 mm.

To the eye, the glow of the window appears uniform when the width of the discharge gap is everywhere the same and d/l is within the limits of 0.1-10 (d is the width of the discharge gap and l is the mean free path of an electron). At pressures greater than 50 mm Hg, contrac-

tion of the discharge begins. At pressures lower than 2mm Hg, various kinds of nonuniformities appear in the discharge. The regions near the electrodes are obscured for a distance of 2 mm and cannot be observed. It was possible to observe the radiation coming from a ring ~5 mm wide.

By means of spectrum photography, with the help of visual observations and the photoelectric method, 16 lines of HeI and 24 lines of NeI were found and identified in the red part of the spectrum. One must particularly note that no ionic lines were observed in either the helium or the neon. A comparison of the oscillograms of the light pulse, the uhf power envelope from the channel, and of the envelope of the leakage power showed that:

1. The intensity of the helium and neon lines follows the amplitude changes of the uhf signal (Fig. 2,a) almost exactly up to pressures of 10 mm Hg for helium but only up to 5 mm Hg for neon.

2. As the pressure is increased, one observes characteristic flashes at the beginning and after the termination of the light pulse (Fig. 2,b). The duration of the first flash is less than 0.5 μsec. The second flash lasts longer. The amplitudes of both flashes vary with pressure changes and they may be different for different lines.

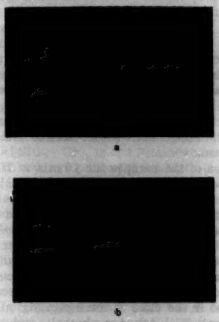

Fig. 2. Forms of the light pulse emitted by a discharge, for a gap width of 0.5 mm in helium, λ = 5876 A. a—Pressure 5 mm Hg; b—pressure 200 mm Hg. 1—uhf impulse envelope from the channel; 2—uhf impulse envelope of the leakage from the gap; 3—line intensity during a 2 μsec impulse.

3. In the quasi-stationary stage of the impulse, the intensity decreases as the pressure is increased.

4. At pressures above 20 mm Hg, there is a background in some spectral regions; this is most pronounced near the 4143 A line.

The appearance of a flash at the beginning of the impulse and the increase of its amplitude with increasing pressure may be connected with the increase in the velocity of the electrons during the development of the discharge. This assumption may be confirmed by the rise in the peak of the leakage power with increasing pressure. As a result of increasing electron velocity, the effectiveness of stepwise excitation may increase and the role of the direct excitation may become noticeable. Similarly, one may apparently explain the drop in intensity during the quasi-stationary period of the discharge as due to a decrease in electron velocity (and perhaps also to a change in the character of the electron velocity distribution). The glow during the period after the discharge may be a result of a recombination, which, perhaps, is of the dissociative type.[1] This assumption is confirmed by the increase in the amplitude of the flash at increased pressure, and the increase in efficiency with increasing pressure which is characteristic of volume recombination processes. A certain amount of shift of the radiation maximum with respect to the end of the impulse is perhaps connected with the redistribution of the particle density in the volume as a result of the impulse discharge, as observed by Shukhtin.[2] A more detailed investigation will be required to explain the physical processes occurring during the phenomena described.

REFERENCES

1. H. S. W. Massey and E. H. S. Burhop, "Electronic and Ionic Impact Phenomena." Oxford, Clarendon Press, 1952; Russian translation by Foreign Literature Press, Moscow, 1958.
2. A. M. Shukhtin, Izvest. Akad. Nauk SSSR, Ser. Fiz. 22, 711 (1958); Opt. i Spektr. 7, 838 (1959), Optics and Spectroscopy 7, 491 (1959).

ELECTRON PARAMAGNETIC RESONANCE IN CRYSTALS OF TRIPHENYLMETHANE DYES

F. P. Chernyakovskii, A. E. Kalmanson, and L. A. Blyumenfel'd

Received 6 June 1960

In the literature, several cases have been described of the appearance of electron paramagnetic resonance (e.p.r.) in compounds with an extended system of conjugated double bonds, which according to existing concepts about structure should not contain unpaired electrons.[1-4] From this point of view, it is of interest to study, by the e.p.r. method, compounds from the series of triphenylmethane dyes whose structure is sufficiently well known and which are characterized by a high degree of conjugation. The results of a preliminary investigation of the e.p.r. spectra of several compounds of this series are presented below.

The following dyes were studied: crystal violet, methyl violet, basic bright green, malachite green, the fuchsines—basic and acid, fluorescein (uranin), rhodamine G, rhodamine GB, thymol- and phenolphthaleins (as the colorless inner-carbinol forms and the colored potassium salts), and also indigo carmine and Congo red, which do not belong to this class. The e.p.r. spectra were recorded for the crystalline dye powders, in the form of the first derivative, with the help of an apparatus described in the literature[5] which uses high frequency modulation of the magnetic field (as an illustration, the e.p.r. spectra of two dyes, obtained under identical conditions, are presented in the Figure).

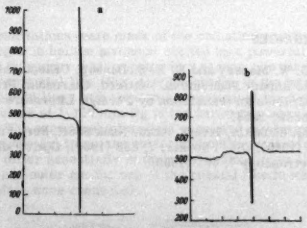

Electron paramagnetic resonance spectra of crystal violet (a) and basic bright green (b).

In all cases (with the exception of the colorless phthaleins, malachite green, and the colored potassium salt of thymolphthalein), a narrow solitary singlet without hyperfine structure was observed. The intensity of the signal varied from compound to compound, amounting to 10^{16}-10^{18} paramagnetic particles per gram of sample. As for the connection between the intensity of the signal and molecular structure, one may come to the conclusion that the signal increases as the conditions for conjugation improve. Thus, for example, colorless phenolphthalein (I) with a tetrahedral central carbon atom (and without a continuous system of conjugated bonds) gives no e.p.r. signal within the limits of sensitivity of the apparatus, while the potassium salt of this compound (II) (a planar structure with a continuous system of conjugated bonds) gives a signal with an intensity around 10^{17} paramagnetic particles per gram.

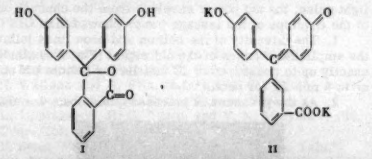

I II

In some cases, line broadening on account of strong saturation was observed. On lowering the temperature to 77° K, the signal intensity grows in approximate agreement with the Curie law. On the basis of this, one may consider that the electron paramagnetic absorption in the samples is associated not with an excited state but with the ground state.

Evacuation of the sample for 15 min at 10^{-3} mm Hg leads to a three- to fivefold increase in the signal, and it diminishes reversibly after admission of air (a second evacuation leads once more to an increase in the signal). This phenomenon was varified for crystal violet, basic bright green, and indigo carmine. The absence of a signal in the case of the original samples of malachite green and potassium thymolphthalein is probably associated with the absorption of oxygen (analogous effects have been discerned in the case of the e.p.r. signals of coals).

Experiments with aqueous alcoholic solutions of indigo carmine and crystal violet showed that the signal disappears on solution and reappears when the sample is dried. In order to check the extent to which the Q of the cavity was lowered when a solution was introduced into it, the e.p.r. lines were recorded on the background of a manganese standard. The disappearance of the signal on solution cannot be explained solely on the basis of the lowering of Q.

As a preliminary conclusion, we may express the hypothesis that the e.p.r. signal of triphenylmethane dyes relates not to the structure of the molecule itself but to the crystalline state, which leads to an increase of conjugation in the system.

REFERENCES

1. B. M. Kozyrev, Doklady Akad. Nauk SSSR 81, 427 (1951).
2. B. M. Kozyrev, Dokt. diss. (Dissertation), Fiz. Inst. Akad. Nauk SSSR, Moscow, 1957.
3. A. A. Berlin, L. A. Blyumenfel'd, M. I. Cherkashin, A. E. Katsnel'son, and O. G. Sil'skaya, Vysokomolekulyarnye Soedinenyia 1, 1361 (1959).
4. Yu. Sh. Moshkovskii, Doklady Akad. Nauk SSSR 130, 1277 (1960).
5. A. G. Semenov and N. N. Bubnov, Pribory i Tekh. Ekspt. No. 1, 92 (1959).

THE RELAXATION SPECTRUM OF KYANITE

N. A. Tolstoi and Liu Shun-Fu

Received 22 June 1960

The method of the pulse taumeter[1] has made it possible to study the distribution of the luminescence decay time over the various lines and bands (the "relaxation spectrum") of synthetic ruby.[2] In contrast to the widespread views that the luminescence of ruby decays according to an exponential law with a single decay constant τ, experiment shows that, generally speaking, to the different lines and bands there correspond different values of τ—which, moreover, depend in different ways on the temperature and the chromium concentration. Against the background of these diverse and complex dependences, one simple and stable fact stands out: the τ values of the two components of the principal doublet (R_2 = 6917 A, R_1 = 6932 A at −193°C) are always equal to each other. The same is also valid for the principal doublets in the spectra of $Ga_2O_3 \cdot Cr$ and $BeAl_2O_4 \cdot Cr$; detailed articles with the results of a study of the relaxation spectra of these substances are being prepared for publication. We have considered it of interest to carry out similar studies on kyanite ($Al_2SiO_5 \cdot Cr$), in the luminescence spectrum of which there are two principal doublets (λ_1 = 7049.3 A and λ_2 = 7034.5 A; λ_3 = 6893.5 A and λ_4 = 6876.3 A).[3,4]

The measurements were carried out on an apparatus which reproduced with some improvements the one described in ref. 2. In Fig. 1 are presented the luminescence spectra of kyanite at the temperatures −180°C and 20°C, taken point by point with the help of a pulse lamp. On the same figure are traced the relaxation spectra at the same temperatures. It is easy to see that at room temperature the value of τ changes from 2×10^{-5} to 9×10^{-4} sec over the spectrum; i.e., by a factor of 45. The τ values for adjacent lines—λ_1 and λ_2, and also λ_3 and λ_4—differ at room temperature by one power of ten. At low temperature, the lines λ_3 and λ_4 disappear from the luminescence spectrum, and for the remaining lines—λ_1 and λ_2—the values of τ differ by a factor of more than 5. It is to be noted that, at room temperature, the line λ_1 is somewhat "smeared" by the long wavelength wing of the line λ_2. With this is associated the fact that the value of τ measured for λ_1 has a lower precision than τ for the other lines, and in general it is approximate, inasmuch as "rectification" of the taumeter loop on the oscillograph screen is not achieved. Nevertheless, the identity of the τ values for the lines λ_2 and λ_3 on the one hand and for the lines λ_1 and λ_4 on the other is evident. The fact that these coincidences are apparently not accidental is clear from the Table, in which are presented the values of τ for the lines of both doublets at different temperatures.

t (°C)	$\tau \cdot 10^4$ (sec)			
	λ_1	λ_2	λ_3	λ_4
−180	31	5.9	—	—
−122	28	3.9	—	—
−42	14	1.3	1.4	14
−5	8	1.1	1.1	10
+20	7	0.8	0.8	9

One attempt to interpret the luminescence spectra of chromium luminors belongs to Deutschbein.[3,4] He showed, in particular, that the term diagram corresponding to the principal doublet in the spectrum of $Al_2O_3 \cdot Cr$, $Ga_2O_3 \cdot Cr$, etc., has the form sketched in Fig. 2,a. The temperature independence of the intensity of the absorption lines in the principal doublet (the latter, as is well known, is a resonance doublet) led Deutschbein to the conclusion that both lines result from one and the same thermally unexcited lower state. On the contrary, the abrupt weakening, when cooled, of one component (R_2) of the doublet in emission led Deutschbein to the conclusion that the line R_2 is emitted after thermal excitation of an electron from level 1 to level 2 (Fig. 2,a). Since equilibrium thermal exchange takes place between levels 1 and 2, the values of τ must be the same for the two lines R_1 and R_2, even if the transition probabilities from these levels to the lower state are different. For the same reasons, Deutschbein proposes the diagram sketched in Fig. 2,b to explain the double doublet in the kyanite spectrum.[4] This diagram well reflects the experimental facts established

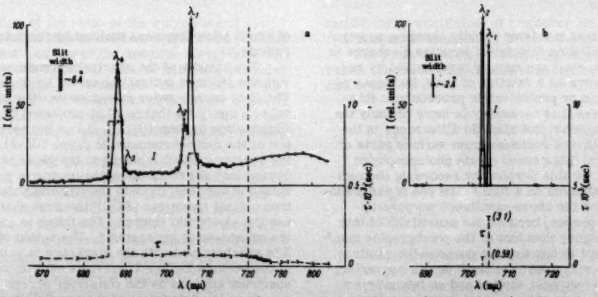

Fig. 1. Emission spectra (solid lines) and relaxation spectra (dashed lines) of kyanite at +20°C (a) and −180°C (b).

by Deutschbein, namely: (1) the lines λ_3 and λ_4 in absorption are preserved at low temperature, but the lines λ_1 and λ_2 are weakened; (2) the lines λ_1 and λ_2 in emission are preserved at low temperature, but the lines λ_3 and λ_4 disappear. Thus Deutschbein considers the pair of lines λ_3 and λ_4 as one doublet and the pair λ_1 and λ_2 as the second. The second doublet, in his opinion, arises in consequence of Stark splitting of the lines of the first doublet in the field of the lattice. We note that originally Deutschbein considered the natural pairs λ_1, λ_2 and λ_3, λ_4 as doublets.[3]

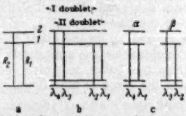

Fig. 2. Term diagrams. a—diagram of the principal doublet of ruby, $Ga_2O_3 \cdot Cr$, etc.; b—diagram proposed by Deutschbein for kyanite; c—diagram suggested by the relaxation data. α—First doublet ("outer" lines); β—second doublet ("inner" lines). There is no thermal exchange between α and β.

The data obtained by us on the decay of the lines λ_1, λ_2, λ_3, and λ_4 disprove the interpretation presented above for the doublets in the kyanite spectrum. Specifically, if the upper level is the same for the pair of lines λ_1 and λ_2, then their τ values must also be the same; as we have seen, in actuality they differ by an order of magnitude. The same applies to the pair λ_3 and λ_4. The equalities $\tau_1 = \tau_2$ and $\tau_3 = \tau_4$ must be valid even if there is no thermal exchange (or if it is insufficiently complete) between the two upper levels in the diagram of Fig. 2,b. If thermal equilibrium is established, then we must have $\tau_1 = \tau_2 = \tau_3 = \tau_4$. It is not difficult to verify that no other diagram with four levels for one luminescence center can accord with the above-cited experimental facts. Thosar[5] expressed the assumption that the environment of the chromium ion in kyanite may be of two sorts, and therefore the presence of two types of luminescence centers is responsible for the appearance of two doublets. If this is so (and if Deutschbein's data on the temperature dependence of the absorption are true), then λ_1 and λ_4 (the "outside" lines) are to be considered as one of the doublets in the kyanite spectrum and the pair λ_2 and λ_3 (the "inside" lines) as the other. The term diagrams for these doublets are presented in Fig. 2,c.

We did not have an opportunity to vary the concentration of chromium in our samples and to elucidate its influence on the relaxation regularities of the luminescence (this influence, as the investigation of other chromium luminors shows, is considerable). Apparently the kyanite samples investigated by us contained a very small quantity of chromium, since, first, they were colorless and, secondly, they had only the two lines λ_1 and λ_2 in the luminescence spectrum at low temperature. The absence of the longwavelength (in comparison with the doublet) part of the spectrum is typical for analogous chromium luminors with a low chromium concentration.

The authors cordially thank their collaborators of the department of mineralogy of Leningrad University for furnishing the samples of Siberian kyanite for the investigation.

REFERENCES

1. N. A. Tolstoi, Opt. i Spektr. 4, 279 (1958).
2. N. A. Tolstoi and A. M. Tkachuk, Opt. i Spektr. 6, 659 (1959), Optics and Spectroscopy 6, 427 (1959).
3. O. Deutschbein, Ann. Physik 14, 737 (1933).
4. O. Deutschbein, Ann. Physik 20, 828 (1934).
5. B. V. Thosar, J. Appl. Phys., Suppl. No. 4, S 84 (1955).

SPARK DISCHARGE SPECTRA RESOLVED IN TIME AND ALONG THE CHANNEL CROSS SECTION AS RECORDED WITH AN ELECTRON OPTICAL CONVERTER

I. F. Balashov, M. P. Vanyukov, V. R. Muratov, and E. V. Nilov

Received 22 June 1960

Light phenomena involving rapidly changing spectral composition of radiation (electrical impulse discharge in gases, explosions, etc.) are usually investigated by recording their spectra as a function of time, by means of either photographic or photoelectric procedures. However, in many cases it is necessary to know not only the time changes of spectra, but also the differences in the spectral composition of radiation from various parts of the emitting object. High speed movie photography of spectra was used for this purpose by recording the radiation under investigation on a film.[1] The use of the photoelectric method for the above-mentioned purpose appears to be quite proper, because the sensitivity of this method is much higher than that of the photographic one.[2] It is quite expedient to use for this purpose the electron optical converter with a fast shutter.[3] Such a converter, equipped with an electronic shutter and an intensity amplifier, permits the use of very short exposures (down to 10^{-8} sec) and has a sensitivity sufficient for the recording of single photoelectrons emitted by the entrance photocathode.[4,5]

The scheme of the spectral arrangement, together with the electron optical converter is given in Fig. 1. The light source under investigation (the horizontal channel of a spark discharge e) is projected by means of the illuminating system (O_1, O_2, O_3) on the vertical entrance slit of the monochromator M (Type UM-2). The image of the spectrum which appears in the plane of the fully opened exit slit of the monochromator is projected by means of the lens O_4 onto the photocathode of the electron optical converter (EOC), the first chamber of which has the electronic shutter. The latter is controlled by the square-wave generator 3. The action of the generator 3 is synchronized with the discharge in question by means of the photomultiplier 1 and the synchronizing unit 2. A spectrum appears on the converter screen which corresponds to the delay time of the opening of the electronic shutter relative to the beginning of the discharge, and

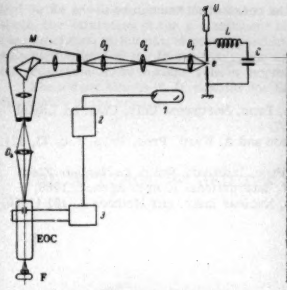

Fig. 1

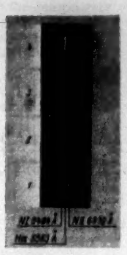

Fig. 2

Fig. 1. Experimental setup.
Fig. 2. Section of the spectrum of the luminescence of the channel of a spark discharge in air, obtained with an exposure of 1 μsec, for different times. Time from the beginning of the discharge (in μsec): 1—1; 2—5; 3—10; 4—21.

also to the exposure time determined by the shutter. The lengths of the spectral lines lie within the limits determined by the diameter of the channel for a given moment of time.

Our arrangement enabled us to obtain pictures of spectra with exposures from 0.1 to 10 μsec, and at different times, starting from 0.07 up to 21 μsec from the beginning of the discharge. Pictures of the spectrum of the spark discharge in air made with this apparatus have demonstrated that it is quite suitable for the determination of the space and time distribution of the emitting atoms in the discharge channel.

Figure 2 depicts a section of a spectrum of a spark discharge in air, in which a group of three lines can be seen. The first is composed of the unresolved nitrogen arc lines N I (6482 A-6484 A), the second is the hydrogen line H_α (6536 A) and the third is the spark line of nitrogen N II (6610 A). The spectral width of the monochromator slit exceeded the halfwidths of the investigated nitrogen lines. The discharge was maintained with the following conditions: U = 10 kv, C = 0.04 μf, L = 5 μh, the electrode gap 1 = 4 mm.

An essential difference in the behavior of the lines of hydrogen and those of nitrogen should be mentioned. The hydrogen line luminesces through the whole channel, and its radiation varies little with the periodic changes of power dissipated in the discharge channel (the period of free oscillations in the circuit was T ≈ 8 μsec). The nitrogen lines are less stable: their intensity changes periodically according to the energy input in the discharge gap. The difference in the length of spectral lines of hydrogen and nitrogen at any given time indicates a nonuniformity of the channel. The change of the length of spectral lines gives information about the change of the diameter of the channel with time.

REFERENCES

1. L. Zernow and G. E. Hauver, Proc. Third Intern. Congr. High Speed Photography, London, 1957, p. 305.
2. W. A. Baum, Sci. American 194, 81 (1956).
3. M. P. Vanyukov, Uspekhi Fiz. Nauk 60, 295 (1956).
4. E. K. Zavoiskii, M. M. Butslov, and G. E. Smolkin, Doklady Akad. Nauk SSSR 111, 996 (1956).
5. M. M. Butslov, Uspekhi Nauch. Foto. 6, 76 (1959).

THE INTENSITY OF THE SLOW COMPONENT OF STILBENE LUMINESCENCE EXCITED BY ALPHA PARTICLES

Yu. A. Nemilov, K. A Gridnev, and A. N. Pisarevskii

Received 23 June 1960

The variation of the ratio of the intensities of the fast and slow components of the luminescence of organic scintillators as a function of the specific energy loss of the exciting particle is useful in discriminating particles with respect to dE/dx.[1-3] It has been shown[3,4] that when stilbene is excited by electrons and protons, the ratios of the intensity of the slow component (τ ~ 0.3 μsec) to the intensity of the total light output are 10% and 20% respectively.

We have measured the above-mentioned intensity ratios for stilbene crystals excited by Pu^{239} α-particles (E_α ~ 4 Mev) and electrons with $E_{\beta\,max}$ = 480 kev (during exposure of the crystals to 660 kev γ-radiation from Cs^{137}). A block diagram of the equipment used for the measurements is shown in the Figure.* The measurements were obtained by a null method which involved measuring the amplification coefficient of amplifier No. 2 with the aid of a calibrated attenuator.

The results of the investigation are shown in the Table. The following conclusions can be drawn from the data obtained:

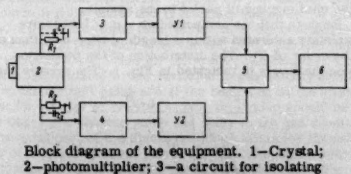

Block diagram of the equipment. 1—Crystal; 2—photomultiplier; 3—a circuit for isolating the slow component; 4—attenuator; 5—a differential comparison circuit; 6—recorder device; Y1 and Y2—amplifiers No. 1 and No. 2.

*An article including a detailed description of the equipment has been submitted for publication in the journal, Pribory i Tekh. Exspt."

Type of excitation	Ratio of the intensity of the slow component to the total light output (%)	Ratio of the intensity of the slow component to the fast component (%)
Electrons	15 ± 2	18 ± 2
α-particles	35 ± 3	54 ± 3

1. When stilbene is excited by electrons, the relative intensity of the slow component is somewhat higher than indicated in ref. 4.

2. The relative intensity of the slow component increases with increasing dE/dx of the exciting particles (transition from protons to α-particles).

3. The results obtained corroborate the views that were expressed in ref. 4 about the nature of the slow component.

REFERENCES

1. F. D. Brooks, Proc. Northwest Univ. Conf. on Liquid Counting, 1957.
2. J. C. Robertson and A. Ward, Proc. Phys. Soc. 73, 471 (1959).
3. R. B. Owen, Proc. Internatl. Symp. on Nuclear Electronics, p. 27. International Atomic Agency, 1959.
4. F. D. Brooks, Nuclear Instr. and Methods 4, 151 (1959).

MAGNITUDE OF THE POLARIZATION OF NUCLEI IN THE NONSTATIONARY OVERHAUSER EFFECT

V. I. Avdeev

Received 4 July 1960

1. Let us consider a system consisting of a nucleus with spin I and an electron with spin S = 1/2, in a strong magnetic field. The energy levels may be characterized by the projections M and m of the spins of the electron and nucleus. We designate the relaxation times of the transitions $\Delta M = \Delta m = \pm 1$; $\Delta M = \pm 1$, $\Delta m = 0$ by T_x and T_e, respectively. If $T_x \ll T_e$ (which is always true in paramagnetic fields, and also for certain impure semiconductors), then it is possible to observe a series of transition phenomena. In ref. 1 Khudishvili computed the degree of orientation of the nuclei upon saturation of one of the forbidden transitions $\Delta M = -\Delta m = \pm 1$. A computation is presented below for the case of successive saturation of two allowed transitions $\Delta M = \pm 1$, $\Delta m = 0$. This nonstationary effect was proposed by Pines, Bardeen, and Schlichter[2] as an explanation of the increase in intensity of one line upon the saturation of a neighboring one.

2. Neglecting the spin-spin interaction of the electron and nucleus, we obtain 2I + 1 pairs of levels. With a precision up to the Zeeman energy of the nucleus, the energy separations of all the components are equal to $\hbar\gamma_e H$.

We shall characterize the degree of polarization of the nucleus by the quantity

$$f = \frac{1}{NI} \sum_m m a_m, \qquad (1)$$

where a_m is the population of the component m, and N is the total number of nuclei in the sample.

Suppose that the component $m = \mu - 1$ becomes completely saturated within a length of time less than or of the order of T_x. The distribution of the population among the levels is indicated in Fig. 1. The arrows designate forbidden and allowed transitions and their relaxation times. Here

$$N_{\pm}^{0} = \frac{N}{2I+1} \frac{e^{\mp 2\delta}}{e^{\delta} + e^{-\delta}}; \quad 2\delta = \frac{\hbar\gamma_n H}{kT}.$$

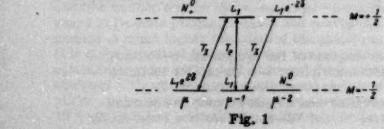

Fig. 1

Considering only hyperfine interactions, we obtain the expressions

$$f = \frac{1}{I(2I+1)} \operatorname{th}\delta, \quad \text{and } I > \frac{1}{2}, \qquad (2a)$$

$$f = \frac{e^{2\delta} - 1}{(e^{-2\delta}+1)(e^{2\delta}+2)}, \quad \text{and } I = \frac{1}{2}. \qquad (2b)$$

for the magnitude of polarization at this stage.

At the second stage, we saturate the component $m = \mu$, the interval of time between saturations being much shorter than T_x. The distribution of the nuclei over the levels after the two processes is shown in Fig. 2.

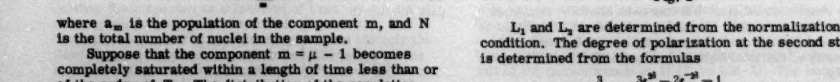

Fig. 2

L_1 and L_2 are determined from the normalization condition. The degree of polarization at the second stage is determined from the formulas

$$f = \frac{3}{2I(2I+1)} \frac{3e^{2\delta} - 2e^{-2\delta} - 1}{(e^{\delta} + e^{-\delta})^2}, \quad \text{and } I > 1, \qquad (3a)$$

$$f = \frac{e^{2\delta} - 1}{e^{2\delta} + 1} \frac{2e^{2\delta} + 2e^{-2\delta} + 3}{2e^{2\delta} + 2e^{-2\delta} + 5}, \quad \text{and } I = \frac{1}{2}. \qquad (3b)$$

For the case I = 1/2 and $\delta \ll 1$, at the first stage $f \approx \delta/3$; at the second stage, $f \approx 7/9\ \delta$.

In this manner, considerable polarization of the nucleus occurs. It is easy to understand the physical significance of the result. On saturation of the component $\mu - 1$, the population of the μ component increases, and

that of the $\mu - 2$ component decreases. At the second stage, the saturation of the μ component leads to further overpopulation of the nuclei with regard to the components with high values of m. In summary, the average value of the projection of the nuclear spin is increased.

The author thanks N. D. Sokolov for his interest and discussion of the results.

REFERENCES

1. G. R. Khutsishvili, Zhur. Eksptl. i Teoret. Fiz. 38, 942 (1960).
2. D. Pines, J. Bardeen, and C. P. Slichter, Phys. Rev. 106, 489 (1957).
3. A. Honig, Phys. Rev. 96, 234 (1954).

THE AFTERGLOW AND ITS RELATION TO GAS DENSITY IN A PULSE DISCHARGE IN Ne

V. S. Egorov and A. M. Shukhtin

Received 11 July 1960

In a recent communication we discussed research on a pulse discharge in Ne by the Rozhdestvenskii "hook" method.[1] We found that the populations of the $2p^53s$, $^3P_{0,1,2}$ and $^1P_1$ excited states are low during the discharge, but increase considerably after the current pulse ends, reach a maximum shortly thereafter, and then gradually decline.

The investigations were carried out with initial Ne pressures of 1-4 mm Hg in the discharge tube. Various current pulses were studied—$\simeq$ 200 μsec trapezoidal pulses and $\simeq$ 16 μsec bell-shaped pulses. The current densities reached $\simeq$ 100 amp/cm^2. We found that the concentration of excited atoms increases much faster, and to a higher maximum, after the end of the short current pulse.

This phenomenon occurs even if the current amplitude in the long pulse is greater than in the short pulse, although just the opposite would be expected. In fact, the longer current pulse introduces much more energy, and it would seem that this should create more ionization. Consequently there should be more recombinations, resulting in more excited Ne atoms, since it was clear from the beginning that the increase in the concentration of excited atoms after the end of the discharge pulse resulted from transitions from the upper states and from the volume recombination of ions. However, there was uncertainty about the character of the recombinations and the mechanism leading to a more rapid increase in the concentrations of excited atoms, and a greater maximum in the case of the shorter, instead of the longer, current pulse.

It is well known that different types of volume recombination of charged particles have very different values of the recombination coefficient. Therefore, to determine which type of recombination is most important under the conditions of our experiment, we attempted to evaluate the recombination coefficient.

The decrease in the number of charged particles within the volume of a collapsing plasma at the end of the current pulse can be expressed by the equation:

$$\left(\frac{dn_i}{dt}\right)_{t=t_0} = -\alpha n_{i_0}^2. \qquad (1)$$

The recombination of ions leads to an increase in the concentration of excited atoms. The decay rate of the latter in the first moments of the afterglow is smaller than the rate of production, so that

$$\left(\frac{dn_b}{dt}\right)_{t=t_0} = -j\left(\frac{dn_i}{dt}\right)_{t=t_0} = \alpha j n_{i_0}^2, \qquad (2)$$

where n_b is the concentration of Ne atoms in the $^3P_{0,1,2}$ and $^1P_1$ levels; n_i is the concentration of charged particles; j is a coefficient proportional to the probability of an atom falling into one of the $2p^53s$ levels during the recombination.

To use E_4. (2) to determine the value of α, we must know the values of $(dn_b/dt)_{t=t_0}$ and n_{i_0} when the current pulse ends, and the value of j. Data from the literature[2] give a value of j close to unity. The concentration of charged particles n_{i_0} at the end of the current pulse was determined by probe and interferometric measurements. In one actual case, where the recombination rate was greatest, $n_{i_0} \simeq 5 \times 10^{13}$ to 10^{14} cm^{-3}, and a value of approximately 10^{-8} to 10^{-9} cm^{3}sec^{-1} was obtained for the volume recombination coefficient. Comparison of the value of α obtained with the values for the different volume recombination processes leaves no doubt that in the collapsing plasma of the pulse discharge that we studied, the neutralization of charged particles in the initial stages of the afterglow results from dissociative recombination. The dissociative recombination process occurs in two stages. The first stage involves transformation of the atomic ion into a molecular ion by a three-body collision:

$$Ne^+ + 2Ne \rightarrow Ne_2^+ + Ne. \qquad (I)$$

This is followed by a direct recombination process:

$$Ne_2^+ + e \rightarrow Ne_2^* \rightarrow Ne^* + Ne. \qquad (II)$$

where Ne_2^* is an unstable excited molecule and Ne* is a highly excited Ne atom.

The excited Ne* atom falls by successive steps into the $^3P_{0,1,2}$ and $^1P_1$ states. It follows from the nature of reaction (I) that the probability of transformation of an atomic Ne^+ ion into molecular Ne_2^+ varies rapidly with gas density (it is proportional to the square of the density). Because of this, the speed with which the concentration of excited atoms increases in the afterglow should also vary rapidly with the actual value of the gas density when the current pulse ends, and in the first stages of the afterglow. The nature of the time variation of the concentration of excited Ne atoms after the end of the current pulse was found to be different for different pulse lengths. This is obviously related to the variation in gas density at the end of the current pulse and at the beginning of the afterglow; for a pulse of greater length, this value should be less than for a shorter pulse (we refer to the gas density in the axial part of the discharge tube). Thus for the afterglow of a longer current pulse, the rate of transformation of atomic Ne^+ ions into Ne_2^+ molecules decreases, the volume recombination rate decreases, and consequently the rates at which the $^3P_{0,1,2}$ and $^1P_1$ levels are filled decrease.

With the decrease in gas density in the axial part of the tube, the importance of volume recombination in this region diminishes somewhat and then the proportion of the particles which is neutralized at the walls of the discharge tube increases. This should lead to a drop in the maximum concentration of excited Ne atoms in the afterglow.

Direct observation of the variation of the gas density in the pulse discharge, carried out by the method given in ref. 5, qualitatively confirmed the results given in the present paper.

With a short current pulse, the decrease in gas density does not exceed 25% of the initial value (p_0 = 4 mm Hg). The results of observations on the variation in the gas density in the 200 μsec current pulse are given in the Figure. In fact, we see that as we move along the flat part of the current pulse the gas density falls monotonically from its initial value and a distinct fall (exceeding the experimental error) occurs starting at about 40-50 μsec after the start of the pulse. With an initial gas density corresponding to a pressure of 4 mm Hg, the density at the end of the flat top of the current pulse had fallen to about 30% of the initial value.

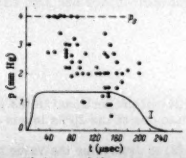

Variation with time of the gas density during the plateau of the current pulse (p_0 = 4 mm Hg, I = 300 amp, discharge tube diameter = 14 mm).

In conclusion, we thank S. E. Frish for his constant attention to and interest in our work.

REFERENCES

1. A. M. Shukhtin and V. S. Egorov, Vestnik Leningrad. Univ. No. 16, 61 (1959).
2. J. M. Richardson, Phys. Rev. 88, 895 (1952).
3. W. I. Loeb, "Basic Processes of Gaseous Electronics." Univ. of California Press, 1955.
4. V. L. Granovskii, "Elektricheskii tok v gase" (Electric Currents in Gases). Moscow, 1952.
5. A. M. Shukhtin, Opt. i Spektr. 7, 838 (1959), Optics and Spectroscopy 7, 491 (1959).

NEWS ITEMS

INTERNATIONAL CONFERENCE ON THE PHYSICS OF SEMICONDUCTORS

An International Conference on the Physics of Semiconductors, in which more than 500 scientists from Czechoslovakia, Hungary, Poland, Bulgaria, the USSR, the German Democratic Republic, the Federal Republic of Germany, England, France, the USA, Belgium et al. participated, was held in Prague from August 29 to September 2, 1960.

During the plenary session, the paper by Academician A. F. Ioffe (USSR; deceased) entitled "New methods of investigation in semiconductor physics" and the paper by Nobel Laureate W. Shockley (USA) entitled "Problems related to p-n junctions in silicon" were received with great interest. More than 100 papers were presented in numerous sessions devoted to the band structure of crystals, transport phenomena, recombination, radiation effects, excitons, photoconductivity, surface phenomena, resonance effects, thermoelectricity, ionic crystals, etc.

In this brief report, it is not even possible to list the most interesting of the contributions. We shall therefore limit ourselves to a brief review of the papers presented during the sessions on "Ionic Crystals" and "Excitons." These investigations were concerned mostly with crystal spectroscopy. A long paper by S. I. Pekar (USSR) summarizing the well-known work of the author and his co-workers was devoted to the theory of localized electronic centers in crystals. Special attention was given to the shape of the absorption and emission bands of the centers and their temperature dependence. In a general paper by O. Stasiw (German Democratic Republic), the optical properties of silver halides containing various cation and anion impurities were considered and interpreted. K. Vacek (Czechoslovakia) spoke on the luminescence of AgCl crystals. W. Martienssen (Federal Republic of Germany) delivered a paper on the establishment of a correspondence between the absorption bands of ionic crystals and electron transitions in the free ions of which the crystal is composed. There was great interest in the paper contributed by W. Känzig (USA). His study of the anisotropy of paramagnetic absorption and dichroism in colored alkali halide crystals at low temperatures showed that the self-trapping of holes at regular crystal lattice sites can last a long time. The paper by A. A. Shatalov (USSR) summarized the results of many years of work by the author on the photochemical transformation of color centers in alkali halide crystals. In the paper by Ch. B. Lushchik, G. G. Liid'ya, and J. V. Yaek (USSR), the spectra of F-center formation in ionic crystals were discussed, and the electron, exciton, and "delocalized" mechanisms for F-center production were considered. C. C. Klick (USA) proposed a mechanism for low temperature coloration of ionic crystals by x-rays, based on the idea of doubly ionized anions and the presence of Frenkel defects in crystals. H. Rabin and J. Schulman (USA) reported on the fine structure of F-center absorption spectra in crystals of CsCl and CsBr. J. Markham and G. Noble (USA) described the optical and paramagnetic properties of "pure" F-centers in crystals which do not contain additive electronic color centers introduced by special treatment. The contribution of A. Bohun and co-workers (Czechoslovakia) concerning physical processes in colored NaCl crystals containing various impurities was received with interest. In their paper, A. Halperin and his co-workers (Israel) considered the relation between thermoluminescence and thermal bleaching of alkali halide crystals. The spectral characteristics of color centers in cubic crystals was the subject of a paper by A. Smakula (USA). Great interest was aroused by the contribution of E. F. Gross (USSR) entitled "Optical and magneto-optical phenomena in semiconductors." On the basis of a broad investigation of various properties of Cu_2O and other crystals, numerous arguments were presented for the existence in crystals of the uncharged, mobile excited state predicted by Frenkel and known as the exciton. The theory of exciton spectra in Cu_2O was the subject of an interesting paper by R. Elliott (England). The results of experimental in-

vestigations of exciton states in various crystals were presented in a group of papers, among which the papers of S. Nikitin and co-workers (France) and of J. Pastrnyak (Czechoslovakia) were noteworthy.

The Prague conference on semiconductor physics was held in a setting permitting fruitful friendly discussions between scientists from various countries. The successful work of the conference was facilitated largely by the exceptional cordiality and careful organization of activities by the conference hosts, the scientists of the Czechoslovak Socialist Republic.

Ch. B. Lushchik.

LETTER TO THE EDITOR

Please publish the following correction to my paper "The Transfer of Electronic Excitation Energy with the Aid of a Virtual Exciton Mechanism."[1]

An incorrect relationship for the variation of transition probability with distance resulted from using an approximation to the effective exciton mass in calculating the probability of energy transfer by the virtual exciton mechanism.[1] It is possible to avoid this approximation and calculate the transition probability exactly. Putting $E(q) = E_0' + 2M\cos qd$ for the exciton energy and introducing the complex variable $z = e^{iqd}$, we find, (using the notation of ref. 1):

$$\sum_s \frac{M_{gs}M_{sk}}{E_g - E_s} = i\frac{M_{aa}M_{ab}}{2\pi M}\oint \frac{z^{|n-m|}}{z^2+\nu z+1}\,dz,$$

where the path of integration in the complex plane is the unit circle, and $\nu = (E_0' - E_H)/M$. We assume that the impurity level lies outside the exciton zone, so that $|\nu| > 2$. The line integral is evaluated by the theory of residuals. As a result, instead of the formula given in ref. 1 we obtain

$$\frac{W_{ab}'}{W_{ab}} = \frac{z^2(\omega)}{\sqrt{z^2-4}}\cdot\frac{M_{aa}^2M_{ab}^2}{M^2\overline{M}_{ab}^2}(n-m)^6\,e^{-\beta|n-m|},$$

where $\beta = -2\ln\left[|\nu|/2 - 1/2\sqrt{\nu^2-4}\right]$. It follows from this formula that the probability ratio is determined by the oscillator strength of a transition in the base substance, and also by the value of $|\nu|$. The probability ratio reaches a maximum at $|n-m| = 6/\beta$. Therefore, for sufficiently small $|\nu|$, the mechanism considered in ref. 1 is important over a wider range of impurity concentrations than indicated. Of course, when the exciton energy $E(q) = E_0 + \alpha q^2$, the conclusions arrived at in ref. 1 remain valid.

V. Agranovich

REFERENCE

1. V. M. Agronovich, Opt. i Spektr. 9, 113 (1960), Optics and Spectroscopy 9, 59 (1960).

ERRATA TO VOL. IX

Page	Line	Printed as	Should be
9 col. 2	12 from bottom	If $kT \geq \varepsilon_0$ then ε may replaced in (2) by $\bar{\varepsilon}$. Under the condition $kT < \varepsilon_0$ it is necessary to use formula (11)	If $\chi_1 kT \gg \varepsilon_0$, then in (12) we can replace $\varepsilon - \varepsilon_0$ by kT and take account in addition of the Boltzmann factor $\exp(-\varepsilon_0/kT)$. When $\chi_1 kT \approx \varepsilon_0$ we must use Eq. (11).
172	At the end of the text		Add: The spectra of guanylurea were obtained with the collaboration of Yu. I. Muchkin.
226 col. 2	At the end of the text		The author thanks V. M. Tatevskii and N. A. Tolstikova for their help in this work.
248 col. 2	12 lines above Table 1.	$V_{ev} = 2 + 54.03$ e/a	$V_{ev} = 2 + 54.93$ e/a
248 col. 2	Table I line 8	$2MgO \cdot Li_2OWO_3 \cdot 0.05$ Mn	$MgO \cdot 2LiO \cdot WO_3 \cdot 0.05$ Mn
248 col. 2	Table 1 line 17	$3Zno \cdot B_2O_3 \cdot 1Mn$	$3ZnO \cdot B_2O_3 \cdot 1Mn$
249 col. 1	Table 2 line 5	$Mg_3(PO_4)_2 \cdot 1Mn$	$Mg_3(PO_4)_2 \cdot 1Mn$
249 col. 1	Table 2 line 6	white	red
249 col. 1	Table 3 last line	$Li_2TiO_3 \cdot 0.1Mn$	$Li_2TiO_3 \cdot 0.1Mn$

AUTHOR LIST

VOLUME IX: JULY-DECEMBER

(Numbers in parentheses refer to pages in Russian original)

Abarenkov, I. V., (418) 218, (527) 276, (765) 402
Adrianova, I. I., (501) 260
Agranovich, V. (798) 421
Agranovich, V. M., (113) 59
Aivazova, A. A., (415) 215
Aksel'rod, V. S., (326) 170
Aleksandrov, I. V., (679) 359
Aleksandrovskaya, A. M., (273) 144
Anufrieva, E. V., (547) 290
Avdeev, V. I., (793) 418

Bagdyk'yants, G. O., (644) 339
Bakakina, V. V., (784) 412
Bakhshiev, N. G., (124) 65
Balashov, I. F., (790) 416
Bancie-Grillot, M., (542) 287
Barkov, V. I., (376) 195
Batsanov, S. S., (264) 137
Bersuker, I. B., (685) 363
Biyumenfel'd, L. A., (786) 414
Bobovich, Ya. S., (669) 352, (747) 392
Bochkova, O. P., (271) 142
Bogomolov, A. M., (311) 162
Bogomolov, S. G., (127) 68
Boitsov, E. N., (51) 26
Bokut, B. V., (635) 334
Bonch-Bruevich, A. M., (134) 73
Borisov, A. Yu., (115) 60
Borisov, M. G., (432) 227
Borod'ko, Yu. G., (677) 358
Bresler, P. I., (22) 11
Bystrov, D. S., (460) 239

Cherkasov, A. S., (540) 285
Cheremisinov, V. P., (446) 233
Chernyakovskii, F. P., (786) 414
Chuiko, L. I., (621) 327

Derkacheva, L. D., (209) 110
Dianov, E. M., (261) 136
Dokunikhin, N. S., (593) 313
Dubinin, V. G., (360) 187, (472) 246, (531) 279

Egorov, V. N., (692) 367
Egorov, V. S., (794) 419
Erkovich, S. P., (269) 141
Eremenko, V. V., (621) 327
Ermolaev, V. L., (353) 183
Ezhik, I. I., (772) 405

Fedorov, F. I., (635) 334
Filimonov, V. N., (460) 239
Finkel'shtein, A. I., (46) 24, (51) 26, (330) 172
Fok, M. V., (775) 407

Gal'pern, D. Yu., (549) 291
Georgobiani, A. N., (775) 407
Gerlovin, Ya. I., (664) 349
Girin, O. P.. (673) 355
Glazkov, V. I., (417) 217
Godnev, I. N., (273) 144
Gorban', I. S., (482) 250, (759) 398
Gorbatov, I. A., (415) 215
Gotlib, Yu. Ya., (319) 166
Gribov, L. A., (176) 93, (658) 346, (666) 350
Gridnev, K. A., (792) 417
Grillot, E., (542) 287
Gross, E. G., (542) 287
Gurevich, M. M. (253) 131

Ioffe, A. F., (551) 292
Irisova, N. A., (261) 136
Ivanov, V. N., (553) 293

Kalmanson, E. A., (786) 414
Kamenetskii, V. D., (111) 58
Kard, P. G., (95) 49, (248) 129, (386) 200
Karpovich, I. A., (653) 343
Kartashev, A. I., (394) 204
Karyakin, A. V., (666) 350
Kataev, D. I., (713) 376
Khachkuruzov, G. A., (721) 380
Khaikin, A. S., (487) 253
Khalupovskii, M. D., (525) 274
Khrshanovskii, S. A., (399) 207
Kiselev, A. A., (765) 402
Klement'eva, A. Yu., (648) 341
Klochkovskii, Yu. V., (728) 383
Kochelaev, B. I., (257) 133
Kochemirovskii, A. S., (544) 288
Kolobkov, V. P., (349) 181
Kolyadin, K. L., (253) 131
Kondilenko, I. I., (26) 13, (524) 273
Kondrasheva, L. D., (281) 149
Korolev, F. A., (648) 341
Korotkov, P. A., (26) 13
Kotlyar, I. P., (353) 183
Koval'chuk, D. S., (34) 18
Kovner, M. A., (170) 90
Krasnitskaya, N. D., (544) 288
Kremenchugskii, L. S., (530) 278
Kristofel', N. N., (527) 276, (615) 324
Kruchek, M. P., (467) 243
Kruglyakov, E. P., (538) 284
Krylova, T. N., (644) 339
Kubarev, S. I., (1) 1
Kudryashov, P. I., (203) 107, (341) 177
Kukina, V. S., (728) 383
Kuzyakov, Yu. Ya., (156) 84

Lapina, A. V., (501) 260
Lazarev, A. N., (195) 103, (326) 170
Leonov, Yu. S., (275) 145
Levshin, V. L., (132) 71, (223) 118
Liid'ya, G. G., (70) 35
Limareva, L. A., (203) 107
Lisitsa, M. P., (130) 70, (188) 99, (438) 229, (742) 389
Liu Shun-Fu, (787) 415
Lukirskii, A. P., (505) 262, (511) 265, (653) 343
Lushchik, Ch. B., (70) 35, (215) 113, (797) 420
Lushchik, N. E., (215) 113

Makhanek, A. G., (412) 214
Maksimova, G. V., (478) 248
Mal'nev, A. F., (530) 278
Mal'tsev, A. A., (428) 225, (713) 376
Malykh, V. D., (425) 223
Markov, M. N., (487) 253, (538) 284
Markin, E. P., (587) 309
Markovskii, L. Ya., (77) 40
Matora, I. M., (707) 373
Mazalov, L. N., (264) 137
Melik-Gaikazyan, I. Ya., (83) 43, (516) 268, (782) 411
Meleshina, A. M., (564) 299
Meshcheryakova, T. F., (648) 341
Mezhueva, T. D., (728) 383
Milosalvskii, V. K., (640) 337
Mirumyants, S. O., (7) 4, (124) 65
Mokeeva, G. A., (601) 317
Morgenshtern, Z. L., (676) 357
Morozov, V. P., (34) 18, (166) 88
Moskalenko, S. A., (369) 192
Muratov, V. R., (790) 416

Naberukhin, Yu. I., (576) 304
Naugol'nikov, B. I., (166) 88
Nemilov, Yu. A., (792) 417
Neporent, B. S., (7) 4
Nikitin, E. E., (16) 8
Nilov, E. V., (790) 416
Nosulenko, N. A., (640) 337
Nurmukhametov, P. N., (593) 313

Odintsov, A. I., (137) 75
Orlov, I. N., (626) 329
Orshanskaya, N. S., (77) 40
Ortenberg, F. S., (147) 80, (151) 82
Osiko, V. V., (478) 248
Ostrovskaya, G. V., (142) 78
Ostrovskii, Yu. I., (703) 371
Ovander, L. N., (571) 302

Padalka, V. G., (119) 63
Palistrant, M. E., (608) 320
Paranichev, V. N., (117) 62
Penkin, N. P., (680) 360, (703) 371
Perlin, Yu. E., (608) 320
Peregudov, G. V., (295) 155
Petrash, G. G., (121) 64, (423) 221
Petrashen', M. I., (527) 276
Pilipovich, V. A., (754) 396
Pisarevskii, A. N., (792) 417
Pisarevskii, Yu. V., (269) 141
Pivovarov, V. M., (266) 139
Plyavin', I. K., (365) 189
Podmoshenskii, I. V., (281) 149
Popov, Yu. M.. (260) 135

Popov, Yu. V., (501) 260
Popova, E. G., (593) 313
Prima, A. M., (452) 236
Prishivalko, A. P., (493) 256
Prokof'eva, N. I., (184) 97

Raikhbaum, Ya. D., (425) 223
Ratner, E. S., (101) 52
Razbirin, B. S., (542) 287
Razumovskaya, L. P., (271) 142
Rebane, K. K., (521) 272, (557) 295
Red'ko, T. P., (680) 360
Reznikova, I. I., (544) 288
Rombakh, V. P., (258) 134
Rozhdestvenskii Lecture, (129) 69
Rumsh, M. A. (505) 262, (511) 265, (653) 343
Ruzin, B. N., (22) 11
Rybakova, G. I., (34) 18, (166) 88

Saganenko, A. A., (349) 181
Selivanenko, A. S., (260) 135
Serdyuk, V. V., (407) 210
Shablya, A. V., (533) 280
Shaevich, A. B., (127) 68
Shatilov, A. V., (86) 44, (233) 123
Sheka, E. F., (57) 29
Shirokov, V. I., (341) 177
Shklyarevskii, I. N., (119) 63, (640) 337
Shovlo, S. T., (772) 405
Shpak, M. T., (57) 29
Shuba, Yu. A., (631) 332
Shukhtin, A. M., (794) 419
Shvarts, K. K., (215) 113
Sidorov, N. K., (546) 289
Sil'd, O. I., (521) 272
Slonim, I. Ya., (244) 127
Smirnov, L. A., (505) 262, (511) 265
Snegirev, B. N., (170) 90
Sobolev, N. N., (446) 233 (587) 309
Soera, T. Ya., (407) 210
Sokolov, V. A., (421) 219
Sokolovskaya, A. I., (582) 307
Strizhevskii, V. L., (26) 13
Sukhorukov, B. I., (46) 24, (330) 172
Sumarokova, T. N., (460) 239
Sushchinskii, M. M., (576) 304
Sverdlov, L. M., (40) 21, (184) 97, (304) 159, (432) 227, (671) 353, (728) 383
Sveshnikova, B. Ya., (203) 107, (341) 177, (601) 317
Syrkin, Ya. K., (677) 358

Taborko, N. I., (626) 329
Tarasova, N. V., (304) 159
Tatevskii, V. M., (713) 376
Terenin, A. N., (533) 280
Terpugova, A. F., (162) 86
Tetevskii, L. N., (156) 84
Tiisler, E. S., (70) 35
Timofeev, V. B., (482) 250
Tkachuk, A. M., (261) 136
Tolstoi, N. A., (261) 136, (421) 219, (787) 415
Trapeznikova, Z. A., (360) 187, (472) 246
Treskina, M. N., (83) 43, (782) 411
Tsyashchenko, Yu. P., (188) 99, (438) 229, (742) 389
Tulub, T. P., (669) 352, (747) 392
Tunitsky, L. N., (156) 84
Tunitskaya, V. F., (223) 118
Tyutikov, A. M., (631) 332

Vanyukov, M. P., (790) 416
Vasil'eva, N. N., (676) 357
Vereshchagin, I. K., (519) 270
Vernyi, E. A., (692) 367
Viktorova, E. N., (349) 181, (544) 288
Vinetskii, V. L., (64) 32
Vitol, I. K., (365) 189, (535) 282
Vlasenko, N. A., (640) 337
Vol'kenshtein, M. V., (467) 243
Vorob'eva, G. A., (524) 273
Voronov, Yu. V., (108) 57
Vuks, M. F., (92) 47

Yaek, I. V., (70) 35
Yakubov, I. T., (409) 212
Yazykova, S. M., (517) 269
Yukhnevich, G. V., (335) 174

Zaidel, A. N., (142) 78
Zavadovskaya, E. K., (83) 43, (516) 268, (782) 411
Zheenbaev, Zh., (288) 152
Zhirnov, N. I., (734) 385
Zhmyreva, I. A., (349) 181

CONTENTS

VOLUME IX: JULY-DECEMBER

(Numbers in parentheses refer to pages in Russian original)

No. 1—July

S. I. Kubarev: Some Problems in the Spectroscopy of Complex Molecules—(1) 1

S. O. Mirumyants and B. S. Neporent: Effect of Foreign Gases on the Intensity of the Electronic Absorption of 3-Dimethylamino-6-Aminophthalimide Vapor—(7) 4

E. E. Nikitin: Nonadiabatic Vibrational Excitation of Molecules During Molecular Collisions—(16) 8

P. I. Bresler and B. N. Ruzin: An Optico-Acoustic Phenomenon in the Visual and Ultraviolet Spectral Regions and its Relation to the Photochemical Processes in Gases—(22) 11

I. I. Kondilenko, P. A. Korotkov, and V. L. Strizhevskii: On the Intensities of Raman Lines—(26) 13

G. I. Rybakova, D. S. Koval'chuk, and V. P. Morozov: Force Constants and Interaction Coefficients of Pyramidal Hydrides—(34) 18

L. M. Sverdlov: Conditions for Specificity of Infrared Band Intensities in Polyatomic Molecules—(40) 21

B. I. Sukhorukov and A. I. Finkel'shtein: Optical Investigation of the Molecular Structure of Cyanamide and its Derivatives. III. Infrared and Ultraviolet Spectra and Molecular Structure of the Products of the Interaction of Cyanamide with Ketones (N-Cyanoketimines)—(46) 24

E. N. Boitsov and A. I. Finkel'shtein: Optical Investigation of the Molecular Structure of s-Triazine Derivatives. VI. Ultraviolet Absorption Spectra of Aqueous Solutions of Cyanuric Acid Derivatives at Various pH—(51) 26

M. T. Shpak and E. F. Sheka: The Influence of Impurities on the Luminescence of Crystalline Naphthalene—(57) 29

V. L. Vinetskii: Light Absorption and Luminescence of M-Centers in a Macroscopic Approximation—(64) 32

Ch. B. Lushchik, G. G. Liid'ya, I. V. Yaek, and E. S. Tiisler: The Mechanism of the Recombination Luminescence of Activated Alkali Halide Crystals—(70) 35

L. Ya. Markovskii and N. S. Orshanskaya: The Luminescence Properties of Selenium-Activated Zinc Oxide—(77) 40

I. Ya. Melik-Gaikazyan, E. K. Zavadovskaya, and M. N. Treskina: Effect of Annealing on the Absorption Spectra and Electrical Conductivity of Crystalline NaCl:Pb and KCl:Pb Phosphors—(83) 43

A. V. Shatilov: On the Scattering of Light by Dielectric Ellipsoids Comparable with the Wavelength. I. A General Expression for the Indicatrix of Scattering of an Ellipsoidal Particle—(86) 44

M. F. Vuks: Comparison of the Activation Energy for the Reorientation of Molecules with the Activation Energy of Viscous Flow—(92) 47

P. G. Kard: New Recursion Formulas in the Theory of Multilayer Optical Coatings—(95) 49

E. S. Ratner: Threshold Sensitivity of Radiation Receivers—(101) 52

Yu. V. Voronov: Intensity Ratio of the Luminescence Bands of ZnS:Mn and ZnS:Ag:Mn Phosphors as a Function of the Density of Cathodoexcitation and Photoexcitation—(108) 57

V. D. Kamenetskii: The Theory and Calculations of Collisions of Slow Electrons with Atoms—(111) 58

V. M. Agranovich: The Transfer of Electronic Excitation Energy with the Aid of a Virtual Excitation Mechanism—(113) 59

A. Yu. Borisov: High-Sensitivity Modulation Photometer—(115) 60

V. N. Paranichev: On the Spin Lattice Relaxation of Excitons in an Ionic Crystal—(117) 62

V. G. Padalka and I. N. Shklyarevskii: A Method for Making Low-Temperature Measurements of the Optical Constants of Metals—(119) 63

G. G. Petrash: Width and Shape of Infrared Absorption Bands—(121) 64

N. G. Bakhshiev and S. O. Mirumyants: The Eighth Conference on Luminescence (Molecular Luminescence and Luminescence Analysis)—(124) 65

S. G. Bogomolov and A. B. Shaevich: The Third Urals Symposium on Spectroscopy—(127) 68

Fourteenth Rozhdestvenskii Lecture—(129) 69

M. P. Lisitsa: Optics of Thin-Layer Coatings by G. V. Rozenberg—(130) 70

V. L. Levshin: Polarized Luminescence of Atoms, Molecules and Crystals by P. P. Feofilov—(132) 71

A. M. Bonch-Bruevich: A Direct Experimental Confirmation of the Second Postulate of the Special Theory of Relativity (in connection with Dingle's note)—(134) 73

The Competition for the S. I. Vavilov Gold Medal—(136) 74

No. 2—August

A. I. Odintsov: Hyperfine Structure and Isotopic Shift in the Spectrum of Tl I—(137) 75

A. N. Zaidel and G. V. Ostrovskaya: A Spectroscopic Determination of the Isotopic Composition of Carbon—(142) 78

F. S. Ortenberg: Intensity Distribution in the Bands of the α-System of the TiO Molecule—(147) 80

F. S. Ortenberg: Calculation of the Relative Transition Probabilities for Certain Band Systems of Oxides and Hydrides of the Group II Elements—(151) 82

Yu. Ya. Kuzyakov, V. M. Tetevskii and L. N. Tunitsky: Rotational Analysis of Boron Monoxide Bands Located in the Vacuum Ultraviolet—(156) 84

A. F. Terpugova: The Energy Levels and Wave Functions of the Disubstituted Benzene Molecule Calculated by the Method of the "Metal" Model—(162) 86

G. I. Rybakova, B. I. Naugol'nikov, and V. P. Morozov: Partial Frequencies of Pyramidal Hydrides and Deuterides with Symmetry C_{3v}—(166) 88

M. A. Kovner and B. N. Snegirev: Intensities and Depolarizations in the Raman Spectra of Polymethybenzenes. II. Numerical Calculation for Toluene—(170) 90

L. A. Gribov: Calculation of Intensities and Polarizations in the Vibrational Absorption Spectra of Polyatomic Molecules. II—(176) 93

L. M. Sverdlov and N. I. Prokof'eva: Calculation and Interpretation of the Vibrational Spectra of Naphthenes. IV. The Influence Constants of Cyclopentane—(184) 97

M. P. Lisitsa and Yu. P. Tsyashchenko: Effect of Temperature on the Intensities of the Vibrational Absorption Bands of Liquid Bromoform—(188) 99

A. N. Lazarev: Vibration Spectra of the Silicates. I. Infrared Spectra of Silicates with Anions of the Type $(Si_2O_7)^{-6}$—(195) 103
B. Ya. Sveshnikov, P. I. Kudryashov and L. A. Limareva: Sensitized Fluorescence in Solutions—(203) 107
L. D. Derkacheva: Variation in the Fluorescence of Naphthalene Derivatives as a Function of the Concentration of Hydrogen Ions in Solution—(209) 110
Ch. B. Lushchik, N. E. Lushchik, and K. K. Shvarts: Electronic-Vibrational Processes in the Luminescence Centers of Ionic Crystals—(215) 113
V. L. Levshin and V. F. Tunitskaya: The Nature and Kinetics of Radiation Processes in ZnS-Mn Phosphors During Excitation—(223) 118
A. V. Shatilov: On the Scattering of Light by Dielectric Ellipsoids Comparable with the Wavelength. II. Dependence of the Indicatrix of the Scattering on the Size, Form, and Orientation of the Ellipsoid. The Scattering Coefficient—(233) 123
I. Ya. Slonim: Determination of the Size of Particles by the Scattering of Light. Nomograms for the Determination of the Size of Rod-shaped Particles—(244) 127
P. G. Kard: Theory of Increasing the Transparency of Metallic Coatings—(248) 129
M. M. Gurevich and K. I. Kolyadin: The Spectrovisor—(253) 131
B. I. Kochelaev: The Theory of Spin-Lattice Relaxation of Nuclear Spins Surrounded by an Octahedral Complex—(257) 133
V. P. Rombakh: On the Light Absorption Edge in Alkali-Earth Metal Oxides—(258) 134
Yu. M. Popov and A. S. Selivanenko: Free Exciton Luminescence in a Molecular Crystal—(260) 135
N. A. Irisova and E. M. Dianov: Superhigh-Frequency Absorption of CH_3GeF_3—(261) 136
A. M. Tkachuk and N. A. Tolstoi: Luminescence of Ethanolamine Compounds of Platinum—(261) 136
L. N. Mazalov and S. S. Batsanov: Application of Perturbation Theory to the Calculation of the Ionic Refractions of Lanthanides and Actinides—(264) 137
V. M. Pivovarov: Consideration of the Internal Field in the Determination of Raman Intensities—(266) 139
S. P. Erkovich and Yu. V. Pisarevskii: The Oscillator Strength for the δ-System of the NO-Bands—(269) 141
L. P. Razumovskaya and O. P. Bochkova: Optical and Electrical Properties of "Weak" and "Strong" High Frequency Discharges in Neon—(271) 142
A. M. Aleksandrovskaya and I. N. Godnev: Approximate Prediction of the Normal Vibration Frequencies of the Hafnium Halides—(273) 144
Yu. S. Leonov: A New Luminor: $2Li_2O - WO_3(U)$—(275) 145
The Ninth Conference on Luminescence (Crystal Phosphors)—(277) 146

No. 3—September

L. D. Kondrasheva and I. V. Podmoshenskii: Concentration of Atoms in the Arc Plasma as Determined by the Pulse Absorption Method—(281) 149
Zh. Zheenbaev: Investigation of a High-Frequency Discharge with Hydrodynamic Compression—(288) 152
G. V. Peregudov: Calculation and Interpretation of the Vibrational Spectra of Biphenyl and Some of its Deuterium Substitution Products—(295) 155
L. M. Sverdlov and N. V. Tarasova: Vibrational Spectra of Unsaturated Hydrocarbons. VIII. Vibrational Spectra and Rotational Isomerism of 1,3-Butadiene—(304) 159
A. M. Bogomolov: Vibrational Spectra of Aromatic Compounds. VII. Characteristic Vibrations of Monosubstituted Benzenes—(311) 162
Yu. Ya. Gotlib: Theory of the Vibrational Spectra of Polymers. II. Torsional Skeletal Vibrations in Syndiotactic Polymer Chains—(319) 166
A. N. Lazarev and V. S. Aksel'rod: The Vibrational Spectra of Pyrophosphates—(326) 170
B. I. Sukhorukov and A. I. Finkel'shtein: Spectroscopic Study of the Molecular Structure of Guanyl-Urea and Biuret—(330) 172
G. V. Yukhnevich: Infrared Spectra of Heteropoly-Compounds and Their Structure—(335) 174
P. I. Kudryashov, B. Ya. Sveshnikov, and V. I. Shirokov: The Kinetics of the Concentration Depolarization of Luminescence and of the Intermolecular Transfer of Excitation Energy—(341) 177
E. N. Viktorova, I. A. Zhmyreva, V. P. Kolobkov, and A. A. Saganenko: Study of the Phosphorescence Lifetimes of Solutions of Organic Compounds at −196°—(349) 181
V. L. Ermolaev and I. P. Kotlyar: Influence of the Hydrogen Bond on the Probability of Internal Conversion to the Triplet Level in the Quinoline Molecule—(353) 183
V. G. Dubinin and Z. A. Trapeznikova: An Electron Paramagnetic Resonance Investigation of the Valence Change of the Activator During Excitation of the Phosphor SrS-Eu,Sm—(360) 187
I. K. Vitol and I. K. Plyavin: The Kinetics of the Short-Lived Photoluminescence of Some Activated Alkali Halide Crystals—(365) 189
S. A. Moskalenko: Light Absorption by Excitons in the Cu_2O Crystal. II. Absence of Constant External Fields—(369) 192
V. I. Barkov: Radiation Transfer in a Homogeneous Medium for the Nonconservative Case—(376) 195
P. G. Kard: Principles of the Theory of the Synthesis of Coated Absorbing Layers—(386) 200
A. I. Kartashev: Optical Systems with Enhanced Resolving Power—(394) 204
S. A. Khrshanovskii: On the Properties of the Focal Surfaces of Mirror Spectrographs—(399) 207
T. Ya. Soera and V. V. Serdyuk: A New Band in the Absorption Spectrum of Polycrystalline Layers of Cadmium Sulfide—(407) 210
I. T. Yakubov: The Franck-Condon Factors for the Schumann-Runge Band System in the Oxygen Molecule—(409) 212
A. G. Makhanek: Influence of Vibrations on the Quadrupole Coupling Constants in Alkali Halide Molecules—(412) 214
A. A. Aivazova and I. A. Gorbatov: Study of Molecular Interaction in p-Dichlorobenzene Near the Freezing Point—(415) 215
V. I. Glazkov: Analysis of the Nuclear Magnetic Resonance Spectrum of $A_3B_2X_2$ Groups—(417) 217
I. V. Abarenkov: The Polarizable Point Lattice Approximation in the Theory of Impurity Centers in Ionic Crystals—(418) 218
V. A. Sokolov and N. A. Tolstoi: The Luminescence of Thallous Chloride—(421) 219
G. G. Petrash: Optimum Conditions for the Measurement of the Width of Absorption Bands—(423) 221

No. 4—October

Ya. D. Raikhbaum and V. D. Malykh: A Spectroscopic Method for Studying the Diffusion of Atoms in an Electric Arc—(425) 223
A. A. Mal'tsev: Isotope Effect in the Singlet Spectral Bands of the BF Molecule—(428) 225
L. M. Sverdlov and M. G. Borisov: Vibrational Spectra of Unsaturated Hydrocarbons. IX. Calculation and

Interpretation of the Vibrational Spectra of Methylallene and the Deuterioallenes—(432) 227
M. P. Lisitsa and Yu. P. Tsyashchenko: Temperature Dependence of the Intensities of the Infrared Absorption Bands of Liquid Chloroform—(438) 229
N. N. Sobolev and V. P. Chermisinov: The Vibrational Spectrum and Molecular Structure of Crystalline Arsenic Oxide—(446) 233
A. M. Prima: Vibrational Spectra of Silicates. III. Equations of the Vibrations of Planar Silicon-Oxygen Rings in Silicates—(452) 236
D. S. Bystrov, T. N. Sumarokova, and V. N. Filimonov: Infrared Absorption Spectra of the Complexes of Urea and Thiourea with Tin Chloride and Tin Bromide—(460) 239
M. V. Vol'kenshtein and M. P. Kruchek: Calculation of the Optical Activity of Molecules—(467) 243
V. G. Dubinin and Z. A. Trapeznikova: Use of Electron Paramagnetic Resonance for the Study of Eu-Activated SrS Phosphors—(472) 246
V. V. Osiko and G. V. Maksimova: The Valence of Manganese as an Activator in Phosphors—(478) 248
I. S. Gorban' and V. B. Timofeev: The Properties of the Longest Wavelength Line in the Intrinsic Absorption of Cu_2O—(482) 250
M. N. Markov and A. S. Khaikin: The Optical Properties of Bulk Bismuth in the 3-36μ Region—(487) 253
A. P. Prishivalko: Determination of the Optical Constants of Absorbing Substances from the Measurements of Stokes' Parameters of Reflected Light—(493) 256
I. I. Adrianova, Yu. V. Popov, and A. V. Lapina: Amplitude and Phase Characteristics of an Interference Light Modulator—(501) 260
A. P. Lukirskii, M. A. Rumsh, and L. A. Smirnov: X-Ray Monochromator for Ultrasoft Radiation with the Recording of the Absolute Number of Quanta—(505) 262
A. P. Lukirskii, M. A. Rumsh, and L. A. Smirnov: Measurement of the Photoelectric Yield for Ultrasoft X-Radiation—(511) 265
I. Ya. Melik-Gaikazyan and E. K. Zavadovskaya: The Connection Between F-Band Half-Widths and Defects in Solid Solutions of Alkali Halide Crystals—(516) 268
S. M. Yazykova: Quantum-Mechanical Treatment of the Nonlinearity of a Molecule—(517) 269
I. K. Vereshchagin: The Aging of ZnS Phosphors—(519) 270
K. K. Rebane and O. I. Sil'd: The Relationship Between Electronic-Vibrational Absorption and Emission Bands—(521) 272
I. I. Kondilenko and G. A. Vorob'eva: Annular Low Pressure Mercury Lamp—(524) 273
M. D. Khalupovskii: The Effect of Temperature on the Decay of Phosphorescence in Boron Phosphors—(525) 274
M. I. Petrashen', I. V. Abarenkov, and N. N. Kristofel': Approximate Wave Functions of Free Ions and of Ions in a Crystal—(527) 276
A. F. Mal'nev and L. S. Kremenchugskii: Low Temperature Thermal Radiation Detector—(530) 278
V. G. Dubinin: The Effect of the Flux on the State of the Activator in a Phosphor: An Investigation by the Paramagnetic Resonance Method—(531) 279
A. V. Shablya and A. N. Terenin: The Spectrum of the Negative Molecular Ion of Phthalocyanin—(533) 280
I. K. Vitol: The Nonisothermal Relaxation of the Luminescence Spectra of X-Irradiated KCl Crystals Activated with Tl^+, In^+, Ab^+, and Cu^+ Ions—(535) 282
M. N. Markov and E. P. Kruglyakov: Zonal Sensitivity of PbS Photoconductors—(538) 284
A. S. Cherkasov: Fluorescence Yields of Acetylanthracenes in Some Solvent Mixtures—(540) 285
M. Bancie-Grillot, E. F. Gross, E. Grillot, and B. S. Razbirin: The Influence of Temperature on Two Series of Bands in the Green Fluorescence Spectrum of Pure Cadmium Sulfide at Low Temperature—(542) 287
E. N. Viktorova, A. S. Kochemirovskii, N. D. Krasnitskaya, and I. I. Reznikova: New Examples of a Pronounced Dependence of Fluorescence Yield on the Position of the Emission Spectrum—(544) 288
N. K. Sidorov: The Indicatrix of Raman Scattering—(546) 289
E. V. Anufrieva: The Effect of Vitrification on the Polarization of the Persistent Luminescence of Organic Substances—(547) 290
D. Yu. Gal'pern: Apodization—(549) 291
Abram Fedorovitch Ioffe's 80th Birthday—(551) 292

No. 5—November

V. N. Ivanov: The Influence of Dipolar Molecules on the Absorption of the Mercury Resonance Line at 2537 A—(553) 293
K. K. Rebane: Toward the Theory of Electronic-Vibrational Transitions in Systems with Many Vibrational Degrees of Freedom—(557) 295
A. M. Meleshina: Effect of Vibrations on the Forbidden Transitions in a Molecule—(564) 299
L. N. Ovander: The Form of the Raman Tensor—(571) 302
Yu. I. Naberukhin and M. M. Sushchinskii: Second-Order Lines in the Raman Spectra of Hydrocarbons—(576) 304
A. I. Sokolovskaya: The Temperature Dependence of the Intensity of Raman Lines in the Vapor and Liquid Phases—(582) 307
E. P. Markin and N. N. Sobolev: Infrared Reflection Spectrum of Boric Anhydride and Fused Quartz at High Temperatures—(587) 309
P. N. Nurmukhametov, E. G. Popova, and N. S. Dokunikhin: The Luminescence of Chrysene Solutions and Powders at 77°K—(593) 313
G. A. Mokeeva and B. Ya. Sveshnikov: The Concentration Quenching of Luminescence in Organoluminors—(601) 317
Yu. E. Perlin and M. E. Palistrant: The Theory of Photoionization of F-Centers—(608) 320
N. N. Kristofel': The Interaction Between Activator and Non-Totally Symmetric Local Vibrations—(615) 324
V. V. Eremenko and L. I. Chuiko: Effect of Deformations on the Absorption Spectrum of Cuprous Oxide Crystals at 20°K—(621) 327
I. N. Orlov and N. I. Taborko: Experimental Study of Light Amplification in a "Photoconductor-Ferroelectric-Electroluminor" Element—(626) 329
A. M. Tyutikov and Yu. A. Shuba: Measurement of Small Photocurrents in the Study of Photoelectric Emission—(631) 332
B. V. Bokut and F. I. Fedorov: Reflection and Refraction of Light in Optically Isotropic Active Media—(635) 334
I. N. Shklyarevskii, N. A. Vlasenko, V. K. Milosalvskii, and N. A. Nosulenko: The Magnitude and Sign of the Phase Difference $\Delta = \delta_p - \delta_s$—(640) 337
T. N. Krylova and G. O. Bagdyk'yants: Study of the Optical Properties and Structure of Titanium Dioxide Films—(644) 339
F. A. Korolev, A. Yu. Klement'eva and T. F. Meshcheryakova: Interference Filters with a Transmission Band of 1.5 A Half-Width—(648) 341
A. P. Lukirskii, M. A. Rumsh, and I. A. Karpovich: Meas-

urement of the Photoelectric Yield of the External Photoeffect under the action of X-Rays in the Wavelength Range 1.54-13.3 A—(653) 343
L. A. Gribov: Intensities and Polarizations of Specific Vibrations in the Infrared Absorption Spectra of Polyatomic Molecules—(658) 346
Ya. I. Gerlovin: A Method for Determination of the Radiation Probability of Gases and Vapors—(664) 349
L. A. Gribov and A. V. Karyakin: Infrared Absorption Band Intensities of the Hydroperoxide Group—(666) 350
T. P. Tulub and Ya. S. Bobovich: The Influence of the Refractive Index on the Temperature Shift of Raman Band Intensities—(669) 352
L. M. Sverdlov: Conditions for Specificity of the Polarization of the Infrared Bands of Polyatomic Molecules—(671) 353
O. P. Girin: The Theory of Vibration of Finite Crystal Lattices—(673) 355
N. N. Vasil'eva and Z. L. Morgenshtern: The Luminescence of Nonactivated KI Crystals—(676) 357
Yu. G. Borod'ko and Ya. K. Syrkin: The Intensities of Raman Lines of Mixtures of CCl_4, $SiCl_4$, and $GeCl_4$ with Benzene, Paraxylene, and Cyclohexane—(677) 358
I. V. Aleksandrov: Theory of the Hyperfine Structure of Electron Paramagnetic Resonance Spectra—(679) 359
N. P. Penkin and T. P. Red'ko: The Relative Oscillator Strengths of Certain Lines of ZnI and CdI—(680) 360
XIII Conference on Spectroscopy—(683) 361

No. 6—December

I. B. Bersuker: On Quantum Transitions in the Self-Consistent Field Approximation—(685) 363
E. A. Vernyi and V. N. Egorov: The Isotope Effect in the Spectrum of Thorium—(692) 367
Yu. I. Ostrovskii and N. P. Penkin: f-Number Measurements for the Spectral Lines of Barium—(703) 371
I. M. Matora: The Scattering of Slow Electrons by Helium Atoms, with Excitation of the 2^3S- and 2^1S-Levels—(707) 373
A. A. Mal'tsev, D. I. Kataev, and V. M. Tatevskii: Study of the Electronic Spectra and Isotope Effect of Oxygen Compounds of Boron. III. γ-Bands of the BO Molecule—(713) 376
G. A. Khachkuruzov: Method of Determining the Nonrigidity Corrections to the Higher Rotational Energy Levels of Molecules of the Asymmetric Rotor Type—(721) 380
L. M. Sverdlov, Yu. V. Klochkovskii, V. S. Kukina, and T. D. Mezhueva: Vibrational Spectra and Potential Energy Constants of Haloethylenes Monochloroethylene, Monofluorethylene, 1,1-Dichloroethylene, 1,1-Dibromoethylene, and their Deuterium Substitution Products—(728) 383
N. I. Zhirnov: On the Interpretation of the Vibrational Spectra of Naphthalene and its Deuterium Analog—(734) 385
M. P. Lisitsa and Yu. P. Tsyashchenko: Influence of Temperature on Absorption for Certain Vibrational Bands of Gaseous Chloroform and Bromoform—(742) 389
Ya. S. Bobovich and T. P. Tulub: The Temperature Dependence of Raman Band Intensities in Crystalline and Glassy Solids. I. Experimental Investigation in the Stokes Region of the Spectrum—(747) 392
V. A. Pilipovich: On the Antistokes Phosphorescence of Organophosphors—(754) 396
I. S. Gorban': Quantitative Studies of the Absorption Spectrum of Cuprous Oxide—(759) 398
A. A. Kiselev and I. V. Abarenkov: Optical Transitions in U-Centers in NaCl Crystals—(765) 402
I. I. Ezhik and S. T. Shovlo: The Role of M-, R-, and F'-Color Centers in the Infrared Fluorescence of F-Centers in Alkali Halide Crystals—(772) 405
A. N. Georgobiani and M. V. Fok: Main Peaks in the Light Pulses of Electroluminescence—(775) 407
I. Ya. Melik-Gaikazyan, M. N. Treskina, and E. K. Zavadovskaya: Half-Width of the F-Band and Density of F-Centers in Solid Solutions of KCl-KBr Single Crystals—(782) 411
V. V. Bakakina: Some Results of a Spectral Investigation of an Ultrahigh Frequency Impulse Discharge in a Restricted Discharge Gap—(784) 412
F. P. Chernyakovskii, A. E. Kalmanson, and L. A. Blyumenfel'd: Electron Paramagnetic Resonance in Crystals of Triphenylmethane Dyes—(786) 414
N. A. Tolstoi and Liu Shun-Fu: The Relaxation Spectrum of Kyanite—(787) 415
I. F. Balashov, M. P. Vanyukov, V. R. Muratov, and E. V. Nilov: Spark Discharge Spectra Resolved in Time and Along the Channel Cross Section as Recorded with an Electron Optical Converter—(790) 416
Yu. A. Nemilov, K. A. Gridnev, and A. N. Pisarevskii: The Intensity of the Slow Component of Stilbene Luminescence Excited by Alpha Particles—(792) 417
V. I. Avdeev: Magnitude of the Polarization of Nuclei in the Nonstationary Overhauser Effect—(793) 418
V. S. Egorov and A. M. Shukhtin: The Afterglow and its Relation to Gas Density in a Pulse Discharge in Ne—(794) 419
Ch. B. Lushchik: International Conference on the Physics of Semiconductors—(797) 420
V. Agranovich: Letter to the Editor—(798) 421
Errata in Vol. IX—(820) 421
Author List, Vol. IX—(799) 422
Contents List, Vol. IX—424

OPTICAL SOCIETY *of* AMERICA

THE OPTICAL SOCIETY OF AMERICA was organized in 1916 "to increase and diffuse the knowledge of optics in all its branches, pure and applied, to promote the mutual interests of investigators of optical problems, of designers, manufacturers and users of optical instruments and apparatus of all kinds and to encourage cooperation among them." The Society cordially invites to membership all who are interested in any branch of optics, either in research, in instruction, in optical applications, in the manufacture and distribution of optical equipment of all kinds, or in physiological and medical optics.

APPLICATION FOR MEMBERSHIP

Full Name ..... Date of Birth .....

Present Professional Position .....

.....

Previous Professional Positions *(with approximate dates)* .....

.....

.....

.....

Education *(List Colleges and Universities attended and degrees received, with dates)*

.....

.....

.....

Chief Publications in Optics *(Titles and journal references. Need not be complete.)*

.....

.....

.....

.....

.....

.....

.....

I wish my subscriptions to the Journal of the Optical Society of America and to the Russian translation journal, Optics and Spectroscopy, to begin January first of ☐ the current year ☐ next year

....., 19..... .....

(Date) *(Signature of Applicant)*

Please print or type your name and address in the space below, exactly as they should appear on the addressograph stencil, which will accommodate no more than four typewritten lines with thirty-one characters or spaces in each line. The Executive Secretary should be notified promptly of all changes of address.

.....

.....

.....

.....

All journal subscriptions date from January 1. Dues are assessed and the journals delivered for the complete calendar year in which application is made unless the applicant requests that the subscriptions begin on January 1 of the following year. Do not send payment of dues with this application. Bill will be sent by the American Institute of Physics after the applicant is elected.

FILLER MATERIAL - NOT IN RUSSIAN ORIGINAL

Return to Dr. Mary E. Warga, Executive Secretary, Optical Society of America, 1155 Sixteenth Street, N.W., Washington 6, D. C.

SPONSORS

We recommend that the applicant named on the reverse be elected to membership.

.....
Member

.....
Member

ACTION BY MEMBERS OF BOARD OF DIRECTORS

Elected to Associate Membership by approval of the undersigned.

.....
.....
.....
Directors

EXCERPTS FROM THE BY-LAWS RELATIVE TO MEMBERSHIP AND DUES

(As Amended January 1, and September 11, 1959)

Eligibility: Any person who is interested in optics is eligible for Associate Membership.

Any person who has been an Associate Member for three years, or has contributed materially to the advancement of optics, is eligible for Regular Membership.

Any person who has served with distinction in the advancement of optics is eligible for transfer to the class of Fellow.

Any person who has rendered eminent service in the advancement of optics may be elected to Honorary Membership.

Application for Membership: Applications for membership must state the candidate's name and qualifications for membership and must be signed by two Associate, Regular, Fellow, Emeritus or Honorary Members of the Society.

Election to Membership: Applications from individuals for membership shall be considered first as applications for Associate Membership and shall be acted upon as such. Applicants shall become Associate Members when their duly prepared applications have received the written approval of three members of the Board of Directors.

Associate Members will automatically become Regular Members at the conclusion of three years as Associate Members. Associate Members may also be transferred to Regular Membership before the completion of the three-year period at any regular meeting of the Board of Directors by a two-thirds vote of the members of the Board present.

Regular Members may be transferred to the class of Fellow at any regular meeting of the Board of Directors by a two-thirds vote of the members of the Board present. The number of Fellows shall at no time exceed one-tenth of the total membership of the Society, except that no one who has been transferred to the class of Fellow shall be displaced from that class because of a reduction in the total number of members in the Society. Fellows shall pay the same dues as Regular Members.

Honorary Members may be elected at any regularly called meeting of the Board of Directors by the unanimous vote of the entire Board. In case any members of the Board are not in attendance their ballots must be obtained by the Executive Secretary. The number of Honorary Members shall at no time exceed five

Duties and Privileges: On payment of their dues,* as determined from time to time by the Board of Directors, Associate Members have the following privileges: The right to attend meetings and receive the Journal of the Society and such other publications as the Board of Directors may direct.

On payment of their dues,* as determined from time to time by the Board of Directors, Regular Members and Fellows have the following privileges: The right to vote, hold office, attend meetings, and receive the Journal of the Society and such other publications as the Board of Directors may direct.

Honorary Members pay no dues. They have the following privileges: The right to vote, hold office, attend meetings, and receive the Journal of the Society and such other publications as the Board of Directors may direct.

Termination of Membership: Membership in the Society may be suspended or terminated by vote of the Board of Directors. Failure to pay dues for one year shall be deemed sufficient cause for suspension or termination of membership.

---

* By action of the Board of Directors, effective April 1, 1959, the annual dues are: Associate Members, $13.00; Fellows and Regular Members, $17.00.

FILLER MATERIAL - NOT IN RUSSIAN ORIGINAL

BACK NUMBERS OF JOSA

The Executive Office is anxious to locate for its Library one copy each of the publications listed below. If any member has a copy available, will he please contact the Assistant Secretary at the OSA Executive Office—1155 Sixteenth Street, N.W., Washington, D. C.

Year	*Vol.*	*Number*	*Month*
1920	IV	5	September
1921	V	1	Jan.–Feb.
1921	V	4	July–Aug.
1921	V	5	Sept.–Oct.
1921	V	6	Nov.–Dec.
1922	VI	2	—
1922	VI	3	—
1923	7	9	September
1923	7	10	October
1925	11	2	August

(FILLER MATERIAL - NOT IN RUSSIAN ORIGINAL)

NEWS ITEMS

International Conference on the Physics of Semiconductors . . . . . Ch. B. Lushchik 420 (797)
Letter to the Editor . . . . . V. Agranovich 421 (798)
Errata to Vol. IX 421 (820)
Author List, Vol. IX 422 (799)
Contents List, Vol. IX 424

EDITOR'S NOTE

Comments on the scientific content of the translated Russian articles published in OPTICS AND SPECTROSCOPY are invited. They should be addressed as a Letter to the Editor of the Journal of the Optical Society of America and forwarded to the Editor of that journal, Dr. D. B. Judd, National Bureau of Standards, Washington 25, D. C.

VOL. IX, NO. 6 OPTICS AND SPECTROSCOPY DECEMBER 1960

CONTENTS

(Numbers in parentheses are original Russian page numbers)

On Quantum Transitions in the Self-Consistent Field Approximation . . . . . I. B. Bersuker 363 (685)

The Isotope Effect in the Spectrum of Thorium . . . . . E. A. Vernyi and V. N. Egorov 367 (692)

f-Number Measurements for the Spectral Lines of Barium . . . . . Yu. I. Ostrovskii and N. P. Penkin 371 (703)

The Scattering of Slow Electrons by Helium Atoms, with Excitation of the 2^3S- and 2^1S-Levels . . . . . I. M. Matora 373 (707)

Study of the Electronic Spectra and Isotope Effect of Oxygen Compounds of Boron III. γ-Bands of the BO Molecule . . . . . A. A. Mal'tsev, D. I. Kataev, and V. M. Tatevskii 376 (713)

Method of Determining the Nonrigidity Corrections to the Higher Rotational Energy Levels of Molecules of the Asymmetric Rotor Type . . . . . G. A. Khachkuruzov 380 (721)

Vibrational Spectra and Potential Energy Constants of Haloethylenes Monochloroethylene, Monofluoroethylene, 1,1-Dichloroethylene, 1,1-Dibromoethylene, and their Deuterium Substitution Products . . . . . L. M. Sverdlov, Yu. V. Klochkovskii, V. S. Kukina, and T. D. Mezhueva 383 (728)

On the Interpretation of the Vibrational Spectra of Naphthalene and its Deuterium Analog . . . . . N. I. Zhirnov 385 (734)

Influence of Temperature on Absorption for Certain Vibrational Bands of Gaseous Chloroform and Bromoform . . . . . M. P. Lisitsa and Yu. P. Tsyashchenko 389 (742)

The Temperature Dependence of Raman Band Intensities in Crystalline and Glassy Solids I. Experimental Investigation in the Stokes Region of the Spectrum . . . . . Ya. S. Bobovich and T. P. Tulub 392 (747)

On the Antistokes Phosphorescence of Organophosphors . . . . . V. A. Pilipovich 396 (754)

Quantitative Studies of the Absorption Spectrum of Cuprous Oxide . . . . . I. S. Gorban' 398 (759)

Optical Transitions in U-Centers in NaCl Crystals . . . . . A. A. Kiselev and I. V. Abarenkov 402 (765)

The Role of M-, R-, and F'- Color Centers in the Infrared Fluorescence of F-Centers in Alkali Halide Crystals . . . . . I. I. Ezhik and S. T. Shovlo 405 (772)

Main Peaks in the Light Pulses of Electroluminescence . . . . . A. N. Georgobiani and M. V. Fok 407 (775)

SHORT COMMUNICATIONS

Half-Width of the F-Band and Density of F-Centers in Solid Solutions of KCl-KBr Single Crystals . . . . . I. Ya. Melik-Gaikazyan, M. N. Treskina, and E. K. Zavadovskaya 411 (782)

Some Results of a Spectral Investigation of an Ultrahigh Frequency Impulse Discharge in a Restricted Discharge Gap . . . . . V. V. Bakakina 412 (784)

Electron Paramagnetic Resonance in Crystals of Triphenylmethane Dyes . . . . . F. P. Chernyakovskii, A. E. Kalmanson, and L. A. Blyumenfel'd 414 (786)

The Relaxation Spectrum of Kyanite . . . . . N. A. Tolstoi and Liu Shun-Fu 415 (787)

Spark Discharge Spectra Resolved in Time and Along the Channel Cross Section as Recorded with an Electron Optical Converter . . . . . I. F. Balashov, M. P. Vanyukov, V. R. Muratov, and E. V. Nilov 416 (790)

The Intensity of the Slow Component of Stilbene Luminescence Excited by Alpha Particles . . . . . Yu. A. Nemilov, K. A. Gridnev, and A. N. Pisarevskii 417 (792)

Magnitude of the Polarization of Nuclei in the Nonstationary Overhauser Effect . . . . . V. I. Avdeev 418 (793)

The Afterglow and its Relation to Gas Density in a Pulse Discharge in Ne . . . . . V. S. Egorov and A. M. Shukhtin 419 (794)

(Contents continued on inside back cover)